Starburst Poly-amidoamine Dendrimer Grafted Gold Nanoparticles as Scaffolds for Targeted Gene Delivery *in vitro*

by

LONDIWE S. MBATHA

Submitted in fulfillment of the academic requirements of

Doctor of Philosophy

in the Discipline of Biochemistry

School of Life Sciences

College of Agriculture, Engineering, and Science

University of KwaZulu-Natal

Durban

South Africa

08 December 2017

PREFACE

The research contained in this dissertation/thesis was completed by the candidate while based in the Discipline of Biochemistry, School of Life Sciences, of the College of Agriculture, Engineering, and Science, University of KwaZulu-Natal, Westville Campus, South Africa. The research was financially supported by National Research Foundation.

The contents of this work have not been submitted in any form to another university and, except where the work of others is acknowledged in the text, the results reported are due to investigations by the candidate.

_____

Signed: Prof M Singh

Date: 08 December 2017

DECLARATION 1: PLAGIARISM

I, Londiwe Simphiwe Mbatha, declare that:

i. The research reported in this dissertation, except where otherwise indicated or acknowledged, is my original work;
ii. This dissertation has not been submitted in full or in part for any degree or examination to any other university;
iii. This dissertation does not contain other persons' data, pictures, graphs or other information unless specifically acknowledged as being sourced from other persons;
iv. This dissertation does not contain other persons' writing unless specifically acknowledged as being sourced from other researchers. Where other written sources have been quoted, then:
    a) Their words have been re-written but the general information attributed to them has been referenced;
    b) Where their exact words have been used, their writing has been placed inside quotation marks, and referenced;
v. Where I have used material for which publications followed, I have indicated in detail my role in the work;
vi. This dissertation is primarily a collection of material, prepared by myself, published as journal articles or presented as a poster and oral presentations at conferences. In some cases, additional material has been included;
vii. This dissertation does not contain text, graphics or tables copied and pasted from the Internet, unless specifically acknowledged, and the source being detailed in the dissertation and in the References sections.

_____

Signed: Londiwe Simphiwe Mbatha

Date: 08 December 2017

DECLARATION 2: PUBLICATIONS

All research presented was conceptualised and designed by Prof Moganavelli Singh and the research was conducted by myself, Londiwe S Mbatha. Conference presentation is indicated.

1. Mbatha, L. and Singh, M. (2016). "Dendrimer functionalised gold nanoparticles for targeting to the folate receptor *in vitro*". Human Gene Therapy. 27 (11): A92-93. DOI: 10.1089/hum.2016. 29035. Abstracts. *Impact factor=4.187*
   Presentation at the Annual Meeting of the European Society of Gene & Cell Therapy and Italian Society of Stem cell Research (Florence, Italy, 18th to 21st October, 2016).

_____

Signed: Londiwe Simphiwe Mbatha

Date: 08 December 2017

ABSTRACT

The major challenge in gene therapy is the development of safe and efficient gene carriers. The merging of gene therapy with nanotechnology provides a new powerful platform which promises to address the safety-efficacy issues. Metal gold nanoparticles (AuNPs) have attracted immense interest over the past few years as gene and drug delivery vehicles, due to their tunable stability, low inherent cytotoxicity and ability to be functionalised. The grafting/stabilizing of metal nanoparticles with starburst dendritic polymers over the conventional polymers has proven to be a promising advancement in the design of highly efficient non-viral gene delivery nano-scaffolds.

The objective of the study was to synthesise, characterise and evaluate the cytotoxicity profiles and capacity of unmodified and folic acid (FA) modified poly-amidoamine generation 5 (PAMAM G5D) grafted gold nanoparticles to deliver pDNA, mRNA, and siRNA in mammalian cell lines. The same parameters were also evaluated using unmodified and folic acid modified PAMAM G5D control nanoparticles (G5D/G5D:FA NPs) for comparative studies. Nanoparticles and their nanocomplexes were characterized by transmission electron microscopy (TEM), nanoparticle tracking analysis (NTA), Ultra-violet (UV) spectroscopy, nuclear magnetic resonance (NMR), band shift, ethidium bromide dye displacement and nuclease protection assays. Nanoparticles appeared as spherical, unilamellar vesicles, while their nanocomplexes appeared as globular clusters. Cytotoxicity profiles, gene expression, and silencing were evaluated in the HEK293, HepG2, Caco-2, MCF-7, KB, and HeLa-Tat-*Luc* cell lines using the MTT and luciferase reporter gene assays respectively. Nanocomplexes prepared at optimum weight/weight ratios protected the pDNA/mRNA/siRNA against nucleases, and were well tolerated by all cell lines. Transgene expression (pDNA and mRNA) and gene silencing (siRNA) was highest with FA targeted dendrimer grafted AuNPs (Au:G5D:FA), in FA-receptor overexpressing cells (MCF-7, KB), and HeLa-Tat-*Luc* cells respectively, and decreased significantly ($p < 0.05$) in the presence of excess competing FA ligand, confirming nanocomplex uptake via receptor mediation. Overall, transgene expression and silencing of the Au:G5D and Au:G5D:FA nanocomplexes were significantly better than that of the G5D/G5D:FA nanocomplexes confirming the key roles played by dendrimer modification and the AuNPs in the design of these delivery systems.

ACKNOWLEDGMENTS

I would like to express my heartfelt gratitude and appreciation to:

- God. Because of his amazing love, strength, and grace, I was able to persevere through the challenges that I faced during the course of this study.
- My supervisor, Professor M. Singh for her guidance, assistance, patience and steadfast supervision, during the course of this thesis.
- Professor M. Ariatti for his guidance.
- My colleagues for their assistance and guidance.
- My friends, Miss, F. Maiyo, Miss, A. Daniels, Miss, S.P.F. Nxumalo, Mr, J. Akinyelu, and Dr. M.P. Mokoena for their moral support and encouragement.
- Mr. P. Christopher for his assistance with the electron microscopy.
- National Research Foundation (NRF), for funding this research project
- My family, for their enduring support, encouragement, and love that made the completion of this thesis possible.

This thesis is dedicated to my family: my grandmother, Mandlovu: my late mother, Maphi: my aunt, Ntobifikile: my sister, Sphesihle and my cousins, Syabonga and Mangaliso

TABLE OF CONTENTS

Page

LIST OF TABLES

LIST OF FIGURES

CHAPTER 1

1. INTRODUCTION

1.1 Rationale/Background of Research

Over the years, a variety of gene delivery treatment modalities have been advanced to treat diseases at the genetic level. However, their clinical application has been limited by two factors viz. high toxicity and low transfection efficiency (Guo and Lee, 1999, Lungwitz *et al.*, 2005). While viral approaches have been very promising due to their high transfection efficiency, the inherent risks of carcinogenicity, insertional inactivation, severe immune responses, limitations in targeting specific cell types, and lack of ability to infect non-dividing cells have motivated for the development of safer non-viral approaches (Kay *et al.*, 2001, Thomas *et al.*, 2003, Ghosh *et al.*, 2008a). Even though non-viral vectors provide some benefits and are low in toxicity, their transfection efficiency is questionable and as a result, basic research in this area is ongoing.

Non-viral vector design based on organic materials, such as micelles, liposomes, and polymers, and have been intensively investigated for gene delivery and have been found to be associated with low to modest transfection efficiency (Xu *et al.*, 2007, Morille *et al.*, 2008). On the contrary, non-viral vectors derived from inorganic materials such as gold nanoparticles, quantum dots, selenium nanoparticles, silver nanoparticles, magnetic iron oxide nanoparticles, platinum nanoparticles and carbon nanotubes promise high transfection efficiency due to the numerous properties that they possess over organic-based non-viral vectors, and hence have recently emerged as favorable scaffolds for gene delivery (Pissuwan *et al.*, 2011, Rana *et al.*, 2012).

The interest in gold nanoparticles, for instance, has been stimulated by their capacity to bind a wide range of organic molecules, due to their rich surface chemistry, low level of cytotoxicity, unique tunable stability, robustness, ease of synthesis, biodegradability, biocompatibility and amenability to synthetic modification (Ghosh *et al.*, 2008a). Numerous studies have demonstrated the effectiveness of gold nanoparticles as plasmid DNA (pDNA) delivery vectors. In the early 2000s, Mclntosh and co-workers demonstrated that gold nanoparticles functionalised with quaternary ammonium and uncharged surface groups could effectively bind plasmid DNA and deliver it to 293T cells (McIntosh *et al.*, 2001).

In 2007, Bhattacharya and co-workers reported that gold nanoparticles functionalised with folic acid and polyethylene glycol-amines complexed with pDNA can be readily targeted to the folate receptors of cancer cells, with high efficiency (Bhattacharya *et al.*, 2007). Moreover, in 2008, Ghosh and co-worker conducted a study using gold nanoparticles functionalized with amino acids to delivery pDNA, which showed compact complexes that provided highly efficient gene delivery without any observed cytotoxicity (Ghosh *et al.*, 2008b). Since then, many studies have been conducted and reported by many research groups to confirm the versatility of gold nanoparticles as efficient gene delivery vectors *in vitro* (Sendroiu *et al.*, 2009, Giljohann *et al.*, 2009, Giljohann *et al.*, 2010, Kim *et al.*, 2011, Rana *et al.*, 2012). More recently, it was shown that gold nanoparticles conjugated to polymers polyethyleneimine, poly-L-lysine, chitosan and the amino acid cysteine were able to efficiently bind and deliver the pCMV-*Luc* DNA to mammalian cancer cells *in vitro* (Lazarus and Singh, 2016). Although the interaction of gold nanoparticles with pDNA has been a focus recently, the delivery of messenger RNA (mRNA) and small interfering RNA (siRNA) is still in its infancy and is yet to be fully exploited.

1.2 Significance/Justification and Novelty of Study

The field of 'nanomedicine' has the potential to dramatically improve the therapeutic outcomes in gene and drug-related therapies. Gold nanoparticles have been more frequently mentioned in nanomedical research than any other inorganic material. Furthermore, the conjugation of gold nanoparticles (AuNPs) to various macromolecules has gained popularity. Despite, the progress in research using AuNPs as delivery systems, they have yet to reach their full potential in the clinic.

The focus of this study was to optimize and enhance gold nanoparticles for efficient *in vitro* transgene expression using pDNA and mRNA, and gene silencing using small interfering RNA (siRNA). Furthermore, this study will compare and contrast the delivery efficiencies of the aforementioned nucleic acids using the same nanoparticle delivery systems in hope of shedding light on the design and formulation of novel non-viral delivery strategies with low cytotoxicity, efficient cellular uptake, and gene delivery.

1.3 Aim

The aim of this study was to evaluate and optimize the delivery efficiencies of functionalised gold nanoparticles for different nucleic acids *in vitro* to effect the required gene expression or silencing.

1.4 Objectives

- To synthesise and functionalise AuNPs with the appropriate polymer and targeting ligand.
- To determine the ultrastructural morphology, colloidal stability, size range, polydispersity, and *zeta* potential of all nanoparticles and nanocomplexes.
- To determine the nucleic acid binding and protection of all nanoparticles.
- To evaluate the cytotoxicity and apoptotic activity of the nanoparticles and their respective nanocomplexes in selected cancer cell lines.
- To determine the efficiency of the prepared functionalised AuNPs in gene delivery, expression, and silencing.

1.5 Outline of Thesis

The thesis is compiled in paper format, with chapters 3-5 presented as research papers.

- **Chapter 1** describes the background, novelty, aims, and objectives of the current study.
- **Chapter 2** provides an in-depth literature review on the research topic, including past and present utilization of AuNPs in gene delivery.
- **Chapter 3** describes the synthesis, formulation, characterisation and *in vitro* assessment of the nanoparticles and their nanocomplexes with plasmid DNA (pCMV-*Luc* DNA).
- **Chapter 4** investigates the formulated nanoparticles as nanocomplexes with F*luc* mRNA. All nanocomplexes and nanocomplexes were fully characterized and assessed *in vitro* for transgene expression.
- **Chapter 5** describes the complexation of siRNA with the nanoparticles. All nanocomplexes are characterised, with the cytotoxicity and luciferase gene silencing potential of the siRNA nanocomplexes in the HeLa-Tat-*Luc* cell line discussed.

- **Chapter 6** provides a conclusion and covers the significant results obtained from the study. Included are future studies that could be undertaken.

1.6 References

BHATTACHARYA, R., PATRA, C. R., EARL, A., WANG, S., KATARYA, A., LU, L., KIZHAKKEDATHU, J. N., YASZEMSKI, M. J., GREIPP, P. R. & MUKHOPADHYAY, D. 2007. Attaching folic acid on gold nanoparticles using noncovalent interaction via different polyethylene glycol backbones and targeting of cancer cells. *Nanomedicine: Nanotechnology, Biology and Medicine,* 3**,** 224-238.

CHOI, Y., MECKE, A., ORR, B. G., BANASZAK HOLL, M. M. & BAKER, J. R. 2004. DNA-directed synthesis of generation 7 and 5 PAMAM dendrimer nanoclusters. *Nano Letters,* 4**,** 391-397.

GHOSH, P., HAN, G., DE, M., KIM, C. K. & ROTELLO, V. M. 2008a. Gold nanoparticles in delivery applications. *Advanced drug delivery reviews,* 60**,** 1307-1315.

GHOSH, P. S., KIM, C.-K., HAN, G., FORBES, N. S. & ROTELLO, V. M. 2008b. Efficient gene delivery vectors by tuning the surface charge density of amino acid-functionalized gold nanoparticles. *ACS nano,* 2**,** 2213.

GILJOHANN, D. A., SEFEROS, D. S., DANIEL, W. L., MASSICH, M. D., PATEL, P. C. & MIRKIN, C. A. 2010. Gold nanoparticles for biology and medicine. *Angewandte Chemie International Edition,* 49**,** 3280-3294.

GILJOHANN, D. A., SEFEROS, D. S., PRIGODICH, A. E., PATEL, P. C. & MIRKIN, C. A. 2009. Gene regulation with polyvalent siRNA− nanoparticle conjugates. *Journal of the American Chemical Society,* 131**,** 2072-2073.

GUO, W. & LEE, R. J. 1999. Receptor-targeted gene delivery viafolate-conjugated polyethylenimine. *The AAPS Journal,* 1**,** 20-26.

KAY, M. A., GLORIOSO, J. C. & NALDINI, L. 2001. Viral vectors for gene therapy: the art of turning infectious agents into vehicles of therapeutics. *Nature medicine,* 7**,** 33-40.

KIM, D.-W., KIM, J.-H., PARK, M., YEOM, J.-H., GO, H., KIM, S., HAN, M. S., LEE, K. & BAE, J. 2011. Modulation of biological processes in the nucleus by delivery of DNA oligonucleotides conjugated with gold nanoparticles. *Biomaterials,* 32**,** 2593-2604.

LAZARUS, G. G. & SINGH, M. 2016. Cationic modified gold nanoparticles show enhanced gene delivery in vitro. *Nanotechnology Reviews,* 5**,** 425-434.

LUNGWITZ, U., BREUNIG, M., BLUNK, T. & GÖPFERICH, A. 2005. Polyethylenimine-based non-viral gene delivery systems. *European Journal of Pharmaceutics and Biopharmaceutics,* 60**,** 247-266.

MCINTOSH, C. M., ESPOSITO, E. A., BOAL, A. K., SIMARD, J. M., MARTIN, C. T. & ROTELLO, V. M. 2001. Inhibition of DNA transcription using cationic mixed monolayer protected gold clusters. *Journal of the American Chemical Society,* 123**,** 7626-7629.

MORILLE, M., PASSIRANI, C., VONARBOURG, A., CLAVREUL, A. & BENOIT, J.-P. 2008. Progress in developing cationic vectors for non-viral systemic gene therapy against cancer. *Biomaterials,* 29**,** 3477-3496.

PISSUWAN, D., NIIDOME, T. & CORTIE, M. B. 2011. The forthcoming applications of gold nanoparticles in drug and gene delivery systems. *Journal of controlled release,* 149**,** 65-71.

RANA, S., BAJAJ, A., MOUT, R. & ROTELLO, V. M. 2012. Monolayer coated gold nanoparticles for delivery applications. *Advanced drug delivery reviews,* 64**,** 200-216.

SENDROIU, I. E., WARNER, M. E. & CORN, R. M. 2009. Fabrication of silica-coated gold nanorods functionalized with DNA for enhanced surface plasmon resonance imaging biosensing applications. *Langmuir,* 25**,** 11282-11284.

THOMAS, C. E., EHRHARDT, A. & KAY, M. A. 2003. Progress and problems with the use of viral vectors for gene therapy. *Nature Reviews Genetics,* 4**,** 346-358.

TURKEVICH, J., STEVENSON, P. C. & HILLIER, J. 1951. A study of the nucleation and growth processes in the synthesis of colloidal gold. *Discussions of the Faraday Society,* 11**,** 55-75.

XU, P., VAN KIRK, E. A., ZHAN, Y., MURDOCH, W. J., RADOSZ, M. & SHEN, Y. 2007. Targeted Charge-Reversal Nanoparticles for Nuclear Drug Delivery. *Angewandte Chemie International Edition,* 46**,** 4999-5002.

CHAPTER 2

2 LITERATURE REVIEW

2.1 Introduction

"Golden therapy" has indeed revolutionized gene therapy over the years. The role that gold nanoparticles have played as delivery systems of therapeutic genes and drugs is commendable and has advanced cancer therapy tremendously over the years. This can be attributed to their unique optical and physicochemical properties such as inertness, low cytotoxicity and a rich surface platform that is amenable to synthetic modification. This review will provide the background of cancer, gene therapy, previously used gene and drug delivery systems, insight into the synthesis and functionalisation of gold nanoparticles for tailored biomedical applications, particularly, gene and drug delivery.

2.2 Cancer

Cancer is a global problem and one of the leading cause of deaths in developing countries. Annually, there are approximately 14 million new cancer cases that are reported worldwide with half of them resulting in death (Ferlay *et al.*, 2013).

Cancer is a disease characterised by uncontrolled growth and spread of abnormal cells. During normal cell growth and division, the genetic material (DNA) of the cells may be damaged or changed resulting in mutations, that lead to uncontrolled proliferation of abnormal cells, which ultimately form masses of tissues called tumours (benign or malignant) (Figure 2.1). Benign tumours do not invade nearby tissues or spread throughout the body (metastasize). They are uncommon and not harmful unless they grow in vital parts of the body such as nerves, blood vessels, or in confined areas such as the brain. Malignant tumours on the other hand, are invasive and metastasize causing havoc to the body (Martin *et al.*, 2013). There are many different types of cancers, each characterized by the type of cell that is primarily affected. Cancer is caused by both internal (e.g. genetic mutations) and external factors (e.g. infectious organisms, tobacco, and an unhealthy diet). Traditional cancer treatments including surgery, radiation therapy, hormone therapy and chemotherapy have proven to be inadequate in treating cancer as they either prolong the patient's life or result in severe side effects (Liu *et al.*, 2008).

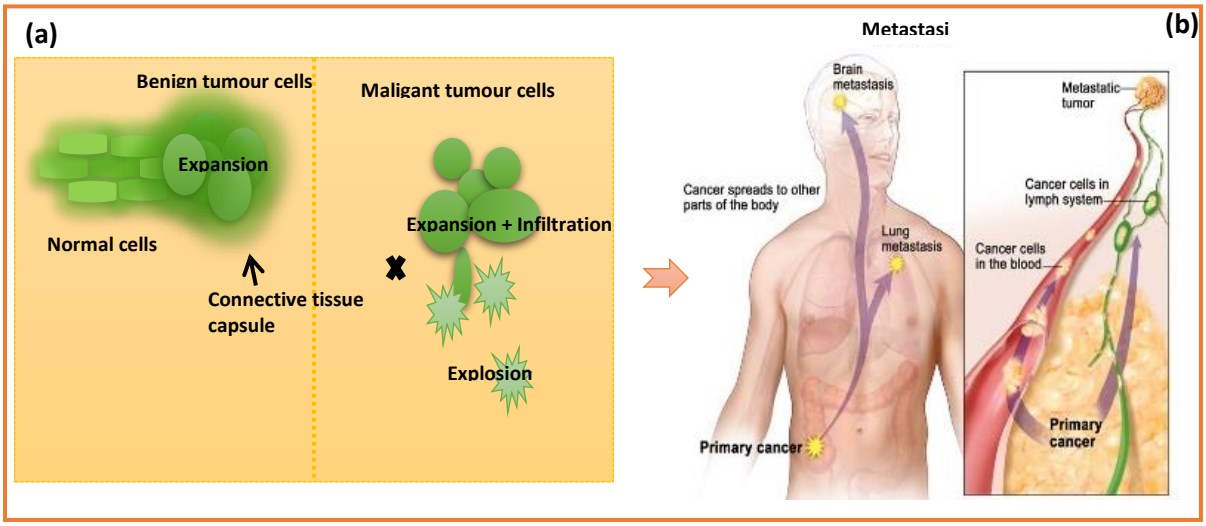

Figure 2.1: Illustration of benign and malignant tumours (a), and the process of metastasis (b). Adapted from https://www.cancer.gov/publications/dictionaries/cancer-terms?cdrid=46283, accessed on the 12th September 2016.

2.3 Gene Therapy: Alternative Approach

Gene therapy has emerged as a useful therapeutic approach for the treatment of cancer (Cho-Chung, 2005), and many other genetic and infectious disorders including haemophilia, cystic fibrosis (Davies *et al.*, 2001), acquired immune deficiency syndrome (AIDS) (Guo and Huang, 2012), muscular dystrophy, and familial hypercholesteremia (Ropert, 1999). Since Rosenberg and colleagues successfully conducted the first clinical application of human gene therapy in the early 1990s, more than 1500 gene therapy clinical trials have been conducted up to 2010 (Rosenberg *et al.*, 1990, Herzog *et al.*, 2010). Over 66% were for cancer treatment, 9.1% were for treatment of cardiovascular disorders, and 8.3% were for treating monogenic genetic diseases (Edelstein *et al.*, 2007). These statistics are indeed a testament of the ability of gene therapy to treat a broad range of inherited and acquired disorders. Gene therapy (Figure: 2.2) is based on the principle of correcting the basis of a disease at its origin by integrating new genes, replacing non-functional genes, or modulating gene expression in the cells (Müller-Reible, 1993).

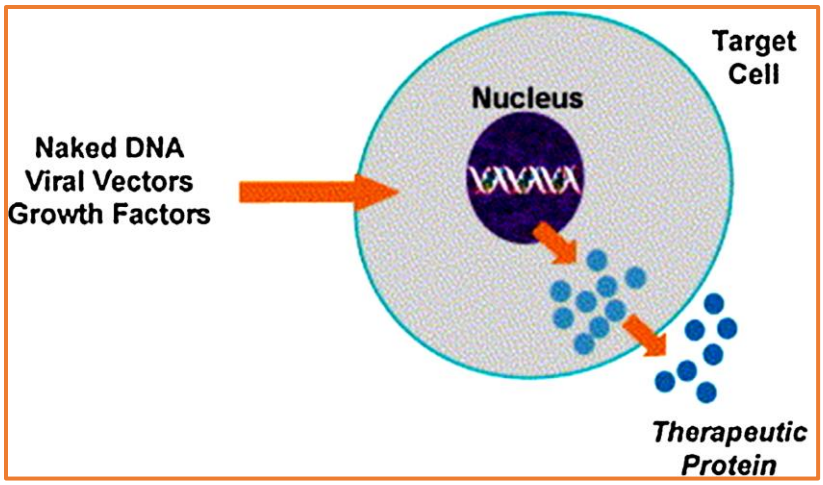

Figure 2.2: Illustration of the principle of gene therapy (Kendirci *et al.*, 2006).

Based on the nature of targeted diseased cells, this approach can be classified into two categories namely germline gene therapy and somatic gene therapy. Germline gene therapy involves correcting inherited genetic disorders by directly inserting the functional gene into the germ cells (reproductive cells). Due to moral, ethical and legal reasons, this method has been prohibited in humans and only allowed in lower level species such as mice (Katragadda *et al.*, 2010, Ibraheem *et al.*, 2014).

Somatic gene therapy, on the other hand, involves the introduction of functional genes into somatic cells (non-reproductive cells). The resulting genetic modifications are not hereditary and restricted to one generation. This approach is further grouped into *ex vivo*, *in situ*, *in vitro* and *in vivo* (Figure 2.3). *Ex vivo* (conducted outside the animal model) delivery involves the extraction of genes from specific tissues or cells, followed by their modification *in vitro*, and then transferred back into the original tissue or cells. This approach is limited by the small number of cells extracted from a specific living tissue. *In situ* involves direct delivery of delivery genes into the target tissue. This approach has been employed in treating cystic fibrosis but does suffer from poor transfection efficiency. *In vitro* (conducted in a tissue culture plate/system) and *in vivo* (conducted inside the animal model) involve the use of a vector that transports the gene to specific cells (Katragadda *et al.*, 2010). These methods are considered very useful in gene therapy, but, are limited by inadequate targeting of vectors to the correct tissue.

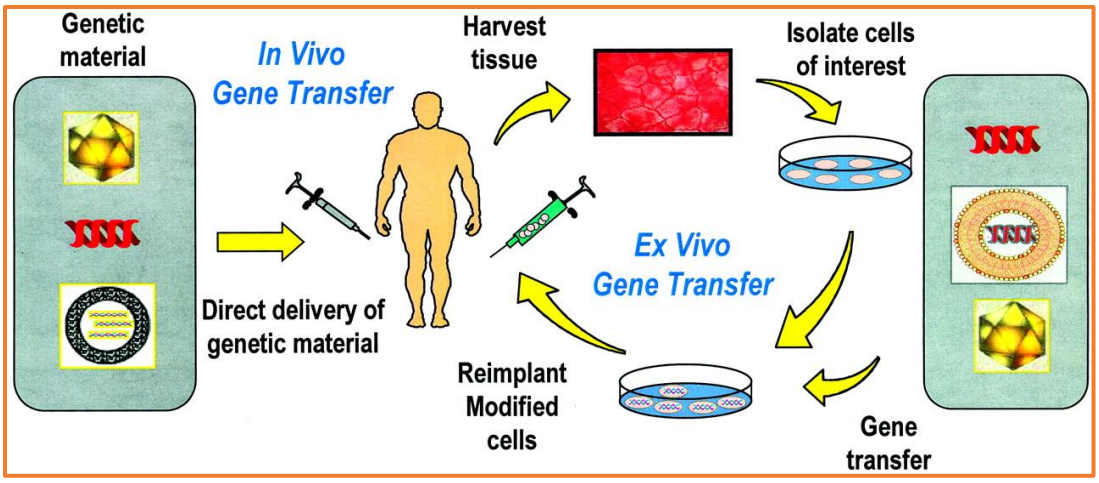

Figure 2.3: Illustration of *in vivo* and *ex vivo* gene transfer. Adapted from http://jasn.asnjournals.org/content/13/suppl_1/S117/F3.expansion, accessed on the 10/26/17.

2.4 Genes and Physiological Barriers

2.4.1 Genes

Several genes/genetic materials/nucleic acids have been used in gene therapy depending on the intended therapeutic effect. These include single-stranded DNA, double-stranded DNA, plasmid DNA (pDNA), messenger RNA (mRNA), antisense oligonucleotides, small interfering RNA (siRNA), micro RNA (miRNA), and small hairpin RNA (shRNA) (Knipe *et al.*, 2013). Based on the scope of this study, we will provide a brief background on pDNA, mRNA, and siRNA.

2.4.1.1 Plasmid DNA

Plasmid DNA (pDNA) (Figure 2.4) is a circular double-stranded deoxyribonucleotide (dsDNA), ranging from 100-1000 base pairs in length and is derived from plasmids of eukaryotic cells (Yin *et al.*, 2005). It produces usable proteins by transcription into messenger RNA, which is, in turn, translated into desired proteins. pDNA contains four main domains e.g. a promoter, enhancer, polyadenylation, and splicing sites which regulate gene expression as well as the transgene that encodes for a specific protein. Promoters initiate transcription by recognizing RNA polymerase and are normally derived from viruses e.g. roux sarcoma virus and cytomegalovirus (CMV), to guarantee high transcription. Enhancers are situated upstream or downstream from the promoter and they improve transcription efficacy by enhancing the binding of proteins that initiate gene transcription.

Polyadenylation and splicing sites ensure correct processing of the mRNA transcript (Elsabahy *et al.*, 2011). Additionally, pDNA has transcription termination sites as well as antibiotic resistance genes. Due to it structural stability, pDNA is extensively used in gene expression studies, especially *in vitro*. However, difficulty in production, inability to transfect non-dividing cells, possible insertional mutagenesis due to integration into the host genome, possible immune responses owing to the unmethylated CpG motifs, and restricted nuclear entry due to its relative large size have limited its *in vivo* application.

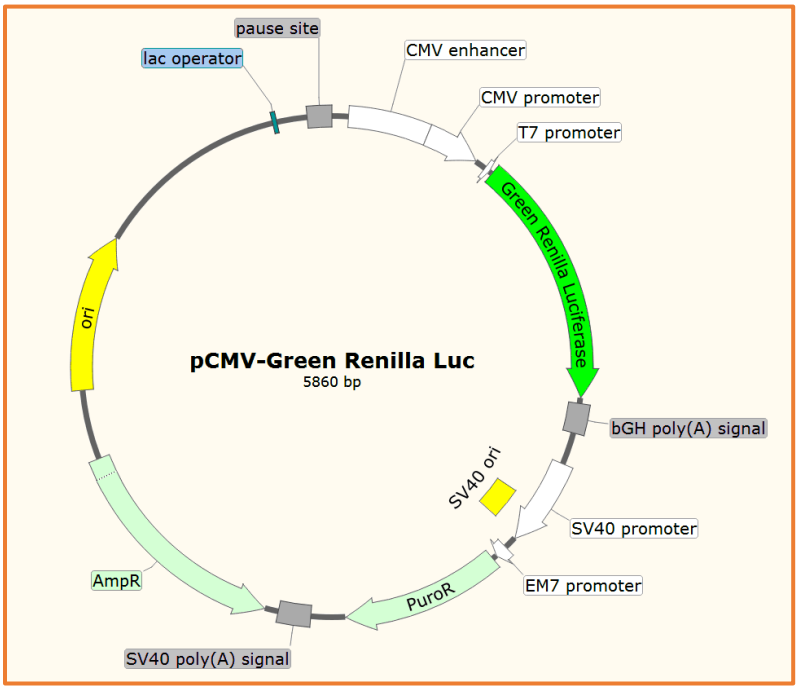

Figure 2.4: Structure of pDNA containing a Green Renilla Luciferase (Luc) gene under the control of CMV promoter. Lac operator (Lac 01) and Transcription termination site (Ter) reduce background by minimizing transcriptional read-through. Ampicillin (Amp) and puromycin (Pur) are markers for drug selection in bacterial and mammalian cells respectively. Adapted from http://www.biofeng.com/zaiti/buru/pCMV-Green-Renilla-Luc.html, accessed on the 10/26/17.

2.4.1.2 Messenger RNA (mRNA)

Mature mRNA is a single-stranded RNA (ssRNA) that transfers genetic material from DNA to ribosomes found in the cytosol of eukaryotic cells, where it acts as a template for protein synthesis. It undergoes extensive processing (Figure 2.5) before it is transported into the cytosol. It comprises five main domains, including a 5' cap (e.g. m7Gp3G), a 5' untranslated region (UTR), an open reading frame (ORF)/protein coding sequence (PCS), a 3' untranslated region (UTR), and a poly (A) tail of adenosine residues (100–250), which ensures proper protein synthesis (Yamamoto *et al.*, 2009). The cap aids in the attachment of mRNA to the ribosome. The 5' UTR is a region before the start codon that is responsible for the stability, localization and translation efficiency of mRNA. The ORF/PCS comprise of start and stop codons that regulates mRNA translation into protein by the ribosomes. The 3' UTR is a region after the stop codon that is responsible for the stability, localization and translation efficiency of mRNA. The poly (A) tail stimulates mRNA transfer from the nucleus to the cytosol (where translation occurs) and stabilizes mRNA by shielding it from enzymatic degradation (Sioud, 2010).

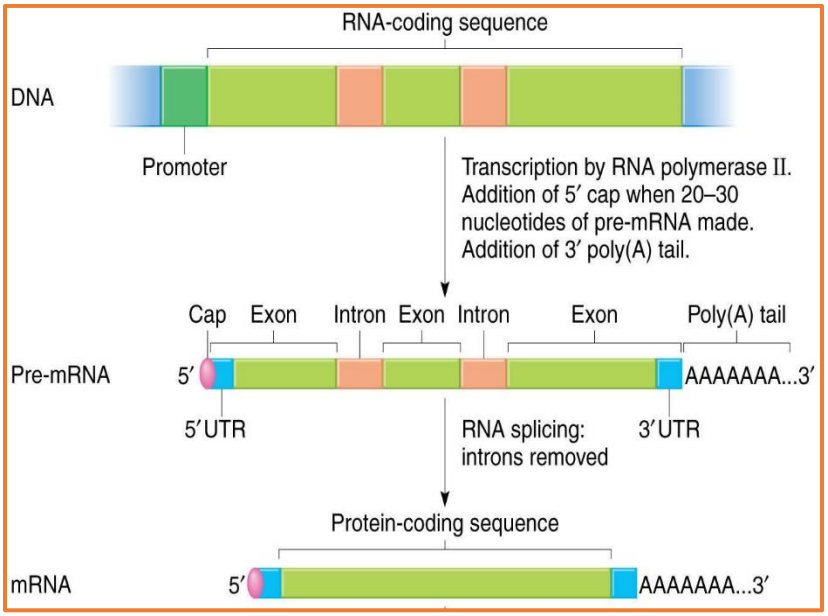

Figure 2.5: Illustration of eukaryotic mRNA structure and processing process from DNA (Russel, 2010). Exons are coding/expresses DNA sequences. Introns are non-coding/suppressed DNA sequences.

Synthetic/functional mRNA, therefore, can be derived from pDNA with a bacteriophage promoter e.g. T7, SP6, or T3 through *in vitro* transcription and is produced without a cap and a poly A tail (Tavernier *et al.*, 2011). It has seldom been used in gene expression studies due to its instability caused by the lack of a cap and a poly A tail. However, its ease of production, ability of transfecting both dividing and non-dividing cells, non- toxicity (does not integrate into the genome), and delivery into cytoplasm (nuclear membrane not a barrier) makes it ideal over pDNA.

2.4.1.3 Small Interfering RNA

Small (or short) interference RNA (siRNA) (Figure 2.6) is commonly used to mediate gene silencing/knockdown via a gene regulatory mechanism that takes place in the cytoplasm of various eukaryotic cells, known as RNA interference (RNAi). SiRNA is a double-stranded/duplex RNA that is synthetically formulated using solid-phase synthesis approaches, to target a specific mRNA for degradation. This duplex consists of a guide/antisense strand and a passenger/sense strand which ranges from 19-22 bp in size, with distinctive 3' dinucleotide overhangs that permits recognition by the RNAi (Elsabahy *et al.*, 2011). Moreover, siRNA transfection into a specific cell usually involves the loading of the guide strand into RNA-induced silencing complexes (RISC). This complex then stimulates gene silencing by binding, cleaving and degrading the complementary strand of the target mRNA. Like mRNA, siRNA is easy to produce, relatively small, non-toxic, and is delivered into the cytoplasm avoiding the nuclear membrane barrier. However, its application is limited by transient gene silencing which leads to time-restricted experiments (Banan and Puri, 2004).

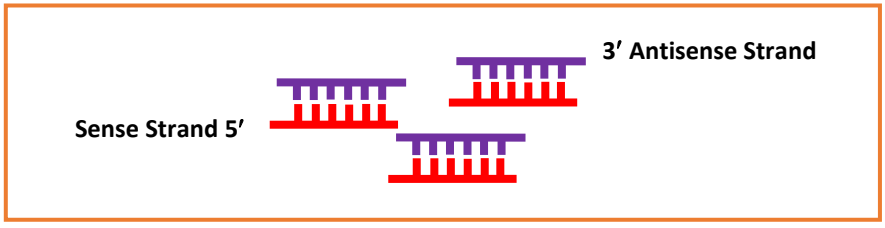

Figure 2.6: General structure of siRNA duplexes.

2.4.2 Physiological Barriers

The direct introduction of naked genes, into diseased cells is associated with unsatisfactory gene expression/silencing due to a number of extra-and intracellular physiological barriers that the gene encounters on its way to the target site, which ultimately affects its cellular biodistribution and bioavailability.

2.4.2.1 Low Intracellular Bioavailability

Subsequent to introduction, the naked DNA/RNA is quickly degraded by extra and intracellular enzymes before it even reaches the target site, resulting in a compromised therapeutic outcome due to low bioavailability. Also, due to the hydrophilicity and enormous size of genes, their cellular uptake is usually limited. However, the little that can be absorbed by cells are done so via a process known as endocytosis. During this process, genes are internalized into vesicles known as endosomes, which are later converted into lysosomes, where they are subsequently degraded by lysozymes. This degradation prevents the genes from reaching the target sites e.g. cytoplasm (RNA) or nucleus (pDNA).

2.4.2.2 Limited Nuclear Uptake

In order for gene expression to take place, some genes e.g. pDNA must be translocated to the nucleus. The nuclear translocation of genes is a procedure that involves both nuclear trafficking and nuclear membrane penetration. The nuclear membrane is impermeable and comprises of a nuclear pore complexes (NPC), of approximately 25 nm in size, which regulates the transport of biomolecules entering and exiting the nucleus (Liu *et al.*, 2003). Generally, biomolecules less than 40 kDa diffuse passively through the membranes, while larger biomolecules are impeded (Roth and Sundaram, 2004). Hence, the nuclear uptake of pDNA is limited by its enormous size and charge diminishing its therapeutic effect.

2.4.2.3 Induction of Cytokines

Foreign/exogenous genes (e.g. DNA/RNA) usually stimulate and activate the immune system, which in turn triggers the release of cytokines which are capable of inducing inflammatory responses. The mechanism that is responsible of inducing inflammatory cytokine release is known as the Toll-like receptor (TLR), and possess four main receptors including TLR3, TLR7, TLR8 and TLR9, which recognizes nucleic acids or structures that resemble nucleic acids (Yoshida *et al.*, 2009). TLR3, recognizes dsRNA e.g. siRNA, whereas TLR7 and TLR8 recognizes single-stranded RNA e.g. mRNA. TLR9 on the other hand only recognizes the sequences in the pDNA that stimulate immune response (e.g. unmethylated CpG motifs) (Sioud, 2010). Such motifs are frequently found in bacterial DNA rather than in mammalian DNA, which explains the strong immune responses that are associated with the application of bacterial DNA *in vivo*.

2.4.3 Overcoming the Barriers

The successful application of gene therapy greatly relies on the delivery of the therapeutic gene into the targeted cell with little to no degradation. Consequently, several methods have been explored to improve the bioavailability of genes, including the chemical modification of the structure of genes, and encapsulation of genes into delivery modalities/vectors/systems. Chemical modification is a very effective approach in reducing cytotoxicity while increasing the stability of nucleic acids. It involves the removal of toxic motifs, in the case of pDNA (Krieg *et al.*, 1995), and addition of stable compounds e.g. pseudouridine (Ψ-mRNA), 2-thiouridine, and 5-methylcytidine in the case of mRNA (Tavernier *et al.*, 2011). However, this approach is difficult, expensive and time-consuming and hence its application is limited. Chemical encapsulation, on the other hand, is a simple, cheap, and very effective approach of protecting therapeutic genes from enzymatic degradation, by encapsulating them into delivery modalities.

2.5 Delivery Modalities

An ideal gene delivery modality must fulfill a number of standards (Somia and Verma, 2000):

- It must be easy to prepare, and inexpensive.
- It must be non-toxic (should not trigger any strong immune response).
- It should be biocompatible and biodegradable.
- It must have a large carrying capacity (able to carry genes of all size).
- It must be able to shield and protect the exogenous gene from degrading extracellular and intracellular enzymes.
- It must ensure stable gene expression or silencing.
- It must infect both non-dividing and dividing cells.
- It must be small and specific enough to be transfected into the into the target site for specific uptake of the exogenous gene.

2.5.1 Viral Modalities

In the last decade, viral modalities have advanced greatly at delivering genes, due to their ability to protect and deliver the genes to specific cells, while evading immunologic detection by an infected host. These modalities are well-known biological products derived from modified viruses (Merten and Gaillet, 2016). Viral modification involves the removal of pathogenic genes, with the most widely studied modified viruses being retroviruses, lentiviruses, adenoviruses, herpes simplex viruses (HSV), adeno-associated viruses (AVV) and poxviruses. The retroviruses were the first to enter clinical trials in the early 1990s and were commercialized because of their remarkable high gene efficacy. These viruses possess unique advantages and limiting properties (Figure 2.7), which need to be considered before their application in gene delivery. In general, viral vectors are excellent gene transfection agents, as evidenced by their associated high transfection efficiency. However, due to limited scale-up techniques (production is expensive) and severe biosafety issues such as insertional mutagenesis, immunogenicity, and carcinogenesis, other safe alternatives such as non-viral modalities have been developed (Jin *et al.*, 2014a).

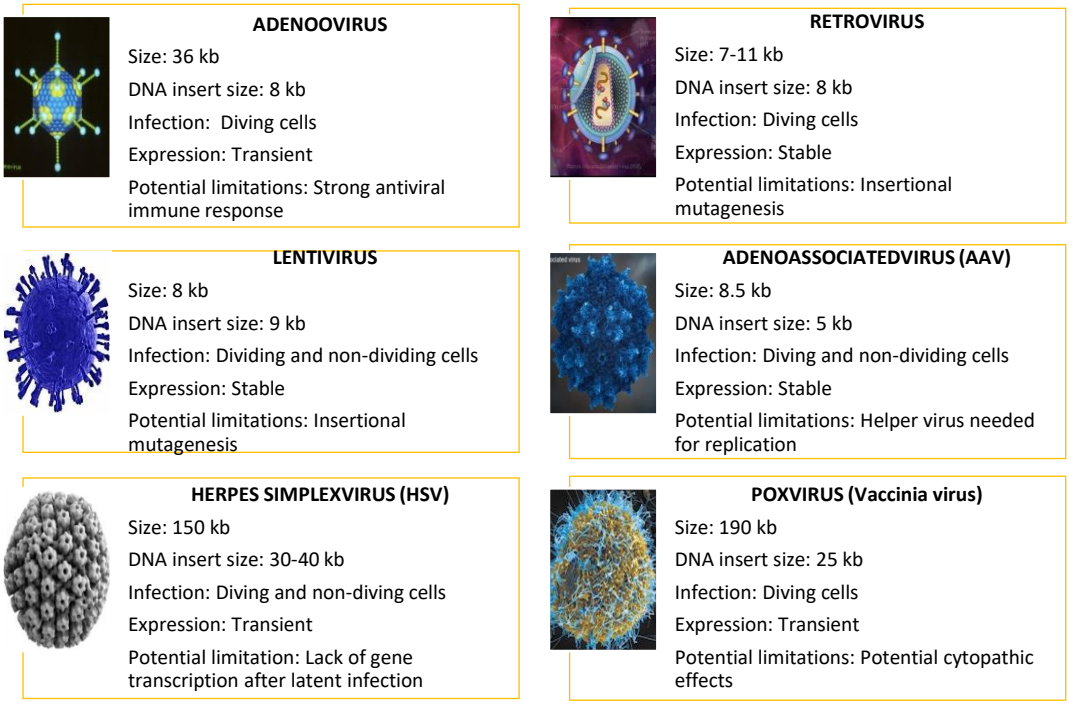

Figure 2.7: Summary of different advantages and limitations of viral vectors which are currently studied and employed in gene therapy (Katragadda *et al.*, 2010).

2.5.2 Non-Viral Modalities

Non-viral modalities present attractive advantages over inherently toxic viral modalities, although not as highly efficient in gene delivery. These synthetic vectors can be produced on a large-scale, are cheap, less toxic, non-immunogenic, biodegradable, biocompatible, possess an unlimited DNA carrying capacity, and can be modified synthetically to enhance gene transfection efficiency (Yin *et al.*, 2014). They can be divided into physical and chemical approaches.

Physical approaches applies physical force to aid in the transfer of the exogenous gene through the cell membrane. Though this approach is easy to perform, its application is limited by potential cell membrane damage and the number of cells that can be treated. Examples of physical approaches include; electroporation, microinjection, gene gun, ultrasound, magnetofection, photo-chemical internalization, occlusion, hydrodynamic injection, laser irradiation, hyperthermia (Balazs and Godbey, 2010). The **chemical approach** conversely, uses inorganic or organic chemicals to complex the gene via electrostatic interaction, forming nanocomplexes that protect the gene against degrading enzymes but are small enough to extravasate the cell membrane without causing any physical damage (Chuang and Chang, 2015).

2.5.2.1 Inorganic Non-viral Modalities

2.5.2.1.1 Cationic Lipids (CLs)

CLs represent the largest group of non-viral vectors that have been extensively studied and used in gene therapy for the last three decades. In the early 1980s, Felgner and co-workers discovered that when the cationic lipid, N[1-(2,3 dioleyloxy) propyl]-N,N,N-trimethylammonium chloride (DOTMA) was mixed with a neutral fusogenic phospholipid such as dioleoyl-phosphatidylethanolamine (DOPE), it spontaneously formed uniform, small liposomes that were able to complex, protect and deliver DNA to a variety of mammalian cells with high efficiency. Later studies produced the formulation, evaluation and commercialization of various other cationic lipids including; 1,2-dioleyl- 3 trimethylammonium propane (DOTAP), N-(2-hydroxyethyl)-N,N-dimethyl 2,3-bis(tetradecycloxy-1-propanaminium bromide (DMRIE), N,N,N-trimethylammonium chloride (DOSPA); dioctadecylamido- glycylspermine (DOGS), 1,2-Distearoyl-*sn*-glycero-3-phosphorylcholine (DSPC), DC-Cholesterol (DC-Chol), DOTIM (Figure 2.8).

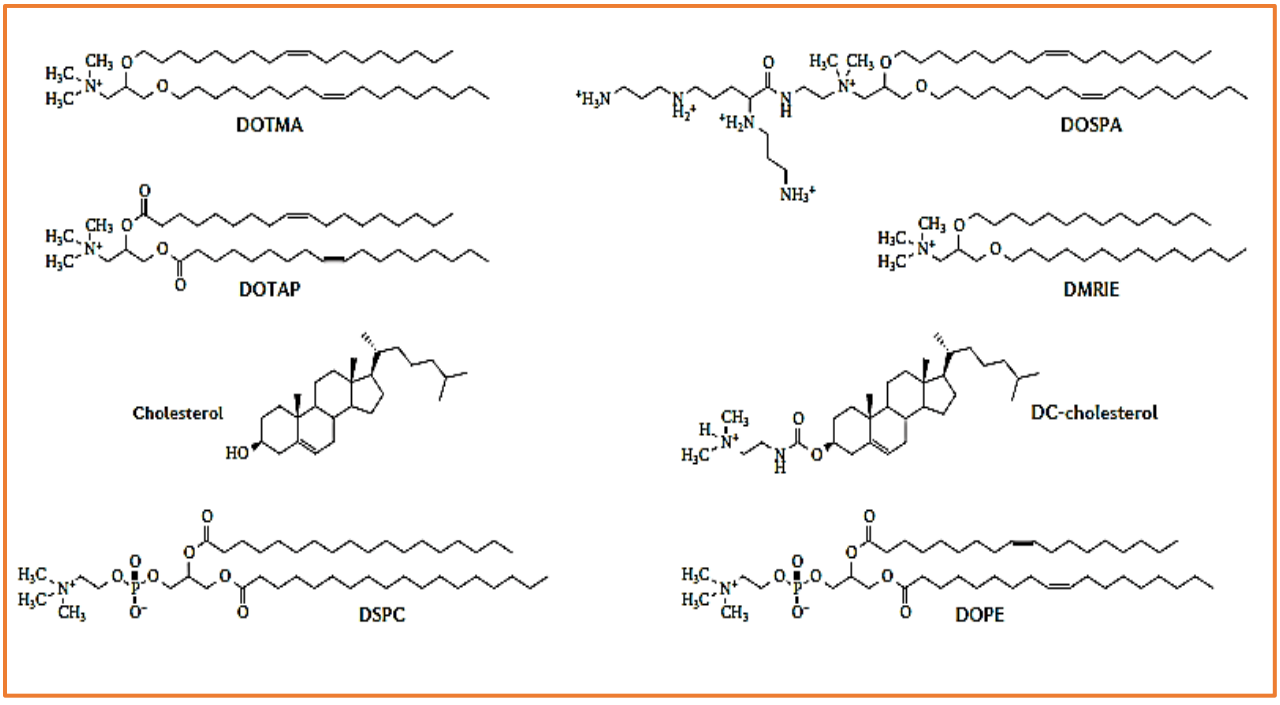

Figure 2.8: Chemical structures of commonly used cationic lipids (Yin *et al.*, 2014).

CLs are amphiphilic systems that are structurally characterized by three functional components namely; a hydrophilic cationic head group, a linking group, and a hydrophobic tail (Junquera and Aicart, 2014). The hydrophilic cationic head group generally contains either a polyamine or tertiary amine ligand or an ammonium group, which binds with the phosphate groups of nucleic acids. The linking groups or arms in lipids are of various lengths and have specific bonds, such as ester, ether, phosphate, amine, carbamate or disulfide bonds, which bridge the cationic head and the tail, controls stability, flexibility, biodegradability and most importantly, transfection efficacy. The hydrophobic tail group contains either sterol rings such as cholesterol or lipid chains such as multivalent or monovalent aliphatic hydrocarbons which facilitates bilayer vesicle (micelles or liposomes) formation in aqueous solutions. CLs mixed with a helper/neutral/fusogenic phospholipid such as DOPE, dioleoylphosphatidyl choline (DOPC) or the membrane component cholesterol, form spherical unilamellar or multilamellar vesicles (20 nm to > 0.5 µm), called liposomes which bind and compact nucleic acids via electrostatic interactions (Figure 2.9), forming lipoplexes, capable of interacting with the cell membrane and delivering the nucleic acid without any immune response (Mintzer and Simanek, 2008, Junquera and Aicart, 2014).

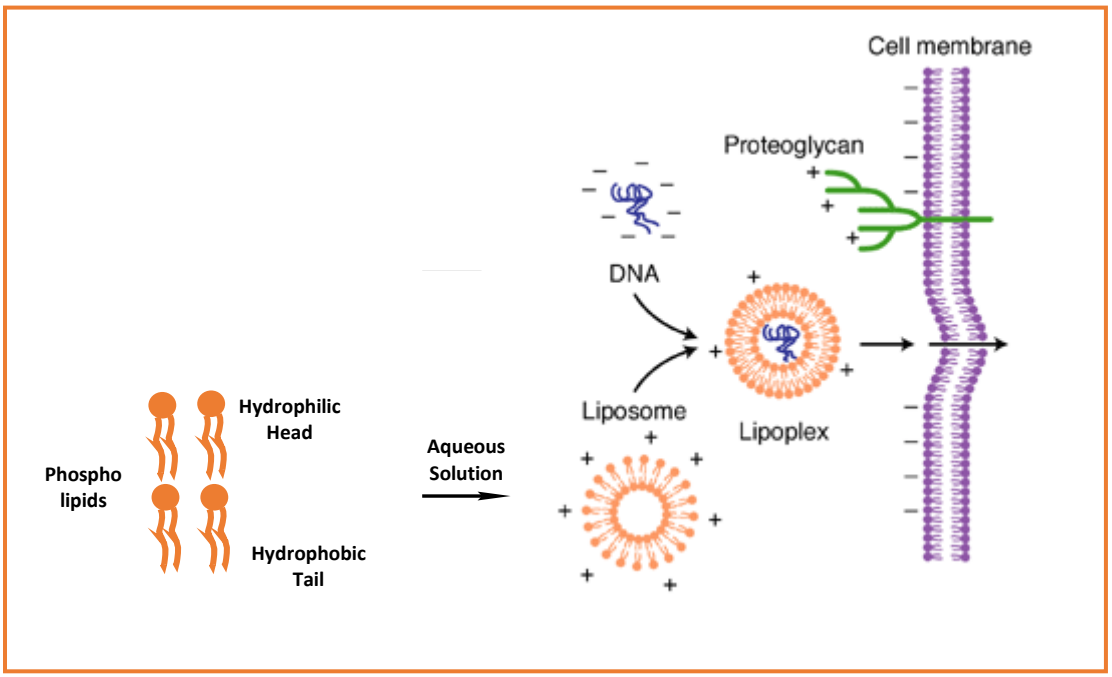

Figure 2.9: Liposome formation via phospholipid assembling and lipoplex formation via electrostatic interaction. Adapter from (Parker *et al.*, 2003) with modifications.

Liposomes are distinctly biodegradable, biocompatible, soluble, reproducible, non-immunogenic, and are amenable to synthetic modification. They possess a large gene/drug carrying capacity, are easy to handle and prepare. However, due to their poor stability, liposomes may experience non-specific binding with negatively charged extra- or intracellular constituents (e.g. serum degrading enzymes and proteins), which may lead to rapid clearance, hence resulting in low transfection efficacy. Additionally, the harmful organic material (e.g. chloroform) that is used to prepare liposomes may potentially cause some cytotoxicity or inflammatory/anti-inflammatory responses, limiting their clinical application. Recently, a phase III clinical trial study conducted to treat metastatic melanoma using allovectin-7-DMRIE-DOPE and pDNA failed due to low efficacy. Nevertheless, several liposomal formulations such as GL67A-DOPE-DMPE-polyethylene glycol, GAP-DMORIE–DPyPE, and DOTAP–cholesterol are still being clinically developed (Junquera and Aicart, 2014).

2.5.2.1.2 Cationic Polymers (CPs)

CPs are also non-viral vectors that have been evaluated in gene delivery studies due to their chemical diversity, which allows for various synthetic modifications. They bind nucleic acids via electrostatic interaction, through their ammonium ions and/ or amines forming polyplexes. The size and morphology of the complex is usually dictated by the number of phosphates in the nucleic acid and the number of amine groups in the vector, known as the N/P ratio. Polyplexes have shown low cytotoxicity, good biodegradability, excellent buffering capacity, structural diversity and reasonably high transfection efficacy compared to lipoplexes (Jin *et al.*, 2014a). Various polymers that have been used in gene therapy, and can be categorized into two groups, namely natural polymers e.g. peptides, proteins, polysaccharides (chitosan), and synthetic polymers e.g. poly (ethyleneimine) (PEI), poly (L-lysine) (PLL), poly (d,l-lactide-co-glycolide) (PLG), and dendrimers (Xun *et al.*, 2014) (Figure 2.10). Among them, poly (L-lysine) (PLL), polyethyleneimine (PEI), polyamidoamine dendrimer (PAMAM), and chitosan are currently the most commonly used with PEI and PAMAM being more frequently applied.

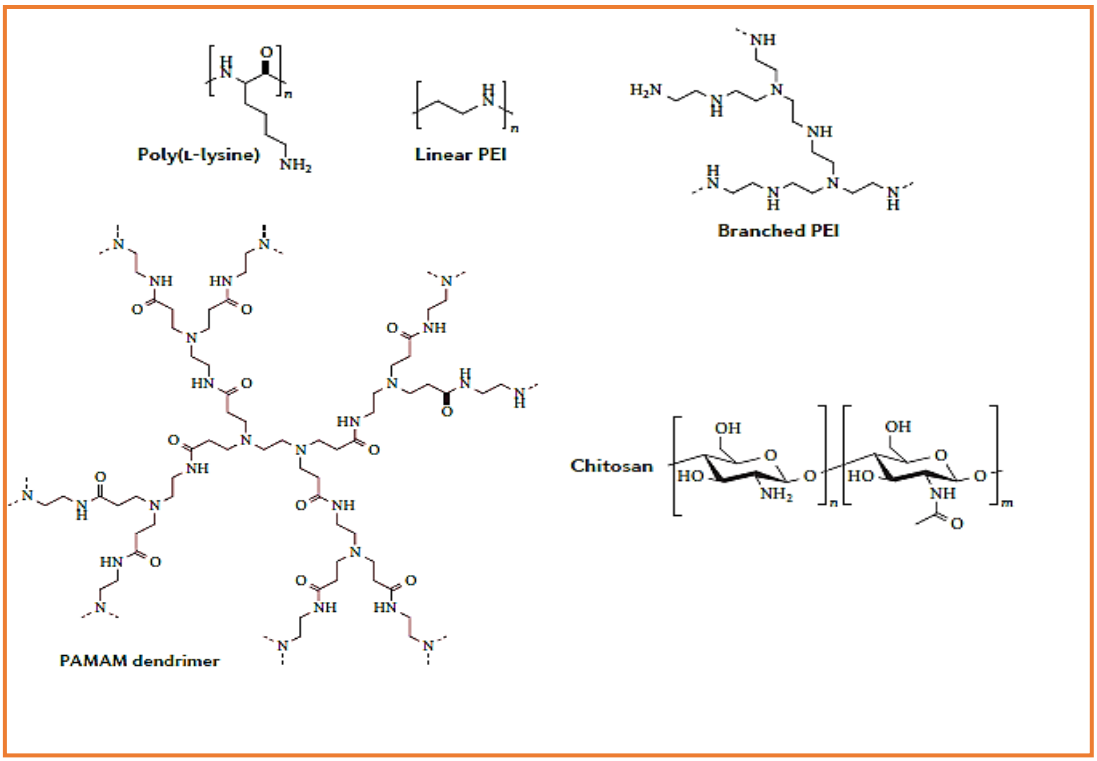

Figure 2.10: Chemical structures of cationic polymers (Yin *et al.*, 2014).

2.5.2.1.2.1 Chitosan

Chitosan has been one of the most widely used natural cationic polymers in both drug and gene delivery applications. This is mainly due to its outstanding biodegradability, excellent biocompatibility, non-toxicity (even at high concentrations and at all molecular weights), low immunogenicity, antimicrobial activity, ease of synthetic modification and abundance in nature (Yin *et al.*, 2014). However, due to their low charge, insolubility under physiological conditions, and low transfection efficiency, its application in gene therapy has been limited. Chitosan-DNA nanocomplexes, are easy to formulate, but have been associated with poor transfection efficiency in some cell lines. It has been suggested that this could have been due to factors such as the chitosan molecular weight (MW), degree of deacetylation, polyplex physicochemical properties, and the N/P ratio. Consequently, various chitosan derivatives have been employed to formulate nanocomplexes to improve transfection efficiency (Katragadda *et al.*, 2010). These include chitosan methoxy polyethylene glycol-cholesterol 20 (LCP-Ch), thiolated-chitosan, low molecular weight alkylated chitosan, and aminoethyl- chitin (ABC).

Chitosan has also been conjugated to folic acid (FA) for targeted delivery and to improve transfection efficiency (Mansouri *et al.*, 2006). The greatest successful application of chitosan/DNA nanocomplexes has been seen in oral and nasal therapy, due to chitosan's mucoadhesive nature. Currently, the development of chitosan-based gene delivery modalities involves the use of chitosan derivatives or chitosan in combination with other nanoparticles (Unsoy *et al.*, 2012).

2.5.2.1.2.2 Poly (ethylenimine) (PEI)

PEI (linear and branch form), is another interesting polycation that has been extensively studied in gene delivery over the years. Its capacity to aid gene transfection both *in vitro* and *in vivo* was initially demonstrated in 1995 (Boussif *et al.*, 1995). PEI has a high charge density and a high buffering capacity that enables it to bind with nucleic acids and facilitate endosomal escape through a process known as the "proton sponge effect" (Figure 2. 11). Due to its compacting and buffering capacities, transfection efficiency is satisfactory and is comparable to that of viral vectors (Katragadda *et al.*, 2010). Studies have suggested a strong dependency of the polyplex structural and physicochemical properties (e.g. MW, N/P ratio and morphology), on the transfection efficiency and cytotoxicity.

For instance, PEI-DNA polyplexes designed with high MW PEI (e.g. 25 kDa), at high N/P ratios are associated with high *in vitro* transfection, while, PEI-DNA polyplexes designed with low MW PEI are associated with low cytotoxicity and poor transfection efficiency. Furthermore, the clinical application of PEI polyplexes is limited due to their non-biodegradability and associated high cytotoxicity as a result of their high positively charged density.

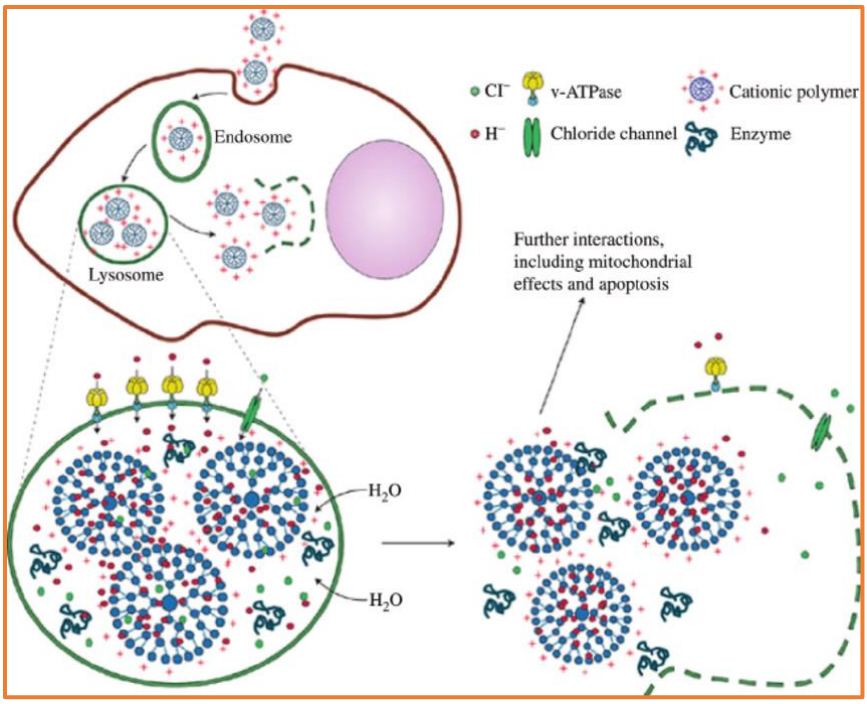

Figure 2.11: Illustration of the "proton sponge effect" (Meng Lin *et al.*, 2010).

Over the years, various PEI/PEI polyplex structural modifications or physicochemical properties including pegylation, alkylation, methylation, and acetylation have been studied to improve their stability, biocompatibility, reduce toxicity and improve transfection efficacy (Petersen *et al.*, 2002, Thomas and Klibanov, 2002, Neu *et al.*, 2005, Lv *et al.*, 2006, Fortune *et al.*, 2011). Currently, lipopolymer, PEG-PEI–cholesterol is being clinically investigated for immunotherapy (cytokine interleukin-12 (IL-12) expression) of colorectal and ovarian cancers (Yin *et al.*, 2014).

2.5.2.1.2.3 Dendrimers

Dendrimers are among the polymers that have been widely studied for numerous biomedical applications, specifically, as delivery vectors of anticancer drugs due to their unique properties. The name dendrimer can be broken down into Din =Greek, Dendron= tree and meros = branch. Hence by definition, dendrimers are globular-tree like, branched, nano-sized (1–100 nm), three-dimensional macromolecules with a well-defined size, structure, and multiple surface functional groups that are either neutral, negative, or positively charged (Xu *et al.*, 2013, Kompella *et al.*, 2013).

They can be easily synthesized by the polymerization method (Luten *et al.*, 2008, Yamano *et al.*, 2010), which originates from an inner core and then grows in layers or generation number (Gn), with the systematic addition of amine groups producing a branch-like structural architecture comprising three main domains namely; an inner or central core; a hyperbranched layer; and surface multivalent functionalities. These components collectively facilitate unique interactions with tissues, maintain structural integrity, encapsulate or entrap various biomolecules such as drugs, genes, antibodies, and targeting moieties for biomedical applications (Honda *et al.*, 2013, Chaplot and Rupenthal, 2014). The tunability of the structural architecture of dendrimers makes them virtually perfect gene and drug delivery vectors with predictable features (Kannan *et al.*, 2014).

To date, more than 100 architecturally different dendrimers have been formulated and exploited in gene and drug delivery (Bravo-Osuna *et al.*, 2016). Amongst these, polyamidoamine (PAMAM) has been the most widely studied, characterized and commercialized since its early discovery by Haensler and Szoka Jr, (1993). This can be attributed to their unique features including excellent solubility, high loading ability, non-immunogenicity, tunable size, defined structure, mono-dispersity, and rich surface functionalities (amine groups, NH_2), which are amenable to synthetic modification (Kompella *et al.*, 2013, Chaplot and Rupenthal, 2014). PAMAM dendrimers possess surface cationic primary (1^o), and tertiary (3^o) NH_2 groups which are protonated at physiological conditions, an intrinsic feature that enables them to bind with and condense nucleic acids to form highly soluble and stable nanocomplexes. These nanocomplexes enhance the cellular uptake of the nucleic acid, and aid in its release from the endosome by destabilizing the endosomal membrane through the "proton sponge effect" (Kesharwani *et al.*, 2015).

However, there are still challenges that need to be addressed regarding the use of these polymers as drug and gene delivery vectors. Firstly, in spite of the fact that some PAMAM dendrimers such as Priofect and Superfect are commercially available, their high-cost and laborious production are still issues (Killops *et al.*, 2008). Secondly, the cytotoxicity and transfection efficiency of these polymers is generation-dependent, and hence said to be influenced by the surface amines of these polymers. For instance, low-generation (LG) PAMAM, e.g. G0-G3 display low gene transfection efficacy with low cytotoxicity, while high-generation (HG) PAMAM, e.g. G4-G8 display high gene transfection efficacy with high cytotoxicity (Shah *et al.*, 2011, Liu *et al.*, 2012, Pan *et al.*,

2013). Hence, an ideal gene delivery vector must exhibit both high transfection efficacy and low cytotoxicity (Kim *et al.*, 2006, Nakhlband *et al.*, 2010).

Many studies have shown that modifying the surface amines of dendrimers by pegylation, methylation, acetylation, etc., greatly increases their biocompatibility and decreases their toxicity (Villanueva *et al.*, 2016). Liu *et al.* formulated a disulfide cross-linked LG PAMAM dendrimer for gene delivery, that exhibited low cytotoxicity and increased transfection efficiency, comparable to that of the PEI (25 kDa), but greater than that of the G2 and G5 PAMAM dendrimers (Liu *et al.*, 2012). Arima *et al.* synthesized a cyclodextrin-modified LG PAMAM dendrimer for gene delivery which exhibited low cytotoxicity and reasonably high gene transfection efficacy (Wada *et al.*, 2005, Arima *et al.*, 2010). Nam *et al.* formulated an arginine-modified PAMAM dendrimer for gene delivery which displayed significant transfection efficiency and low cytotoxicity from G2-G4 (Nam *et al.*, 2008). Patil *et al.* synthesized a surface-acetylated internally quaternized G4 PAMAM dendrimer for siRNA delivery, which showed reasonable gene silencing and low cytotoxicity in A2780 ovarian cancer cells (Patil *et al.*, 2008). Likewise, in another study conducted by Patil *et al.* a tri-block complex (PAMAM-PEG-PLL) G4-PAMAM-dendrimer efficiently delivered siRNA with low cytotoxicity in human plasma (Patil *et al.*, 2011).

Alternatively, other studies have reported on the modification of the dendrimer core instead, which increases the flexibility of the dendrimer, which in turn increases its nucleic acid binding capability. For example, Aydin *et al.* synthesized a partially degraded Jeffamine-cored PAMAM dendrimer (JCPD) for gene delivery, which displayed low cytotoxicity and significantly higher transfection efficiency (Aydin *et al.*, 2012). Lastly, the transfection efficiency of some dendrimers is cell type dependent, which may be attributed to the many architecturally different dendrimers that exist and various structures of cell types (Bhakta *et al.*, 2009, Jin *et al.*, 2014b).

Issues regarding cost, production and transfection efficiency associated with these vectors, has led to the use of non-viral vectors formulated with inorganic materials to try and resolve these issues (Edinger and Wagner, 2011, Ibraheem *et al.*, 2014).

2.5.2.2 Organic Non-Viral Vectors

Organic non-viral vectors provide an alternative over inorganic non-viral vectors. They are low in toxicity and are capable of enhancing gene transfection due to the properties that they possess, including small or "nano" size, robustness, large drug and gene carrying capacity, enhanced cell binding affinity, and robustness. The most frequently researched metal nanoparticles include magnetic nanoparticles, quantum dots, silver, and gold (Tiwari *et al.*, 2011).

2.5.2.2.1 Magnetic Nanoparticles (MNPs)

MNPs show great promise as suitable drug and gene delivery vectors, and much effort is now being dedicated in their advancement (Katragadda *et al.*, 2010). These are metal clusters that operate under an external magnetic field which can be directed to target a specific tissue and be removed upon completion of therapy. This is vital in gene therapy and can significantly improve the gene transfection efficiency and deliver the nucleic acid in a rapid manner. Moreover, these NPs possess size dimensions of < 100 nm, comparable to those of a protein, a virus, and a gene. MNPs are superparamagnetic, meaning that they do not retain magnetization once the electric field has been removed, hence presenting an advantage of reducing particle aggregation (Zhu *et al.*, 2010). The commonly used MNPs include cobalt and their oxides such as magnetite (Fe_3O_4), cobalt ferrite ($FeCoO_4$), maghemite (γ–Fe_2O_3), chromium dioxide (CrO_2), and iron-nickel (Katragadda *et al.*, 2010). Among these, iron oxide NPs (Fe_3O_4) are commonly used in biological applications due to their stability and biocompatibility (Indira and Lakshmi, 2010). The use of these NPs is still at its infancy but holds great potential.

2.5.2.2.2 Quantum Dots (QDs)

QDs are nanoparticles with tunable optical, mechanical and electrical physicochemical properties. Their semiconductor crystalline with high luminescence, broad UV excitation and unique size-dependent characteristics make them appealing vectors for applications including light emitting diodes (LEDs), catalysis, photovoltaic, phosphors, and biological labeling. These properties together with their small size and amenability for synthetic modification presents great potential for medical and biological applications, particularly in imaging (Katragadda *et al.*, 2010). QDs have been used in several gene (pDNA, RNA) delivery studies, particularly in gene silencing both

in vivo and *in vitro* (Chen *et al.*, 2005, Tan *et al.*, 2007, Klein *et al.*, 2009). Recently, Li and co-workers used QD-siRNA nanocomplexes to silence the HPV18 E6 oncogene which resulted in the growth inhibition of HeLa cells. It was postulated that these complexes served as dual-vectors; providing a luminescence tool to analyze gene silencing, and intracellular imaging (Li *et al.*, 2011).

2.5.2.2.3 Silver Nanoparticles (AgNPs)

AgNPs are composed of silver or silver oxide, ranging in size from 1 to 100 nm. For centuries, AgNPs have been known for their antimicrobial action, and hence have been commonly used in medical devices (Ahamed *et al.*, 2010). They are also used in biomedicine due to their unique chemical and physical properties which increases their efficiency, however, their size-dependent toxicity remains a concern (Singh *et al.*, 2008). Previous studies have shown that AgNPs can be toxic to a number of mammalian cells. However, some reports have shown that these NPs are also capable of inducing genes that are involved in cell growth, and apoptosis in mammalian cells at low concentrations (Xia *et al.*, 2006). Recently, Bouwmeester and co-workers conducted an *in vitro* study which demonstrated the ability of AgNPs to efficiently deliver mRNA to colon cancer (Caco-2) and epithelial cells of mucosa-associated lymphoid (M-cells) (Bouwmeester *et al.*, 2011).

2.5.2.2.4 Gold Nanoparticles (AuNPs)

AuNPs are the most studied metal nanoparticles in biomedicine, since their discovery centuries ago. Colloidal suspensions of AuNPs with nanometer sizes exhibit various shapes such as spheres, rod, cubes, triangles, cages, shells depending on the synthesis method (Liu *et al.*, 2016). They have a broad range of colors that depends on their shape, size, refractive index as well as aggregation (Figure 2.12) (Dreaden *et al.*, 2012).

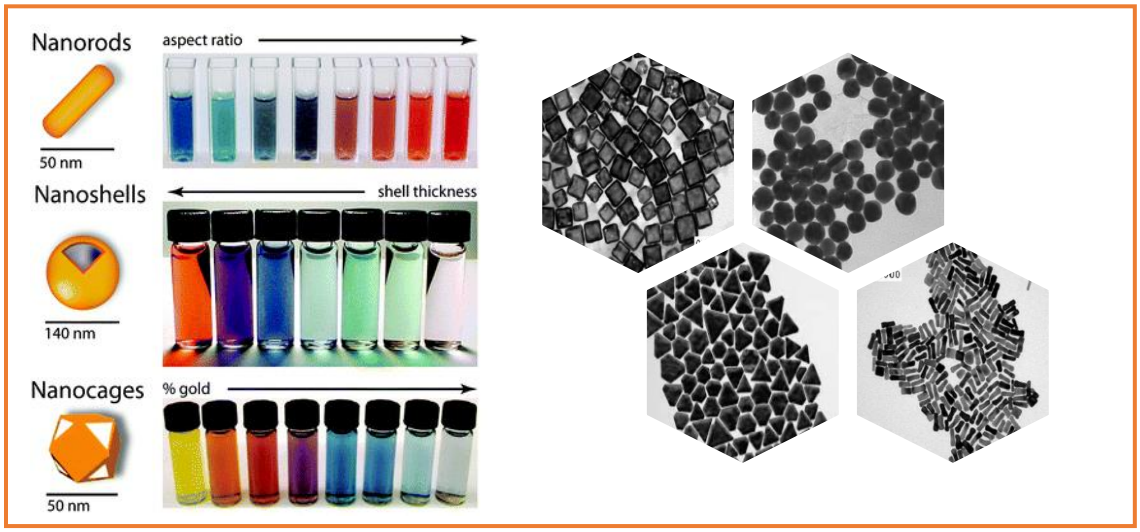

Figure 2.12: Gold nanoparticles frequently used in biomedical applications. Adapted from (Dreaden *et al.*, 2012) with modifications.

Historically, gold has been used by artists to stain glasses due to the vibrant colors produced when they interact with visible light (Duncan *et al.*, 2010). The colors are said to be as a result of localized surface plasmon resonance (LSPR) (Figure 2.13), where the free electrons on the metal NP surface, oscillate in resonance with absorbed light (Sun *et al.*, 2016). The general consensus is that the size of the NP is directly proportional to the wavelength of absorbed light, therefore, AuNPs with sizes between 10 and 30 nm have an absorption peak at ~530 nm.

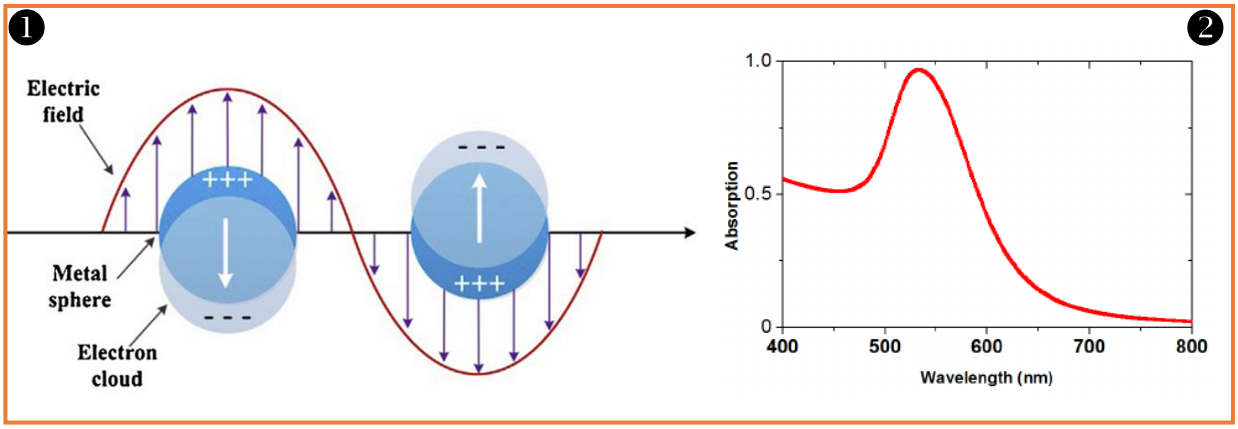

Figure 2.13: (1) Illustration of LSPR process (Sun *et al.*, 2016) and (2) spectrum of AuNPs with an absorption peak at ~530 nm (Atar *et al.*, 2013).

Recently, AuNPs have made their way into high impact biomedical applications due to their unique optoelectronic and physicochemical properties (Figure 2.14). These NPs possess intense optical properties which have allowed them to be used in diagnostic and imaging applications. Their ability to effectively absorb and scatter light has allowed for specific thermal removal of tumors.

In addition, AuNPs possess tunable physicochemical properties which are key for their use in cancer therapy. They have an inert core that is essentially non-toxic, and are biocompatible, providing a platform for construction of suitable gene or drug delivery carriers (Connor *et al.*, 2005). AuNPs are generally highly dispersed with sizes that can be tuned based on the desired therapeutic application (Daniel and Astruc, 2004). Their nanometer sizes (1-200 nm), allow them to accumulate in tumor sites and transfect cells rapidly using various mechanisms. They have a high surface area-to-volume ratio which allows loading of vast biomolecules including therapeutic drugs, genes, and proteins, which in turn facilities their integration into biological systems (Tiwari *et al.*, 2011). Their surface chemistry, allows them to behave as synthetic antibodies with tunable binding affinities. Their multivalent surface enables them to host multiple therapeutic drugs (unstable) or bio-macromolecules by covalent or non-covalent conjugation, and aiding in their delivery to remote or target sites (Ghosh *et al.*, 2008a, Kim *et al.*, 2013). Hence, all these properties of AuNPs can be combined to form a non-viral vector which is multi-functional, and which can be tailored for a specific disease.

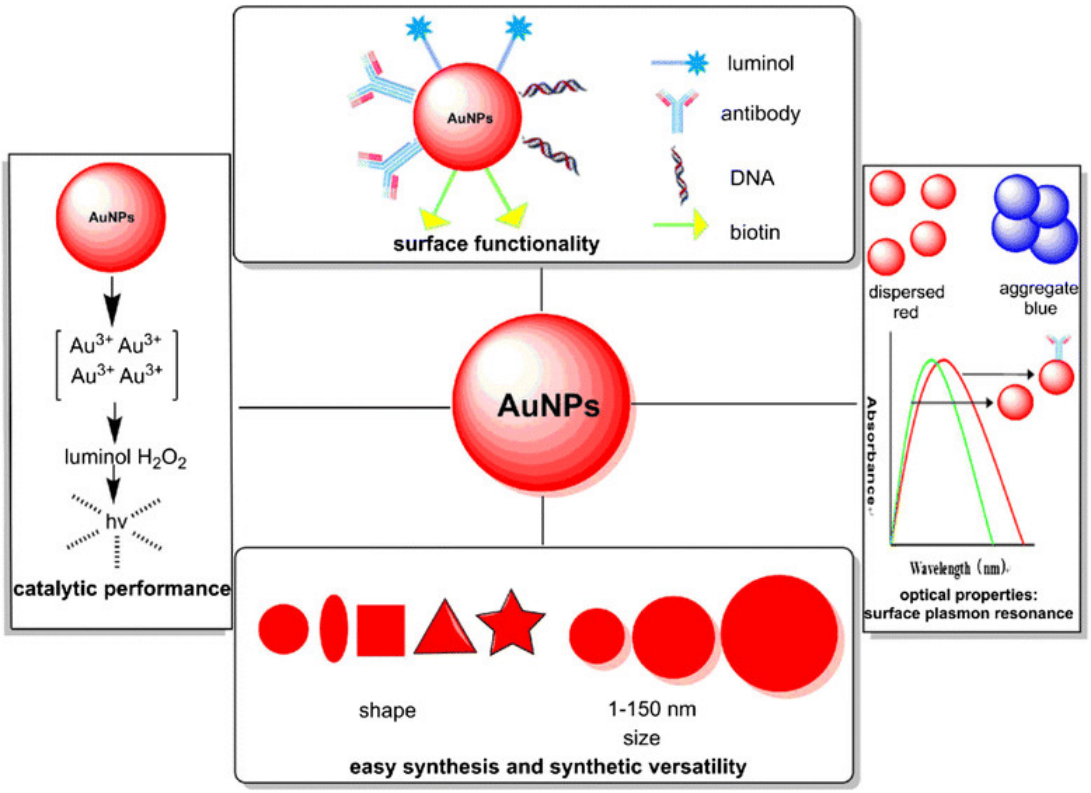

Figure 2.14: Illustration of the properties of gold nanoparticles (Liu *et al.*, 2016).

2.6 Synthesis of Gold Nanoparticles

Various methods have been developed to synthesise gold nanoparticles with surfaces that confer unique physicochemical properties required for enhanced delivery of drugs and biomolecules. These can be categorized as "top-down" and "bottom-up" methods. The "top-down" method involves the mechanical grinding of large quantities of metals, followed by the stabilization of the resultant nano-sized metals with a protecting agent (Bradley, 1994). This method is very versatile as it can produce a variety of nanoparticles in small-scale laboratories; however, the demanding apparatus operation and the difficulties in generating small sized particles limits it use. The "bottom-up" method, on the other hand, involves chemical reduction of metal salts in aqueous solutions by stabilizing agents such as solvents (THF, THF/MeOH), polymers, donor ligands (amines, phosphanes, thioethers), and surfactants (sodium citrate/borohydride), which control the size of the nanoparticles, and prevent them from aggregating (Zhou *et al.*, 2009). This strategy is considered the most powerful and hence is commonly used in many laboratories.

2.6.1 Citrate Reduction/Turkevich Method

This method was first derived by Turkevich *et al.* in 1951 and later modified by Frens *et al.* in 1973. It is the simplest and most frequently used approach for the synthesis of monodisperse spherical AuNPs in the 10-20 nm size range. This approach involves the reduction of gold ions (chloroauric acid, $HAuCl_4$) by trisodium citrate in water at 100 $^{\circ}$C to form AuNPs (Rana *et al.*, 2012) (Figure 2.15). In this reaction, the citrate ions act as both a reducer and a stabilizer. Stabilizers are essential during NP synthesis, as they prevent the aggregation of NPs. The size of these AuNPs depends on the temperature, salt concentration and the ratio of the added reactants (citrate: gold ions ratio). Larger particles (>20 nm) can be synthesized by adjusting these factors. The shape and monodispersity of AuNPs can be disrupted when the size is greater than 50 nm. Furthermore, the modification of this basic method using other forms of stabilizing agents including glucose (Zhang *et al.*, 2006), methanol extract of medicinal plants (Ramezani *et al.*, 2008), L-tryptophane and polyethylene glycol (Akbarzadeh *et al.*, 2009), and derivative of serrapeptase (Ravindra, 2009), and hydroquinone (Perrault and Chan, 2009) have also been reported.

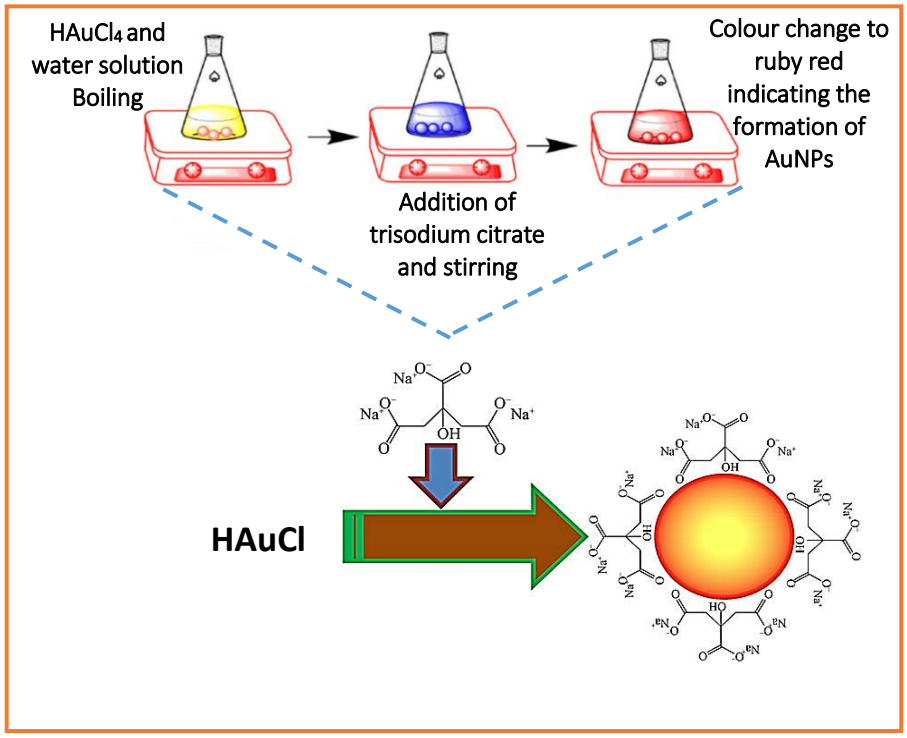

Figure 2.15: Illustration of the synthesis of AuNPs via the citrate reduction method. Adapted from (Ghosh and Chattopadhyay, 2013), (Liu *et al.*, 2016) with modifications.

2.6.2 Brush-Schiffrin Method

This is the second popular biphasic toluene-water method of synthesising AuNPs anchored with monolayer protected clusters (MPCs), with diameters ranging from 5-6 nm under ambient conditions. This approach was derived by Brust-Schiffrin and co-workers in 1994 (Brust *et al.*, 1994), and involves the chemical replacement of the native surfactant ligand with a hydrophilic ligand. During synthesis, $AuCl_4$ ions are reduced with sodium borohydride ($NaBH_4$) in the presence of the chosen thiol stabilizing ligand e.g. tetraoctylammonium bromide (TOAB) (Ghosh *et al.*, 2008a, Rana *et al.*, 2012). $NaBH_4$ acts as a reducing agent, while TOAB acts as both a phase transfer catalyst and as a stabilizing agent. Moreover, direct or post-functionalisation of these AuNPs anchored with MPCs using various ligands in a place-exchange reaction derived by Murray and co-workers, resulted in the formation of functionally diverse MPCs known as mixed monolayer protected clusters (MMPCs) (Figure 2.16) (Rana *et al.*, 2012).

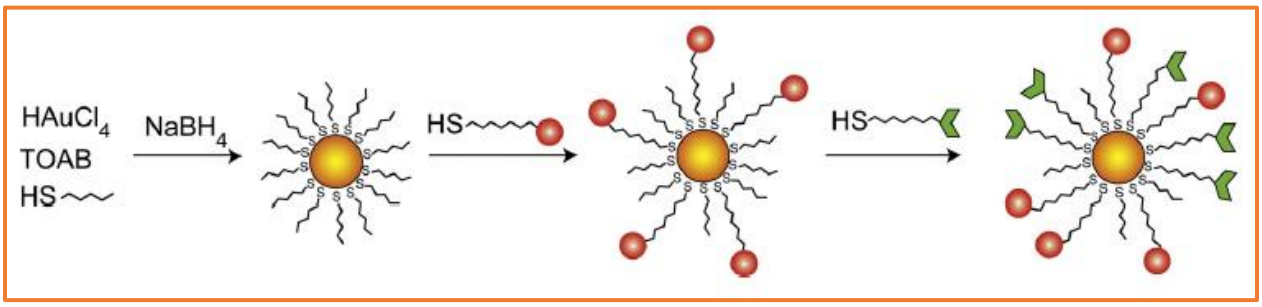

Figure 2.16: Formation of MPCs and MMPCs using the Brust-Schiffrin and Murray's place-exchange reactions (Rana *et al.*, 2012).

Over the years, an array of other approaches to synthesise AuNPs with various shapes e.g. hexagons, rods, cubes, and cages based on the specific research application have been proposed e.g. seeding growth, microemulsion, sonochemistry, photochemistry, reversed micelles, and radiolysis (Hu *et al.*, 2008, Huang *et al.*, 2010).

2.7 Functionalisation of Gold Nanoparticles

The surface of AuNPs, particularly citrate coated AuNPs presents a platform that is filled with vast biological possibilities due to its ease of modification (e.g. carboxyl groups are readily reactive due to weak bonding). Functionalisation of AuNPs occur subsequent to the initial synthesis and can be achieved via a ligand exchange reaction (e.g. Brush-Schiffrin method) or by addition of

polymers and biomolecules on the surface of AuNPs for tailored therapeutic applications (Fratoddi *et al.*, 2014). Functionalisation can be broken down into primary coating, and biomolecule coating (Figure 2.17).

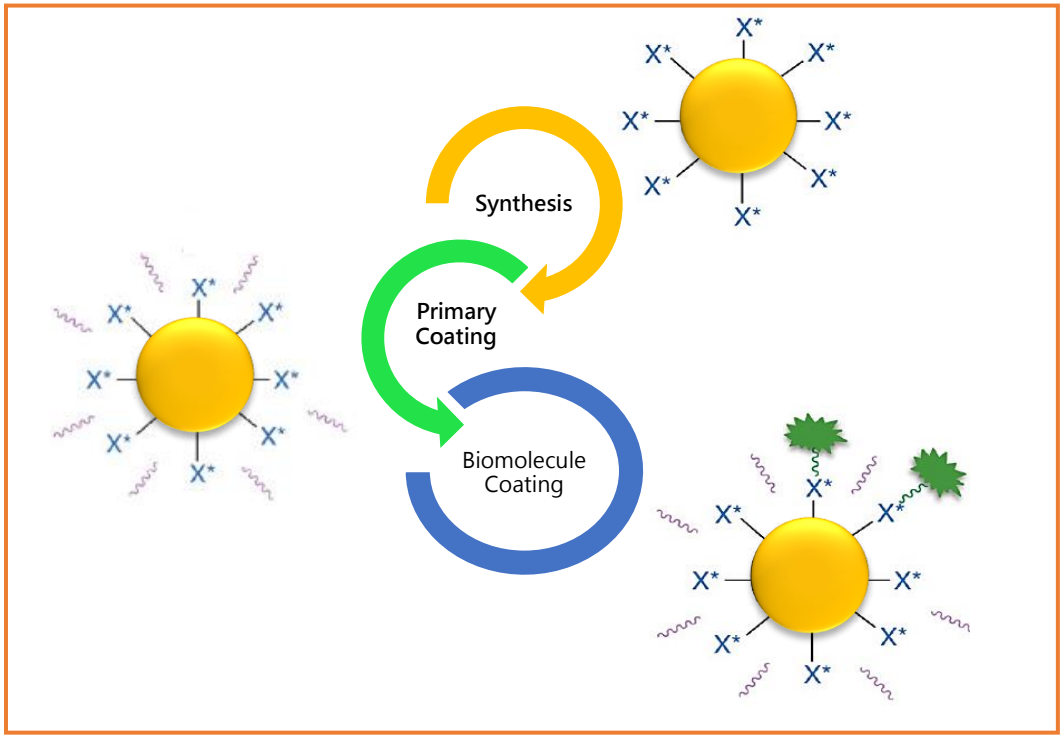

Figure 2.17: Functionalisation process from synthesis. Adapted from (Fratila *et al.*, 2014) with modifications.

2.7.1 Primary Coating of Gold Nanoparticles

Colloidal stability is an important property that determines the successful biological application of NPs. Colloidal stability is affected by high content of salt, carbohydrates, amino acids, lipids, proteins, and enzymes normally found in physiological media, which consequently cause NP aggregation via van der Waals interactions (Fratila *et al.*, 2014).

An ideal NP must be capable of overcoming biological barriers, avoid being recognized by the immune system, and prevent accumulation in unspecific sites e.g. the spleen and liver, which compromise their desired effect. Generally, when NPs enter the body, the immune system recognizes them as foreign molecules and responds by releasing serum proteins called opsonins

which bind onto the surface of the NPs, resulting in their recognition by phagocytes/macrophages which degrades and eliminates them from the bloodstream.

The primary coating of AuNPs is important for the following reasons (Mout *et al.*, 2012, Llevot and Astruc, 2012, Fratila *et al.*, 2014, Liu *et al.*, 2016):

- It increases NP stability and solubility.
- It preserves the NPs' physicochemical properties.
- It defines the NPs' interaction with the surrounding environment.
- It helps NPs to escape uptake by phagocytes/macrophages, increasing circulation time.
- It reduces non-specific uptake of NPs.
- It decreases cytotoxicity.
- It protects NPs from enzymatic degradation *in vivo.*
- Finally, it provides a flexible and rich surface chemistry that can be further functionalized with biomolecules for specific biological applications.

Typical primary coating strategies of AuNPs include ligand exchange (as previously mentioned), polymer coating, silica coating, and layer-by-layer coating, with polymer coating being more commonly used.

2.7.1.1 Polymer Coating

Since it discovery in 1718, polymer coating has by far been the most effective and widely used approach to increase NP stability in aqueous solutions, as well as its circulation in the blood (Daniel and Astruc, 2004). This approach involves the modification of the surface of NPs with polymers such as poly (ethylene glycol) (PEG), which results in a stealth shield around the NP, preventing NP self-aggregation and non-specific binding to extra-/intracellular degrading proteins (Kumar *et al.*, 2014). Several other polymers such as heparin, dextran, PEI, PLL and chitosan derivatives have been used to stabilize AuNPs, due to their high biocompatibility, extreme buffering capacity and rich surface functionalities that can be used for further bioconjugations (Fratila *et al.*, 2014). Polymer coated AuNPs are capable of passively targeting tumour sites via the leaky tumor vasculatures, because of their small size as well as due to the "enhanced permeability and retention" (EPR) effect. This ability is crucial in the delivery of therapeutic molecules for cancer treatments (Nichols and Bae, 2014).

2.7.2 Biomolecule Coating

Coating gold nanoparticles with biomolecules allows for efficient delivery of the biomolecules to the specific cells with less damage, a feature that synthetic materials fail to achieve. Various biomolecules have been covalently/non-covalently conjugated onto the surface of AuNPs viz., antibodies, genes (e.g. DNA/RNA/oligonucleotides), peptides, Herceptin, carcinoembryonic antigen (CEA), epidermal growth factor (e.g. EGF58), vitamins (e.g. folic acid), and sugars (e.g. galactose) (Figure 2.18) (Rana *et al.*, 2012). Biomolecule coated AuNPs are capable of actively targeting specific cell surface receptors or proteins on tumours, and direct their therapeutic effect, which destroys the tumors with little injury to normal cells (Choi *et al.*, 2010).

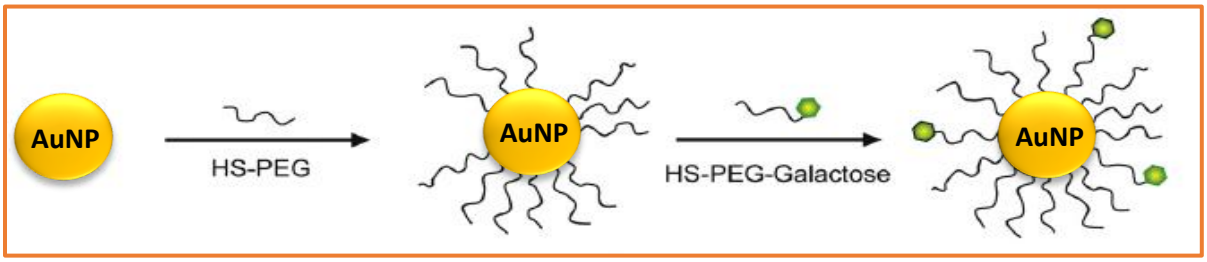

Figure 2.18: Polymer and biomolecule (e.g galactose ligand) coated AuNPs (Ghosh *et al.*, 2008a).

2.8 Application of Functionalised Gold Nanoparticles

2.8.1 Gene Therapy: Gene Delivery

The successful delivery of genes into target sites requires effective binding and condensation of the genes, effective cellular uptake via endocytosis, effective endosomal escape, effective protection against degrading intracellular enzyme, and delivery to the target site (Rana *et al.*, 2012). Gold nanoparticles provides an excellent platform for gene delivery due to their large payload carrying capacity, efficient gene compaction and tenable surface which permits enhancement of transfection efficiency. Gold nanoparticles for gene delivery have been applied in two ways (Shan *et al.*, 2012):

(a) Cationic polymer coated AuNPs to bind/condense genes and release them inside the cell.
(b) Thiolated biomolecule coated AuNPs to target the components of the cytoplasm.

Over the years, many studies have been conducted to demonstrate their gene delivery ability. In the early 1990s, Mirkin *et al* and Alivisatos *et al* reported an oligonucleotide coated AuNP via the thiol-gold bond formation and its application in cancer therapy (Mirkin *et al.*, 1996, Alivisatos *et al.*, 1996). They showed that these NPs could efficiently protect siRNA against degrading RNAses and deliver it to the cytoplasm with no toxicity. They further demonstrated the gene silencing ability of polyvalent RNA-AuNP conjugates *in vitro*. The gene silencing ability of siRNA-PEG-poly (β-aminoester)-AuNPs conjugates was also shown in human cells (Lee *et al.*, 2009). A study conducted by Rosi and co-workers showed that DNA coated AuNP nanocomplexes could also efficiently silence genes through an antisense mechanism (Rosi *et al.*, 2006).

Furthermore, Oishi and co-workers demonstrated the *in vitro* (HuH-7 cells) gene silencing ability of PEG-block-poly (2-(N,N-dimethylamino) ethylmethacrylate) copolymer coated siRNA conjugated to AuNPs (Oishi *et al.*, 2006). Giljohann and colleagues further demonstrated the *in vivo* gene silencing ability of PEG-coated-siRNA conjugated AuNPs (Giljohann *et al.*, 2009). Braun *et al*. demonstrated the gene silencing ability of siRNA-Au-nanoshell coated with a TAT-lipid layer (Braun *et al.*, 2009). Several other studies have demonstrated the efficiency of AuNPs in delivering siRNA and gene silencing (Guo *et al.*, 2010, Wadhwani *et al.*, 2010).

Early studies by Niidome and colleagues reported on the ability of primary amine-coated AuNPs to effectively deliver pDNA with a luciferase gene into HeLa cells (Niidome *et al.*, 2004). Later studies by Ghosh *et al*. showed that the first-generation lysine dendron (G1-Lys)-coated dsDNA Au nanocomplexes was more efficient than polylysine in gene expression (Ghosh *et al.*, 2008b). Jiang and co-workers demonstrated the efficiency of Herceptin coated gold-silver NPs in targeting the Her-2 receptor overexpressed in breast and ovarian carcinoma cells (Jiang *et al.*, 2008).

Recent studies have shown that combining phototherapy with gene therapy can enhance the gene delivery efficiency. For instance, Niidome and co-workers demonstrated laser-induced gene expression using PEG-ortho-pyridyl-disulfide (PEG-OPSS)-coated-pDNA conjugated AuNPs (Figure 2.19) (Niidome *et al.*, 2006). EI-Sayed and colleagues demonstrated the targeting and light scattering ability of AuNPs coated with anti-EGFR. They showed that these NPs had a 6-fold higher affinity for cancerous cells than non-cancerous cells, and when incubated with cancer cells, activated with a laser, and local heating, cell death was observed (El-Sayed *et al.*, 2005).

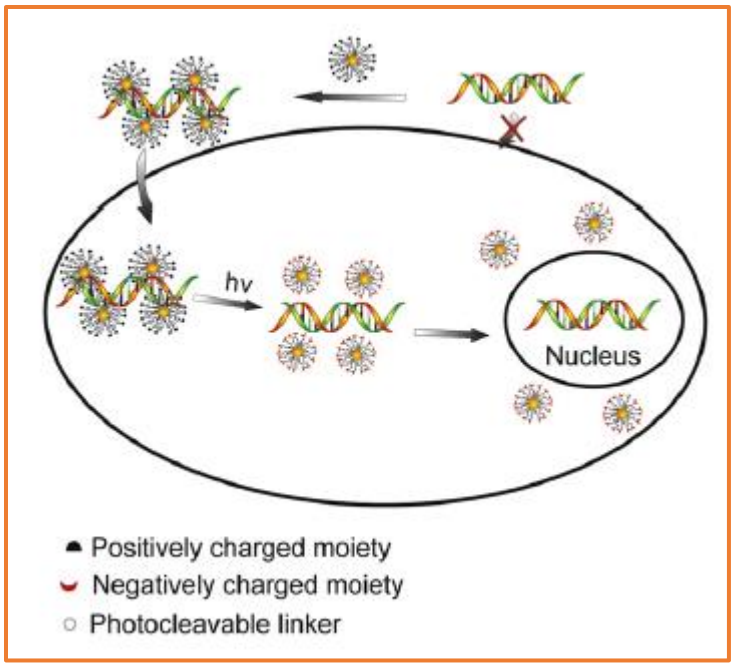

Figure 2.19: Illustration of DNA delivery using photolabile functionalized AuNPs (Ghosh *et al.*, 2008a).

Oligonucleotide coated AuNPs have also been used in other molecular diagnostic biomedical applications, such as in the detection of adenosine triphosphate (ATP) and nucleic acids (Seferos *et al.*, 2007, Zheng *et al.*, 2009). A study conducted by Seferos and co-workers demonstrated the use of oligonucleotide coated AuNP probes as "nanoflares" in visualization and quantification of intercellular mRNA. These vectors were found to be non-toxic, resistant to enzyme degradation without the need for any additional transfection reagents.

2.8.2 Chemotherapy: Drug Delivery

Chemotherapy uses anti-cancer drugs to treat cancer. Delivery of these drugs into cancer cells is usually associated with low therapeutic effects due to rapid clearance and non-specific distribution as a result of their small size. Poor drug distribution and delivery can result in severe side effects and multidrug resistance (Conde *et al.*, 2011). Several factors affect the performance of drug delivery vectors, including NP size, surface functionalities, NP rapture/breakdown, and rate of drug release. Functionalized AuNPs (FAuNPs) can selectively target anticancer drugs to tumours passively or actively (Figure 2.20).

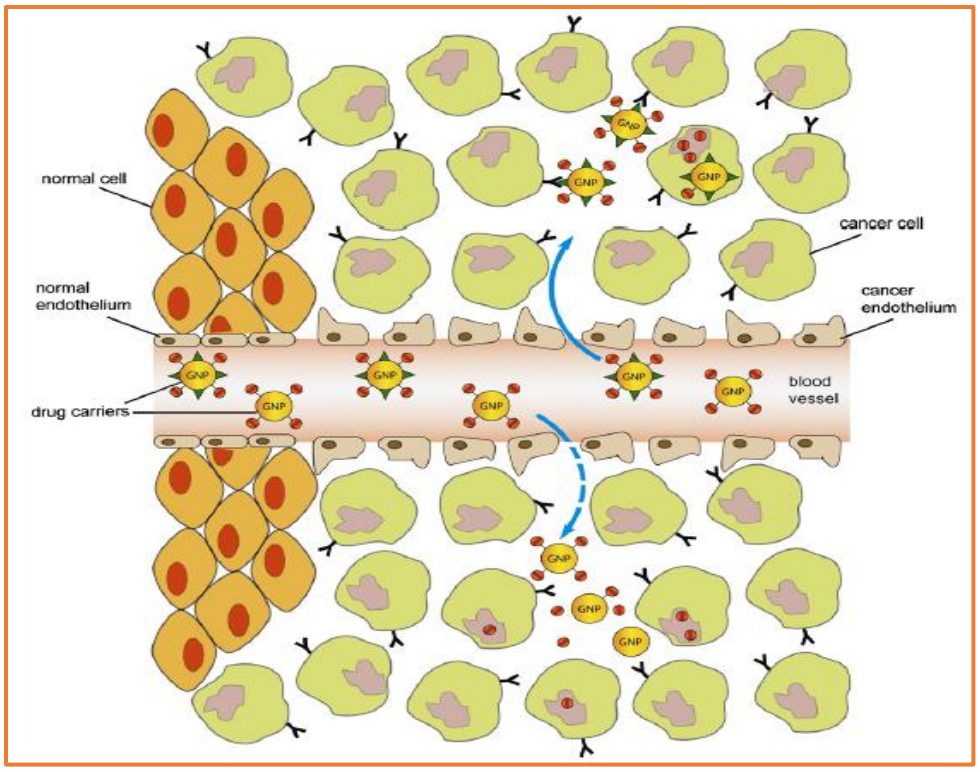

Figure 2.20: Illustration of active and passive therapeutic drug targeting using FAuNPs (Ghosh *et al.*, 2008a).

Anticancer drug loading in AuNPs has been achieved by several methods (Fratoddi *et al.*, 2014):

(a) Partitioning, which uses the monolayer or bilayer coating on the surface of AuNPs to partition hydrophobic anticancer drugs.

(b) Surface complexation, which uses the amine and thiol binding affinity of AuNPs by forming Au-N or Au-S bonds.

(c) Attachment to stabilizing agents using the peripheral functional groups of the stabilizing agent to attach drugs.

(d) Charge interaction, which uses electrostatic interactions to bind the surface of AuNPs with oppositely charged anticancer drugs.

(e) Encapsulation, which uses the interior of AuNPs to condense hydrophobic drugs.

A number of anticancer drugs including curcumin, paclitaxel, doxorubicin, docetaxel, oxaliplatin, methotrexate, tamoxifen and 3-mercaptopropionic acid have been delivered using functionalized AuNPs (Manju and Sreenivasan, 2012, Chen *et al.*, 2013, Jang *et al.*, 2013, Lu *et al.*, 2013, Ding *et al.*, 2013, Zhou *et al.*, 2013a, de Oliveira *et al.*, 2013, Webster *et al.*, 2013). Furthermore, studies on the development of Au-Au sulfide nanoshells coated with a thermosensitive hydrogel matrix as photothermal stimulated drug-delivery vectors has been reported (Strong and West, 2011).

2.8.3 Other Cancer Applications: Immunotherapy

Immunotherapy is amongst the strategies that promise to treat cancer, by stimulating the immune system of the host, so as to identify and kill tumor cells. Generally, tumors evade immune system recognition by developing various mechanisms (Almeida *et al.*, 2014). For example, cancer cells are capable of down-regulating the expression of stimulatory molecules and surface antigens which in turn suppress recognition and stimulation of T cells (Cruz *et al.*, 2012, Guo and Huang, 2014).

Tumor cells are also capable of inhibiting dendritic cells (DCs) by releasing the cytokines e.g. TGF-β and IL-10 that suppress immune responses (Zhou *et al.*, 2013b). Tumor cells are also capable of inducing cell death in T cells by activating pro-apoptotic factors such as FasL and TRAIL (Kichev *et al.*, 2014). Hence, immunotherapy aims at establishing stable immune responses against malignant tumors by developing novel strategies.

One of these strategies involves efficiently delivering antigens to DCs which stimulate cytotoxic $CD8^+$ T cell response upon maturation. DCs are antigen presenting cells that are abundantly found in lymph nodes along with other macrophages, and immune cells, hence delivering antigens to the lymph nodes is regarded as a smart tactic (Bal *et al.*, 2010). Nanoparticles, specifically, AuNPs have therefore been used as antigen delivering vectors in immunotherapy due to their tunable size, non-toxicity, biocompatibility, and tendency to accumulate in immune cells. Various immunotherapeutic pre-clinical studies have been reported recently. Lee *et al*. formulated AuNP conjugated-RFP-CpG (Figure 2.21) for antigen delivery to the lymph nodes. Red fluorescent protein (RFP) was selected as a test antigen and was formulated to contain a C terminus with additional cysteines, enabling conjugation to AuNPs via an Au-S bond formation.

A thiol modified CpG 1668 oligodeoxynucleotide containing a spacer of a 10 adenine nucleotide (A_{10}) conjugate was also linked to the RFP-AuNP since CpG 1668 is capable of stimulating strong immune responses via TLR-9 activation. It was found that this AuNP-based antigen vector displayed significant antitumor efficiency in RFP-overexpressing melanoma tumor models, hence showing potential as a vaccine adjuvants for the prevention of cancer.

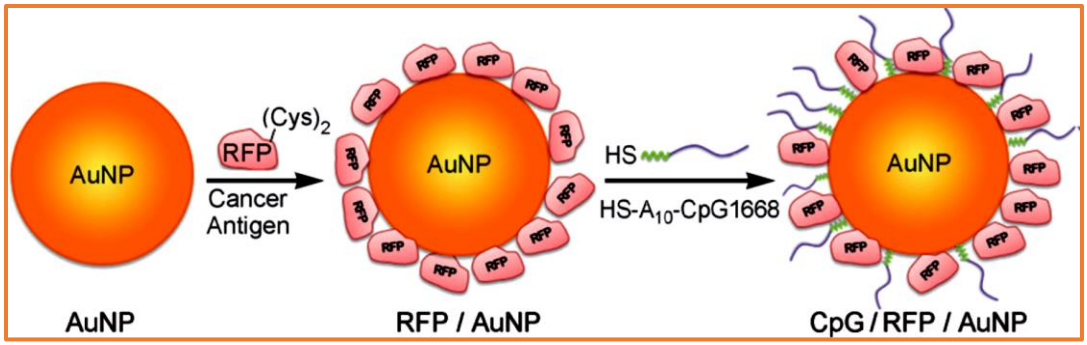

Figure 2.21: Preparation of RFP/AuNP and CpG/RFP/AuNP for immunotherapeutic application (Lee *et al.*, 2012).

Lin *et al*. synthesized AuNPs conjugated to a modified CpG oligodeoxynucleotide-linked triethylene glycol (TEG) for DNA delivery. The use of a TEG spacer in addition of the conventional poly-thymidine spacer stimulated CpG macrophages which resulted in improved particle uptake without compromising the DNA content. They observed that these TEG modified CpG-AuNP nanocomplexes induced infiltration of dendritic and macrophage tumor cells, prohibited tumor growth, and stimulated survival in mice, therefore, showing potential as vaccine adjuvants for the prevention of cancer (Lin *et al.*, 2013).

Andersson *et al*. demonstrated the ability of HSP70-conjugated gold nanorods (AuNRs) to induce site-specific, heat-inducible gene expression. HSP70 is a heat shock protein that is promoter-driven. AuNRs are capable of absorbing light and converting it into heat, and hence inducing the stimulation of photothermal expression of the cytokines. For *in vitro* studies, they transfected human-murine B16 and HeLa cells with nanocomplexes of PEI-conjugated AuNRs/HSP70-enhanced EGFP plasmid, followed by exposure to near-infrared (NIR) light or heat shock at 42 °C resulting in significant gene expression. For *in vivo* studies, mice with B16 melanoma cancer cells were transfected with the same nanocomplex and gene expression was verified after 6 and 24-hours (Andersson *et al.*, 2014).

Combination techniques were also demonstrated in FAuNPs mediated immunotherapy. It was shown that when synthesized PEGylated AuNPs (~30 nm) conjugated to necrosis factors were transfected into prostate tumour bearing mice, efficient uptake within 24-hours was observed (Kim and Jon, 2012). Sun *et al*. synthesized immunoglobulin G (IgG)-linked-co-factor (PEG-protein G) FAuNPs for antigen delivery since co-factors were found to improve AuNP's NIR plasmonic resonance. Thus, when breast tumor cells (SK-BR-3) were transfected with these immune-FAuNPs followed by exposure to the laser light, significant cell membrane rapture occurred (Sun *et al.*, 2013). Furthermore, antigen-conjugated AuNPs as vaccine adjuvants for image cancer immunotherapy were developed (Coulie *et al.*, 2014). These reports all attest to the potential and applicability of FAuNPs in cancer immunotherapy.

2.9 Gold Nanoparticle Toxicity

Toxicity is an important aspect that can limit the applicability of NPs in biological systems. Physico-chemical properties such as size and surface charge greatly influence the toxicity of NPs. These properties play a crucial role in the ability of the NP to avoid recognition by macrophages/phagocytes, which in turn means avoiding immune stimulation and renal filtration clearance. Hydrophilic NPs ranging from 10 and 100 nm in size are said to be small enough to avoid recognition by macrophages/phagocytes but are large enough to avoid renal clearance (Gil and Parak, 2008).

AuNPs are inherently non-toxic; however, size, additional coating, and targeting ligands compromise their cytotoxicity *in vitro* or *in vivo*. Several studies have reported on the cytotoxicity of AuNPs. Investigation of the size-dependence of AuNP's cytotoxicity *in vitro* revealed that the cytotoxicity of 1-2 nm sized AuNPs was cell-type-dependent with high IC50s, while those that were around 15 nm were non-toxic to all cells even at high concentrations (Pan *et al.*, 2007). It was reported that small sized AuNPs were capable of suppressing immune responses by macrophages, and activating the inflammatory responses by interleukin-1and 6 genes (Yen *et al.*, 2009).

Studies investigating the shape-dependence of AuNPs cytotoxicity *in vivo* using KM mice demonstrated that the rod-shaped AuNPs were highly toxic, while the cube-shaped AuNPs was moderately toxic. Sphere-shaped AuNPs, however, showed the best biocompatibility, proving that toxicity is also shape-dependent (Sun *et al.*, 2011). High toxicity was observed with the Au-NRs due to the surface charges of the cationic CTAB cap/surfactant that is used to synthesize them (Qiu *et al.*, 2010).

2.10 References

AHAMED, M., ALSALHI, M. S. & SIDDIQUI, M. 2010. Silver nanoparticle applications and human health. *Clinica chimica acta,* 411**,** 1841-1848.

AKBARZADEH, A., ZARE, D., FARHANGI, A., MEHRABI, M. R., NOROUZIAN, D., TANGESTANINEJAD, S., MOGHADAM, M. & BARARPOUR, N. 2009. Synthesis and characterization of gold nanoparticles by tryptophane. *American Journal of Applied Sciences,* 6**,** 691-695.

ALIVISATOS, A. P., JOHNSSON, K. P., PENG, X. & WILSON, T. E. 1996. Organization of'nanocrystal molecules' using DNA. *Nature,* 382**,** 609.

ALMEIDA, J. P. M., FIGUEROA, E. R. & DREZEK, R. A. 2014. Gold nanoparticle mediated cancer immunotherapy. *Nanomedicine: Nanotechnology, Biology and Medicine,* 10**,** 503-514.

ANDERSSON, H. A., KIM, Y.-S., O'NEILL, B. E., SHI, Z.-Z. & SERDA, R. E. 2014. HSP70 promoter-driven activation of gene expression for immunotherapy using gold nanorods and near infrared light. *Vaccines,* 2**,** 216-227.

ARIMA, H., YAMASHITA, S., MORI, Y., HAYASHI, Y., MOTOYAMA, K., HATTORI, K., TAKEUCHI, T., JONO, H., ANDO, Y. & HIRAYAMA, F. 2010. In vitro and in vivo gene delivery mediated by lactosylated dendrimer/α-cyclodextrin conjugates (G2) into hepatocytes. *Journal of Controlled Release,* 146**,** 106-117.

ATAR, F. B., BATTAL, E., AYGUN, L. E., DAGLAR, B., BAYINDIR, M. & OKYAY, A. K. 2013. Plasmonically enhanced hot electron based photovoltaic device. *Optics express,* 21**,** 7196-7201.

AYDIN, Z., AKBAS, F., SENEL, M. & KOC, S. N. 2012. Evaluation of Jeffamine®-cored PAMAM dendrimers as an efficient in vitro gene delivery system. *Journal of Biomedical Materials Research Part A,* 100**,** 2623-2628.

BAL, S. M., DING, Z., VAN RIET, E., JISKOOT, W. & BOUWSTRA, J. A. 2010. Advances in transcutaneous vaccine delivery: do all ways lead to Rome? *Journal of controlled release,* 148**,** 266-282.

BALAZS, D. A. & GODBEY, W. 2010. Liposomes for use in gene delivery. *Journal of drug delivery,* 2011.
BANAN, M. & PURI, N. 2004. The ins and outs of RNAi in mammalian cells. *Current pharmaceutical biotechnology,* 5**,** 441-450.

BHAKTA, G., SHRIVASTAVA, A. & MAITRA, A. 2009. Magnesium phosphate nanoparticles can be efficiently used in vitro and in vivo as non-viral vectors for targeted gene delivery. *Journal of biomedical nanotechnology,* 5**,** 106-114.

BOUSSIF, O., LEZOUALC'H, F., ZANTA, M. A., MERGNY, M. D., SCHERMAN, D., DEMENEIX, B. & BEHR, J.-P. 1995. A versatile vector for gene and oligonucleotide transfer into cells in culture and in vivo: polyethylenimine. *Proceedings of the National Academy of Sciences,* 92**,** 7297-7301.

BOUWMEESTER, H., POORTMAN, J., PETERS, R. J., WIJMA, E., KRAMER, E., MAKAMA, S., PUSPITANINGANINDITA, K., MARVIN, H. J., PEIJNENBURG, A. A. & HENDRIKSEN, P. J. 2011. Characterization of translocation of silver nanoparticles and effects on whole-genome gene expression using an in vitro intestinal epithelium coculture model. *ACS nano,* 5**,** 4091-4103.

BRADLEY, J. S. 1994. The chemistry of transition metal colloids. *Clusters and colloids: from theory to applications***,** 459-544.

BRAUN, G. B., PALLAORO, A., WU, G., MISSIRLIS, D., ZASADZINSKI, J. A., TIRRELL, M. & REICH, N. O. 2009. Laser-activated gene silencing via gold nanoshell− siRNA conjugates. *Acs Nano,* 3**,** 2007-2015.

BRAVO-OSUNA, I., VICARIO-DE-LA-TORRE, M., ANDRÉS-GUERRERO, V., SÁNCHEZ-NIEVES, J., GUZMÁN-NAVARRO, M., DE LA MATA, F., GÓMEZ, R., DE LAS HERAS, B., ARGUESO, P. & PONCHEL, G. 2016. Novel water-soluble mucoadhesive carbosilane dendrimers for ocular administration. *Molecular pharmaceutics,* 13**,** 2966-2976.

BRUST, M., WALKER, M., BETHELL, D., SCHIFFRIN, D. J. & WHYMAN, R. 1994. Synthesis of thiol-derivatised gold nanoparticles in a two-phase liquid–liquid system. *Journal of the Chemical Society, Chemical Communications***,** 801-802.

CHAPLOT, S. P. & RUPENTHAL, I. D. 2014. Dendrimers for gene delivery–a potential approach for ocular therapy? *Journal of Pharmacy and Pharmacology,* 66**,** 542-556.

CHEN, A. A., DERFUS, A. M., KHETANI, S. R. & BHATIA, S. N. 2005. Quantum dots to monitor RNAi delivery and improve gene silencing. *Nucleic acids research,* 33**,** e190-e190.

CHEN, Q., LI, K., WEN, S., LIU, H., PENG, C., CAI, H., SHEN, M., ZHANG, G. & SHI, X. 2013. Targeted CT/MR dual mode imaging of tumors using multifunctional dendrimer-entrapped gold nanoparticles. *Biomaterials,* 34**,** 5200-5209.

CHO-CHUNG, Y. 2005. DNA drug design for cancer therapy. *Current pharmaceutical design,* 11**,** 2811-2823.

CHOI, C. H. J., ALABI, C. A., WEBSTER, P. & DAVIS, M. E. 2010. Mechanism of active targeting in solid tumors with transferrin-containing gold nanoparticles. *Proceedings of the National Academy of Sciences,* 107**,** 1235-1240.

CHUANG, C.-C. & CHANG, C.-W. 2015. Complexation of bioreducible cationic polymers with gold nanoparticles for improving stability in serum and application on nonviral gene delivery. *ACS applied materials & interfaces,* 7**,** 7724-7731.

CONDE, J., DORIA, G. & BAPTISTA, P. 2011. Noble metal nanoparticles applications in cancer. *Journal of drug delivery,* 2012.

CONNOR, E. E., MWAMUKA, J., GOLE, A., MURPHY, C. J. & WYATT, M. D. 2005. Gold nanoparticles are taken up by human cells but do not cause acute cytotoxicity. *Small,* 1**,** 325-327.

COULIE, P. G., VAN DEN EYNDE, B. J., VAN DER BRUGGEN, P. & BOON, T. 2014. Tumour antigens recognized by T lymphocytes: at the core of cancer immunotherapy. *Nature reviews. Cancer,* 14**,** 135.

CRUZ, L. J., TACKEN, P. J., RUEDA, F., CARLES DOMINGO, J., ALBERICIO, F. & FIGDOR, C. G. 2012. 8 Targeting Nanoparticles to Dendritic Cells for Immunotherapy. *Methods in enzymology,* 509**,** 143.

DANIEL, M.-C. & ASTRUC, D. 2004. Gold nanoparticles: assembly, supramolecular chemistry, quantum-size-related properties, and applications toward biology, catalysis, and nanotechnology. *Chemical reviews,* 104**,** 293-346.

DAVIES, J. C., GEDDES, D. M. & ALTON, E. W. 2001. Gene therapy for cystic fibrosis. *The journal of gene medicine,* 3**,** 409-417.

DE OLIVEIRA, R., ZHAO, P., LI, N., DE SANTA MARIA, L. C., VERGNAUD, J., RUIZ, J., ASTRUC, D. & BARRATT, G. 2013. Synthesis and in vitro studies of gold nanoparticles loaded with docetaxel. *International journal of pharmaceutics,* 454**,** 703-711.

DING, Y., ZHOU, Y.-Y., CHEN, H., GENG, D.-D., WU, D.-Y., HONG, J., SHEN, W.-B., HANG, T.-J. & ZHANG, C. 2013. The performance of thiol-terminated PEG-paclitaxel-conjugated gold nanoparticles. *Biomaterials,* 34**,** 10217-10227.

DREADEN, E. C., ALKILANY, A. M., HUANG, X., MURPHY, C. J. & EL-SAYED, M. A. 2012. The golden age: gold nanoparticles for biomedicine. *Chemical Society Reviews,* 41**,** 2740-2779.

DUNCAN, B., KIM, C. & ROTELLO, V. M. 2010. Gold nanoparticle platforms as drug and biomacromolecule delivery systems. *Journal of Controlled Release,* 148**,** 122-127.

EDELSTEIN, M. L., ABEDI, M. R. & WIXON, J. 2007. Gene therapy clinical trials worldwide to 2007—an update. *The journal of gene medicine,* 9**,** 833-842.

EDINGER, D. & WAGNER, E. 2011. Bioresponsive polymers for the delivery of therapeutic nucleic acids. *Wiley interdisciplinary reviews: nanomedicine and nanobiotechnology,* 3**,** 33-46.

EL-SAYED, I. H., HUANG, X. & EL-SAYED, M. A. 2005. Surface plasmon resonance scattering and absorption of anti-EGFR antibody conjugated gold nanoparticles in cancer diagnostics: applications in oral cancer. *Nano letters,* 5**,** 829-834.

ELSABAHY, M., NAZARALI, A. & FOLDVARI, M. 2011. Non-viral nucleic acid delivery: key challenges and future directions. *Current drug delivery,* 8**,** 235-244.

FERLAY, J., SOERJOMATARAM, I., ERVIK, M., DIKSHIT, R., ESER, S., MATHERS, C., REBELO, M., PARKIN, D., FORMAN, D. & BRAY, F. 2013. Cancer Incidence and Mortality Worldwide: IARC CancerBase No. 11. Lyon, France: International Agency for Research on Cancer. GLOBOCAN 2012 v1. 0, 2013.

FORTUNE, J. A., NOVOBRANTSEVA, T. I. & KLIBANOV, A. M. 2011. Highly effective gene transfection in vivo by alkylated polyethylenimine. *Journal of drug delivery,* 2011.

FRATILA, R. M., MITCHELL, S. G., DEL PINO, P., GRAZU, V. & DE LA FUENTE, J. S. M. 2014. Strategies for the biofunctionalization of gold and iron oxide nanoparticles. *Langmuir,* 30**,** 15057-15071.

FRATODDI, I., VENDITTI, I., CAMETTI, C. & RUSSO, M. 2014. Gold nanoparticles and gold nanoparticle-conjugates for delivery of therapeutic molecules. Progress and challenges. *Journal of Materials Chemistry B,* 2**,** 4204-4220.

GHOSH, D. & CHATTOPADHYAY, N. 2013. Gold nanoparticles: acceptors for efficient energy transfer from the photoexcited fluorophores. *Optics and Photonics Journal,* 3**,** 18.

GHOSH, P., HAN, G., DE, M., KIM, C. K. & ROTELLO, V. M. 2008a. Gold nanoparticles in delivery applications. *Advanced drug delivery reviews,* 60**,** 1307-1315.

GHOSH, P. S., KIM, C.-K., HAN, G., FORBES, N. S. & ROTELLO, V. M. 2008b. Efficient gene delivery vectors by tuning the surface charge density of amino acid-functionalized gold nanoparticles. *ACS nano,* 2**,** 2213.

GIL, P. R. & PARAK, W. J. 2008. Composite nanoparticles take aim at cancer. *ACS nano,* 2**,** 2200-2205.

GILJOHANN, D. A., SEFEROS, D. S., PRIGODICH, A. E., PATEL, P. C. & MIRKIN, C. A. 2009. Gene regulation with polyvalent siRNA− nanoparticle conjugates. *Journal of the American Chemical Society,* 131**,** 2072-2073.

GUO, S. & HUANG, L. 2014. Nanoparticles containing insoluble drug for cancer therapy. *Biotechnology advances,* 32**,** 778-788.

GUO, S., HUANG, Y., JIANG, Q., SUN, Y., DENG, L., LIANG, Z., DU, Q., XING, J., ZHAO, Y. & WANG, P. C. 2010. Enhanced gene delivery and siRNA silencing by gold nanoparticles coated with charge-reversal polyelectrolyte. *ACS nano,* 4**,** 5505-5511.

GUO, X. & HUANG, L. 2012. Recent advances in non-viral vectors for gene delivery. *Accounts of chemical research,* 45**,** 971.

HAENSLER, J. & SZOKA JR, F. C. 1993. Polyamidoamine cascade polymers mediate efficient transfection of cells in culture. *Bioconjugate chemistry,* 4**,** 372-379.

HERZOG, R. W., CAO, O. & SRIVASTAVA, A. 2010. Two decades of clinical gene therapy–success is finally mounting. *Discovery medicine,* 9**,** 105.

HONDA, M., ASAI, T., OKU, N., ARAKI, Y., TANAKA, M. & EBIHARA, N. 2013. Liposomes and nanotechnology in drug development: focus on ocular targets. *International journal of nanomedicine,* 8**,** 495.

http://jasn.asnjournals.org/content/13/suppl_1/S117/F3.

http://www.biofeng.com/zaiti/buru/pCMV-Green-Renilla-Luc.html.

https://www.cancer.gov/publications/dictionaries/cancer-terms?cdrid=46283.

HU, M., QIAN, L., BRIÑAS, R. P., LYMAR, E. S., KUZNETSOVA, L. & HAINFELD, J. F. 2008. Gold nanoparticle–protein arrays improve resolution for cryo-electron microscopy. *Journal of structural biology,* 161**,** 83-91.

HUANG, Y., YU, F., PARK, Y.-S., WANG, J., SHIN, M.-C., CHUNG, H. S. & YANG, V. C. 2010. Co-administration of protein drugs with gold nanoparticles to enable percutaneous delivery. *Biomaterials,* 31**,** 9086-9091.

IBRAHEEM, D., ELAISSARI, A. & FESSI, H. 2014. Gene therapy and DNA delivery systems. *International journal of pharmaceutics,* 459**,** 70-83.

INDIRA, T. & LAKSHMI, P. 2010. Magnetic nanoparticles–a review. *Int. J. Pharm. Sci. Nanotechnol,* 3**,** 1035-1042.

JANG, H., RYOO, S.-R., KOSTARELOS, K., HAN, S. W. & MIN, D.-H. 2013. The effective nuclear delivery of doxorubicin from dextran-coated gold nanoparticles larger than nuclear pores. *Biomaterials,* 34**,** 3503-3510.

JIANG, W., KIM, B. Y., RUTKA, J. T. & CHAN, W. C. 2008. Nanoparticle-mediated cellular response is size-dependent. *Nature nanotechnology,* 3**,** 145-150.

JIN, L., ZENG, X., LIU, M., DENG, Y. & HE, N. 2014a. Current progress in gene delivery technology based on chemical methods and nano-carriers. *Theranostics,* 4**,** 240.

JUNQUERA, E. & AICART, E. 2014. Cationic lipids as transfecting agents of DNA in gene therapy. *Current topics in medicinal chemistry,* 14**,** 649-663.

KANNAN, R., NANCE, E., KANNAN, S. & TOMALIA, D. 2014. Emerging concepts in dendrimer-based nanomedicine: from design principles to clinical applications. *Journal of internal medicine,* 276**,** 579-617.

KATRAGADDA, C. S., CHOUDHURY, P. K. & MURTHY, P. 2010. Nanoparticles as non-viral gene delivery vectors. *Indian J Pharm Educ Res,* 44**,** 109-111.

KENDIRCI, M., TELOKEN, P. E., CHAMPION, H. C., HELLSTROM, W. J. & BIVALACQUA, T. J. 2006. Gene therapy for erectile dysfunction: fact or fiction? *european urology,* 50**,** 1208-1222.

KESHARWANI, P., BANERJEE, S., GUPTA, U., AMIN, M. C. I. M., PADHYE, S., SARKAR, F. H. & IYER, A. K. 2015. PAMAM dendrimers as promising nanocarriers for RNAi therapeutics. *Materials Today,* 18**,** 565-572.

KICHEV, A., ROUSSET, C. I., BABURAMANI, A. A., LEVISON, S. W., WOOD, T. L., GRESSENS, P., THORNTON, C. & HAGBERG, H. 2014. Tumor necrosis factor-related apoptosis-inducing ligand (TRAIL) signaling and cell death in the immature central nervous system after hypoxia-ischemia and inflammation. *Journal of Biological Chemistry,* 289**,** 9430-9439.

KILLOPS, K. L., CAMPOS, L. M. & HAWKER, C. J. 2008. Robust, efficient, and orthogonal synthesis of dendrimers via thiol-ene "click" chemistry. *Journal of the American Chemical Society,* 130**,** 5062-5064.

KIM, C. S., DUNCAN, B., CRERAN, B. & ROTELLO, V. M. 2013. Triggered nanoparticles as therapeutics. *Nano today,* 8**,** 439-447.

KIM, D. & JON, S. 2012. Gold nanoparticles in image-guided cancer therapy. *Inorganica Chimica Acta,* 393**,** 154-164.

KIM, J.-B., CHOI, J. S., NAM, K., LEE, M., PARK, J.-S. & LEE, J.-K. 2006. Enhanced transfection of primary cortical cultures using arginine-grafted PAMAM dendrimer, PAMAM-Arg. *Journal of controlled release,* 114**,** 110-117.

KLEIN, S., ZOLK, O., FROMM, M., SCHRÖDL, F., NEUHUBER, W. & KRYSCHI, C. 2009. Functionalized silicon quantum dots tailored for targeted siRNA delivery. *Biochemical and biophysical research communications,* 387**,** 164-168.

KNIPE, J. M., PETERS, J. T. & PEPPAS, N. A. 2013. Theranostic agents for intracellular gene delivery with spatiotemporal imaging. *Nano today,* 8**,** 21-38.

KOMPELLA, U. B., AMRITE, A. C., RAVI, R. P. & DURAZO, S. A. 2013. Nanomedicines for back of the eye drug delivery, gene delivery, and imaging. *Progress in retinal and eye research,* 36**,** 172-198.

KRIEG, A. M., YI, A.-K., MATSON, S., WALDSCHMIDT, T. J., BISHOP, G. A., TEASDALE, R., KORETZKY, G. A. & KLINMAN, D. M. 1995. CpG motifs in bacterial DNA trigger direct B-cell activation. *Nature,* 374**,** 546-549.

KUMAR, S. S. D., SURIANARAYANAN, M., VIJAYARAGHAVAN, R., MANDAL, A. B. & MACFARLANE, D. 2014. Curcumin loaded poly (2-hydroxyethyl methacrylate) nanoparticles from gelled ionic liquid–In vitro cytotoxicity and anti-cancer activity in SKOV-3 cells. *European Journal of Pharmaceutical Sciences,* 51**,** 34-44.

LEE, I. H., KWON, H. K., AN, S., KIM, D., KIM, S., YU, M. K., LEE, J. H., LEE, T. S., IM, S. H. & JON, S. 2012. Imageable Antigen-Presenting Gold Nanoparticle Vaccines for Effective Cancer Immunotherapy In Vivo. *Angewandte Chemie,* 124**,** 8930-8935.

LEE, J.-S., GREEN, J. J., LOVE, K. T., SUNSHINE, J., LANGER, R. & ANDERSON, D. G. 2009. Gold, poly (β-amino ester) nanoparticles for small interfering RNA delivery. *Nano letters,* 9**,** 2402-2406.

LI, J.-M., ZHAO, M.-X., SU, H., WANG, Y.-Y., TAN, C.-P., JI, L.-N. & MAO, Z.-W. 2011. Multifunctional quantum-dot-based siRNA delivery for HPV18 E6 gene silence and intracellular imaging. *Biomaterials,* 32**,** 7978-7987.

LIN, A. Y., ALMEIDA, J. P. M., BEAR, A., LIU, N., LUO, L., FOSTER, A. E. & DREZEK, R. A. 2013. Gold nanoparticle delivery of modified CpG stimulates macrophages and inhibits tumor growth for enhanced immunotherapy. *PLoS One,* 8**,** e63550.

LIU, B., YANG, M., LI, R., DING, Y., QIAN, X., YU, L. & JIANG, X. 2008. The antitumor effect of novel docetaxel-loaded thermosensitive micelles. *European Journal of Pharmaceutics and Biopharmaceutics,* 69**,** 527-534.

LIU, G., LI, D., PASUMARTHY, M. K., KOWALCZYK, T. H., GEDEON, C. R., HYATT, S. L., PAYNE, J. M., MILLER, T. J., BRUNOVSKIS, P. & FINK, T. L. 2003. Nanoparticles of compacted DNA transfect postmitotic cells. *Journal of Biological Chemistry,* 278**,** 32578-32586.

LIU, H., WANG, H., YANG, W. & CHENG, Y. 2012. Disulfide cross-linked low generation dendrimers with high gene transfection efficacy, low cytotoxicity, and low cost. *Journal of the American Chemical Society,* 134**,** 17680-17687.

LIU, Z., ZHAO, F., GAO, S., SHAO, J. & CHANG, H. 2016. The Applications of Gold Nanoparticle-Initialed Chemiluminescence in Biomedical Detection. *Nanoscale research letters,* 11**,** 460.

LLEVOT, A. & ASTRUC, D. 2012. Applications of vectorized gold nanoparticles to the diagnosis and therapy of cancer. *Chemical Society Reviews,* 41**,** 242-257.

LU, S., NEOH, K. G., HUANG, C., SHI, Z. & KANG, E.-T. 2013. Polyacrylamide hybrid nanogels for targeted cancer chemotherapy via co-delivery of gold nanoparticles and MTX. *Journal of colloid and interface science,* 412**,** 46-55.

LUTEN, J., VAN NOSTRUM, C. F., DE SMEDT, S. C. & HENNINK, W. E. 2008. Biodegradable polymers as non-viral carriers for plasmid DNA delivery. *Journal of Controlled Release,* 126**,** 97-110.

LV, H., ZHANG, S., WANG, B., CUI, S. & YAN, J. 2006. Toxicity of cationic lipids and cationic polymers in gene delivery. *Journal of Controlled Release,* 114**,** 100-109.

MANJU, S. & SREENIVASAN, K. 2012. Gold nanoparticles generated and stabilized by water soluble curcumin–polymer conjugate: Blood compatibility evaluation and targeted drug delivery onto cancer cells. *Journal of colloid and interface science,* 368**,** 144-151.

MANSOURI, S., CUIE, Y., WINNIK, F., SHI, Q., LAVIGNE, P., BENDERDOUR, M., BEAUMONT, E. & FERNANDES, J. C. 2006. Characterization of folate-chitosan-DNA nanoparticles for gene therapy. *Biomaterials,* 27**,** 2060-2065.

MARTIN, T. A., YE, L., SANDERS, A. J., LANE, J. & JIANG, W. G. 2013. Cancer invasion and metastasis: molecular and cellular perspective.

MENG LIN, M., KIM, H.-H., KIM, H., MUHAMMED, M. & KYUNG KIM, D. 2010. Iron oxide-based nanomagnets in nanomedicine: fabrication and applications. *Nano reviews,* 1**,** 4883.

MERTEN, O.-W. & GAILLET, B. 2016. Viral vectors for gene therapy and gene modification approaches. *Biochemical Engineering Journal,* 108**,** 98-115.

MINTZER, M. A. & SIMANEK, E. E. 2008. Nonviral vectors for gene delivery. *Chemical reviews,* 109**,** 259-302.

MIRKIN, C. A., LETSINGER, R. L., MUCIC, R. C. & STORHOFF, J. J. 1996. A DNA-based method for rationally assembling nanoparticles into macroscopic materials. *Nature,* 382**,** 607-609.

MOUT, R., MOYANO, D. F., RANA, S. & ROTELLO, V. M. 2012. Surface functionalization of nanoparticles for nanomedicine. *Chemical Society Reviews,* 41**,** 2539-2544.

MÜLLER-REIBLE, C. 1993. Principles, possibilities and limits of gene therapy. *Zeitschrift fur Kardiologie,* 83**,** 5-8.

NAKHLBAND, A., BARAR, J., BIDMESHKIPOUR, A., HEIDARI, H. R. & OMIDI, Y. 2010. Bioimpacts of anti epidermal growth receptor antisense complexed with polyamidoamine dendrimers in human lung epithelial adenocarcinoma cells. *Journal of biomedical nanotechnology,* 6**,** 360-369.

NAM, H. Y., HAHN, H. J., NAM, K., CHOI, W.-H., JEONG, Y., KIM, D.-E. & PARK, J.-S. 2008. Evaluation of generations 2, 3 and 4 arginine modified PAMAM dendrimers for gene delivery. *International journal of pharmaceutics,* 363**,** 199-205.

NEU, M., FISCHER, D. & KISSEL, T. 2005. Recent advances in rational gene transfer vector design based on poly (ethylene imine) and its derivatives. *The journal of gene medicine,* 7**,** 992-1009.

NICHOLS, J. W. & BAE, Y. H. 2014. EPR: evidence and fallacy. *Journal of Controlled Release,* 190**,** 451-464.

NIIDOME, T., NAKASHIMA, K., TAKAHASHI, H. & NIIDOME, Y. 2004. Preparation of primary amine-modified gold nanoparticles and their transfection ability into cultivated cells. *Chemical Communications***,** 1978-1979.

NIIDOME, Y., NIIDOME, T., YAMADA, S., HORIGUCHI, Y., TAKAHASHI, H. & NAKASHIMA, K. 2006. Pulsed-laser induced fragmentation and dissociation of DNA immobilized on gold nanoparticles. *Molecular Crystals and Liquid Crystals,* 445**,** 201/[491]-206/[496].

OISHI, M., NAKAOGAMI, J., ISHII, T. & NAGASAKI, Y. 2006. Smart PEGylated gold nanoparticles for the cytoplasmic delivery of siRNA to induce enhanced gene silencing. *Chemistry Letters,* 35**,** 1046-1047.

PAN, S., CAO, D., HUANG, H., YI, W., QIN, L. & FENG, M. 2013. A Serum-Resistant Low-Generation Polyamidoamine with PEI 423 Outer Layer for Gene Delivery Vector. *Macromolecular bioscience,* 13**,** 422-436.

PAN, Y., NEUSS, S., LEIFERT, A., FISCHLER, M., WEN, F., SIMON, U., SCHMID, G., BRANDAU, W. & JAHNEN-DECHENT, W. 2007. Size-dependent cytotoxicity of gold nanoparticles. *Small,* 3**,** 1941-1949.

PARKER, A. L., NEWMAN, C., BRIGGS, S., SEYMOUR, L. & SHERIDAN, P. J. 2003. Lipoplex-mediated transfection and endocytosis. *Expert Reviews in Molecular Medicine,* 5.

PATIL, M. L., ZHANG, M., BETIGERI, S., TARATULA, O., HE, H. & MINKO, T. 2008. Surface-modified and internally cationic polyamidoamine dendrimers for efficient siRNA delivery. *Bioconjugate chemistry,* 19**,** 1396-1403.

PATIL, M. L., ZHANG, M. & MINKO, T. 2011. Multifunctional triblock nanocarrier (PAMAM-PEG-PLL) for the efficient intracellular siRNA delivery and gene silencing. *ACS nano,* 5**,** 1877-1887.

PERRAULT, S. D. & CHAN, W. C. 2009. Synthesis and surface modification of highly monodispersed, spherical gold nanoparticles of 50− 200 nm. *Journal of the American Chemical Society,* 131**,** 17042-17043.

PETERSEN, H., FECHNER, P. M., MARTIN, A. L., KUNATH, K., STOLNIK, S., ROBERTS, C. J., FISCHER, D., DAVIES, M. C. & KISSEL, T. 2002. Polyethylenimine-graft-poly (ethylene glycol) copolymers: influence of copolymer block structure on DNA complexation and biological activities as gene delivery system. *Bioconjugate chemistry,* 13**,** 845-854.

QIU, Y., LIU, Y., WANG, L., XU, L., BAI, R., JI, Y., WU, X., ZHAO, Y., LI, Y. & CHEN, C. 2010. Surface chemistry and aspect ratio mediated cellular uptake of Au nanorods. *Biomaterials,* 31**,** 7606-7619.

RAMEZANI, N., EHSANFAR, Z., SHAMSA, F., AMIN, G., SHAHVERDI, H. R., ESFAHANI, H. R. M., SHAMSAIE, A., BAZAZ, R. D. & SHAHVERDI, A. R. 2008. Screening of medicinal plant methanol extracts for the synthesis of gold nanoparticles by their reducing potential. *Zeitschrift für Naturforschung B,* 63**,** 903-908.

RANA, S., BAJAJ, A., MOUT, R. & ROTELLO, V. M. 2012. Monolayer coated gold nanoparticles for delivery applications. *Advanced drug delivery reviews,* 64**,** 200-216.

RAVINDRA, P. 2009. Protein-mediated synthesis of gold nanoparticles. *Materials Science and Engineering: B,* 163**,** 93-98.

ROPERT, C. 1999. Liposomes as a gene delivery system. *Brazilian journal of medical and biological research,* 32.

ROSENBERG, S. A., AEBERSOLD, P., CORNETTA, K., KASID, A., MORGAN, R. A., MOEN, R., KARSON, E. M., LOTZE, M. T., YANG, J. C. & TOPALIAN, S. L. 1990. Gene transfer into humans—immunotherapy of patients with advanced melanoma, using tumor-infiltrating lymphocytes modified by retroviral gene transduction. *New England Journal of Medicine,* 323**,** 570-578.

ROSI, N. L., GILJOHANN, D. A., THAXTON, C. S., LYTTON-JEAN, A. K., HAN, M. S. & MIRKIN, C. A. 2006. Oligonucleotide-modified gold nanoparticles for intracellular gene regulation. *Science,* 312**,** 1027-1030.

ROTH, C. M. & SUNDARAM, S. 2004. Engineering synthetic vectors for improved DNA delivery: insights from intracellular pathways. *Annu. Rev. Biomed. Eng.,* 6**,** 397-426.

SEFEROS, D. S., GILJOHANN, D. A., HILL, H. D., PRIGODICH, A. E. & MIRKIN, C. A. 2007. Nano-flares: probes for transfection and mRNA detection in living cells. *Journal of the American Chemical Society,* 129**,** 15477-15479.

SHAH, N., STEPTOE, R. J. & PAREKH, H. S. 2011. Low-generation asymmetric dendrimers exhibit minimal toxicity and effectively complex DNA. *Journal of Peptide Science,* 17**,** 470-478.

SHAN, Y., LUO, T., PENG, C., SHENG, R., CAO, A., CAO, X., SHEN, M., GUO, R., TOMÁS, H. & SHI, X. 2012. Gene delivery using dendrimer-entrapped gold nanoparticles as nonviral vectors. *Biomaterials,* 33**,** 3025-3035.

SINGH, M., SINGH, S., PRASAD, S. & GAMBHIR, I. 2008. Nanotechnology in medicine and antibacterial effect of silver nanoparticles. *Digest Journal of Nanomaterials and Biostructures,* 3**,** 115-122.

SIOUD, M. 2010. Development of TLR7/8 small RNA antagonists. *RNA Therapeutics: Function, Design, and Delivery***,** 385-392.

SOMIA, N. & VERMA, I. M. 2000. Gene therapy: trials and tribulations. *Nature Reviews Genetics,* 1**,** 91-99.

STRONG, L. E. & WEST, J. L. 2011. Thermally responsive polymer–nanoparticle composites for biomedical applications. *Wiley Interdisciplinary Reviews: Nanomedicine and Nanobiotechnology,* 3**,** 307-317.

SUN, L., CHEN, P. & LIN, L. 2016. Enhanced Molecular Spectroscopy via Localized Surface Plasmon Resonance. *Applications of Molecular Spectroscopy to Current Research in the Chemical and Biological Sciences.* InTech.

SUN, X., ZHANG, G., KEYNTON, R. S., O'TOOLE, M. G., PATEL, D. & GOBIN, A. M. 2013. Enhanced drug delivery via hyperthermal membrane disruption using targeted gold nanoparticles with PEGylated Protein-G as a cofactor. *Nanomedicine: Nanotechnology, Biology and Medicine,* 9**,** 1214-1222.

SUN, Y.-N., WANG, C.-D., ZHANG, X.-M., REN, L. & TIAN, X.-H. 2011. Shape dependence of gold nanoparticles on in vivo acute toxicological effects and biodistribution. *Journal of nanoscience and nanotechnology,* 11**,** 1210-1216.

TAN, W. B., JIANG, S. & ZHANG, Y. 2007. Quantum-dot based nanoparticles for targeted silencing of HER2/neu gene via RNA interference. *Biomaterials,* 28**,** 1565-1571.

TAVERNIER, G., ANDRIES, O., DEMEESTER, J., SANDERS, N. N., DE SMEDT, S. C. & REJMAN, J. 2011. mRNA as gene therapeutic: how to control protein expression. *Journal of controlled release,* 150**,** 238-247.

THOMAS, M. & KLIBANOV, A. M. 2002. Enhancing polyethylenimine's delivery of plasmid DNA into mammalian cells. *Proceedings of the National Academy of Sciences,* 99**,** 14640-14645.

TIWARI, P. M., VIG, K., DENNIS, V. A. & SINGH, S. R. 2011. Functionalized gold nanoparticles and their biomedical applications. *Nanomaterials,* 1**,** 31-63.

UNSOY, G., YALCIN, S., KHODADUST, R., GUNDUZ, G. & GUNDUZ, U. 2012. Synthesis optimization and characterization of chitosan-coated iron oxide nanoparticles produced for biomedical applications. *Journal of Nanoparticle Research,* 14**,** 964.

VILLANUEVA, J. R., NAVARRO, M. G. & VILLANUEVA, L. R. 2016. Dendrimers as a promising tool in ocular therapeutics: Latest advances and perspectives. *International journal of pharmaceutics,* 511**,** 359-366.

WADA, K., ARIMA, H., TSUTSUMI, T., HIRAYAMA, F. & UEKAMA, K. 2005. Enhancing effects of galactosylated dendrimer/α-cyclodextrin conjugates on gene transfer efficiency. *Biological and Pharmaceutical Bulletin,* 28**,** 500-505.

WADHWANI, A., KLEIN, W. & LACOR, P. 2010. Efficient gene silencing in neural cells by functionalized gold nanoparticles. *Nanoscape,* 7**,** 6-10.

WEBSTER, D. M., SUNDARAM, P. & BYRNE, M. E. 2013. Injectable nanomaterials for drug delivery: carriers, targeting moieties, and therapeutics. *European Journal of Pharmaceutics and Biopharmaceutics,* 84**,** 1-20.

XIA, T., KOVOCHICH, M., BRANT, J., HOTZE, M., SEMPF, J., OBERLEY, T., SIOUTAS, C., YEH, J. I., WIESNER, M. R. & NEL, A. E. 2006. Comparison of the abilities of ambient and manufactured nanoparticles to induce cellular toxicity according to an oxidative stress paradigm. *Nano letters,* 6**,** 1794-1807.

XU, Q., KAMBHAMPATI, S. P. & KANNAN, R. M. 2013. Nanotechnology approaches for ocular drug delivery. *Middle East African journal of ophthalmology,* 20**,** 26.

XUN, M.-M., LIU, Y.-H., GUO, Q., ZHANG, J., ZHANG, Q.-F., WU, W.-X. & YU, X.-Q. 2014. Low molecular weight PEI-appended polyesters as non-viral gene delivery vectors. *European journal of medicinal chemistry,* 78**,** 118-125.

YAMAMOTO, A., KORMANN, M., ROSENECKER, J. & RUDOLPH, C. 2009. Current prospects for mRNA gene delivery. *European Journal of Pharmaceutics and Biopharmaceutics,* 71**,** 484-489.

YAMANO, S., DAI, J. & MOURSI, A. M. 2010. Comparison of transfection efficiency of nonviral gene transfer reagents. *Molecular biotechnology,* 46**,** 287-300.

YEN, H. J., HSU, S. H. & TSAI, C. L. 2009. Cytotoxicity and immunological response of gold and silver nanoparticles of different sizes. *Small,* 5**,** 1553-1561.

YIN, H., KANASTY, R. L., ELTOUKHY, A. A., VEGAS, A. J., DORKIN, J. R. & ANDERSON, D. G. 2014. Non-viral vectors for gene-based therapy. *Nature reviews. Genetics,* 15**,** 541.

YIN, W., XIANG, P. & LI, Q. 2005. Investigations of the effect of DNA size in transient transfection assay using dual luciferase system. *Analytical biochemistry,* 346**,** 289-294.

YOSHIDA, H., NISHIKAWA, M., YASUDA, S., MIZUNO, Y., TOYOTA, H., KIYOTA, T., TAKAHASHI, R. & TAKAKURA, Y. 2009. TLR9-dependent systemic interferon-β production by intravenous injection of plasmid DNA/cationic liposome complex in mice. *The journal of gene medicine,* 11**,** 708-717.

ZHANG, J., DU, J., HAN, B., LIU, Z., JIANG, T. & ZHANG, Z. 2006. Sonochemical formation of single-crystalline gold nanobelts. *Angewandte Chemie,* 118**,** 1134-1137.

ZHENG, D., SEFEROS, D. S., GILJOHANN, D. A., PATEL, P. C. & MIRKIN, C. A. 2009. Aptamer nano-flares for molecular detection in living cells. *Nano letters,* 9**,** 3258-3261.

ZHOU, J., RALSTON, J., SEDEV, R. & BEATTIE, D. A. 2009. Functionalized gold nanoparticles: synthesis, structure and colloid stability. *Journal of Colloid and Interface Science,* 331**,** 251-262.

ZHOU, M., ZHANG, X., YANG, Y., LIU, Z., TIAN, B., JIE, J. & ZHANG, X. 2013a. Carrier-free functionalized multidrug nanorods for synergistic cancer therapy. *Biomaterials,* 34**,** 8960-8967.

ZHOU, Z., MA, X., JIN, E., TANG, J., SUI, M., SHEN, Y., VAN KIRK, E. A., MURDOCH, W. J. & RADOSZ, M. 2013b. Linear-dendritic drug conjugates forming long-circulating nanorods for cancer-drug delivery. *Biomaterials,* 34**,** 5722-5735.

ZHU, H., JIANG, R., XIAO, L. & ZENG, G. 2010. Preparation, characterization, adsorption kinetics and thermodynamics of novel magnetic chitosan enwrapping nanosized γ-Fe 2 O 3 and multi-walled carbon nanotubes with enhanced adsorption properties for methyl orange. *Bioresource technology,* 101**,** 5063-5069.

CHAPTER 3

Starburst Poly-amidoamine Dendrimer Grafted Gold Nanoparticles as a Scaffold for Folic Acid-Targeted Plasmid DNA Delivery *in vitro*

Submitted to Colloids and Surfaces B Biointerfaces

Londiwe Simphiwe Mbatha and Moganavelli Singh*

Non-Viral Gene Delivery Laboratory, Discipline of Biochemistry University of KwaZulu-Natal, School of Life Sciences, Private Bag X54001, Durban 4000, South Africa Corresponding Author:singhm1@ukzn.ac.za

Abstract

Gene therapy has opened doors for the treatment of genetic disorders such as cancer. However, for years, its clinical application has been limited by safety-efficacy issues. Recently, dendritic stabilized metal nanoparticles have shown great potential as efficient non-viral modalities for plasmid DNA (pDNA) delivery. The objective was to synthesise, characterise and evaluate the cytotoxicity profiles and capacity of unmodified and folic acid (FA) modified poly-amidoamine generation 5 (PAMAM G5D) grafted gold nanoparticles (AuNPs) to deliver pDNA containing a luciferase gene (pCMV *Luc*-DNA) to various cancer cell lines. The same parameters of unmodified and folic acid modified PAMAM G5D control nanoparticles (G5D/G5D:FA NPs) were also evaluated for comparative studies. Nanocomplexes prepared with folic acid untargeted/targeted PAMAM grafted gold nanoparticles and pDNA were characterised by TEM, NTA, UV spectroscopy, NMR spectroscopy, band shift, ethidium bromide dye displacement and nuclease protection assays. Cytotoxicity profiles and gene expression were evaluated in five mammalian cell lines, HEK293, HepG2, Caco-2, MCF-7, and KB, using the MTT and luciferase reporter gene assays. Nanocomplexes at optimum $^{w}/_{w}$ ratios of 5.2:1 and 6.0:1, protected the pDNA against serum nucleases and were well tolerated by all cell lines. Transgene expression was higher with FA targeted dendrimer grafted AuNPs (Au:G5D:FA), in FA-receptor overexpressing MCF-7 and KB cells, compared to the G5D/G5D:FA NPs, decreasing significantly ($p < 0.05$) in the presence of excess FA ligand, confirming nanocomplex uptake via receptor mediation. Overall, the transfection efficiency of the Au:G5D:FA nanocomplexes superseded that of the G5D/G5D:FA nanocomplexes indicating the importance of dendrimer modification and the significant role of AuNPs in the formulation of these delivery systems.

Keywords*:* *pDNA, PAMAM dendrimers, Gold nanoparticles, Folic acid, Gene expression*

3.1 Introduction

Cancer, characterised by deregulated cell growth, has remained one of the leading causes of deaths around the world (Ferlay *et al.*, 2013), with treatments such as surgery, radiation, hormone, and chemotherapy not producing the ultimate desired effect (Liu *et al.*, 2008). Gene therapy has emerged as a useful therapeutic approach for the treatment of cancer, and other acquired and inherited disorders (Xiao *et al.*, 2013).

The introduction of a naked gene such a plasmid DNA (pDNA) into diseased cells is usually associated with poor gene expression due to the physiological barriers encountered by the DNA on its way to the target site, ultimately affecting its cellular biodistribution and bioavailability. These barriers include degradation by extracellular enzymes (nucleases and proteases), limited cellular uptake due to its hydrophilicity and size, accumulation and degradation by intracellular enzymes (lysozymes) and limited uptake into the nucleus of targeted cells due to nuclear pore size restriction (Elsabahy *et al.*, 2011). Consequently, a number of viral and non-viral gene delivery modalities, have been formulated and extensively studied both *in vitro* and *in vivo,* in an effort to enhance delivery. However, the safety-efficacy balance has limited their clinical application.

Viral systems, elicit high gene expression, but their associated inherent toxicity and immunogenicity are hurdles encountered in gene therapy studies (Merten and Gaillet, 2016). Non-viral based modalities formulated with peptides, polymers, lipids, and liposomes are safer alternatives but are associated with modest transfection efficiency (Nayerossadat *et al.*, 2012).

The merging of gene therapy and nanotechnology provides a powerful platform which promises to address the issues of safety and gene transfection efficiency associated with non-viral delivery systems (Scholz and Wagner, 2012). A combination of the unique properties of metal nanoparticles such as gold (Au), silver (Ag), selenium (Se), iron oxide, and platinum (Pt), with those of cationic polymers, have the potential to produce safe and efficient delivery systems (Katragadda *et al.*, 2010). AuNPs have been used in various biomedical applications, due to their ease of synthesis, robustness, tunable stability, biodegradability, biocompatibility, low cytotoxicity, and synthetic surface amenability (Sardar *et al.*, 2009, Fratoddi *et al.*, 2014, Lazarus and Singh, 2016).

Many cationic polymers such as dendrimers, poly-L-lysine (PLL), polyethyleneimine (PEI), polyethylene glycol (PEG), poly-D-lactide-co-glycolide (PLGA), and chitosan have been used as stabilizers of metal nanoparticles (Xiao *et al.*, 2013), with dendrimers being the least exploited. The stabilizing of metal nanoparticles with dendrimers such as PAMAM is preferred mainly due to their hyperbranched, well-defined tree-like structure with surface functionalities that can host multiple therapeutic biomolecules (Chaplot and Rupenthal, 2014). Dendrimers are protonated at physiological pH, enabling them to complex with and condense pDNA, enhancing its efficient delivery into cells (Smith, 2008). Their buffering capacity due to the hydrophilic tertiary internal amines, facilitate rapid dissociation of the DNA cargo in the cytoplasm, avoiding lysosomal degradation, and improving transgene expression (Kambhampati *et al.*, 2015). It has been reported that these amines along with those situated at the periphery (primary) of the dendrimers can also elicit increased cytotoxicity when abundant, especially at higher generations (>5) (Xiao *et al.*, 2013). Modifying surface amines via pegylation, methylation, alkylation, acetylation, and conjugation with vitamins or amino acids, greatly decreased their cytotoxicity, without compromising their desired effects (Luo *et al.*, 2002, Lee *et al.*, 2003, Kim *et al.*, 2004). Since Crooks and colleagues first introduced dendrimers as suitable metal nanoparticle stabilizers, a number of studies have been reported over the years (Crooks *et al.*, 2001, Shan *et al.*, 2012, Yuan *et al.*, 2013, Figueroa *et al.*, 2014).

Polymers possess a surface that can host multiple biomolecules at a time and can be synthetically modified with targeting ligands such as carbohydrates, antibodies, proteins, and vitamins for targeted gene expression to the site of pathology (Chaplot and Rupenthal, 2014). FA has been extensively used due to its regulation of replication, cell growth and protein synthesis (Llevot and Astruc, 2012), is small, non-immunogenic, readily available, biodegradable, and easily conjugated to other biomolecules (Chen *et al.*, 2013). Furthermore, it has a high affinity for FA receptors (FA-Rs) (glycophosphatidylinositols membrane proteins) overexpressed by a majority of cancer cells, particularly breast (MCF-7), and cervical (KB) cells, (Figure 3.1) (Mansoori *et al.*, 2010). This study focused on designing, characterising and evaluating the cytotoxicity profiles and ability of untargeted and FA targeted PAMAM grafted AuNPs to deliver a reporter plasmid (pCMV-*Luc* DNA) to various mammalian cell lines.

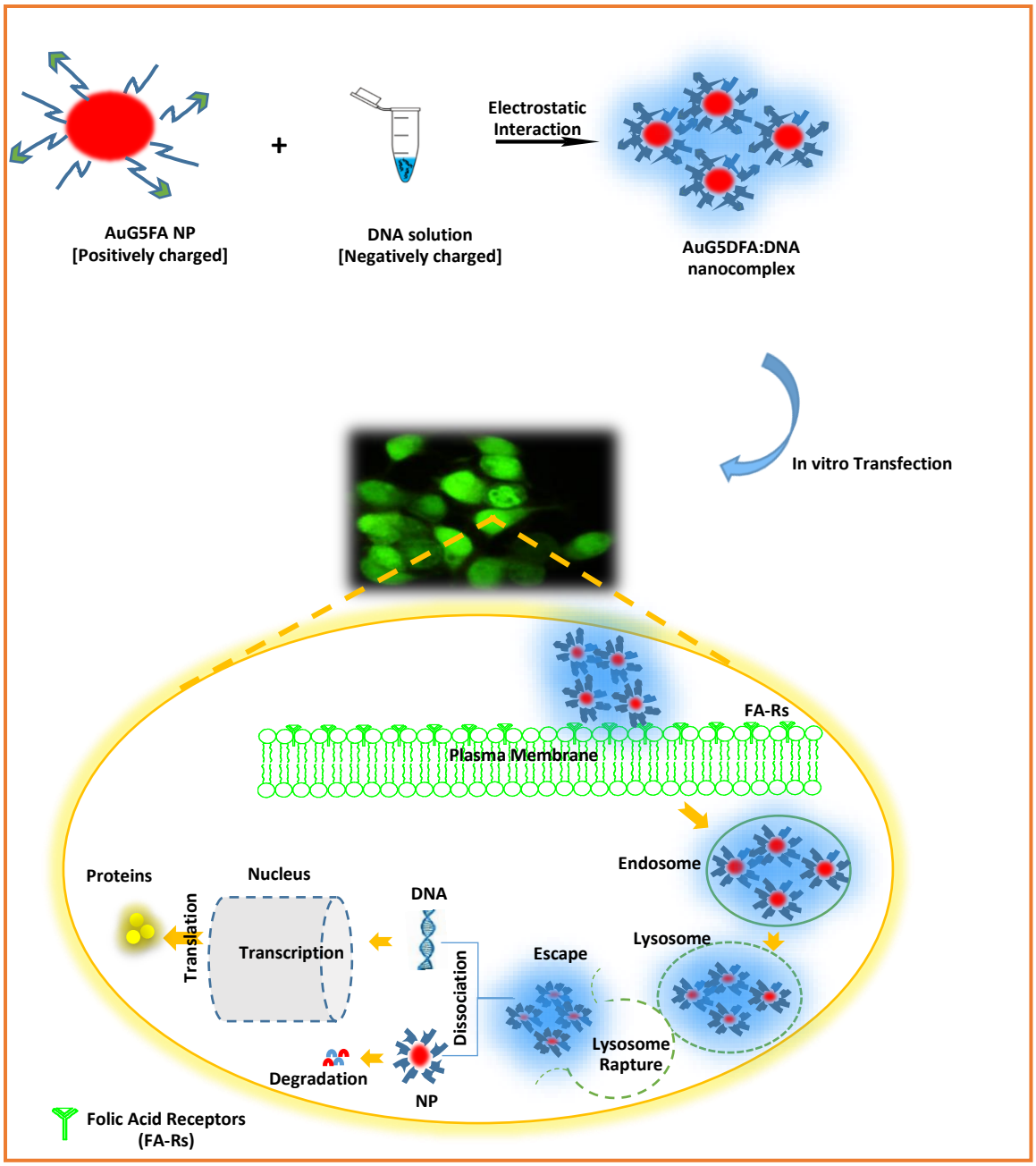

Figure 3.1: Schematic representation of FA receptor-mediated uptake of AuG5DFA:DNA nanocomplex.

3.2 Materials and Methods

3.2.1 Materials

Methanolic solution of starburst PAMAM dendrimer, generation five (PAMAM G5D), (Mw 28,826, 128 surface amino groups), gold (III) chloride trihydrate ($HAuCl_4$), bicinchoninic acid (BCA), folic acid, 1-(3-dimethylaminopropyl)-3-ethylcarbodiimide (EDC), dimethylformamide (DMF), sodium dodecylsulphate (SDS) and benzolylated dialysis tubing (MWCO 12,000 Da) were supplied by Sigma-Aldrich (St. Louis, MO, USA). Ultra-pure DNA grade agarose was acquired from Bio-Rad Laboratories (Richmond, VA, USA). Tris (hydroxymethyl)-aminomethane hydrochloride (Tris-HCl), 3-(4, 5-dimethylthiazol- 2-yl)-2,5- diphenyltetrazolium bromide (MTT), 2-[4-(2-hydroxyethyl)-1-piperazinyl] ethane sulphonic acid (HEPES), dimethyl sulphoxide (DMSO), and ethidium bromide (ETB) were purchased from Merck (Darmstadt, Germany). Minimum Essential Medium (EMEM) containing Earle's salts and L-glutamine, penicillin (500 units/mL)/streptomycin (5000 µg/mL) and trypsin-versene were purchased from Lonza-BioWhittaker (Walkersville, MD, USA). Foetal bovine serum (FBS) was purchased from Hyclone (Utah, USA). Human breast adenocarcinoma cells (MCF-7) and Human embryonic kidney cells (HEK293) were obtained from American Type Culture Collection (Manassas, VA, USA). Human hepatocellular carcinoma cells (HepG2) and Human epithelial colorectal adenocarcinoma cells (Caco-2) were purchased from Highveld Biologicals (Pty) Ltd. (Kelvin, South Africa). Human cervical adenocarcinoma cells (KB) were obtained from the Institute of Biological Chemistry, Academia Sinica, Nankang, Taipei. Plasmid pCMV-*Luc* DNA (6.2 kbp) was purchased from Plasmid Factory (Bielefeld, Germany).

3.2.2 Methods

3.2.2.1 Modification of PAMAM G5D with Folic Acid (G5D:FA conjugate)

PAMAM G5 NH_2 (in 5% $^{w}/_{v}$ methanol) was dried under a nitrogen atmosphere and then dissolved in 18 MOhm water. FA ($C_{19}H_{19}N_7O_6$) was conjugated to the amino groups of G5D via a carbodiimide reaction as previously described (Wiener *et al.*, 1997, Wang *et al.*, 2011) (Figure 3.2). Briefly, FA, 2.8 µmol (1.23 mg), was dissolved in 3 mL of DMF and reacted with 38.2 µmol (7.3 mg) of EDC for 45 minutes under N_2 with constant stirring.

Thereafter, the activated FA was added drop-wise into G5D solution (3 µmol, 100 µL) solution with vigorous stirring. The pH of the solution was adjusted to 9.5, followed by a further 3 days stirring under nitrogen. This solution was then dialyzed (MWCO 12, 000 Da) against 18 MOhm water for 24 hours, to remove excess unreacted by-products.

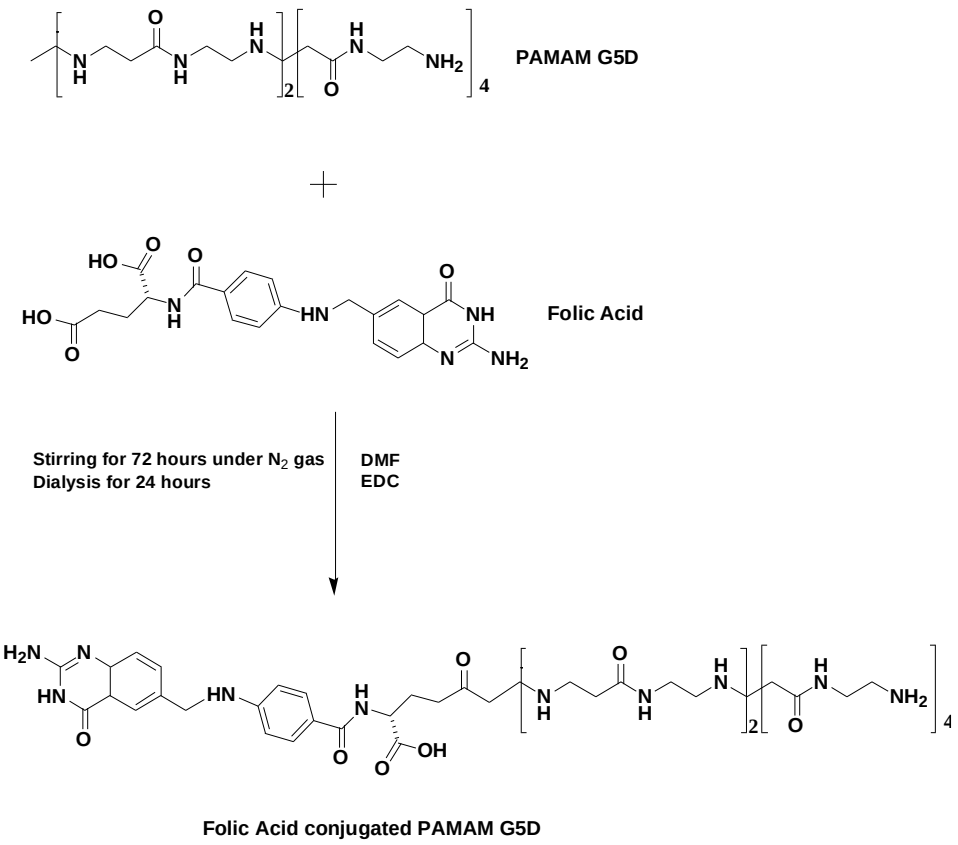

Figure 3.2: Schematic representation of the synthesis of folic acid conjugated PAMAM G5D.

3.2.2.2 Synthesis of Gold Nanoparticles (AuNPs)

AuNPs were synthesised by an adaptation of the Turkevich method (Turkevich *et al.*, 1951). Briefly, 0.1 mL of 0.03 M chloroauric acid ($HAuCl_4$) solution was dissolved in 25 mL of MOhm water, stirred vigorously and heated until boiling (15 minutes). Thereafter, 1 mL of 1% Trisodium citrate ($Na_3C_6H_5O_7$) solution was slowly added with stirring to the reaction mixture until a cherry red colour change was evident. The mixture was then removed from the heat and stirred until it cooled to room temperature.

3.2.2.3 Synthesis of Dendrimer Grafted AuNPs (Au:G5D NPs) and Folic Acid Targeted Dendrimer Grafted AuNPs (Au:G5D NPs)

The unmodified G5D and previously synthesised G5D:FA conjugates were used as templates as demonstrated**:**

$$\text{G5D} \xrightarrow[\text{EDC}]{\text{FA}} \text{G5D:FA} \xrightarrow[\text{Na}_3\text{C}_6\text{H}_5\text{O}_7]{\text{HAuCl}_4} \text{Au:G5:FA}$$

The Au:G5D and Au:G5D:FA NPs were synthesised as in section 3.2.2.2 to contain a 25:1 gold/dendrimer molar ratio (Shi *et al.*, 2009). All AuNPs were dialyzed against 18 MOhm water for 1 day, to remove unreacted by-products. A total of four nano-scaffolds were successfully prepared (Figure 3.3).

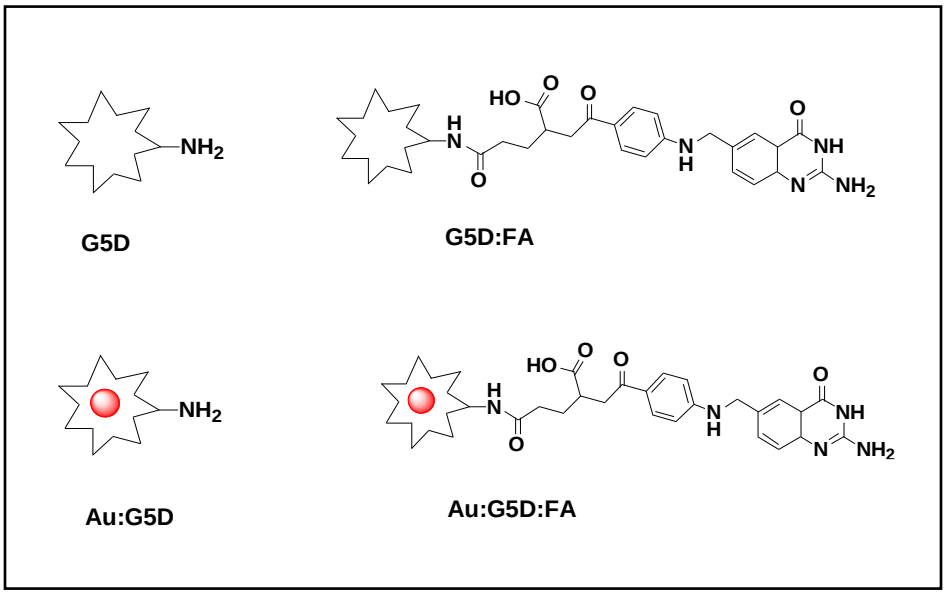

Figure 3.3: Structural illustrations of the prepared control NPs (G5D and G5D:FA) and test NPs (Au:G5D and Au:G5D:FA).

3.2.2.4 Nanocomplex Preparation

Nanocomplexes used for binding, cell viability, and transfection studies were prepared by mixing increasing amounts of G5D, Au:G5D, G5D:FA and Au:G5D:FA with 0.25 µg pCMV-*Luc* DNA in 32 µL sterile HBS. This was followed by brief mixing and centrifugation at 13000 revolutions/ minute (rpm) for 5 minutes, and a 60 minute maturation period at room temperature.

3.3.2.5 Characterisation: Transmission Electron Microscopy (TEM) and Nanoparticle Tracking Analysis (NTA)

The morphology of the synthesised nano-scaffolds and their nanocomplexes prepared at optimum binding ratios ($^{w}/_{w}$), as determined from the band shift assay were viewed at an acceleration voltage of 200 kV in a Jeol JEM-1010 transmission electron microscope, containing a Soft Imaging Systems (SIS) fitted with a MegaView III digital camera with iTEM UIP software (Tokyo, Japan). The sizes (z-average hydrodynamic diameter) and *zeta* potentials of the nano-scaffolds and their nanocomplexes were determined by nanoparticle tracking analysis (NanoSight LM10; Malvern Instruments Ltd., Worcestershire, UK) at room temperature.

3.2.2.6 Ultra-Violet (UV) and Proton Nuclear Magnetic Resonance (^{1}H NMR) Spectroscopy

The conjugation of FA and G5D onto the surface of AuNPs was monitored by UV-Vis spectroscopy (UV-1650PC, Shimadzu, Japan), followed by ^{1}H NMR spectroscopy (Bruker DRX 400), using deuterated (D_2O) water as a solvent.

3.2.2.7 DNA Binding Studies:

Band Shift Assay

To determine the ability of the prepared nano-scaffolds to bind and complex pDNA, band shift assays were conducted. Briefly, samples of preformed nanocomplexes (32 µL) containing gel loading buffer (6.4 µL, 50% glycerol, 0.05% bromophenol blue, 0.05% xylene cyanol) were subjected to electrophoresis on a 1% ($^{w}/_{v}$) agarose gels with ETB (1 µg/mL, Merck, Darmstadt,

Germany), in a Bio-Rad mini-sub electrophoresis tank containing 1 X electrophoresis buffer [36 mM Tris-HCl, 30 mM, sodium phosphate (NaH_2PO_4), 10 mM ethylenediamine tetra-acetic acid (EDTA), pH 7.5], for 1.5 hours at 50 Volts. Thereafter, the gels were viewed under UV_{300} transillumination and images captured at exposure times of 1-2 second (s) using a Vacutec Syngene G: Box BioImaging system (Syngene, Cambridge, UK).

Ethidium Bromide Intercalation Assay

The degree of complexation of the nano-scaffolds was monitored by detecting the fluorescence quenching of the DNA-ethidium bromide interaction using a Glomax®-Multi+ detection system (Promega), set at an excitation wavelength of 520 nm and an emission wavelength of 600 nm (Tros de Ilarduya *et al*., 2002). Briefly, a mixture of ETB solution (24 µL, 100 µg/mL) and HBS (100 µL) was prepared in a 96-well FluorTrac flat bottom black plate. The relative fluorescence (RF) obtained was set to 0% and was used as a baseline fluorescence reading. To set a 100% relative fluorescence, 4.8 µL (3 µg) pCMV-*Luc* DNA was then introduced to the mixture, followed by a step-wise addition of 1 µL aliquots of the prepared NPs. The RF values were recorded after each addition until a plateau in fluorescence readings was noticed.

3.2.2.8 Nuclease Protection Assay

Nuclease protection assays were conducted to monitor the integrity of the pDNA and the stability of the preformed nano-scaffolds in the presence of serum nucleases (Singh *et al*., 2003). Briefly, nanocomplexes prepared at sub-optimum, optimum, supra-optimum ratios as previously determined in section 3.2.2.7 by band shift assays, were exposed to 10% FBS for 4 hours at 37 °C. Thereafter, EDTA and SDS were introduced to the samples to final concentrations of 10 mM and 0.5% ($^{w}/_{v}$), respectively, and samples incubated at 55 °C for 20 min, followed by electrophoresis as described earlier.

3.2.2.9 Cell Culture

All cells were maintained and propagated at 37 °C and 5% CO_2, in 25 cm^2 flasks containing sterile EMEM, FBS (10%, $^{v}/_{v}$), penicillin G (100 U/mL) and streptomycin sulphate (100 μg/mL). The cells were split into desired ratios when necessary and the medium changed routinely.

3.2.2.9.1 MTT Cell Viability Assay

To monitor cell viability after treatment with prepared nanocomplexes in selected cell lines, MTT assays were conducted (Singh *et al*., 2007). Briefly, HEK293, HepG2, Caco-2, MCF-7 and KB cells were trypsinised and plated into 48-well plates at densities of 2.3 x 10^4, 2.0 x 10^4, 1.8 x 10^4, 1.3 x 10^4, 2.7 x 10^5 cells/well, respectively, and incubated for 24 hours at 37 °C. Nanocomplexes prepared in triplicate at sub-optimum, optimum and supra-optimum ratios were added thereafter, followed by a 48-hour incubation at 37 °C.

Thereafter, the medium was replaced with fresh medium (0.3 mL) and MTT reagent (0.3 mL, 5 mg/mL in PBS), followed by incubation for 4 hours at 37 °C. The EMEM/MTT mixture was then removed, cells washed with PBS (2 x 0.3 mL) and treated with DMSO (0.3 mL). Absorbance values of the samples were recorded at 570 nm in a Mindray MR-96A microplate reader. Cell viability was related to control untreated cells (100%).

3.2.2.9.2 Apoptosis Assay

Cell death was investigated using the apoptosis assay as described by Bezabeh *et al*., (2006), Maiyo *et al*., (2016). Cells with densities of 2.0-2.9 x 10^5 cells/well, were plated into 12-well plates and incubated for 24 hours at 37 °C. Thereafter, nanocomplexes at optimum ratios were introduced to the cells and incubated for 24 hours at 37 °C. Cells were washed with PBS and then treated with 10 μL of AO/ETB (acridine orange/ethidium bromide) dye (100 μg/mL AO and 100 μg/mL ETB). Morphological changes of the cells were observed using an Olympus fluorescent microscope (X200 magnification), fitted with a CC12 fluorescent camera (Olympus Co., Tokyo, Japan).
Apoptotic cell death was quantified by calculating the apoptotic index (AI) as below:

$$Apoptotic\ Index = \frac{Number\ of\ apoptotic\ cells}{Total\ number\ of\ cells}$$

3.2.2.9.3 Transfection Assay

Transfection was conducted as described by Singh *et al.* (2007). HEK293, HepG2, Caco-2, MCF-7 and KB cells with densities of 2.3- 2.7 x 10^5 cells/well, were seeded into 48-well plates and incubated for 24 hours at 37 °C. The nanocomplexes were added as previously described, and the cells were incubated for 48 hours at 37 °C. The medium was then removed, cells washed with PBS (2 x 0.5 mL) and lysed with 80 µL/well cell lysis buffer (Promega) for 15 min with shaking at 30 rpm in a Scientific STR 6 platform rocker. Cell lysates were collected by centrifugation at 12,000×g for 1 min. To 20 µL of the cell-free extract was added 50 µL luciferase assay reagent (Promega), mixed, and luminescence measured in relative light units (RLU) in a Glomax®-Multi+Detection System (Promega Biosystem, Sunnyvale, USA).

Protein concentrations of the cell-free extracts were determined using the BCA assay as described Smith *et al*., (1985), and the luciferase activity was expressed as RLU/mg protein.

3.2.2.9.4 Competition Assay

Receptor-mediated delivery of the FA-targeted nanocomplexes was confirmed by a competition assay (Singh *et al.*, 2007). FA (250 µg) was added to the cells and incubated for 20 min at 37 °C prior to addition of the nanocomplexes, followed by determination of luciferase activity as described above.

3.2.2.10 Statistical Analysis

Cell viability and transfection studies were performed in triplicate and results expressed as means ± standard deviation (S.D). The experimental data was analyzed by two-way ANOVA and *t*-test, using GraphPad Prism 6.0 and statistical significant values are indicated by $*p < 0.05$, $**p < 0.01$, and $***p < 0.001$.

3.3 Results and Discussion

3.3.1 Morphology, Size and *Zeta* Potential of Nanoparticles and Nanocomplexes

The stability of the nanoparticles under physiological conditions is essential for their biological applications. The NPs appeared spherical in shape with uniform distribution, and mean diameter sizes ranging between 65-128 nm (Figure 3.4-3.5 and Table 3.1). Nanocomplexes prepared at optimum binding ratios presented as clusters of smaller particles with mean diameters ranging from 100-150 nm, which is within the optimal size range (100-200 nm) requirements for efficient gene delivery via non-specific or receptor-specific endocytosis (Azzam and Domb, 2004, Rejman *et al.*, 2004, Grosse *et al.*, 2005). A significant difference ($p < 0.05$) in nanocomplex size is seen between the Au:G5D and G5D nanocomplexes. This could be due to the attachment of the dendrimer on the AuNP surface (Qi *et al.*, 2009).

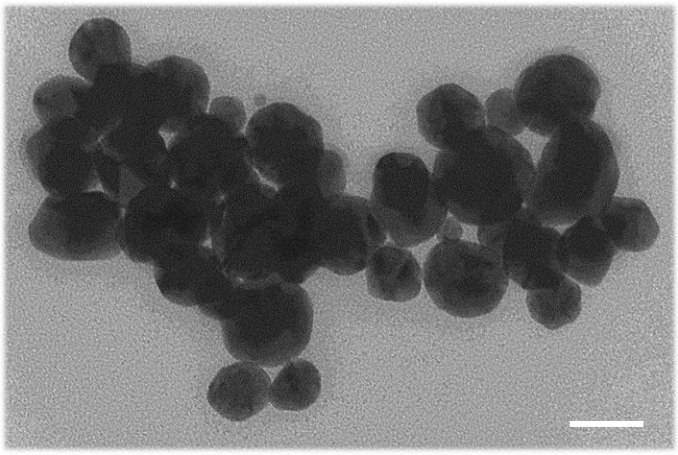

Figure 3.4: TEM micrograph of AuNPs. Scale bar = 100 nm

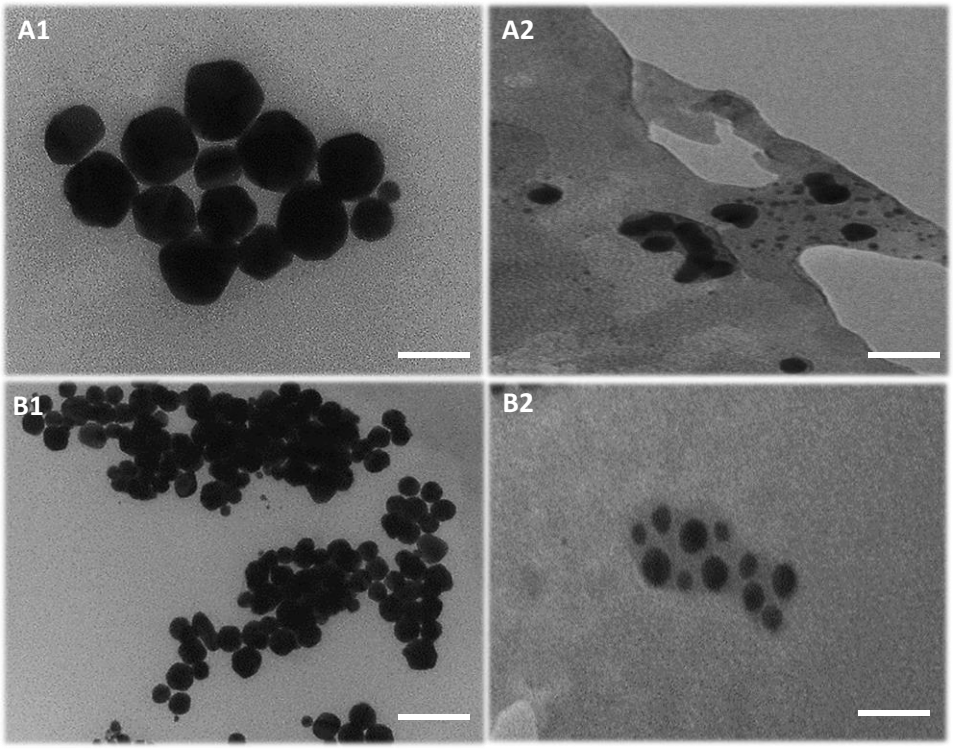

Figure 3.5: TEM micrographs of (A1) Au:G5D, (A2) Au:G5D-pDNA, (B1) Au:G5D:FA and (B2) Au:G5D:FA-pDNA. Nanocomplexes prepared at optimum weight ratio of 6.0:1 and 5.2:1 $^{w}/_{w}$ respectively. Scale bar = 100 nm

Zeta (ζ) potential reflects the degree of repulsion between the surface charge of the NPs and the surrounding solvent (Ostolska and Wiśniewska, 2014), and is closely related to stability, with the magnitude (positive or negative) predicting the degree of stability or aggregation of the NPs. Good stability has been associated with ζ potentials greater than +25 mV or less than -25 mV (Honary and Zahir, 2013). The synthesized AuNPs showed poor stability as indicated by a ζ-potential measurement of -7.3 mV (Table 3.1). However, upon conjugation with G5D and folic acid, the stability of the nano-scaffolds greatly improved as indicated by the increased ζ potentials of +20.9 mV (Au:G5D) and +29 mV (Au:G5D:FA). These findings support the notion that the ζ potential is affected by the bioconjugation of molecules onto the surface of the NPs (Ostolska and Wiśniewska, 2014).

Table 3.1: Mean size and ζ potential measurements of nano-scaffolds and their nanocomplexes. Data presented as mean diameter or ζ potential ± standard deviation (SD).

Nanoparticles and Nanocomplexes	NP:DNA ($^{w}/_{w}$) Ratio	Mean Diameter (nm) ± SD	ζ Potential (mV) ± SD
Au	-	65.90 ± 9.80	-7.3 ± 1.6
G5D	-	161.3 ± 11.9	+ 87.2 ± 2.4
Au:G5D	-	100.5 ± 44.1	+ 20.9 ± 2.2
G5D:FA	-	128.0 ± 1.20	+ 71.2 ± 3.4
Au:G5D:FA	-	77.70 ± 12.5	+ 29.0 ± 0.5
Au:G5D-pDNA	5.2:1	247.9 ± 15.3 *	- 25.0 ± 0.0
Au:G5D:FA-pDNA	6.0:1	111.7 ± 55.1	- 38.1 ± 0.4 ***
G5D-pDNA	5.2:1	144.4 ± 8.30 *	- 19.7 ± 2.0
G5D:FA-pDNA	6.0:1	114.5 ± 0.60	- 14.2 ± 0.4 ***

*$p < 0.05$, **$p < 0.01$, ***$p < 0.001$ when test nanocomplexes are compared with control nanocomplexes. NTA size and *zeta* potential distribution is reflected in the Appendix.

In general, all nano-scaffolds displayed ζ potentials ranging from +29 mV to +87 mV, while their nanocomplexes displayed ζ potentials ranging from -14 mV to -38 mV. The Au:G5D and Au:G5D:FA nanocomplexes seemed to be highly stable, based on their ζ potentials of -25 mV and -38.1 mV respectively) compared to the G5D and G5D:FA nanocomplexes, suggesting that these nano-scaffolds may be better gene delivery vectors. The improved stability is said to be due to the combined shielding effect of the targeting ligand and the encapsulated Au ions on the positive charges of the dendrimer, preventing particle aggregation. From these findings, it can be predicted that the test nano-scaffolds would be better at delivering pDNA than the control nano-scaffolds.

3.3.2 UV-Spectroscopy and ^{1}H NMR Spectroscopy

The formation of Au:G5D and Au:G5D:FA nano-scaffolds was first confirmed by UV spectroscopy. UV spectroscopy showed an absorption band at 536 nm for the AuNPs which was within the known absorption range of AuNPs (520-550 nm) (Haiss *et al.*, 2007). Moreover, a broadening and red-shift (bathochromic shift) of the absorption band to a longer wavelength of

566 nm, for the Au:G5D was evident (Figure 3.6). This is said to be due to the intermolecular hydrogen bonding in the AuNPs-G5D interaction (Pan *et al.*, 2003). The covalent attachment of FA onto the surface of NPs produces an absorption maxima at 280 nm, and a saddle point at 360 nm (Zhang *et al.*, 2003, Mansoori *et al.*, 2010) (Figure A3, Appendix A), which corresponds with the absorption peak of Au:G5D:FA observed at 287 nm.

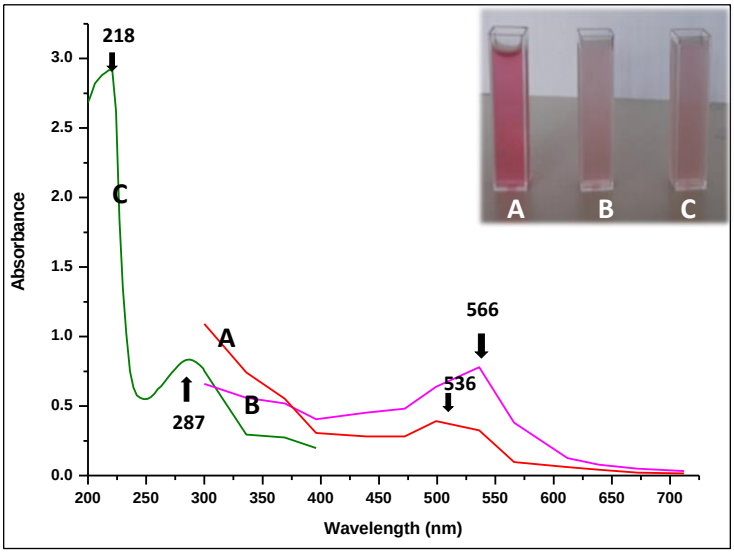

Figure 3.6: UV- Spectra of (A) AuNPs, (B) Au:G5D NPs and (C) Au:G5D:FA NPs.

The formation of Au:G5D and Au:G5D:FA nanoparticles was also verified by ^{1}H NMR spectroscopy. Significant differences in the chemical shift of protons related to Au:G5D (a), Au:G5D:FA (b), G5D:FA (c) were observed when compared to G5D (Figure A5, Appendix A). The ^{1}H NMR of the G5D shows 6 broad peaks as indicated by a chemical shift ranging from 2.25-3.34 ppm, which represents the protons of the amino (NH_2) and methylene groups (CH_2). The formation of Au:G5D nano-scaffolds resulted in the downfield shift of protons 4, 5 and 6 of G5D, which indicated the interaction of the surface of the AuNPs with the internal amines of the dendrimers (Shi *et al.*, 2009). Moreover, the three peaks between 6.50-8.63 ppm observed in Figure A5 (A-B), indicated the attachment of the FA protons [H-Ar (7 and 13), NH (18)].

All findings were correlated to those reported in literature (Zhang *et al.*, 2010, Santos *et al.*, 2010, Chang *et al*., 2012). Based on the above results it can be concluded that G5D and FA were successfully conjugated to the AuNPs.

3.3.3 Binding Studies

Band Shift Assay

The complexation of the prepared NPs with pDNA and the binding efficiency or endpoint ratios (amount of cationic NPs needed to fully compact pDNA) was first determined using the band shift assay. This is a fast and sensitive technique that was first described in the 1980s' (Fried and Crothers, 1981) and (Garner and Revzin, 1981). It is based on the principle that the mobility of the nanocomplex is usually retarded compared to that of free nucleic acid during electrophoresis (Hellman and Fried, 2007).

Figure 3.7 shows that all prepared nano-scaffolds effectively bound the pDNA, as indicated by the complete retardations at different weight ratios (indicated by the arrows). The G5D and Au:G5D NPs both completely retarded at (+/-) charge ratio of 12:1 corresponding to 5.2:1 ($^{w}/_{w}$)] ratio. Similarly the endpoint (+/-) ratios of both Au:G5D:FA and G5D:FA was at 21:1 corresponding to 6.0:1 ($^{w}/_{w}$) ratios. All FA-targeted NPs displayed higher binding charge ratios than untargeted NPs, suggesting that the cationic charges were potentially shielded by the FA moieties on the surface of the targeted NPs. As a result, an increased amount of positive charges were required to fully neutralize a fix amount (0.25 µg) of negatively charged pDNA for targeted NPs, compared to untargeted NPs (Mbatha *et al.*, 2016). Therefore, these findings verify the ability of the prepared NPs to effectively bind pDNA.

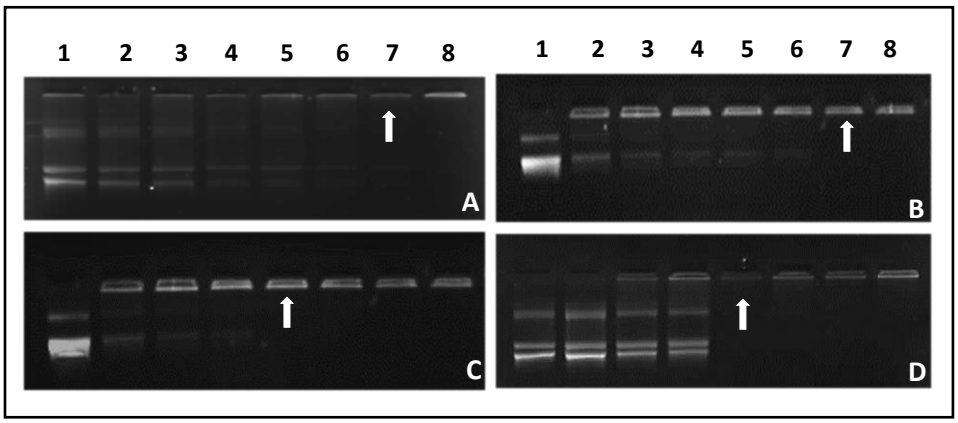

Figure 3.7: Band shift of the interaction between various nanoparticles (A) G5D, (B) Au:G5D, (C) G5D:FA, (D) Au:G5D:FA and pCMV-*Luc* plasmid DNA. Incubation mixtures (20 µL) in HBS contained varying amounts of nanoparticle preparation and 0.25 µg plasmid DNA corresponding to charge ratios of 7:1, 8:1, 9:1, 10:1, 11:1, 12:1 (5.2:1 $^{w}/_{w}$) and 13:1 in lanes 2-8 respectively (A-B); and 18:1, 19:1, 20:1, 21:1 (6.0:1 $^{w}/_{w}$), 22:1, 23:1 and 24:1 in lanes 2-8 respectively (C-D). Lane 1: naked pDNA. Arrows indicate endpoint ratios.

Ethidium Bromide Intercalation Assay

Since its early discovery in the 1960s, the ethidium bromide displacement/intercalating assay has been another simple and fast technique that is widely used to monitor the complexation and condensation of genes (LePecq and Paoletti, 1967). This assay takes advantage of the fact that when ethidium bromide (ETB), a cationic, fluorescent (excited at UV $_{300\ nm}$ light) dye intercalates between the base pairs of DNA, its fluorescence is enhanced and decreases upon interaction of the DNA with increasing amounts of cationic nano-scaffolds, until no further displacement occurs (point of infection or complete complexation) (Geall and Blagbrough, 2000, De Ilarduya *et al.*, 2002).

From figure 3.8, we can observe that all nano-scaffolds were able to displace ETB, hence confirming a possible degree of DNA compaction. The ETB displacement ranged from 10-30% for the untargeted nano-scaffolds (G5D and Au:G5D) and 50-70% for the FA-targeted nano-scaffolds. The higher displacement observed for the targeted nano-scaffolds suggest a higher degree of pDNA compaction and hence a weak binding of pDNA (Chuang and Chang, 2015). Therefore, these findings support the idea that the targeted nanocomplexes would easily release the DNA cargo upon transfection, sparing it from lysosomal degradation, hence enhancing gene transfection efficacy.

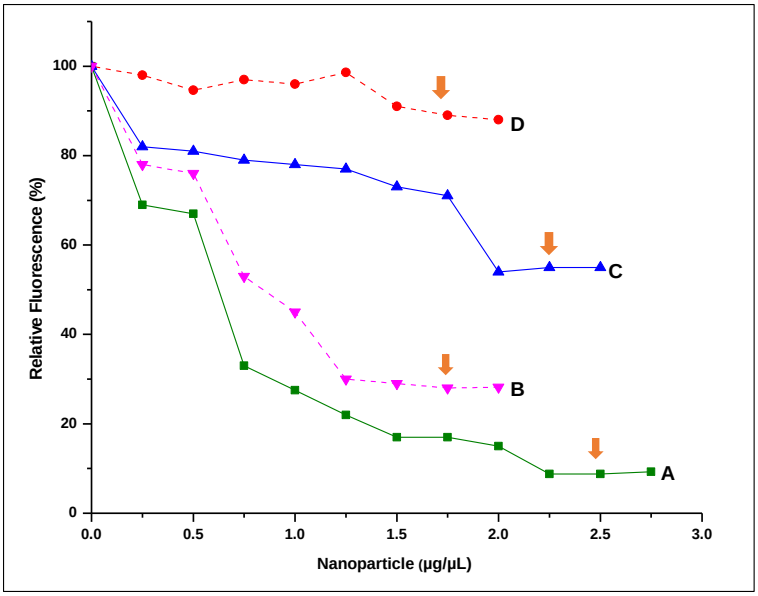

Figure 3.8: Ethidium bromide displacement assay of (A) G5D, (B) Au:G5D, (C) G5D:FA, (D) Au:G5D:FA nanoparticles. Arrows indicate point of complexation.

3.3.4 Nuclease Digestion Assay

It is known that nucleic acids are subjected to nuclease degradation upon direct or intravenous injection of nanocomplexes into cells or organs, which results in premature clearance from the bloodstream, and a decrease in gene expression (Obata *et al.*, 2009). This is a limitation that all gene delivery systems need to overcome prior to use in *in vivo* systems. Therefore, the ability of the nano-scaffolds to stably deliver the cargo DNA into the target sites in "*in vivo* like" conditions was evaluated using a nuclease digestion assay.

As expected, naked pDNA treated with 10% FBS was completely degraded as illustrated by the absence of bands. In contrast, the pDNA complexed to nano-scaffolds was partially protected as indicated by the presence of two of the three band forms of pDNA (closed circular and superhelical), and partial degradation of the linear form (Figure 3.9). This could be attributed to the highly organized globular structures that forms as a result of the electrostatic interaction between negatively charged pDNA and cationic nano-scaffolds (Pitard, 2002). In general, it can be concluded that all nano-scaffolds afforded sufficient protection to the pDNA.

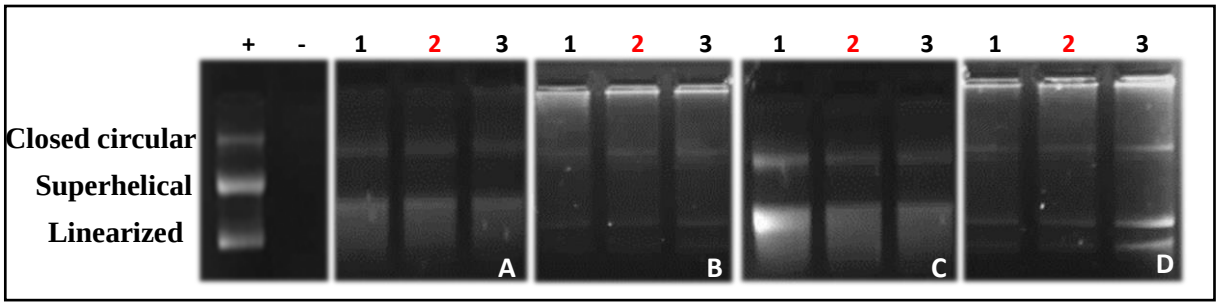

Figure 3.9: Nuclease digestion assay of nanocomplexes. (A) G5D, (B) Au:G5D, (C) G5D:FA, (D) Au:G5D:FA. Control: naked pDNA in the absence (+ = positive control) or presence (- = negative control) of FBS. Lanes 1-3 contains nanocomplexes at sub-optimum, optimum and supra-optimum nanoparticle: DNA ratios. (A) 5.5:1, 6.0:1, 6.5:1; (B) 5.5:1, 6.0:1, 6.5:1; (C) 5.0:1, 5.2:1, 5.5:1 ($^{w}/_{w}$). Red colored numbers indicate endpoint ratios.

3.3.5 MTT Cell Viability Assay

Successful gene delivery depends largely on the ability to deliver the gene safely and efficiently to the target site (Singh *et al*., 2007). Hence, cytotoxicity evaluation of the nano-carriers prior to use in transfection studies is mandatory. The MTT assay, which is based on the reduction of the tetrazolium salt, MTT, by living cells to form a blue formazan product which is spectroscopically quantified and reported as a measure of cell viability was employed (Denizot and Lang, 1986, Berridge *et al.*, 2005) to assess the cytotoxicity profiles of the nanocomplexes in four mammalian cancer cell lines, and one non-cancer cell line (HEK293).

High cell viabilities, ranging from 70%-97% were observed in the HEK293, HepG2, Caco-2 cell lines for all tested ratios after treatment with test nanocomplexes (Au:G5D:DNA and Au:G5D:FA:DNA), compared to the G5D:DNA and G5D:FA:DNA nanocomplexes (60-89%) (Figure 3.10A-B). This significant ($p < 0.05$) decrease in cytotoxicity indicated that the test nano-scaffolds were less toxic than the control nanocomplexes at these ratios. This is postulated to be due to the reduced portion of the 1^{o} amines of G5D since some are accountable for stabilizing the entrapped AuNPs (Shan *et al.*, 2012). From the test nanocomplexes, the FA-targeted G5D grafted Au nanocomplexes seemed to be the least toxic (average cell viability of 82%) compared to the untargeted G5D grafted Au nanocomplexes. This can be attributed to the G5D surface modification by the FA moieties, which may have shielded a portion of the positive charges, hence reducing the strong electrostatic interaction between the cells and the NPs (Xiao *et al.*, 2013).

Overall, there was over 70% cell survival after exposure to the test nanocomplexes, suggesting that these nanocomplexes were well tolerated in all tested cell lines, and hence safe to use in therapeutic applications.

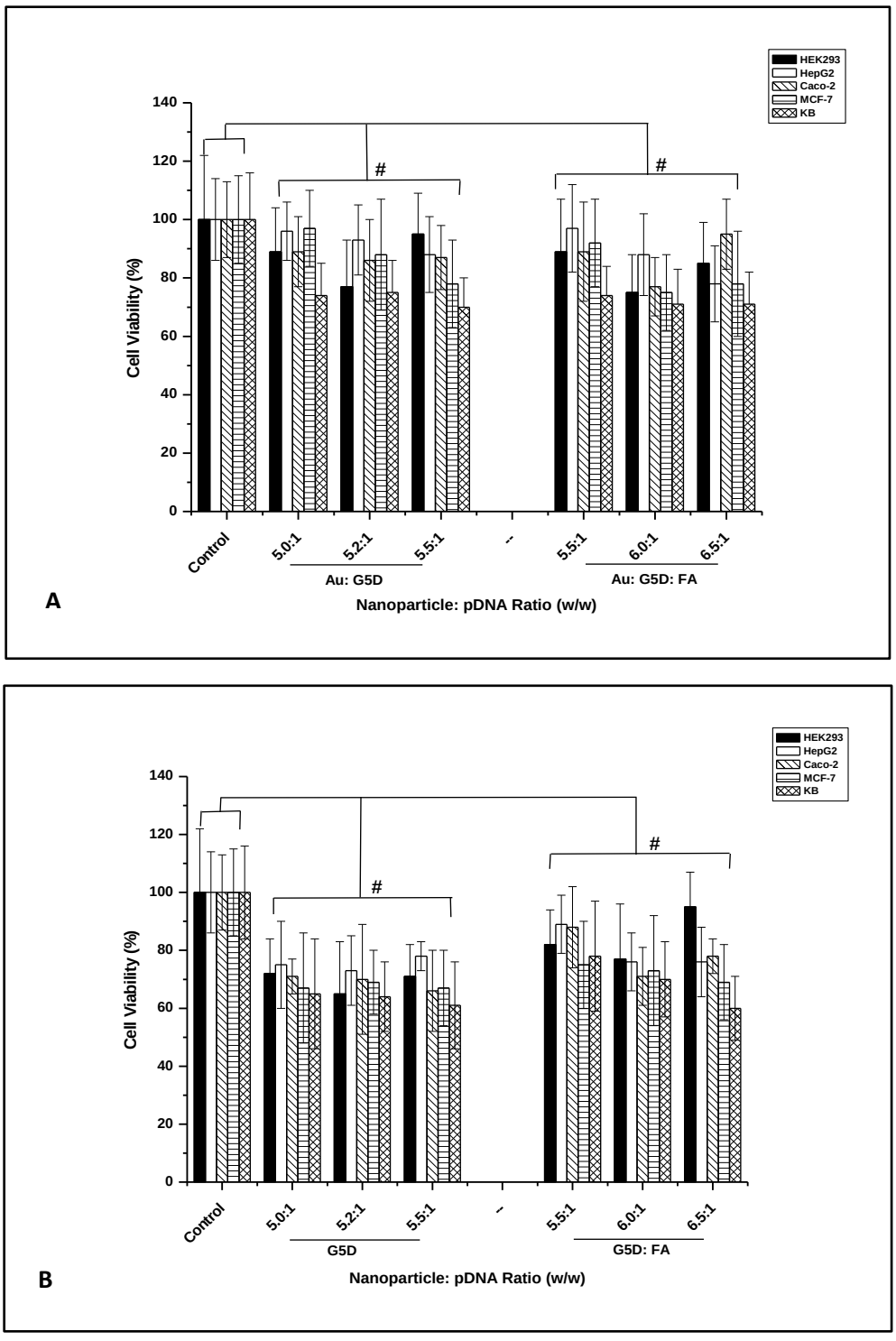

Figure 3.10 (A-B): Cell viability assay of nanocomplexes in HEK293, HepG2, Caco-2, MCF-7 and KB cells. Cells were incubated with nanocomplexes containing 0.25 µg pDNA-*Luc* at indicated ratios ($^{w}/_{w}$). Data are presented as means ± S.D. (n = 3). Control: untreated cells. #*p* >0.05.

3.3.6 Apoptosis Assay

Following nanocomplex exposure, different outcomes can be observed such as necrosis, "unprogrammed cell death" and apoptosis ("programmed cell death"). During necrosis, the cells swell and rupture the plasma membrane causing it to lose its integrity, which results in cell death due to lysis (Proskuryakov *et al.*, 2003). Apoptosis, on the other hand, is as a result of cytological and molecular events which can be seen as morphological changes such as cytoplasmic shrinkage/condensation and nuclear DNA fragmentation. These morphological changes were identified and quantified microscopically using fluorescence AO/ETB dual staining (Johnstone *et al*., 2007, Elmore, 2007). Viable cells appeared green due to the AO and the non-viable cells (apoptotic) orange due to the ETB (Figure 3.11). The AI (Table 3.2), of the Au:G5D:DNA and Au:G5D:FA:DNA nanocomplexes were significantly ($p < 0.01$) lower than those of the G5D:DNA and G5D:FA:DNA nanocomplexes (Figure 3.12). These findings correlate with the cytotoxicity profiles determined by MTT.

Table 3.2: Apoptotic Indices of NPs in selected cell lines.

Cell lines	**Apoptotic Index**				
	Control	**Au:G5D**	**Au:G5D:FA**	**G5D**	**G5D:FA**
HEK293	0.00	0.02	0.08	0.25	0.11
HepG2	0.00	0.08	0.09	0.17	0.10
Caco-2	0.00	0.07	0.14	0.50	0.31
MCF-7	0.00	0.11	0.08	0.33	0.18
KB	0.00	0.09	0.08	0.15	0.48

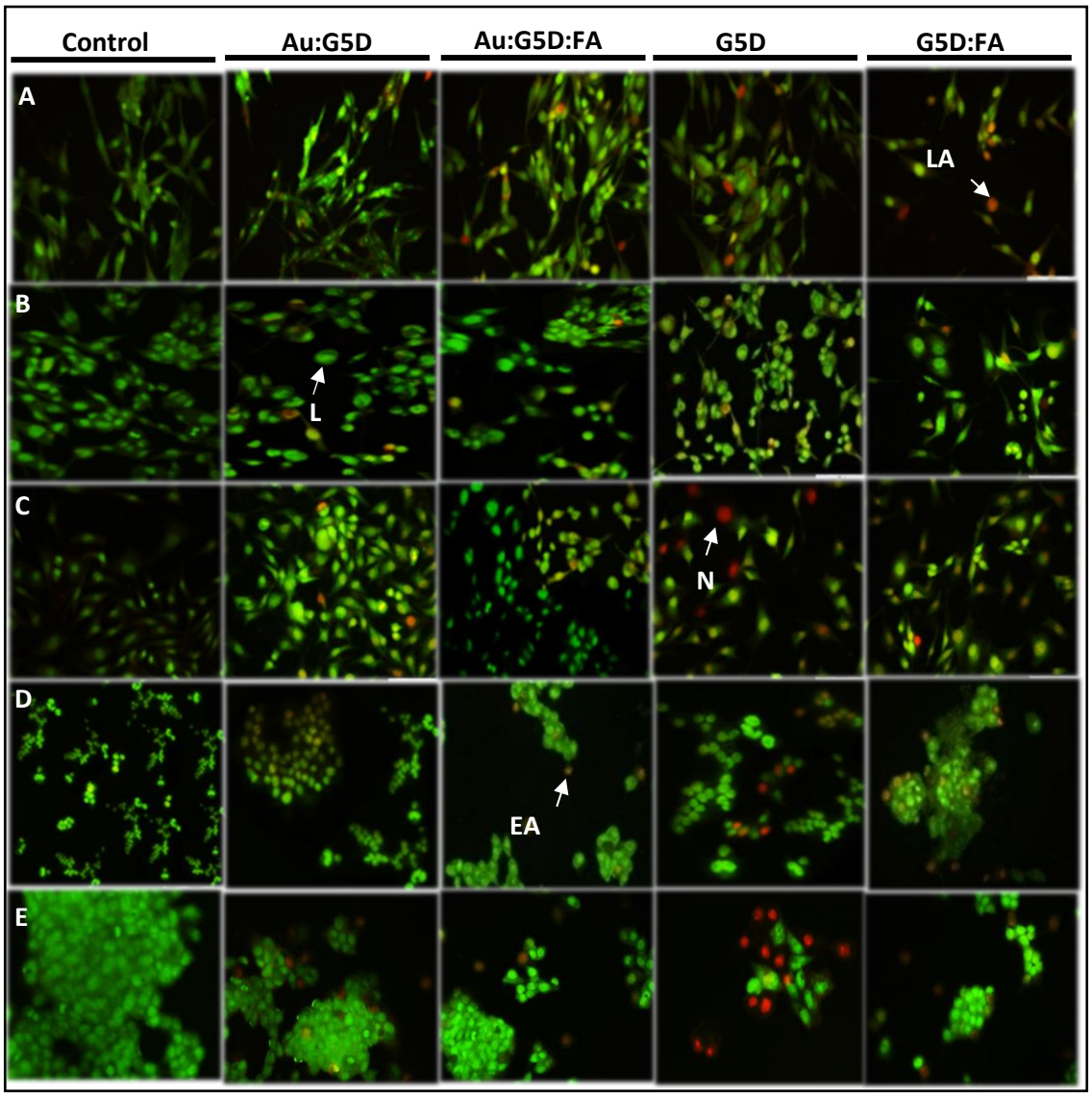

Figure 3.11: Fluorescence images of (A) HEK293, (B) HepG2, (C) Caco-2, (D) MCF-7 and (E) KB cells treated with untargeted/ targeted G5D grafted Au nanocomplexes and untargeted/ targeted G5D nanocomplexes at optimum ratios ($^{w}/_{w}$) for 24 hours showing induction of apoptosis. Green= live (L), orange= early apoptotic (EA); late apoptotic (LA) and red= necrotic (N) cells. Scale bar = 100 μm.

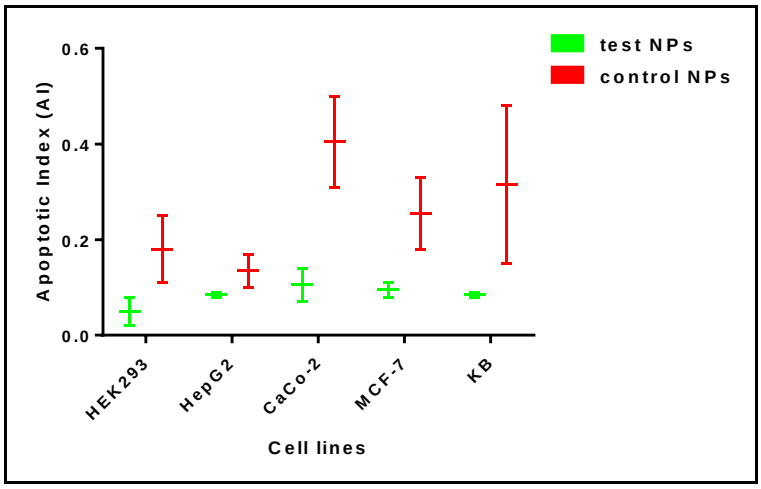

Figure 3.12: Statistical differences in AI values between test and control NPs in tested cell lines. *$p < 0.05$, **$p < 0.01$, ***$p < 0.001$ when control nanocomplexes are compared with test nanocomplexes.

3.3.7 Transfection and Competition Studies

The transfection efficiency of gene delivery systems depends on the NP's physicochemical properties such as shape, size, ζ potential, and stability. The cellular uptake of NPs/nanocomplexes, non-specific or receptor-specific involves two steps (a) attachment and (b) internalization (Sahay *et al*., 2010). NPs bind to the cell membrane mainly via electrostatic interactions. Although, negative charges predominate the cellular membrane, repelling negatively charge NPs, for cells the amount of the negative charges is not significant, suggesting the presence some cationic sites for binding of negatively charged nanocomplexes (Honary and Zahir, 2013).

The sizes of the synthesized NPs fall within the range for efficient specific/non-specific uptake. The Au:G5D:DNA and Au:G5D:FA:DNA nanocomplexes displayed high ζ potentials, indicating good colloidal stability, a property that augurs well for their systemic use. Figure 3.13 (A-B) shows that all nanocomplexes were able to transfect the selected cell lines either by non-specific or specific uptake. The buffering capacity introduced by the presence of the PAMAM G5 dendrimer could have further facilitated the endosomal escape of the nanocomplexes from the degrading lysosomes.

The transfection levels in HEK293, HepG2, Caco-2 cells were significantly ($p < 0.001$) lower than those elicited in MCF-7 and KB cells. This could be due to the lack/overexpression of specific transcription factors and cell-surface receptors (Mansoori *et al.*, 2010). The transfection activity of all nanocomplexes (Figure 3.13A-B) was high, with Au:G5D:DNA and Au:G5D:FA:DNA nanocomplexes showing more than a two-fold increase in transfection activity over the G5D:DNA and G5D:FA:DNA nanocomplexes at certain ratios. This could be due to the entrapment of AuNPs, which helped preserve the 3D spherical structure of the dendrimers, allowing for efficient dendrimer-DNA interaction (Shan *et al.*, 2012). Upon interaction with interfaces, dendrimers, particularly those with generation numbers >4, can lose their 3D spherical morphology resulting in a significant loss of binding sites, hence weakening their DNA binding ability. This explains the lower transfection levels observed for the G5D:DNA and G5D:FA:DNA nanocomplexes (Bosman *et al.*, 1999).

The highest transfection levels (8×10^6 RLU/mg protein) was observed in the FA-R positive cell lines (MCF-7 and KB). In particular, at the optimum ratios, the FA-targeted Au nanocomplexes (Figure 3.13A), showed a significant increase in transfection levels, compared to that of the untargeted Au nanocomplexes. This could be due to the interaction of the cognate FA moiety incorporated on the surface of these nano-scaffolds, with the abundant FA-receptors on the surface of the MCF and KB cells (Srinivasarao *et al.*, 2015). When the FA-R positive cells (KB) were pre-treated with an excess of free folic acid (250 μg), a significant ($p < 0.05$) drop (29%) in transgene activity by folic acid targeted nanocomplexes was observed (Figure 3.13 A-B), suggesting that only a portion of these targeted nano-scaffolds were taken up via receptor-mediated endocytosis (Zhang *et al.*, 2015). This was due to the fact that the free folic acid bound to the FA-R on the cells prior to the addition of the targeted nanocomplexes and prevented their entry into the cell.

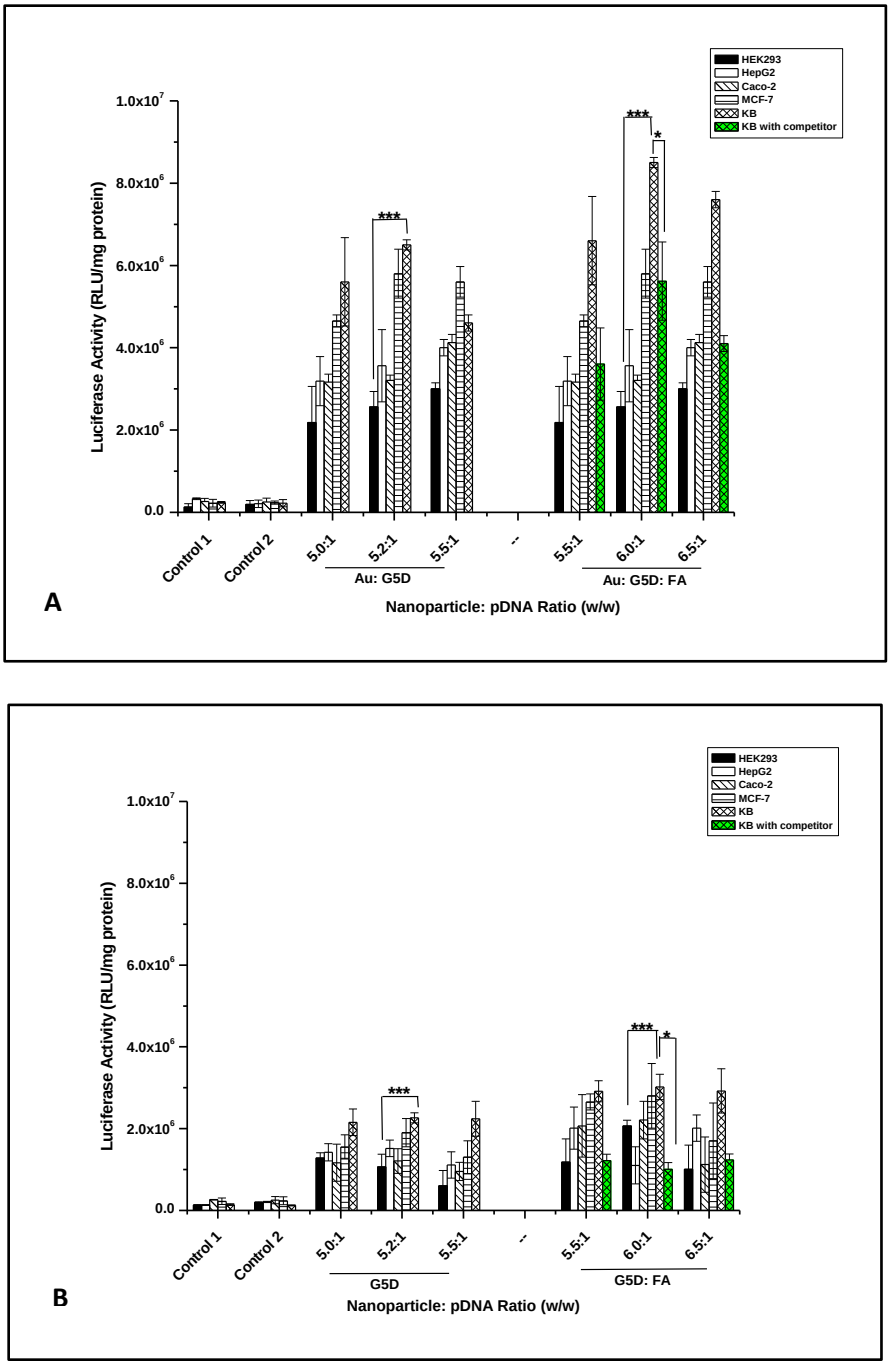

Figure 3.13 (A-B): Transfection studies of NP:pCMV-*Luc* DNA nanocomplexes. HEK293, HepG2, Caco-2, MCF-7 and KB cells were exposed to nanocomplexes constituted with 0.25 µg DNA and varying amounts of nanoparticles at sub-optimum, optimum and supra-optimum ratios. Control 1= untreated cells. Control 2= cells + pDNA. The transgene expression is reported as RLU/mg protein. Data are presented as means ± SD (n=3). *$p < 0.05$, *** $p < 0.001$ for optimum ratios.

3.4 Conclusion

Both Au:G5D and Au:G5D:FA NPs were highly efficient in pCMV-*Luc* DNA binding and delivery. They formed stable nanocomplexes affording good protection to the pDNA against nucleases. Furthermore, >70% cell viability was observed, suggesting that these nanocomplexes were well tolerated by all cell lines. Their transfection efficiency superseded that of the controls indicating the pivotal roles played by both the dendrimer and the AuNPs in their formulation. Receptor-mediated delivery was confirmed by the competition assay, where transfection levels in the FA-receptor negative cell lines, were significantly lower ($p < 0.001$) than that in FA-receptor positive cell lines. Future studies would encompass the NP optimisation for *in vivo* delivery in a mouse model.

3.5 References

AZZAM, T. & DOMB, A. J. 2004. Current developments in gene transfection agents. *Current drug delivery,* 1**,** 165-193.

BEZABEH, T., MOWAT, M., JAROLIM, L., GREENBERG, A. & SMITH, I. 2001. Detection of drug-induced apoptosis and necrosis in human cervical carcinoma cells using 1H NMR spectroscopy. *Cell death and differentiation,* 8**,** 219.

BOSMAN, A., JANSSEN, H. & MEIJER, E. 1999. About dendrimers: structure, physical properties, and applications. *Chemical reviews,* 99**,** 1665-1688.

C MAIYO, F., MOODLEY, R. & SINGH, M. 2016. Cytotoxicity, antioxidant and apoptosis studies of quercetin-3-O glucoside and 4-(β-D-glucopyranosyl-1→ 4-α-L-rhamnopyranosyloxy)-benzyl isothiocyanate from Moringa oleifera. *Anti-Cancer Agents in Medicinal Chemistry (Formerly Current Medicinal Chemistry-Anti-Cancer Agents),* 16**,** 648-656.

CHANG, Y., LIU, N., CHEN, L., MENG, X., LIU, Y., LI, Y. & WANG, J. 2012. Synthesis and characterization of DOX-conjugated dendrimer-modified magnetic iron oxide conjugates for magnetic resonance imaging, targeting, and drug delivery. *Journal of Materials Chemistry,* 22**,** 9594-9601.

CHAPLOT, S. P. & RUPENTHAL, I. D. 2014. Dendrimers for gene delivery–a potential approach for ocular therapy? *Journal of Pharmacy and Pharmacology,* 66**,** 542-556.

CHEN, Q., LI, K., WEN, S., LIU, H., PENG, C., CAI, H., SHEN, M., ZHANG, G. & SHI, X. 2013. Targeted CT/MR dual mode imaging of tumors using multifunctional dendrimer-entrapped gold nanoparticles. *Biomaterials,* 34**,** 5200-5209.

CHUANG, C.-C. & CHANG, C.-W. 2015. Complexation of bioreducible cationic polymers with gold nanoparticles for improving stability in serum and application on nonviral gene delivery. *ACS applied materials & interfaces,* 7**,** 7724-7731.

CROOKS, R. M., ZHAO, M., SUN, L., CHECHIK, V. & YEUNG, L. K. 2001. Dendrimer-encapsulated metal nanoparticles: synthesis, characterization, and applications to catalysis. *Accounts of Chemical Research,* 34**,** 181-190.

DE ILARDUYA, C. T., ARANGOA, M., MORENO-ALIAGA, M. & DÜZGÜNEŞ, N. 2002. Enhanced gene delivery in vitro and in vivo by improved transferrin-lipoplexes. *Biochimica et Biophysica Acta (BBA)-Biomembranes,* 1561**,** 209-221.

DENIZOT, F. & LANG, R. 1986. Rapid colorimetric assay for cell growth and survival. *Journal of Immunological Methods,* 89**,** 271-277.

ELMORE, S. 2007. Apoptosis: a review of programmed cell death. *Toxicologic pathology,* 35**,** 495-516.

ELSABAHY, M., NAZARALI, A. & FOLDVARI, M. 2011. Non-viral nucleic acid delivery: key challenges and future directions. *Current drug delivery,* 8**,** 235-244.

FIGUEROA, E. R., LIN, A. Y., YAN, J., LUO, L., FOSTER, A. E. & DREZEK, R. A. 2014. Optimization of PAMAM-gold nanoparticle conjugation for gene therapy. *Biomaterials,* 35**,** 1725-1734.

FRATODDI, I., VENDITTI, I., CAMETTI, C. & RUSSO, M. 2014. Gold nanoparticles and gold nanoparticle-conjugates for delivery of therapeutic molecules. Progress and challenges. *Journal of Materials Chemistry B,* 2**,** 4204-4220.

FRIED, M. & CROTHERS, D. M. 1981. Equilibria and kinetics of lac repressor-operator interactions by polyacrylamide gel electrophoresis. *Nucleic acids research,* 9**,** 6505-6525.

GARNER, M. M. & REVZIN, A. 1981. A gel electrophoresis method for quantifying the binding of proteins to specific DNA regions: application to components of the Escherichia coli lactose operon regulatory system. *Nucleic acids research,* 9**,** 3047-3060.

GEALL, A. J. & BLAGBROUGH, I. S. 2000. Rapid and sensitive ethidium bromide fluorescence quenching assay of polyamine conjugate–DNA interactions for the analysis of lipoplex formation in gene therapy. *Journal of pharmaceutical and biomedical analysis,* 22**,** 849-859.

GORLE, S., SEWBALAS, A., ARIATTI, M. & SINGH, M. 2016. Ligand-tagged cationic liposome facilitates efficient gene delivery to folate receptors. *Current Science,* 111**,** 662.

GROSSE, S., ARON, Y., THÉVENOT, G., FRANÇOIS, D., MONSIGNY, M. & FAJAC, I. 2005. Potocytosis and cellular exit of complexes as cellular pathways for gene delivery by polycations. *The journal of gene medicine,* 7**,** 1275-1286.

HAISS, W., THANH, N. T., AVEYARD, J. & FERNIG, D. G. 2007. Determination of size and concentration of gold nanoparticles from UV− Vis spectra. *Analytical chemistry,* 79**,** 4215-4221.

HELLMAN, L. M. & FRIED, M. G. 2007. Electrophoretic mobility shift assay (EMSA) for detecting protein–nucleic acid interactions. *Nature protocols,* 2**,** 1849-1861.

HONARY, S. & ZAHIR, F. 2013. Effect of zeta potential on the properties of nano-drug delivery systems-a review (Part 2). *Tropical Journal of Pharmaceutical Research,* 12**,** 265-273.

JOHNSTONE, R. W., RUEFLI, A. A. & LOWE, S. W. 2002. Apoptosis: A Link between Cancer Genetics and Chemotherapy. *Cell,* 108**,** 153-164.

KAMBHAMPATI, S. P., CLUNIES-ROSS, A. J., BHUTTO, I., MISHRA, M. K., EDWARDS, M., MCLEOD, D. S., KANNAN, R. M. & LUTTY, G. 2015. Systemic and Intravitreal Delivery of Dendrimers to Activated Microglia/Macrophage in Ischemia/Reperfusion Mouse RetinaRetinal Microglia Uptake of Dendrimers. *Investigative ophthalmology & visual science,* 56**,** 4413-4424.

KATRAGADDA, C. S., CHOUDHURY, P. K. & MURTHY, P. 2010. Nanoparticles as non-viral gene delivery vectors. *Indian J Pharm Educ Res,* 44**,** 109-111.

KIM, T.-I., SEO, H. J., CHOI, J. S., JANG, H.-S., BAEK, J.-U., KIM, K. & PARK, J.-S. 2004. PAMAM-PEG-PAMAM: novel triblock copolymer as a biocompatible and efficient gene delivery carrier. *Biomacromolecules,* 5**,** 2487-2492.

LAZARUS, G. G. & SINGH, M. 2016. Cationic modified gold nanoparticles show enhanced gene delivery in vitro. *Nanotechnology Reviews,* 5**,** 425-434.

LEE, J. H., LIM, Y.-B., CHOI, J. S., LEE, Y., KIM, T.-I., KIM, H. J., YOON, J. K., KIM, K. & PARK, J.-S. 2003. Polyplexes assembled with internally quaternized PAMAM-OH dendrimer and plasmid DNA have a neutral surface and gene delivery potency. *Bioconjugate chemistry,* 14**,** 1214-1221.

LEPECQ, J.-B. & PAOLETTI, C. 1967. A fluorescent complex between ethidium bromide and nucleic acids: physical—chemical characterization. *Journal of molecular biology,* 27**,** 87-106.

LUO, D., HAVERSTICK, K., BELCHEVA, N., HAN, E. & SALTZMAN, W. M. 2002. Poly (ethylene glycol)-conjugated PAMAM dendrimer for biocompatible, high-efficiency DNA delivery. *Macromolecules,* 35**,** 3456-3462.

MANSOORI, G. A., BRANDENBURG, K. S. & SHAKERI-ZADEH, A. 2010. A comparative study of two folate-conjugated gold nanoparticles for cancer nanotechnology applications. *Cancers,* 2**,** 1911-1928.

MANSOURI, S., CUIE, Y., WINNIK, F., SHI, Q., LAVIGNE, P., BENDERDOUR, M., BEAUMONT, E. & FERNANDES, J. C. 2006. Characterization of folate-chitosan-DNA nanoparticles for gene therapy. *Biomaterials,* 27**,** 2060-2065.

MBATHA, L., CHAKRAVORTY, S., B DE KONING, C., AL VAN OTTERLO, W., ARBUTHNOT, P., ARIATTI, M. & SINGH, M. 2016. Spacer length: a determining factor in the design of galactosyl ligands for hepatoma cell-specific liposomal gene delivery. *Current drug delivery,* 13**,** 935-945.

MERTEN, O.-W. & GAILLET, B. 2016. Viral vectors for gene therapy and gene modification approaches. *Biochemical Engineering Journal,* 108**,** 98-115.

NAYEROSSADAT, N., MAEDEH, T. & ALI, P. A. 2012. Viral and nonviral delivery systems for gene delivery. *Advanced biomedical research,* 1.

OBATA, Y., SAITO, S., TAKEDA, N. & TAKEOKA, S. 2009. Plasmid DNA-encapsulating liposomes: Effect of a spacer between the cationic head group and hydrophobic moieties of the lipids on gene expression efficiency. *Biochimica et Biophysica Acta (BBA) - Biomembranes,* 1788**,** 1148-1158.

OSTOLSKA, I. & WIŚNIEWSKA, M. 2014. Application of the zeta potential measurements to explanation of colloidal Cr2O3 stability mechanism in the presence of the ionic polyamino acids. *Colloid and polymer science,* 292**,** 2453-2464.

PAN, D., TURNER, J. L. & WOOLEY, K. L. 2003. Folic acid-conjugated nanostructured materials designed for cancer cell targeting. *Chemical Communications***,** 2400-2401.

PITARD, B. 2002. Supramolecular assemblies of DNA delivery systems. *Somatic cell and molecular genetics,* 27**,** 5-15.

PROSKURYAKOV, S. Y., KONOPLYANNIKOV, A. G. & GABAI, V. L. 2003. Necrosis: a specific form of programmed cell death? *Experimental cell research,* 283**,** 1-16.

QI, R., GAO, Y., TANG, Y., HE, R.-R., LIU, T.-L., HE, Y., SUN, S., LI, B.-Y., LI, Y.-B. & LIU, G. 2009. PEG-conjugated PAMAM dendrimers mediate efficient intramuscular gene expression. *The AAPS journal,* 11**,** 395-405.

REJMAN, J., OBERLE, V., ZUHORN, I. S. & HOEKSTRA, D. 2004. Size-dependent internalization of particles via the pathways of clathrin-and caveolae-mediated endocytosis. *Biochemical Journal,* 377**,** 159-169.

SAHAY, G., ALAKHOVA, D. Y. & KABANOV, A. V. 2010. Endocytosis of Nanomedicines. *Journal of controlled release : official journal of the Controlled Release Society,* 145**,** 182-195.

SANTOS, J. L., OLIVEIRA, H., PANDITA, D., RODRIGUES, J., PÊGO, A. P., GRANJA, P. L. & TOMÁS, H. 2010. Functionalization of poly(amidoamine) dendrimers with hydrophobic chains for improved gene delivery in mesenchymal stem cells. *Journal of Controlled Release,* 144**,** 55-64.

SARDAR, R., FUNSTON, A. M., MULVANEY, P. & MURRAY, R. W. 2009. Gold nanoparticles: past, present, and future. *Langmuir,* 25**,** 13840-13851.

SCHOLZ, C. & WAGNER, E. 2012. Therapeutic plasmid DNA versus siRNA delivery: Common and different tasks for synthetic carriers. *Journal of Controlled Release,* 161**,** 554-565.

SHAN, Y., LUO, T., PENG, C., SHENG, R., CAO, A., CAO, X., SHEN, M., GUO, R., TOMÁS, H. & SHI, X. 2012. Gene delivery using dendrimer-entrapped gold nanoparticles as nonviral vectors. *Biomaterials,* 33**,** 3025-3035.

SHI, X., SUN, K. & BAKER JR, J. R. 2009. Spontaneous formation of functionalized dendrimer-stabilized gold nanoparticles. *The journal of physical chemistry. C, Nanomaterials and interfaces,* 112**,** 8251.

SINGH, M., ROGERS, C. B. & ARIATTI, M. 2007. Targeting of glycosylated lipoplexes in HepG2 cells: Anomeric and C-4 epimeric preference of the asialoglycoprotein receptor. *South African Journal of Science,* 103**,** 204-210.

SMITH, P. K., KROHN, R. I., HERMANSON, G., MALLIA, A., GARTNER, F., PROVENZANO, M., FUJIMOTO, E., GOEKE, N., OLSON, B. & KLENK, D. 1985. Measurement of protein using bicinchoninic acid. *Analytical biochemistry,* 150**,** 76-85.

SRINIVASARAO, M., GALLIFORD, C. V. & LOW, P. S. 2015. Principles in the design of ligand-targeted cancer therapeutics and imaging agents. *Nat Rev Drug Discov,* 14**,** 203-219.

TURKEVICH, J., STEVENSON, P. C. & HILLIER, J. 1951. A study of the nucleation and growth processes in the synthesis of colloidal gold. *Discussions of the Faraday Society,* 11**,** 55-75.

WANG, Y., GUO, R., CAO, X., SHEN, M. & SHI, X. 2011. Encapsulation of 2-methoxyestradiol within multifunctional poly (amidoamine) dendrimers for targeted cancer therapy. *Biomaterials,* 32**,** 3322-3329.

WIENER, E. C., KONDA, S., SHADRON, A., BRECHBIEL, M. & GANSOW, O. 1997. Targeting dendrimer-chelates to tumors and tumor cells expressing the high-affinity folate receptor. *Investigative radiology,* 32**,** 748-754.

XIAO, T., CAO, X. & SHI, X. 2013. Dendrimer-entrapped gold nanoparticles modified with folic acid for targeted gene delivery applications. *Journal of Controlled Release,* 172**,** e114-e115.

XUN, M.-M., LIU, Y.-H., GUO, Q., ZHANG, J., ZHANG, Q.-F., WU, W.-X. & YU, X.-Q. 2014. Low molecular weight PEI-appended polyesters as non-viral gene delivery vectors. *European journal of medicinal chemistry,* 78**,** 118-125.

YUAN, X., WEN, S., SHEN, M. & SHI, X. 2013. Dendrimer-stabilized silver nanoparticles enable efficient colorimetric sensing of mercury ions in aqueous solution. *Analytical Methods,* 5**,** 5486-5492.

ZHANG, S., GAO, H. & BAO, G. 2015. Physical principles of nanoparticle cellular endocytosis. *ACS nano,* 9**,** 8655-8671.

ZHANG, Y., THOMAS, T. P., DESAI, A., ZONG, H., LEROUEIL, P. R., MAJOROS, I. J. & BAKER JR, J. R. 2010. Targeted dendrimeric anticancer prodrug: a methotrexate-folic acid-poly (amidoamine) conjugate and a novel, rapid,"one pot" synthetic approach. *Bioconjugate chemistry,* 21**,** 489.

ZHANG, Z., ZHOU, F. & LAVERNIA, E. 2003. On the analysis of grain size in bulk nanocrystalline materials via X-ray diffraction. *Metallurgical and Materials Transactions A,* 34**,** 1349-1355.

CHAPTER 4

Efficient Folic Acid-Targeted Messenger RNA Delivery using Dendrimer Modified Gold Nanoparticles *in vitro*

***Submitted to the* Journal of Acta Pharmaceuticals**

Londiwe Simphiwe Mbatha and Moganavelli Singh*
Non-Viral Gene Delivery Laboratory, Discipline of Biochemistry University of KwaZulu-Natal, School of Life Sciences, Private Bag X54001, Durban 4000, South Africa
Corresponding Author:singhm1@ukzn.ac.za

Abstract

Messenger RNA (mRNA) has not been an attractive candidate for gene therapy due to its instability, and hence has received little attention. Recently, studies have successfully shown the advantage of using mRNA over pDNA in cancer immunotherapy, where transient therapeutic gene expression is needed. The objective of this study was to synthesise, characterise and evaluate the cytotoxicity profiles and capacity of unmodified and folic acid (FA) modified poly-amidoamine generation 5 (PAMAM G5D) grafted gold nanoparticles (AuNPs) to deliver mRNA containing a luciferase gene (F*luc*-mRNA) to various cancer cell lines. Nanocomplexes containing mRNA were characterised by transmission electron microscopy (TEM), nanoparticle tracking analysis (NTA), UV spectroscopy, NMR spectroscopy, band shift, ethidium bromide displacement and nuclease protection assays. Cytotoxicity profiles and gene expression were evaluated in the HEK293, HepG2, Caco-2, MCF-7, and KB, cell lines using the MTT and luciferase reporter gene assays respectively. Nanocomplexes at optimum weight/weight ratios of 2:1, 3:1 and 4:1, protected the mRNA against nucleases and were well tolerated in all cell lines. Transgene expression was significantly ($p < 0.0001$) higher with FA targeted dendrimer grafted AuNPs (Au:G5D:FA), in FA-receptor overexpressing MCF-7 and KB cells, compared to the G5D/G5D:FA NPs, decreasing significantly ($p < 0.01$) in the presence of excess competing FA ligand, confirming nanocomplex uptake via receptor mediation. Overall, transgene expression of the Au:G5D and Au:G5D:FA nanocomplexes exceeded that of the G5D/G5D:FA nanocomplexes, indicating the pivotal role played by the inclusion of a dendrimer in the AuNP delivery system, and the imparting of gold's favourable properties potentiating an increased level of luciferase gene expression.

Keywords: *mRNA, PAMAM dendrimers, Gold nanoparticles, Folic acid, Gene expression*

4.1 Introduction

Over the years, non-viral gene delivery modalities based on plasmid DNA (pDNA) have been extensively evaluated *in vitro* as potential therapeutic treatments of inherited diseases (McCrudden and McCarthy, 2013). However, their failure to demonstrate potency at a clinical level, due to their inability to bypass hurdles posed by the nuclear membrane of non-dividing cells and immunogenic responses of cytosine-phosphate-guanine (CpG) motifs contained by unmethylated DNA, has aroused interest in using mRNA instead of pDNA (Krieg, 2002, Su *et al.*, 2011).

Since the early study conducted by Malone and co-workers, the use of mRNA in gene therapy has been limited by the belief that mRNA is too unstable when transfected into cells (Malone *et al.*, 1989, Tavernier *et al.*, 2011). Recently, researchers have disapproved that notion by successfully demonstrating the feasibility of mRNA-based modalities in several therapeutic applications, including tumor vaccination (Saenz-Badillos *et al.*, 2001) and cancer immunotherapy. Lately, the feasibility and non-toxicity of naked mRNA and mRNA complexed with protamine was demonstrated in human patients via intradermal injections, resulting in promising immunological responses (Weide *et al.*, 2008, Weide *et al.*, 2009).

The recent interest in mRNA based systems is due to the pharmaceutical safety advantages demonstrated over their pDNA-based counterparts. These include, firstly, the ease of mRNA to be formulated into an efficient therapeutic agent, since it doesn't require incorporation of promoters and terminators, like pDNA. It lacks immunogenic CpG motifs, which are present in pDNA, and does not require to traverse the nuclear membrane to elicit expression, as it is delivered into the cytoplasm, resulting in early and improved transfection activities (Mockey *et al.*, 2006). Lastly, mRNA can transfect non-dividing cells, and to integrate into the host genome eliminates insertional mutagenesis, making it safer to deliver than pDNA (Van Tendeloo *et al.*, 2007). However, few studies have explored mRNA transfection over the years and consequently, knowledge regarding mRNA transfection is limited (Lu *et al.*, 1994, Bettinger *et al.*, 2001, Read *et al.*, 2005, Zohra *et al.*, 2007, Yamamoto *et al.*, 2009). Thus far, the general consensus is that the used of cationic non-viral mRNA based delivery systems, particularly, cationic polymers (e.g dendrimers), results in significantly improved transgene activity compared with that elicited by pDNA-based delivery systems (Tavernier *et al.*, 2011).

Dendrimers, particularly, PAMAM, have been shown to elicit high transfection activities *in vitro*, due to their hyperbranched, well-defined, 3 dimensional (3D) structure with multiple surface functionalities, extreme buffering capacity and ability to be protonated at physiological pH for efficient nucleic acid binding (Chaplot and Rupenthal, 2014). However, their high cytotoxic profiles induced by an excess of the surface amines (tertiary, 3^o internal and peripheral primary, 1^o) amines, especially at higher generations (>5), has tarnished their use in drug/gene delivery in the past (Xiao *et al.*, 2013). Many reports, however, have shown that modifying these surface amines via pegylation, methylation, alkylation, acetylation, and conjugation with vitamins or amino acids greatly decrease this cytotoxicity (Luo *et al.*, 2002, Lee *et al.*, 2003, Kim *et al.*, 2004).

Recently, several studies have exploited the incredible properties of dendrimers as stabilizers of metal nanoparticles (Shan *et al.*, 2012, Yuan *et al.*, 2013, Figueroa *et al.*, 2014). This strategy combines the unique properties of metal nanoparticles with those of cationic dendrimers to produce safe and highly efficient non-viral gene delivery systems. To the best of our knowledge, the transfection of mRNA using PAMAM dendrimer grafted gold nanoparticles has never been explored. For that reason, this study focused on designing FA modified PAMAM grafted gold nanoparticles and PAMAM grafted gold nanoparticles and evaluating their cytotoxicity profiles and capacity to deliver F*luc*-mRNA *in vitro.* FA modified PAMAM nano-conjugates and PAMAM nano-conjugates were also evaluated for comparison purposes.

4.2 Materials and Methods

4.2.1 Materials

Methanolic solution of starburst PAMAM dendrimer, generation five (PAMAM G5D), (Mw of 28,826, 128 surface amino groups), bicinchoninic acid (BCA), folic acid, hydrochloride salt of 1-(3-dimethylaminopropyl)-3-ethylcarbodiimide (EDC), dimethylformamide (DMF), sodium dodecylsulphate (SDS), benzolylated dialysis tubing (MWCO, 12,000 Daltons) and ribonuclease A (RNase) were supplied by Sigma-Aldrich (St. Louis, MO, USA). Ultra-pure DNA grade agarose was acquired from Bio-Rad Laboratories (Richmond, VA, USA). Tris (hydroxymethyl)-aminomethane hydrochloride (Tris-HCl), 3-(4, 5-dimethylthiazol- 2-yl)-2,5- diphenyltetrazolium bromide (MTT), 2-[4-(2-hydroxyethyl)-1-piperazinyl] ethane sulphonic acid (HEPES), Dimethyl sulphoxide (DMSO), ethidium bromide (ETB) and gold (III) chloride trihydrate 99% ($HAuCl_4$)

were purchased from Merck (Darmstadt, Germany). Minimum essential medium (EMEM) containing Earle's salts and L-glutamine, penicillin (500 units/mL)/streptomycin (5000 µg/mL) and trypsin-versene were purchased from Lonza-BioWhittaker (Walkersville, MD, USA). Foetal bovine serum (FBS) was purchased from Highveld Biological (Lyndhurst, South Africa). Human embryonic kidney cells (HEK293) were obtained from American Type Culture Collection (Manassas, VA, USA). Human hepatocellular carcinoma cells (HepG2), human breast adenocarcinoma cells (MCF-7) and human epithelial colorectal adenocarcinoma cells (Caco-2) were purchased from Highveld Biologicals (Pty) Ltd. (Kelvin, South Africa). Human cervical adenocarcinoma cells (KB) were obtained from the Institute of Biological Chemistry, Academia Sinica, Nankang, Taipei. F*luc*-mRNA was purchased from TriLink BioTechnologies, Inc (San Diego, CA).

4.2.2 Methods

The methods employed in this chapter are similar to that reported in the preceding chapter, with slight modifications. Hence for completeness of this chapter, some repetition in these protocols is unavoidable.

4.2.2.1 Modification of PAMAM G5D with Folic Acid (G5D:FA)

PAMAM G5D (dried under nitrogen) was dissolved in 18 MOhm water and conjugated to folic acid via carbodiimide chemistry (Wiener *et al.*, 1997, Wang *et al.*, 2011) (Figure A1, Appendix). Folic acid, 2.8 µmol (in 3 mL of DMF) was reacted with 38.2 µmol EDC for 45 minutes with constant stirring in a nitrogen atmosphere. The activated folic acid was then added slowly with stirring into the dendrimer (3 µmol, 100 µL) solution, and the pH maintained at 9.5, The solution was stirred for 3 days under nitrogen, followed by removal of unreacted by-products by dialysis (Mw= 12, 000 Daltons) against 18 MOhm water for 24 hours.

4.2.2.2 Synthesis of Gold Nanoparticles (AuNPs)

An adaptation of the Turkevich method was followed to synthesize the AuNPs (Turkevich *et al.*, 1951). $HAuCl_4$ (0.03 M, 0.1 mL) was dissolved in 25 mL of MOhm water, stirred vigorously and heated for 15 minutes until boiling. This was followed by the slow addition of 1 mL of 1% trisodium citrate ($Na_3C_6H_5O_7$) with stirring until a red colour change was produced. The mixture was then removed from the heat and stirred until it cooled to room temperature.

4.2.2.3 Formulation of Dendrimer Grafted AuNPs (Au:G5D NPs) and Folic Acid Targeted Dendrimer Grafted AuNPs (Au:G5D:FA NPs)

The G5D and G5D:FA were conjugated by addition to the citrate reduced AuNP solution utilising the Turkevich method, to produce Au:G5D and Au: G5D:FA NPs in a 25:1 gold/dendrimer molar ratio ((Turkevich *et al.,* 1951; Shi *et al.*, 2009). NPs were dialyzed as in 4.3.2.1.

4.2.2.4 Nanocomplex Preparation

Nanocomplexes for binding, cell viability, and transfection studies contained a constant amount of F*luc*-mRNA (0.05 µg) together with increasing amounts of G5D, Au:G5D, G5D:FA and Au:G5D:FA NPs. Nanocomplexes were briefly mixed and incubated at room temperature for 60 minutes.

4.2.2.5 Characterisation: Transmission Electron Microscopy (TEM) and Nanoparticle Tracking Analysis (NTA)

The ultrastructural morphology of the NPs and their nanocomplexes at optimum binding ratios ($^{w}/_{w}$), determined from the band shift assay were determined by cryo-TEM, using a Jeol JEM-1010 transmission electron microscope containing a Soft Imaging Systems (SIS) filted with a MegaView III digital camera with iTEM UIP software, operating at an acceleration voltage of 200 kV (Tokyo, Japan). The z-average hydrodynamic diameters and *zeta* (ζ) potentials were determined by nanoparticle tracking analysis (NanoSight LM10; Malvern Instruments Ltd., Worcestershire, UK) at 25°C. NPs were sonicated prior to use and nanocomplexes freshly prepared.

4.2.2.6 Ultra-Violet (UV) and Proton Nuclear Magnetic Resonance (^{1}H NMR) Spectroscopy

Successful functionalisation of the G5D and AuNPs was monitored by UV-Vis spectroscopy (UV-1650PC, Shimadzu, Japan), and ^{1}H NMR spectroscopy (Bruker DRX 400), using deuterated (D_2O) water as a solvent.

4.2.2.7 Binding Studies

Band Shift Assay

Band shift assays were utilised to determine binding of mRNA to the NPs. Nanocomplexes prepared as in 4.3.2.4, were subjected to electrophoresis on a 1% ($^w/_v$) agarose gels containing ethidium bromide (ETB) (1 µg/mL), in a Bio-Rad mini-sub electrophoresis tank containing 1 X electrophoresis buffer [36 mM Tris-HCl, 30 mM, sodium phosphate (NaH_2PO_4), 10 mM ethylenediamine tetra-acetic acid (EDTA), pH 7.5], for 45 minutes at 50 Volts. Gels were viewed and images captured using a Vacutec Syngene G: Box BioImaging system (Syngene, Cambridge, UK).

Ethidium Bromide Dye Displacement Assay

The compaction of the nanocomplexes was assessed using a dye displacement assay (Geall and Blagbrough, 2000, Tros de Ilarduya *et al*., 2002). ETB solution (24 µL, 100 µg/mL) and HBS (100 µL) were initially added to a 96-well FluorTrac flat bottom black plate, and fluorescence read in a Glomax®-Multi+ detection system (Promega) at an excitation wavelength of 520 nm and an emission wavelength of 600 nm. This was set as 0% relative fluorescence (RF). The 100% RF was obtained after the addition of 0.05 µg F*luc*-mRNA. Thereafter, 1 µL aliquots of the respective NPs were added and fluorescence measured until a plateau in fluorescence was achieved.

4.2.2.8 RNase A Protection Assay

The stability of the nanocomplexes and the protection afforded to the mRNA in the presence of degrading enzymes was evaluated by a RNase protection assay, adapted from Singh *et al*., 2003. NP:mRNA nanocomplexes prepared at; sub-optimum, optimum, and supra-optimum ratios were

exposed to 10% RNase A for 2 hours at 37 °C. This was followed by the addition of 10mM EDTA and 0.5% SDS respectively, and samples incubated at 55 °C for 20 min, followed by electrophoresis as described previously.

4.2.2.9 Cell Culture

All cells were maintained and propagated at 37 °C and 5% CO_2, in 25 cm^2 flasks containing sterile EMEM, FBS (10%, $^{v}/_{v}$), penicillin G (100 U/mL) and streptomycin sulphate (100 μg/mL). The cells were split upon confluency into desired ratios when necessary, and the medium changed routinely.

4.2.2.9.1 Cell Viability: MTT Assay

The MTT assay was used to determine the viability of the cells after treatment with the respective nanocomplexes as described previously (Singh *et al*., 2007). HEK293, HepG2, Caco-2, MCF-7 and KB cells were trypsinised and plated into 48-well plates at densities of 2.3 x 10^4, 2.0 x 10^4, 1.8 x 10^4, 1.3 x 10^4, 2.7 x 10^5 cells/well, respectively, and incubated for 24 hours at 37 °C. Thereafter, nanocomplexes at selected ratios were added in triplicate and cells incubated for 24 hours at 37 °C. Cells containing no nanocomplexes were used as the positive control (100% cell survival). After the 24 hour incubation, fresh medium containing the MTT reagent (5 mg/mL in PBS) (0.3 mL, EMEM:MTT 1:1 $^{v}/_{v}$) was then added, followed by a 4 hour incubation at 37 °C. The medium-MTT mixture was then aspirated, cells washed with PBS (2 x 0.3 mL) and 0.3 mL DMSO added. Absorbance was then measured at 570 nm in a Mindray MR-96A microplate reader.

4.2.2.9.2 Apoptosis Assay

To determine if apoptosis was instrumental in the cell death recorded, an apoptosis assay was conducted as previously described (Bezabeh *et al*., 2006, Maiyo *et al*., 2016). Cells (2.0-2.9 x 10^5 cells/well) were plated into 12-well plates and incubated for 24 hours at 37 °C. Following the addition of nanocomplexes at optimum ratios, the cells were incubated for 24 hours at 37 °C. Thereafter, cells were washed with PBS and 10 μL of AO/ETB (acridine orange/ethidium bromide) dye (100 μg/mL AO and 100 μg/mL ETB) was added. Cells were viewed for structural and

morphological changes under an Olympus fluorescent microscope (X200 magnification), fitted with a CC12 fluorescent camera (Olympus Co., Tokyo, Japan). Apoptosis was quantified by calculating the apoptotic index (AI) as below:

$$\textit{Apoptotic Index} = \frac{\textit{Number of apoptotic cells}}{\textit{Total number of cells}}$$

4.2.2.9.3 Transfection and Competition Assay

The transfection and competition assays were conducted as previously described (Singh *et al.* 2007). Cells with densities of 2.3- 2.7 x 10^5 cells/well, were seeded into 48-well plates and incubated for 24 hours at 37 °C. The nanocomplexes (ratios similar to the MTT assay) were then added, and the cells were incubated for 24 hours at 37 °C. Thereafter, the cells were washed with PBS (2 x 0.5 mL) and lysed with 80 µL/well cell lysis buffer (Promega) for 15 min with shaking at 30 rpm in a Scientific STR 6 platform rocker. Cell suspensions were then centrifuged at 12,000×g for 1 min. The cell-free extract (20 µL), was added to 100 µL luciferase assay reagent (Promega), mixed, and luminescence recorded in relative light units (RLU) in a Glomax®-Multi+Detection System (Promega Biosystem, Sunnyvale, USA). The BCA assay was used to determine the protein concentrations of the cell-free extracts as described previously (Smith *et al*., 1985), and the luciferase activity was normalized and expressed as RLU/mg protein.

The competition assay was performed as previously described (Singh *et al.*, 2007). Briefly, FA (250 µg) was incubated with folate receptor positive cells for 20 min at 37 °C, prior to addition of the targeted nanocomplexes. Luciferase activity was determined as described above.

4.2.2.10 Statistical Analysis

Cell viability and transfection studies were performed in triplicate and results expressed as means ± standard deviation (S.D). The experimental data was analyzed by two-way ANOVA and *t* test, using GraphPad Prism 6.0 and statistical significant values are indicated by $*p < 0.05$, $**p < 0.01$, $***p < 0.001$ and $****p < 0.0001$, $\#p > 0.05$.

4.3 Results and Discussion

4.3.1 Morphology, Size and *Zeta* Potential of Nanoparticles and Nanocomplexes

From the TEM and NTA results respectively, the NPs appeared spherical in shape with a uniform distribution and mean diameter sizes ranging between 65-128 nm (Figure 4.1-4.2, Table 4.1, and Figure A6, Appendix A). Nanocomplexes prepared at optimum ratios, presented as clusters of smaller particles with mean diameter sizes ranging from 101-265 nm (Figure 4.1-4.2 and Figure A7, Appendix A). In general, all the nanocomplexes, with the exception of G5D:FA nanocomplexes (265.2 nm), fall within the general size range (100-200 nm) required for gene delivery via non-specific or receptor-specific uptake (Azzam and Domb, 2004, Rejman *et al.*, 2004, Grosse *et al.*, 2005). There was no significant size difference (*#p* >0.05) between the Au:G5D/Au:G5D:FA and G5D/G5D:FA nanocomplexes (Table 4.1).

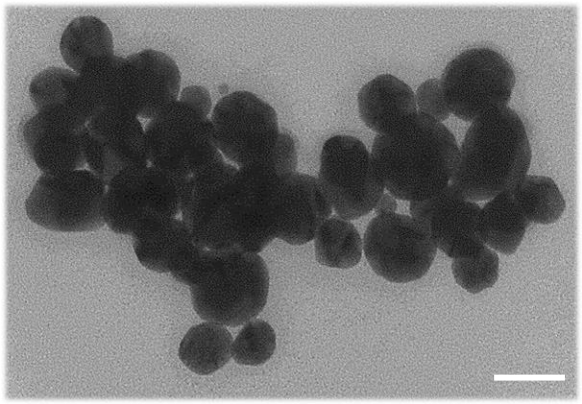

Figure 4.1: TEM micrograph of AuNPs. Scale bar = 100 nm.

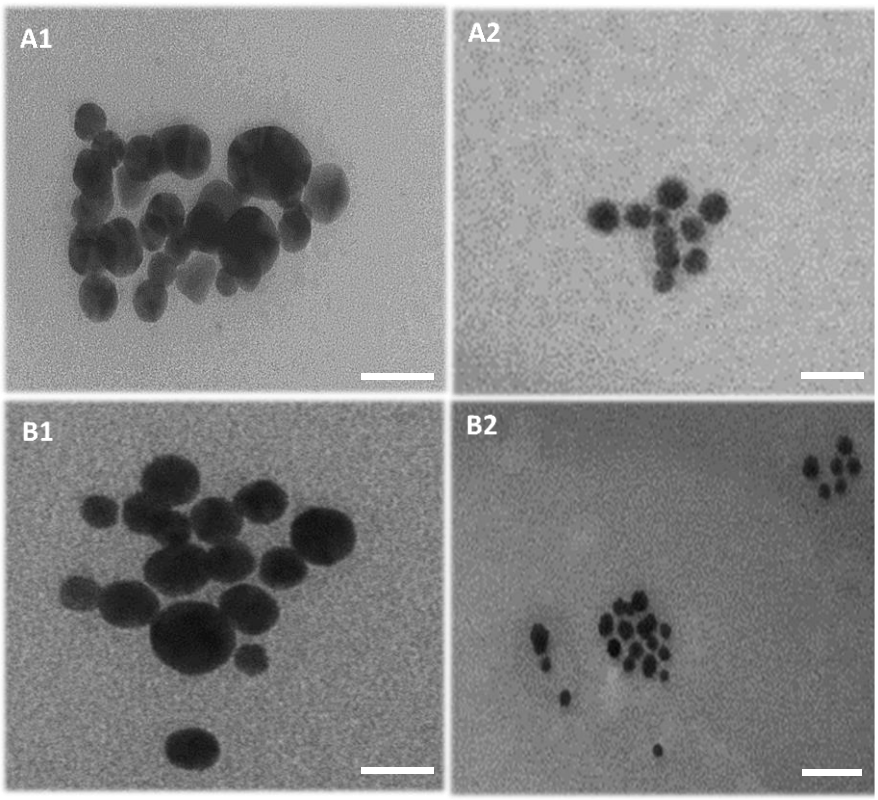

Figure 4.2: TEM micrographs of (A1) Au:G5D, (A2) Au:G5D-mRNA (B1) Au:G5D:FA and (B2) Au:G5D:FA-mRNA nanocomplexes prepared at optimum weight ratio of 3:1 and 4:1 $^{w}/_{w}$ respectively. Scale bar = 100 nm.

Table 4.1: Mean size and ζ potential measurements of gold nanoparticles and their counterparts. Data presented as mean diameter ± standard deviation (SD).

Nanoparticles and Nanocomplexes	NP:mRNA ($^{w}/_{w}$) Ratio	Mean Diameter (nm) ± SD	ζ Potential (mV) ± SD
Au	-	65.9 ± 9.8	-7.3 ± 1.6
G5D	-	161.3 ± 11.9	+87.2 ± 2.4
Au:G5D	-	100.5 ± 44.1	+ 20.9 ± 2.2
G5D:FA	-	128.0 ± 1.20	+71.2 ± 3.4
Au:G5D:FA	-	77.7 ± 12.5	+29.0 ± 0.5
Au:G5D-mRNA	3:1	207.2 ± 35.5 #	-37.3 ± 0.1***
Au:G5D:FA-mRNA	4:1	101.8 ± 36.9 #	-65.7 ± 1.4***
G5D-mRNA	2:1	118.0 ± 6.20 #	-21.0 ± 0.5***
G5D:FA-mRNA	4:1	265.2 ± 51.6 #	-25.8 ± 0.0***

#p > 0.05, **p* < 0.05, ***p* < 0.01, ****p* < 0.001, *****p* < 0.0001 when control nanocomplexes are compared with test nanocomplexes. NTA size and *zeta* potential distribution is reflected in the Appendix.

Zeta potential measurements greater than +25 mV or less than -25 mV are reported to be associated with good colloidal stability (Honary and Zahir, 2013). The AuNPs alone showed poor stability (-7.3 mV), but upon G5D and FA functionalisation, the stability improved immensely to +20.9 mV (Au:G5D), and +29 mV (Au:G5D:FA) (Table 4.1). Overall, functionalised NPs displayed ζ potentials ranging from 20.9 mV to 87.2 mV, and their nanocomplexes ζ potentials ranging from -21.0 mV to -65 mV, all indicating good colloidal stability. Au:G5D and Au:G5D:FA nanocomplexes also seemed to be highly stable with ζ potentials of -37.3 mV and -65.7 mV respectively. This improved stability with the targeted NPs could be due to the shielding or grafting effect imparted by FA and the dendrimer which prevents particle aggregation (Fratila *et al*., 2014). From these findings, it can be predicted that these nanocomplexes would be efficient in delivering mRNA.

4.3.2 UV-Spectroscopy and ^{1}H NMR Spectroscopy

The attachment of G5D and FA on the AuNPs was first confirmed by UV spectroscopy. The absorption band at 536 nm confirmed the formation of AuNPs, since the known absorption band of AuNPs range between 520-550 nm (Haiss *et al.*, 2007). The band shift from 536 nm to 566 nm confirmed the attachment of G5D on the surface of the AuNPs (Figure A2, Appendix A), (Pan *et al*., 2003). Furthermore, the covalent attachment of the FA onto the surface of NPs is known by its absorption maxima at 280 nm with a saddle point at 360 nm (Zhang *et al.*, 2003, Mansoori *et al.*, 2010) (Figure A3, Appendix A), corresponding to the absorption peak of Au:G5D:FA observed at 287 nm.

Moreover, the formation of Au:G5D and Au:G5D:FA nanoparticles was also verified by ^{1}H NMR spectroscopy. Significant differences in the chemical shift of protons related to Au:G5D (a), Au:G5D:FA (b), G5D:FA (c) were observed when compared to G5D (Figure 4.3). The ^{1}H NMR of the G5D shows 6 broad peaks as indicated by a chemical shift ranging from 2.25-3.34 ppm, which represents the protons of the amino groups (NH_2) and the methylene groups (CH_2). These findings correlated with those reported by Zhang *et al.* (2010) and Santos *et al.* (2010). The formation of Au:G5D nano-scaffolds resulted in the downfield shift of protons 4, 5 and 6 of G5D which indicated the interaction of the surface of the AuNPs with the internal amines of the dendrimers (Shi *et al.*, 2009).

Moreover, the three peaks between 6.50-8.63 ppm observed in figure 4.3 (A-B), indicate the attachment of FA protons [H-Ar (7&13), NH (18)]. These findings correlate with previous literature (Chang *et al*., 2012). Therefore, based on the UV information and these findings it can be concluded that the G5D polymer and FA moiety were successful conjugated to the AuNPs.

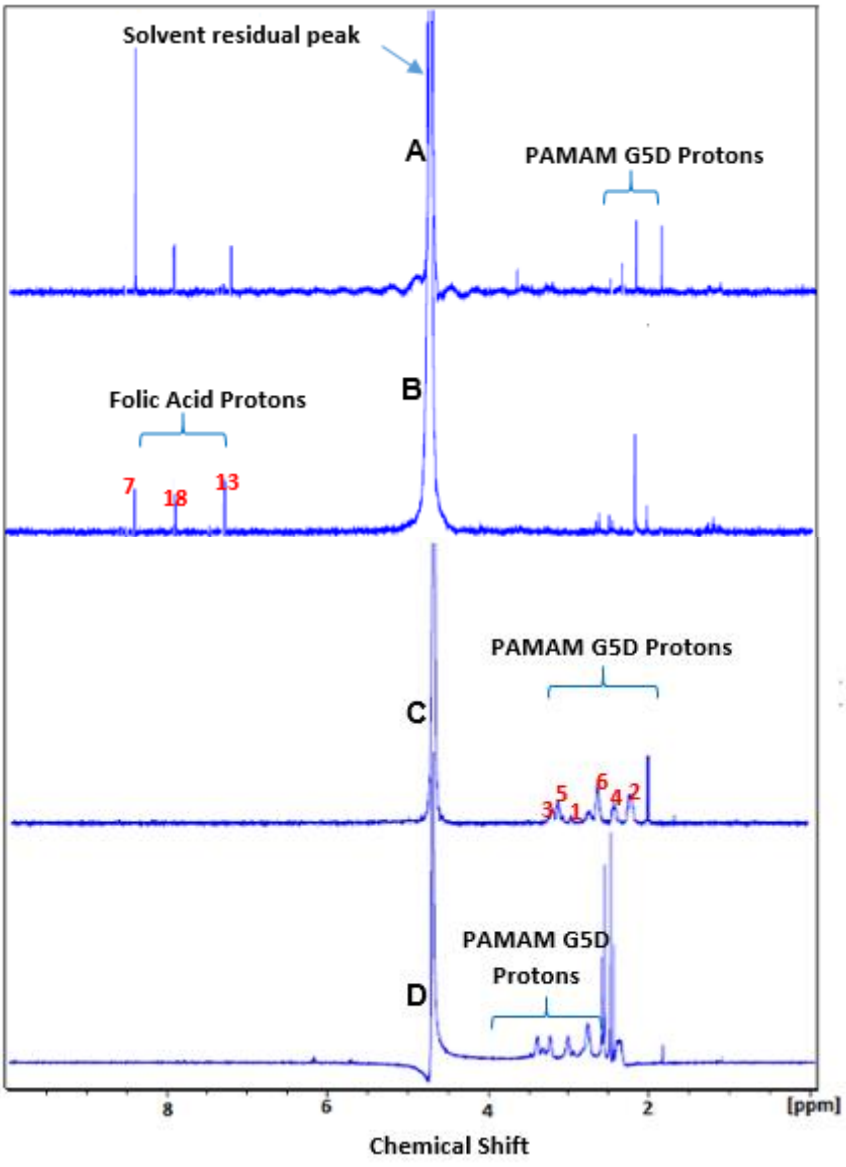

Figure 4.3: The structure of PAMAM G5 dendrimer and ^{1}H NMR spectra of PAMAM dendrimer (G5D) and folic acid functionalised gold nanoparticles in D_2O. (A) G5D:FA, (B) Au:G5D:FA, (C) G5D, (D) Au:G5D.

4.3.3 Binding Studies

Band Shift Assay

The mRNA binding efficiency of the prepared NPs can be seen in Figure 4.4.

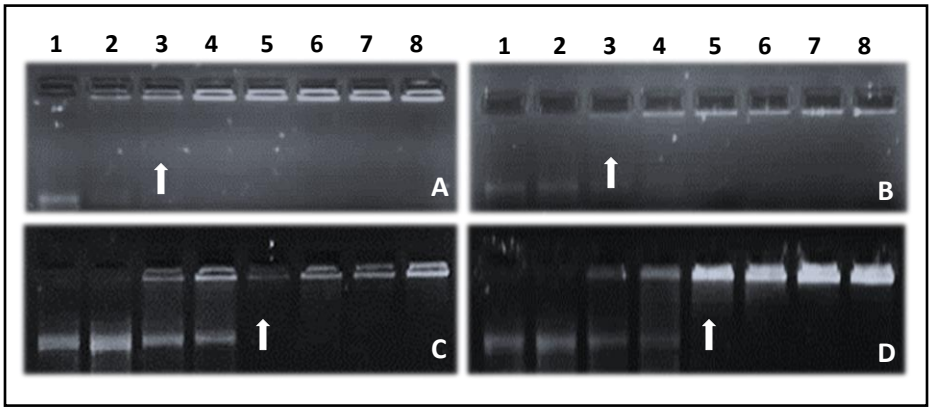

Figure 4.4: Band shift assay of the interaction between various nanoparticles (A) G5D, (B) Au:G5D, (C) G5D:FA, (D) Au:G5D:FA and mRNA. Incubation mixtures (20 µL) in HBS contained varying amounts of nanoparticle preparation and 0.05 µg mRNA-*Luc* corresponding to $^{w}/_{w}$ ratios of 1:1, 2:1, 3:1, 4:1, 5:1, 6:1, 7:1, and 8:1 in lanes 2-8 respectively (A-D). Lane 1: naked mRNA. Arrows indicate endpoint ratios.

All prepared NPs were able to bind and complex with the mRNA. This can be credited to the ability of G5D to become protonated at physiological pH (Chaplot and Rupenthal, 2014). G5D and Au:G5D nano-scaffolds completely retarded the mRNA at ($^{w}/_{w}$) ratios of 2:1 and 3:1, respectively, while both G5D:FA and Au:G5D:FA NPs completely retarded mRNA at a ($^{w}/_{w}$) ratio of 4:1. This difference in binding efficiency between the FA targeted and untargeted NPs, could be due to the possible shielding of the cationic charges on the targeted NPs by the FA moiety, which meant that more positive charges were required to fully neutralize the negative charges on the mRNA (Mbatha *et al.*, 2016). Overall, the complex formation of all nano-scaffolds occurred at very low weight/charge ratios, which could be accredited to the single-stranded nature of mRNA which is quickly embedded by the highly cationic G5D.

Ethidium Bromide Dye Displacement Assay

All NPs displaced ETB, indicating a significant degree of mRNA compaction, which bodes well for their stability and protection under physiological conditions. The degree of mRNA compaction for G5D and Au:G5D nano-scaffolds ranged from 10-30%, while that of G5D:FA and Au:G5D:FA nano-scaffolds ranged from 40-70% (Figure 4.5).

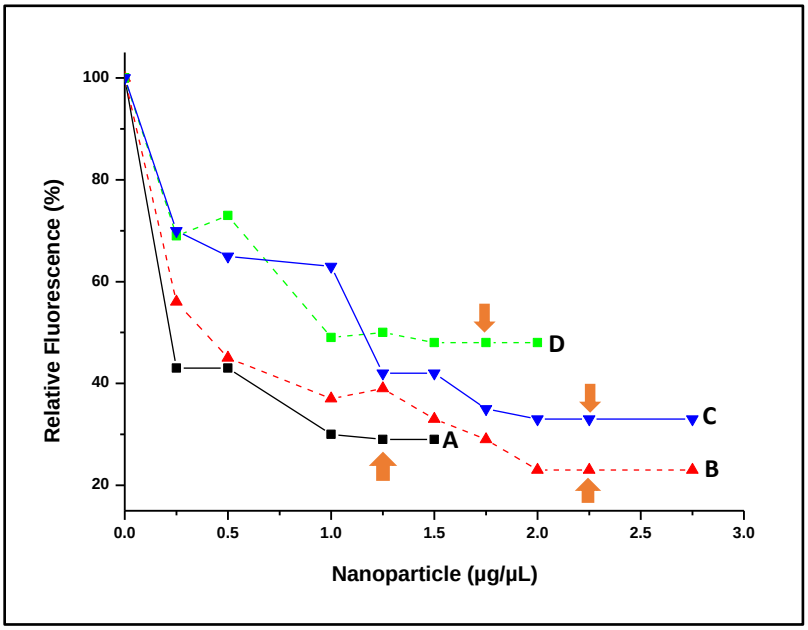

Figure 4.5: Ethidium bromide displacement assay of (A) G5D, (B) Au:G5D, (C) G5D:FA, (D) Au:G5D:FA nano-scaffolds. Arrows indicate point of complexation.

This higher degree of compaction seen for the targeted nanocomplexes, suggest a weaker binding of mRNA, which could translate into easy dissociation of the mRNA from the nanocomplexes during transfection, hence avoiding degradation by the lysosomal compartment, in turn enhancing gene transfection efficiency (Chuang and Chang, 2015). Hence, it can be concluded that all nano-scaffolds were able to efficiently bind and compact mRNA, with the targeted nanocomplexes showing a higher degree of compaction.

4.3.4 RNase A Digestion Assay

The integrity of the nanocomplexes may be compromised by degrading enzymes such as RNase A, leading to a decreased transgene expression (Obata *et al.*, 2009). To assess the ability of the nano-scaffolds to protect the mRNA cargo against these degrading nucleases, which would be encountered in circulation in an *in vivo* system, a RNase A digestion assay was conducted.

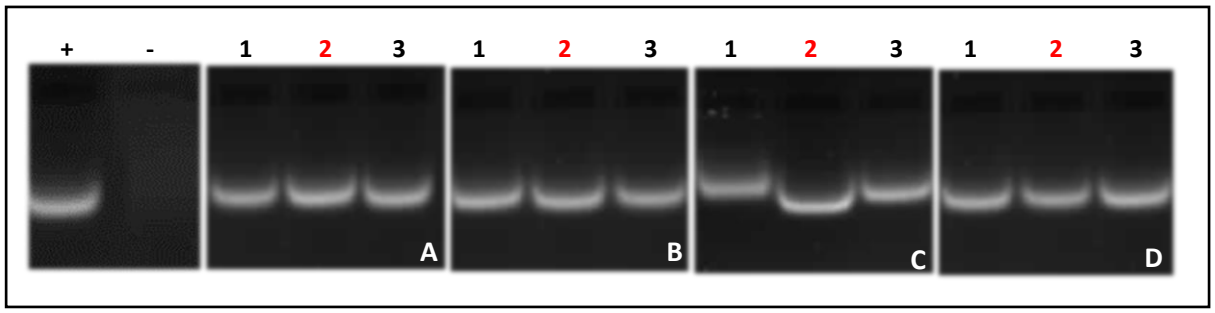

Figure 4.6: Nuclease digestion assay of nanocomplexes. (A) G5D, (B) Au:G5D, (C) G5D: FA, (D) Au:G5D:FA. Control: naked mRNA in the absence (+ = positive control) or presence (- = negative control) of RNase A. Lanes 1-3 contains nanocomplexes at sub-optimum, optimum and supra-optimum nanoparticle: mRNA ratios. (A) 1:1, 2:1, 3:1; (B) 2:1, 3:1, 4:1; (C) 3:1, 4:1, 5:1; (D) 3:1, 4:1, 5:1 ($^{w}/_{w}$). Red colored numbers indicate optimum ratios.

Figure 4.6 clearly shows the exceptional ability of all NPs to fully protect mRNA, following treatment with 10% RNase A, as depicted by the presence of undigested bands in all tested ratios. This could be due to the highly organized globular structures that form as a result of the electrostatic interaction between the negatively charged single-stranded mRNA and the highly cationic G5D containing NPs (Pitard, 2002). By contrast, the treatment of naked mRNA with RNase A showed complete degradation (negative control) as illustrated in figure 4.5, lane 2. The use of the RNase enzyme was a stringent test for these nanoparticles due to its specificity. However, in the circulatory system, the nanoparticles may encounter less specific enzymes and possibly at lower concentrations as well. Therefore, it can be concluded that all nano-scaffolds afforded exceptional protection to the mRNA cargo, boding well for future *in vivo* studies.

4.3.5 MTT Assay

The first step towards understanding how biocompatible a delivery vector will be, often involves the use of cell-culture studies, commencing with the assessment of cytotoxicity. To monitor cell viability after treatment with prepared nanocomplexes in selected cell lines, a series of MTT assays were conducted. This assay uses MTT which enters the cells and passes into the mitochondria where it's reduced to an insoluble, purple coloured formazan product which can be quantified spectroscopically and is used as an indication of metabolically active cells.

No significant ($p > 0.05$) change in cell viability was observed following treatment with all nanocomplexes. Higher cell viabilities (80-97%) were observed in all cell lines for the Au:G5D:mRNA and Au:G5D:FA:mRNA nanocomplexes, compared to the G5D:mRNA and G5D:FA:mRNA nanocomplexes (68-78%) (Figure 4.7A-B). This is assumed to be due to the reduced portion of the cationic charges of the 1^{o} amines of G5D, some of which are responsible for stabilising the entrapped AuNPs (Shan *et al.*, 2012).

Noticeably, all FA targeted nanocomplexes showed higher cell viabilities compared to their untargeted nanocomplex counterparts (average cell viability of 88% for Au:G5D:FA and 72% for G5D:FA. This could be as a result of the shielding effect of FA which may have covered a portion of the positive charges on the surface of G5D, hence reducing the strong electrostatic interaction between the cells and the NPs (Xiao *et al.*, 2013). Overall, more than 80% of cells were still viable after being exposed to the gold containing nanocomplexes at the selected ratios, suggesting that these nanocomplexes were superior and well tolerated in all tested cell lines, and therefore relatively safe to use.

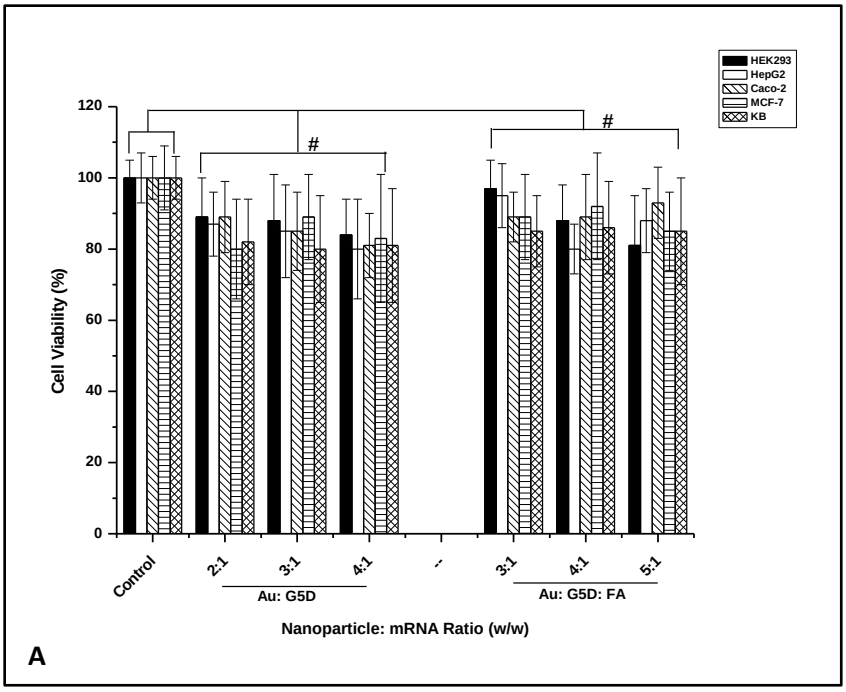

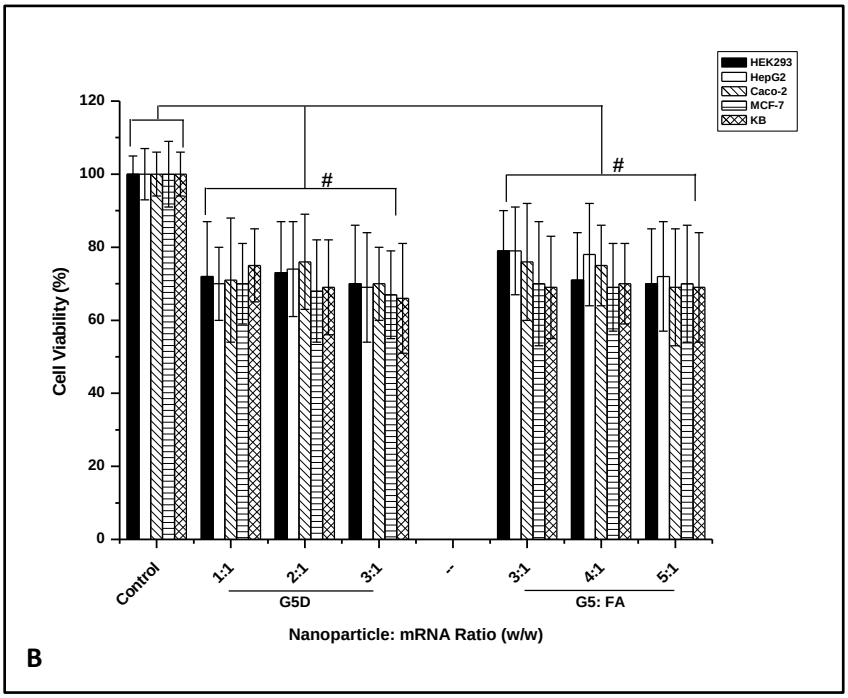

Figure 4.7 (A-B): Cell viability assay of four nanocomplexes in HEK293, HepG2, Caco-2, MCF-7 and KB cells. Cells were incubated with nanocomplexes containing 0.05 µg mRNA-*Luc* at indicated ratios ($^{w}/_{w}$). Nanocomplexes were prepared at sub-optimum, optimum and supra-optimum ratios. Data are presented as means ± S.D. (n = 3). Control = untreated cells. #$p > 0.05$.

4.3.6 Apoptosis Assay

Cell death was also studied by evaluating the ability of NPs to induce apoptosis in selected cell lines. All nanocomplexes induced little apoptosis in the cells, as evidenced by very few apoptotic (yellow-orange/red) cells visible and the low apoptotic indices (AI) (Table 4.2 and Figure 4.8). Noticeably, the AI values of Au:G5D:mRNA and Au:G5D:FA:mRNA nanocomplexes were significantly ($p < 0.0001$) lower than those of the G5D:mRNA and G5D:FA:mRNA nanocomplexes particularly, in all cell lines (Table 4.2; Figure 4.9). These findings suggested that the Au:G5D:mRNA and Au:G5D:FA:mRNA nanocomplexes were safe and stable, and correlates with the cytotoxicity profiles determined by MTT.

Table 4.2: Apoptotic Indices of NPs in selected cell lines.

Cell Lines	**Apoptotic Indices**				
		Test NPs		**Control NPs**	
	Control	**Au:G5D**	**Au:G5D:FA**	**G5D**	**G5D:FA**
HEK293	0.0	0.03	0.04	0.07	0.08
HepG2	0.0	0.06	0.04	0.08	0.09
Caco-2	0.0	0.05	0.04	0.13	0.11
MCF-7	0.0	0.04	0.06	0.25	0.23
KB	0.0	0.05	0.06	0.19	0.20

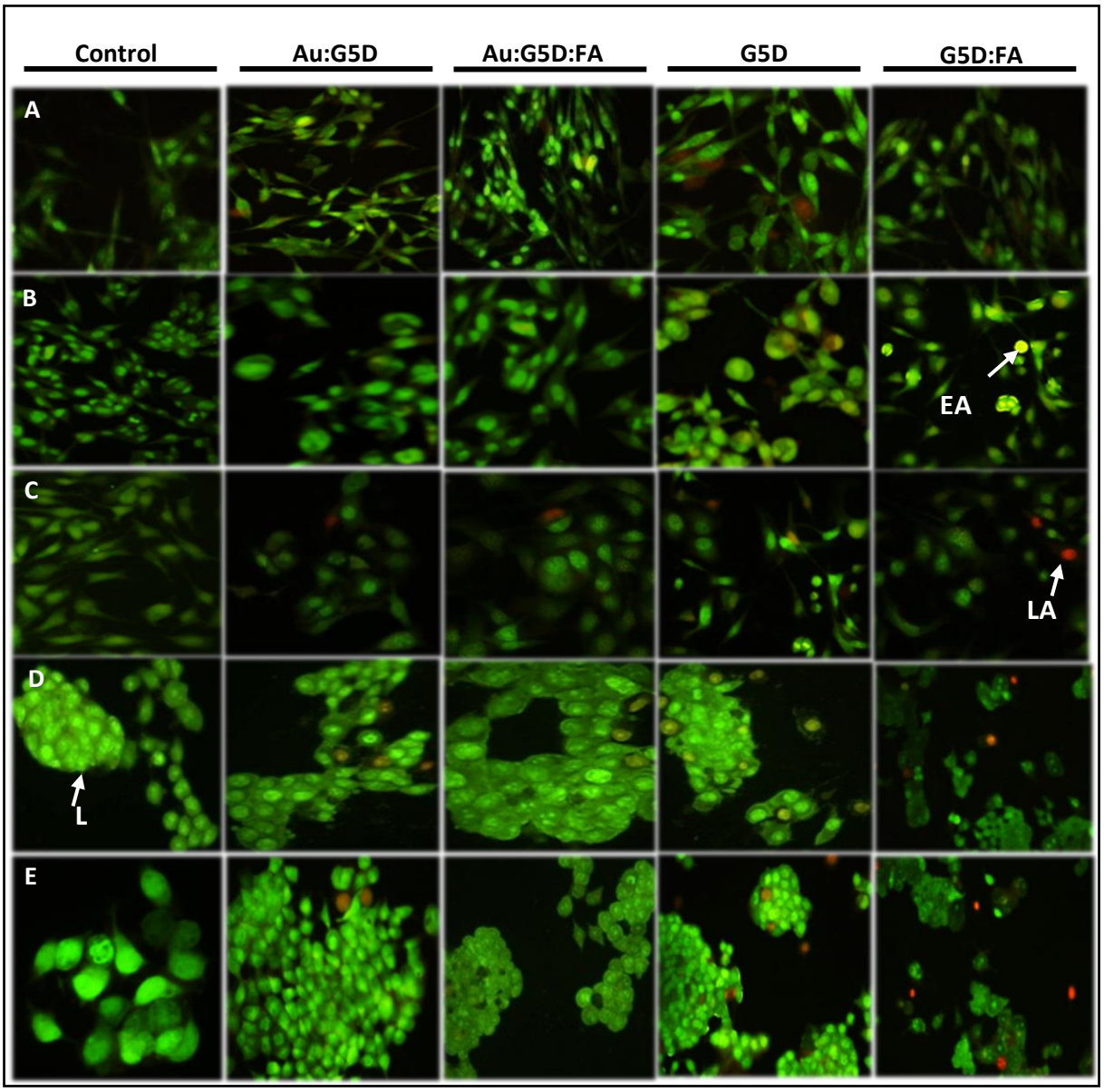

Figure 4.8: Fluorescence images of (A) HEK293, (B) HepG2, (C) Caco-2, (D) MCF-7 and (E) KB cells treated with test and control nanocomplexes prepared at sub-optimum ratios for 24 hours showing induction of apoptosis. Green= live (L), light orange= early apoptotic (EA) and dark orange = late apoptotic (LA) cells. Scale= 100 μm.

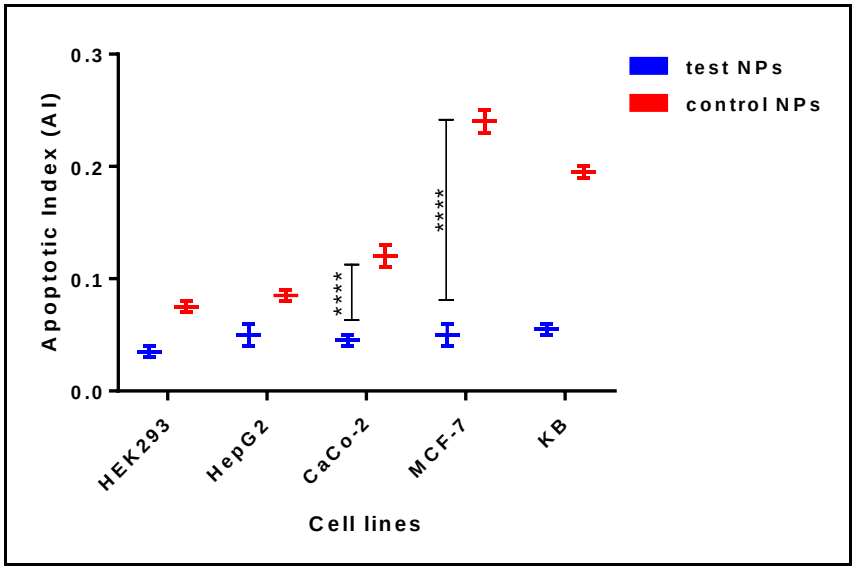

Figure 4.9: Differences in AI values between the test and control NPs in tested cell lines. ****$p < 0.0001$.

4.3.7 Transfection and Competition Assays

The ability of the NPs to deliver mRNA was evaluated in folate receptor negative cell lines, HEK293, Caco-2, and receptor-positive cell lines HepG2, MCF-7 and KB, the latter with low to high folate receptor expression. The transfection efficacy of the nanocomplexes was assessed as a function of weight ratios (sub-optimum, optimum and supra-optimum).

All NPs and their nanocomplexes had sizes appropriate for either specific or non-specific uptake and were reasonably stable, with the nanocomplexes showing excellent stability. The transfection activity of the Au:G5D:mRNA and Au:G5D:FA:mRNA nanocomplexes (Figure 4.10A-B) was much higher than that of the naked mRNA (control). This was expected since the introduction of naked mRNA into the cells is known to be associated with poor transgene expression mainly due to enzymatic degradation (Elsabahy *et al.*, 2011), as evidenced in the RNase A digestion assay. All nanocomplexes were able to significantly transfect the selected cell lines. The high transfection observed could be due to three reasons. Firstly, since the translation of mRNA occurred in the cytoplasm, the major limiting step, which is the nuclear pore entry was avoided, resulting in an increased transgene expression. Secondly, since the transfection studies were conducted over a duration of 24 hours, more protein expression was measured as the lifetime of mRNA is limited

(Tavernier *et al.*, 2011). Lastly, the efficient encapsulation of the mRNA by the highly rigid dendrimer, with an exceptional buffering capacity could have helped protect the mRNA from degradation and facilitated the endosomal escape of the nanocomplexes from degrading lysosomes (Kambhampati *et al.*, 2015). Moreover, the transfection levels in HEK293 and Caco-2 cells were significantly ($p < 0.001$) lower than those elicited in the receptor-positive cells. HepG2 cells also exhibited lower expression, possibly due to fewer receptors on the cell surface compared to the MCF-7 and KB cells. Low targeted expression has been associated with a lack of specific transcription factors and cell-surface receptors (Mansoori *et al.*, 2010).

All nanocomplexes showed excellent transfection activity, with Au:G5D:mRNA and Au:G5D:FA:mRNA nanocomplexes (Figure 4.10A) showing higher transfection efficiencies ranging from $5 \times 10^7 – 6 \times 10^8$ RLU/mg protein. This can be accredited to the entrapment of AuNPs in the 1° amines of the dendrimer which helped preserve the structural integrity of the dendrimers, allowing for efficient interaction between the dendrimers and mRNA (Shan *et al.*, 2012). The decreased transfection activity showed by G5D:mRNA and G5D:FA:mRNA nanocomplexes ($4 \times 10^7 – 3 \times 10^8$ RLU/mg protein) (Figure 4.10B), could, therefore be due to the loss of the structural integrity of the dendrimer due to interaction with interfaces or solid surfaces (Xiao *et al.*, 2013). Furthermore, poor dissociation between the mRNA and the G5D due to the strong binding affinity possessed by these nano-scaffolds, could have attributed to the decreased transfection efficiency. Earlier studies have demonstrated a direct correlation between the binding affinity of the single stranded mRNA to cationic polymers and transgene expression (Bettinger *et al.*, 2001).

Noticeably, the Au:G5D:FA:mRNA nanocomplexes, showed a 4 fold increase in transfection activity ($6x\ 10^8$ RLU/mg protein), compared to Au:G5D:mRNA nanocomplexes (2×10^8 RLU/mg protein) at the optimum ratios in the FA-R positive cell line, MCF-7. This could be due to the interaction that occurs between the targeting ligand, FA, incorporated in these nanocomplexes and the FA-Rs abundantly decorating the surface of the MCF-7 cells (Srinivasarao *et al.*, 2015). It is generally known that FA has a high affinity for FA-Rs overexpressed by a majority of cancer cells (Mansoori *et al.*, 2010).

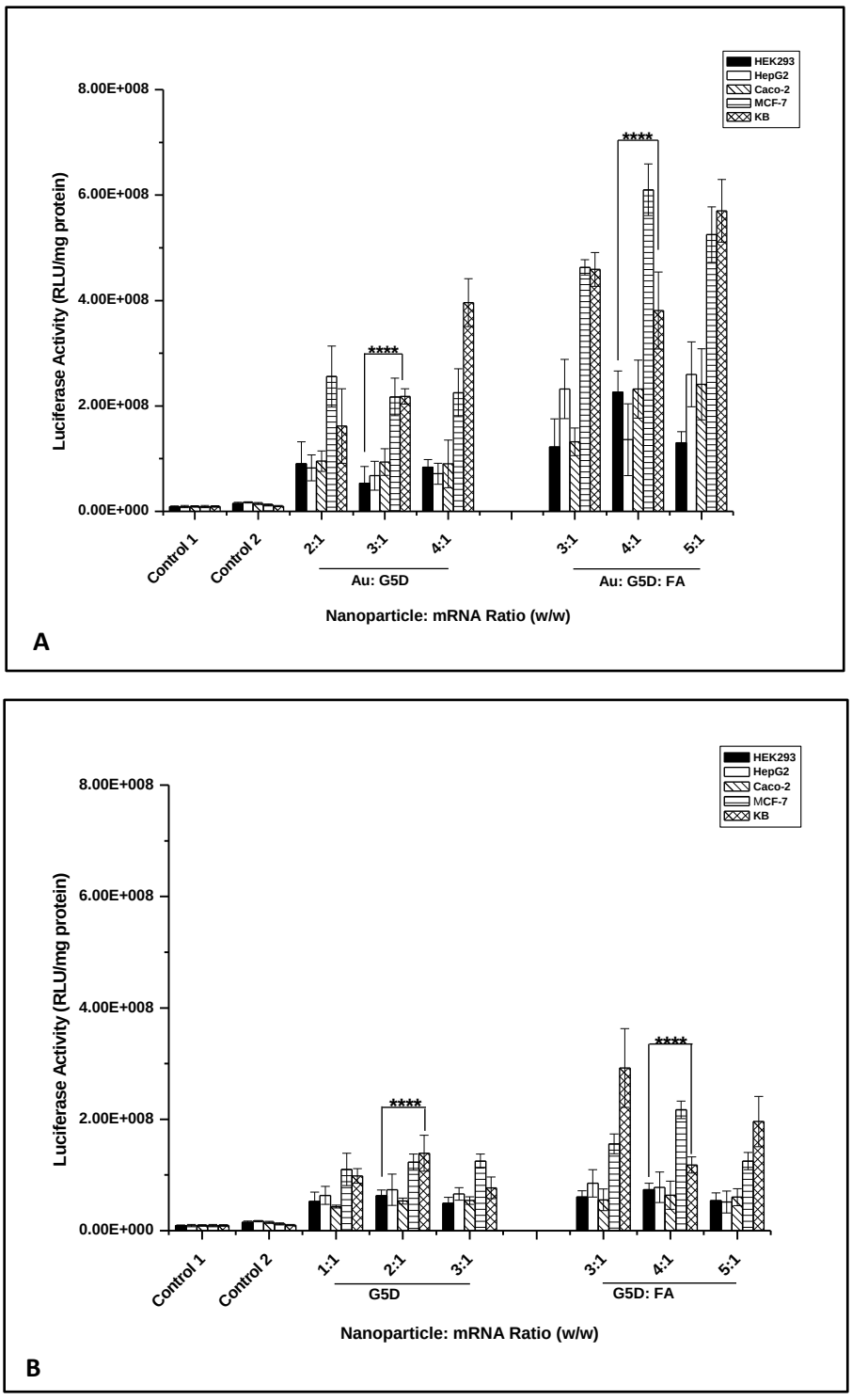

Figure 4.10 (A-B): Transfection studies of (A) Test nanocomplexes (B) Control nanocomplexes. HEK293, HepG2, Caco-2, MCF-7 and KB cells were exposed to nanocomplexes constituted with 0.05 µg mRNA and varying amounts of nanoparticles at sub-optimum, optimum and supra-optimum ratios. Control 1= untreated cells. Control 2= cells + mRNA-*Luc*. The transgene expression is reported as RLU/mg protein. Data are presented as means ± SD (n=3). ****$p < 0.0001$ for optimum ratios.

To confirm the uptake mechanism of the nano-scaffolds, a competition assay was conducted. This involved flooding the cells with excess free FA (250 μg) before exposure to the FA targeted nanocomplexes (Au:G5D:FA:mRNA and G5D:FA:mRNA).The assay was conducted in the cell line with the overall higher targeted transgene expression, viz. MCF-7. A significant ($p < 0.01$) drop of approximately 30% in transgene activity was observed as depicted in figure 4.11, which suggests that a large portion of these nanocomplexes were taken up by receptor-mediated endocytosis (Zhang *et al.*, 2015), confirming that FA receptor mediation was a key player in the high transgene expression obtained.

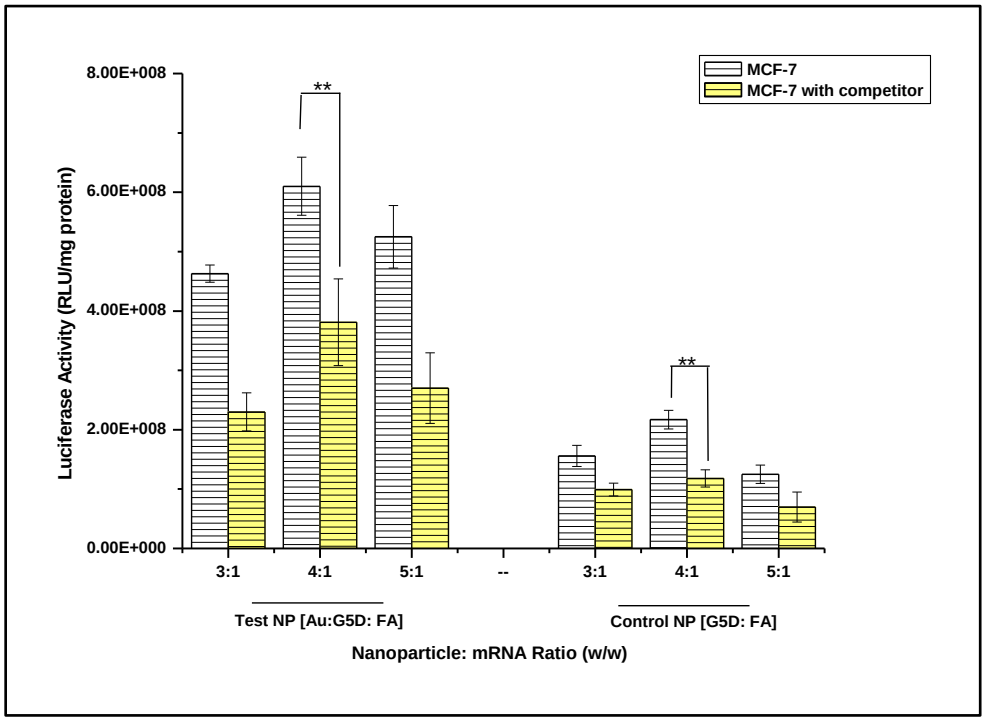

Figure 4.11: Competition studies of FA targeted mRNA nanocomplexes. MCF-7 cells were first exposed to excess folic acid (250 μg), then treated with FA targeted nanocomplexes at optimum ratios. The transgene expression is reported as RLU/mg protein. Data are presented as means ± SD (n=3). $^{**}p < 0.01$.

4.4 Conclusion

Both Au:G5D and Au:G5D:FA NPs were highly efficient in F*luc*-mRNA binding and delivery. They formed stable nanocomplexes and afforded excellent protection to the mRNA against RNases. Furthermore, >80% cell viability was observed, suggesting that these nanocomplexes were well tolerated by all cell lines. This was also demonstrated in their superior transfection efficiency, indicating the significant roles played by both the dendrimer and the AuNPs in their formulation. Lastly, we have confirmed that folate receptor-mediated delivery was the main route of entry into the receptor positive cells, as evidenced by the transfection levels in the FA-receptor negative cell lines, being significantly lower ($p < 0.001$) than that in FA-receptor positive cell lines. Future studies would encompass the NP optimization for *in vivo* delivery.

4.5 References

AZZAM, T. & DOMB, A. J. 2004. Current developments in gene transfection agents. *Current drug delivery,* 1**,** 165-193.

BETTINGER, T., CARLISLE, R. C., READ, M. L., OGRIS, M. & SEYMOUR, L. W. 2001. Peptide-mediated RNA delivery: a novel approach for enhanced transfection of primary and post-mitotic cells. *Nucleic acids research,* 29**,** 3882-3891.

CHAPLOT, S. P. & RUPENTHAL, I. D. 2014. Dendrimers for gene delivery–a potential approach for ocular therapy? *Journal of Pharmacy and Pharmacology,* 66**,** 542-556.

CHUANG, C.-C. & CHANG, C.-W. 2015. Complexation of bioreducible cationic polymers with gold nanoparticles for improving stability in serum and application on nonviral gene delivery. *ACS applied materials & interfaces,* 7**,** 7724-7731.

DE ILARDUYA, C. T., ARANGOA, M., MORENO-ALIAGA, M. & DÜZGÜNEŞ, N. 2002. Enhanced gene delivery in vitro and in vivo by improved transferrin-lipoplexes. *Biochimica et Biophysica Acta (BBA)-Biomembranes,* 1561**,** 209-221.

ELSABAHY, M., NAZARALI, A. & FOLDVARI, M. 2011. Non-viral nucleic acid delivery: key challenges and future directions. *Current drug delivery,* 8**,** 235-244.

FIGUEROA, E. R., LIN, A. Y., YAN, J., LUO, L., FOSTER, A. E. & DREZEK, R. A. 2014. Optimization of PAMAM-gold nanoparticle conjugation for gene therapy. *Biomaterials,* 35**,** 1725-1734.

GEALL, A. J. & BLAGBROUGH, I. S. 2000. Rapid and sensitive ethidium bromide fluorescence quenching assay of polyamine conjugate–DNA interactions for the analysis of lipoplex formation in gene therapy. *Journal of pharmaceutical and biomedical analysis,* 22**,** 849-859.

GROSSE, S., ARON, Y., THÉVENOT, G., FRANÇOIS, D., MONSIGNY, M. & FAJAC, I. 2005. Potocytosis and cellular exit of complexes as cellular pathways for gene delivery by polycations. *The journal of gene medicine,* 7**,** 1275-1286.

HAISS, W., THANH, N. T., AVEYARD, J. & FERNIG, D. G. 2007. Determination of size and concentration of gold nanoparticles from UV− Vis spectra. *Analytical chemistry,* 79**,** 4215-4221.

HONARY, S. & ZAHIR, F. 2013. Effect of zeta potential on the properties of nano-drug delivery systems-a review (Part 2). *Tropical Journal of Pharmaceutical Research,* 12**,** 265-273.

KAMBHAMPATI, S. P., CLUNIES-ROSS, A. J., BHUTTO, I., MISHRA, M. K., EDWARDS, M., MCLEOD, D. S., KANNAN, R. M. & LUTTY, G. 2015. Systemic and Intravitreal Delivery of Dendrimers to Activated Microglia/Macrophage in Ischemia/Reperfusion Mouse RetinaRetinal Microglia Uptake of Dendrimers. *Investigative ophthalmology & visual science,* 56**,** 4413-4424.

KIM, T.-I., SEO, H. J., CHOI, J. S., JANG, H.-S., BAEK, J.-U., KIM, K. & PARK, J.-S. 2004. PAMAM-PEG-PAMAM: novel triblock copolymer as a biocompatible and efficient gene delivery carrier. *Biomacromolecules,* 5**,** 2487-2492.

KRIEG, A. M. 2002. CpG motifs in bacterial DNA and their immune effects. *Annual review of immunology,* 20**,** 709-760.

LEE, J. H., LIM, Y.-B., CHOI, J. S., LEE, Y., KIM, T.-I., KIM, H. J., YOON, J. K., KIM, K. & PARK, J.-S. 2003. Polyplexes assembled with internally quaternized PAMAM-OH dendrimer and plasmid DNA have a neutral surface and gene delivery potency. *Bioconjugate chemistry,* 14**,** 1214-1221.

LU, D., BENJAMIN, R., KIM, M., CONRY, R. & CURIEL, D. 1994. Optimization of methods to achieve mRNA-mediated transfection of tumor cells in vitro and in vivo employing cationic liposome vectors. *Cancer gene therapy,* 1**,** 245-252.

LUO, D., HAVERSTICK, K., BELCHEVA, N., HAN, E. & SALTZMAN, W. M. 2002. Poly (ethylene glycol)-conjugated PAMAM dendrimer for biocompatible, high-efficiency DNA delivery. *Macromolecules,* 35**,** 3456-3462.

MALONE, R. W., FELGNER, P. L. & VERMA, I. M. 1989. Cationic liposome-mediated RNA transfection. *Proceedings of the National Academy of Sciences,* 86**,** 6077-6081.

MANSOORI, G. A., BRANDENBURG, K. S. & SHAKERI-ZADEH, A. 2010. A comparative study of two folate-conjugated gold nanoparticles for cancer nanotechnology applications. *Cancers,* 2**,** 1911-1928.

MBATHA, L., CHAKRAVORTY, S., B DE KONING, C., AL VAN OTTERLO, W., ARBUTHNOT, P., ARIATTI, M. & SINGH, M. 2016. Spacer length: a determining factor in the design of galactosyl ligands for hepatoma cell-specific liposomal gene delivery. *Current drug delivery,* 13**,** 935-945.

MCCRUDDEN, C. M. & MCCARTHY, H. O. 2013. Cancer gene therapy-key biological concepts in the design of multifunctional non-viral delivery systems. *Cancer Gene Therapy. 1st ed. Rijeka, Croatia: InTech***,** 213-235.

MOCKEY, M., GONÇALVES, C., DUPUY, F. P., LEMOINE, F. M., PICHON, C. & MIDOUX, P. 2006. mRNA transfection of dendritic cells: synergistic effect of ARCA mRNA capping with Poly (A) chains in cis and in trans for a high protein expression level. *Biochemical and biophysical research communications,* 340**,** 1062-1068.

OBATA, Y., SAITO, S., TAKEDA, N. & TAKEOKA, S. 2009. Plasmid DNA-encapsulating liposomes: Effect of a spacer between the cationic head group and hydrophobic moieties of the lipids on gene expression efficiency. *Biochimica et Biophysica Acta (BBA) - Biomembranes,* 1788**,** 1148-1158.

PITARD, B. 2002. Supramolecular assemblies of DNA delivery systems. *Somatic cell and molecular genetics,* 27**,** 5-15.

READ, M. L., SINGH, S., AHMED, Z., STEVENSON, M., BRIGGS, S. S., OUPICKY, D., BARRETT, L. B., SPICE, R., KENDALL, M. & BERRY, M. 2005. A versatile reducible polycation-based system for efficient delivery of a broad range of nucleic acids. *Nucleic acids research,* 33**,** e86-e86.

REJMAN, J., OBERLE, V., ZUHORN, I. S. & HOEKSTRA, D. 2004. Size-dependent internalization of particles via the pathways of clathrin-and caveolae-mediated endocytosis. *Biochemical Journal,* 377**,** 159-169.

SAENZ-BADILLOS, J., AMIN, S. & GRANSTEIN, R. 2001. RNA as a tumor vaccine: a review of the literature. *Experimental dermatology,* 10**,** 143-154.

SANTOS, J. L., OLIVEIRA, H., PANDITA, D., RODRIGUES, J., PÊGO, A. P., GRANJA, P. L. & TOMÁS, H. 2010. Functionalization of poly(amidoamine) dendrimers with hydrophobic chains for improved gene delivery in mesenchymal stem cells. *Journal of Controlled Release,* 144**,** 55-64.

SHAN, Y., LUO, T., PENG, C., SHENG, R., CAO, A., CAO, X., SHEN, M., GUO, R., TOMÁS, H. & SHI, X. 2012. Gene delivery using dendrimer-entrapped gold nanoparticles as nonviral vectors. *Biomaterials,* 33**,** 3025-3035.

SHI, X., SUN, K. & BAKER JR, J. R. 2009. Spontaneous formation of functionalized dendrimer-stabilized gold nanoparticles. *The journal of physical chemistry. C, Nanomaterials and interfaces,* 112**,** 8251.

SRINIVASARAO, M., GALLIFORD, C. V. & LOW, P. S. 2015. Principles in the design of ligand-targeted cancer therapeutics and imaging agents. *Nat Rev Drug Discov,* 14**,** 203-219.

SU, X., FRICKE, J., KAVANAGH, D. & IRVINE, D. J. 2011. In vitro and in vivo mRNA delivery using lipid-enveloped pH-responsive polymer nanoparticles. *Molecular pharmaceutics,* 8**,** 774.

TAVERNIER, G., ANDRIES, O., DEMEESTER, J., SANDERS, N. N., DE SMEDT, S. C. & REJMAN, J. 2011. mRNA as gene therapeutic: how to control protein expression. *Journal of controlled release,* 150**,** 238-247.

VAN TENDELOO, V. F., PONSAERTS, P. & BERNEMAN, Z. N. 2007. mRNA-based gene transfer as a tool for gene and cell therapy. *Current opinion in molecular therapeutics,* 9**,** 423-431.

WEIDE, B., CARRALOT, J.-P., REESE, A., SCHEEL, B., EIGENTLER, T. K., HOERR, I., RAMMENSEE, H.-G., GARBE, C. & PASCOLO, S. 2008. Results of the first phase I/II clinical vaccination trial with direct injection of mRNA. *Journal of immunotherapy,* 31**,** 180-188.

WEIDE, B., PASCOLO, S., SCHEEL, B., DERHOVANESSIAN, E., PFLUGFELDER, A., EIGENTLER, T. K., PAWELEC, G., HOERR, I., RAMMENSEE, H.-G. & GARBE, C. 2009. Direct injection of protamine-protected mRNA: results of a phase 1/2 vaccination trial in metastatic melanoma patients. *Journal of Immunotherapy,* 32**,** 498-507.

XIAO, T., CAO, X. & SHI, X. 2013. Dendrimer-entrapped gold nanoparticles modified with folic acid for targeted gene delivery applications. *Journal of Controlled Release,* 172**,** e114-e115.

YAMAMOTO, A., KORMANN, M., ROSENECKER, J. & RUDOLPH, C. 2009. Current prospects for mRNA gene delivery. *European Journal of Pharmaceutics and Biopharmaceutics,* 71**,** 484-489.

YUAN, X., WEN, S., SHEN, M. & SHI, X. 2013. Dendrimer-stabilized silver nanoparticles enable efficient colorimetric sensing of mercury ions in aqueous solution. *Analytical Methods,* 5**,** 5486-5492.

ZHANG, S., GAO, H. & BAO, G. 2015. Physical principles of nanoparticle cellular endocytosis. *ACS nano,* 9**,** 8655-8671.

ZHANG, Y., THOMAS, T. P., DESAI, A., ZONG, H., LEROUEIL, P. R., MAJOROS, I. J. & BAKER JR, J. R. 2010. Targeted dendrimeric anticancer prodrug: a methotrexate-folic acid-poly (amidoamine) conjugate and a novel, rapid,"one pot" synthetic approach. *Bioconjugate chemistry,* 21**,** 489.

ZHANG, Z., ZHOU, F. & LAVERNIA, E. 2003. On the analysis of grain size in bulk nanocrystalline materials via X-ray diffraction. *Metallurgical and Materials Transactions A,* 34**,** 1349-1355.

ZOHRA, F., CHOWDHURY, E., TADA, S., HOSHIBA, T. & AKAIKE, T. 2007. Effective delivery with enhanced translational activity synergistically accelerates mRNA-based transfection. *Biochemical and biophysical research communications,* 358**,** 373-378.

CHAPTER 5

Dendrimer Functionalised Folate-Targeted Gold Nanoparticles for Luciferase Gene Silencing *in vitro*: A Proof of Principle Study

Submitted to the Journal of Acta Pharmaceuticals

Londiwe Simphiwe Mbatha* and Moganavelli Singh
Discipline of Biochemistry, Non- Viral Delivery Laboratory, University of KwaZulu-Natal, Westville Campus, School of Life Sciences, Private Bag X54001, Durban 4000, South Africa
Corresponding Author Email: singhm1@ukzn.ac.za

Abstract

For years, the therapeutic development of gene silencing has relied on the elegant, endogenous RNA interference (RNAi) mechanism. Recently, the use of exogenous small interfering RNA (siRNA) has showed potential and has gained attention as an alternative gene silencing therapeutic. However, delivery to targeted sites remains a hurdle, hence, efficient siRNA delivery vectors are needed for the clinical improvement of gene therapy. This study is aimed at developing and evaluating the safety and efficiency of siRNA delivery using unmodified and folic acid (FA) modified poly-amidoamine generation 5 (PAMAM G5D) functionalised gold nanoparticles (Au:G5D/Au:G5D:FA NPs) in various mammalian cell lines. The same parameters were also evaluated using unmodified PAMAM G5D and FA modified PAMAM G5D nanoparticles (G5D/G5D:FA NPs) for comparative purposes. NPs and their nanocomplexes were formulated and analyzed using TEM, NTA, UV spectroscopy, NMR spectroscopy, band shift, ethidium bromide displacement and nuclease protection assays. Cytotoxicity was assessed in the HEK293, HepG2, Caco-2, and HeLa-Tat-*Luc* using the MTT assay, while the gene silencing efficiency was assessed in HeLa-Tat-*Luc* cells using luciferase reporter gene assay. Nanocomplexes at optimum $^{w}/_{w}$ ratios, bound and protected siRNA against degrading RNases, were well tolerated by the cells, and were able to elicit excellent gene silencing. High gene silencing with Au:G5D and Au:G5D:FA nanocomplexes, with Au:G5D:FA exhibiting a significantly ($p < 0.001$) higher silencing in FA receptor overexpressing HeLa-Tat-*Luc* cells, decreasing significantly ($p < 0.001$) in the presence of excess FA ligand, indicating the uptake mechanism of these NPs to be receptor mediated. These results signify and highlight the synergistic role played by Au and the dendrimer in the enhancement of transgene silencing.

Keywords: *RNA interference, siRNA, Targeted delivery, Dendrimers, Gold nanoparticles, Folic acid.*

5.1 Introduction

Small interfering RNA (siRNA) has evoked much interest as an effective gene knockdown tool in gene therapy and holds great potential in treating various incurable disorders such as cancer and acquired immunodeficiency syndrome (AIDS) (Ziraksaz *et al.,* 2013). This gene knockdown ability of siRNA can be accredited to the endogenous elegant RNAi mechanism (Figure 5.1) that was discovered by Fire and Mello in the late 1990s which regulates gene expression by silencing disease inducing genes. It is said that, upon the delivery of the long, double-stranded RNA (dsRNA) into the cytoplasm of eukaryotic cells, it is subjected to cleavage by the enzyme called Dicer (RNase III-type) into short fragments of 21–25 base pairs, known as small interferences (siRNAs). These siRNAs are then loaded into an RNA-induced silencing complex (RISC), which triggers the activation of the RISC by the guide strand (antisense) of these siRNA duplex. The activated RISC is then said to bind to and cleaves the complementary strand of the target gene (mRNA), resulting in its degradation by intracellular nucleases, which in turn silences/downregulates its expression into respective proteins (Tseng *et al.*, 2009, Dorasamy *et al.*, 2012).

Though siRNA is inherently produced from a long dsRNA, the introduction of synthetic siRNA in various mammalian cancer cell lines has been reported to induce the same effect to the RNAi. The long term gene silencing attained through repeated systemic administrations has aroused much attention in its potential as a key therapeutic agent in the advancement of novel medicines. However, the inability to bypass the cellular membrane due to their hydrophilic and polyanionic nature, and rapid enzymatic degradation, due to the presence of a hydroxyl group at the second carbon atom of the sugar moiety favouring hydrolysis of the phosphodiester backbone, leads to poor gene silencing efficiency, limiting its application to date (Banan and Puri, 2004, Gary *et al.*, 2007). Consequently, designing appropriate vectors that are safe, and that will embody the protection of the siRNA from degrading enzymes while facilitating its targeted cell specific uptake is crucial for its therapeutic application.

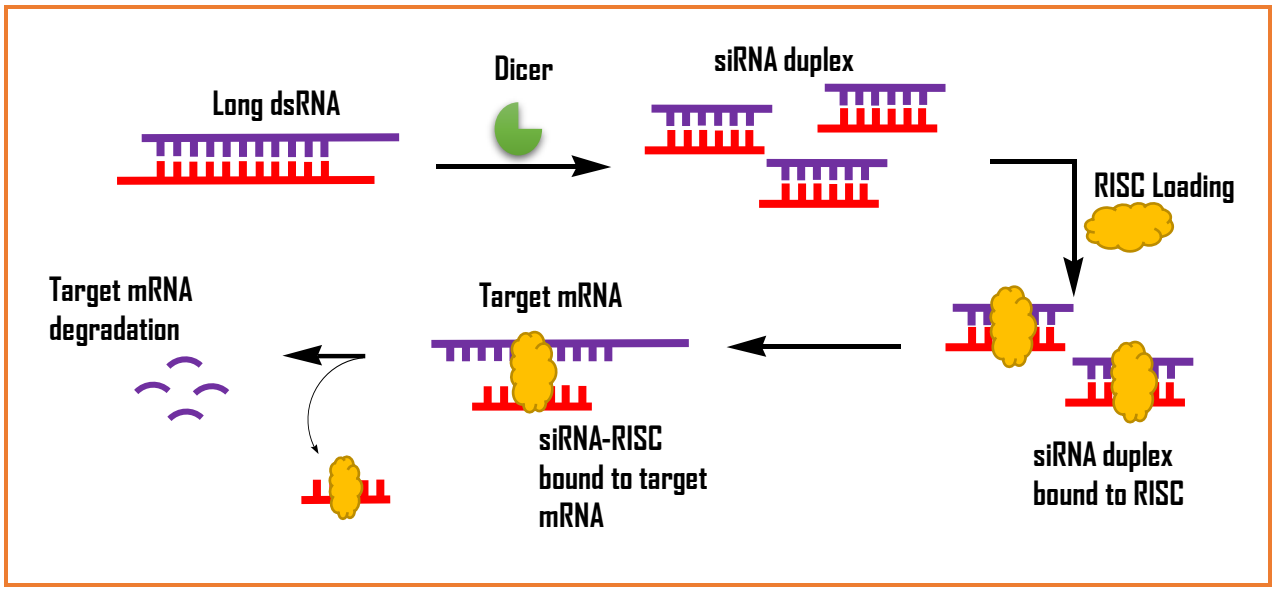

Figure 5.1: Schematic illustration of the siRNA-mediated gene silencing via the RNAi mechanism.

Cationic polymers, such as dendrimers, have been extensively explored as effective pDNA vectors over the years and mildly as metal stabilizers recently, due to their associated high transfection efficiency. The relatively high cytotoxicity of these dynamic well defined cationic dendrimers, PAMAM in particular, which is due to nonspecific interaction of primary amine groups with the cell membrane, is the main concern for their potential application in gene therapy studies. In this present study, two different approaches have been used to reduce the cytotoxicity of PAMAM dendrimers while preserving their gene delivery efficiency. Firstly, the internal amines of the dendrimer were modified with gold nanoparticles, forming less toxic complexes with negatively charged siRNA. Secondly, the surface primary amines of the gold nanoparticle modified dendrimers were partially tailored with a targeting ligand, folic acid producing folate targeted dendrimer grafted gold nanoparticle with reduced toxicity. This study focused on designing, characterising and evaluating the cytotoxicity profiles of untargeted and FA targeted PAMAM grafted AuNPs in various mammalian cell lines and their ability to deliver siRNA to HeLa-Tat-*Luc* cells (Figure 5.2).

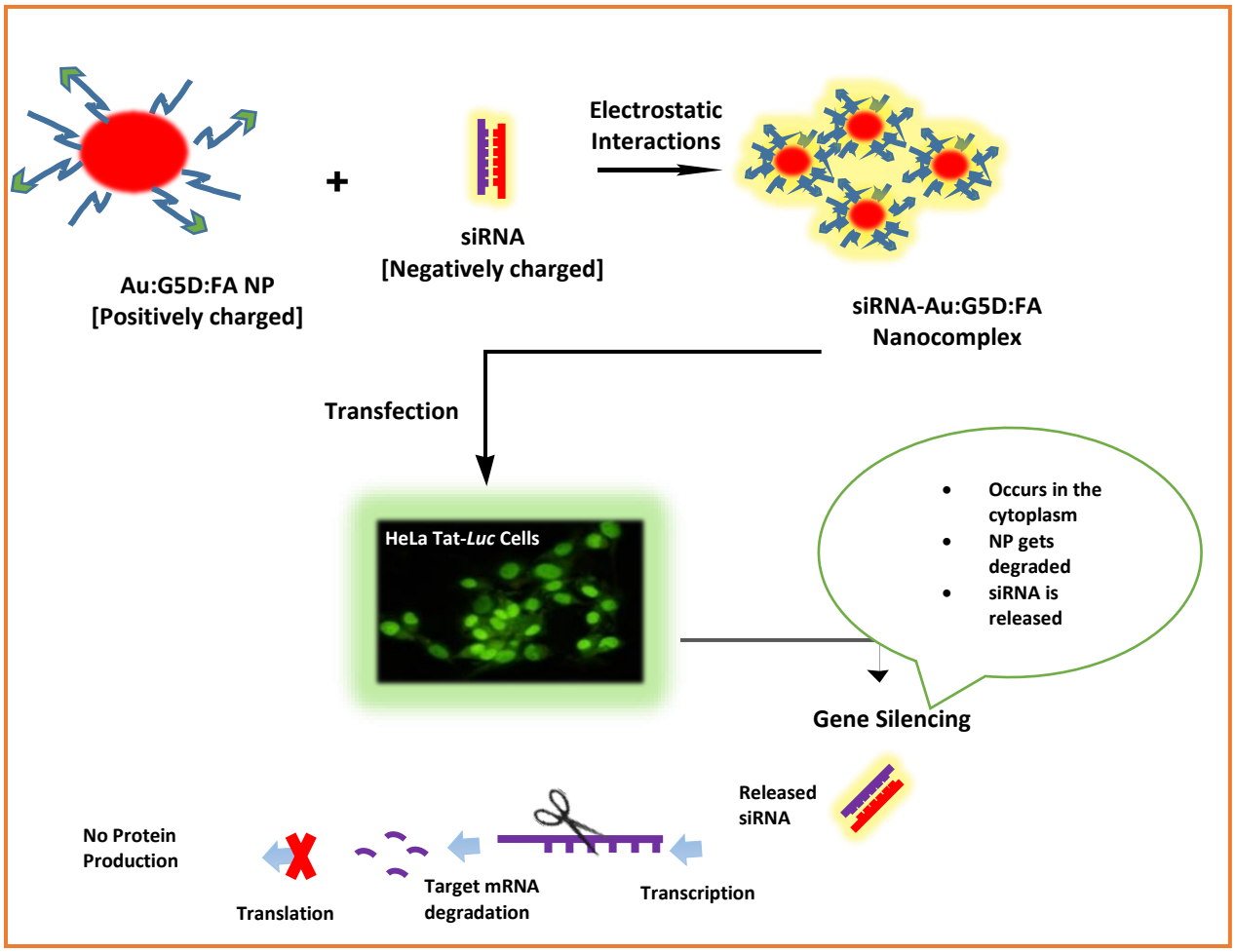

Figure 5.2: Illustration of the delivery of siRNA using Au:G5D:FA NP in HeLa Tat-*Luc* cells.

5.2 Materials and Methods

5.2.1 Materials

Methanolic solution of starburst poly (amidoamine), PAMAM dendrimer, generation five (PAMAM G5D), (Mw 28,826, 128 surface amino groups), bicinchoninic acid (BCA), folic acid, 1-(3-dimethylaminopropyl)-3-ethylcarbodiimide (EDC), dimethylformamide (DMF), sodium dodecylsulphate (SDS), ribonuclease A (RNase A) and benzolylated dialysis tubing (MWCO 12,000 Da) were supplied by Sigma-Aldrich (St. Louis, MO, USA). Ultra-pure DNA grade agarose was acquired from Bio-Rad Laboratories (Richmond, VA, USA). Tris (hydroxymethyl)-aminomethane hydrochloride (Tris-HCl), 3-(4, 5-dimethylthiazol- 2-yl)-2,5- diphenyltetrazolium bromide (MTT), 2-[4-(2-hydroxyethyl)-1-piperazinyl] ethane sulphonic acid (HEPES), dimethyl sulphoxide (DMSO), ethidium bromide (ETB) and gold (III) chloride trihydrate 99% ($HAuCl_4$) were purchased from Merck (Darmstadt, Germany). Minimum essential medium (EMEM) containing Earle's salts and L-glutamine, penicillin (500 units/mL)/streptomycin (5000 µg/mL) and trypsin-versene were purchased from Lonza-BioWhittaker (Walkersville, MD, USA). Foetal bovine serum (FBS) was purchased from Hyclone (Utah, USA). Human embryonic kidney cells (HEK293) was obtained from American Type Culture Collection (Manassas, VA, USA). Human hepatocellular carcinoma cells (HepG2) and Human epithelial colorectal adenocarcinoma cells (Caco-2) were purchased from Highveld Biologicals (Pty) Ltd. (Kelvin, South Africa). The HeLa-Tat-*Luc* cell line was provided by the Department of Physiology (University of KwaZulu-Natal, Durban, South Africa). The luciferase assay kit containing the assay reagent and cell lysis buffer was purchased from the Promega Corporation (Madison, WI). siGENOME non-targeting siRNA (D-001210–01) and anti-*Luc* siRNA (D-002050-01) with sequence: GAUUAUGUCCGGUUAUGUA(UU), were obtained from Thermo Scientific Dharmacon Products (Lafayette, CO). Solutions of duplexes were prepared according to the manufacturer's specifications in 1 × RNA buffer to a final concentration of 20 μM. Stock solutions were routinely stored at –20 ^{o}C. All other reagents were of analytical grade and 18 MOhm water was used throughout.

5.2.2 Methods

The methods employed in this chapter are similar to those reported in the preceding chapters, with slight modifications. Hence for completeness of this chapter, some repetition in these protocols will be evident.

5.2.2.1 Synthesis of PAMAM G5D Modified Folic Acid (G5D:FA conjugate)

PAMAM G5D was modified with folic acid (FA) ($C_{19}H_{19}N_7O_6$) through a carbodiimide reaction as previously described (Wiener *et al*., 1997, Wang *et al*., 2011) (Figure A1, Appendix A). Briefly, FA, 2.8 µmol (1.23 mg) in 3 mL of DMF was reacted under N_2 with 38.2 µmol (7.3 mg) of EDC for 45 minutes with constant stirring. This was then added dropwise with stirring into the G5D solution (3 µmol, 100 µL) and the pH adjusted to 9.5. This solution was further stirred for 3 days under nitrogen atmosphere and was then dialyzed (Mw=12 000 Da) against 18 MOhm water for 24 hours, to remove excess unreacted by-products.

5.2.2.2 Synthesis of Gold Nanoparticles (AuNPs)

AuNPs were synthesised by reduction of $HAuCl_4$ (0.03 M) with trisodium citrate (1%) as previously described (Turkevich *et al*., 1951, Lazarus *et al*., 2014). The colloidal solutions were stored for future use and were stable for 6 months.

5.2.2.3 Synthesis of Dendrimer Grafted Gold Nanoparticles (Au:G5D NPs) and Folic acid Targeted Dendrimer Grafted Gold Nanoparticle (Au:G5D:FA NPs)

Au:G5D and Au:G5D:FA NPs were synthesised by an adaptation of 5.2.2.2, to contain a 25:1 gold/dendrimer molar ratio (Shi *et al*., 2009). The unmodified G5D and previously synthesized G5D:FA conjugates were used as control templates. All AuNPs were dialyzed against 18 MOhm water for 24 hours, to remove unreacted by-products.

5.2.2.4 Nanocomplex Preparation

Increasing amounts of the NPs ranging from 2-8 µg were mixed with either 0.5 µg siCONTROL Tox siRNA for binding studies or 0.27 µg anti-*Luc* siRNA for cytotoxicity and transfection studies in 32 µL sterile HBS. This was followed by brief mixing and centrifugation at 13000 revolutions/ minute (rpm) for 5 minutes, and a 60 minute incubation at room temperature.

5.2.2.5 Characterisation: Transmission Electron Microscopy (TEM) and Nanoparticle Tracking Analysis (NTA)

A Jeol JEM-1010 transmission electron microscope, containing a Soft Imaging Systems (SIS) filtered with a MegaView III digital camera and iTEM UIP software (Tokyo, Japan), set at an acceleration voltage of 200 kV, was used to view the morphology of the synthesized nanoparticles and their nanocomplexes prepared at endpoint ratios ($^{w}/_{w}$). NTA (NanoSight NS500; Malvern Instruments Ltd., Worcestershire, UK) was used to determine the sizes (z-average hydrodynamic diameter) and *zeta* potentials of the nano-scaffolds and their nanocomplexes (prepared at optimum binding ratios ($^{w}/_{w}$) and diluted to 1 mL).

5.2.2.6 Ultra-Violet (UV) and Proton Nuclear Magnetic Resonance (^{1}H NMR) Spectroscopy

The attachment of G5D and FA onto the AuNP surface was confirmed using UV–Vis spectroscopy (UV-1650PC, Shimadzu, Japan) and ^{1}H NMR spectroscopy (Bruker DRX 400), using deuterated (D_2O) water as a solvent.

5.2.2.7 Binding Studies

Gel Retardation Assay

Nanocomplexes at varing ($^{w}/_{w}$) ratios, containing gel loading buffer (6.4 µL, 50% glycerol, 0.05% bromophenol blue, 0.05% xylene cyanol), were subjected to electrophoresis on a 2% ($^{w}/_{v}$) agarose gel containing ETB (1 µg/mL), in a Bio-Rad mini-sub electrophoresis apparatus containing 1 X electrophoresis buffer [36 mM Tris-HCl, 30 mM, sodium phosphate (NaH_2PO_4), 10 mM ethylenediamine tetra-acetic acid (EDTA), pH 7.5], for 1 hour at 50 V. The gels were viewed and images captured at exposure times of 1–2 seconds using a Vacutec Syngene G: Box BioImaging system (Syngene, Cambridge, UK).

Ethidium Bromide Displacement Assay

The compact binding of the siRNA to the NPs was assessed fluorescently using a Glomax®-Multi+ detection system (Promega), set at an excitation wavelength of 520 nm and an emission wavelength of 600 nm (Tros de Ilarduya *et al*., 2010). ETB (24 µL, 100 µg/mL) was first mixed with HBS (100 µL) in a 96-well FluorTrac flat bottom black plate and the relative fluorescence

(RF) was used as a baseline (0%) fluorescence reading. The 100% relative fluorescence, was set by introducing 1.3 µg siRNA to the mixture, which was followed by a systematic addition of 1 µL aliquots of the prepared cationic NPs (0.5 µg). The RF values were recorded after each addition until a plateau in fluorescence was noticed.

5.2.2.8 Ribonuclease A Digestion Assay

Nanocomplexes containing siRNA (0.5 µg) and varying amounts of NPs were prepared at three $^{w}/_{w}$ ratios; sub-optimum, optimum, and supra-optimum as determined from the gel retardation assay. Nanocomplexes were exposed to 10% RNase A for 2 hours at 37 °C, followed by addition of EDTA and SDS to final concentrations of 10 mM and 0.5% ($^{w}/_{v}$), respectively. After an additional 20 min incubation at 55 °C, the samples were subjected to electrophoresis as described previously.

5.2.2.9 Cell Culture

All cells were maintained and propagated at 37 °C and 5% CO_2, in 25 cm^2 flasks containing sterile EMEM, FBS (10%, $^{v}/_{v}$), penicillin G (100 U/mL) and streptomycin sulphate (100 µg/mL). The cells were split upon confluency into desired ratios, and the medium changed routinely.

5.2.2.9.1 Cell Viability: MTT Assay

HEK293, HepG2, Caco-2, and HeLa-Tat-*Luc* cells were trypsinised and seeded into 48-well plates at densities of 2.8 x 10^4, 2.0 x 10^4, 2.3 x 10^4, 2.1 x 10^4 cells/well respectively, and incubated in 0.3 mL complete medium for 24 hours at 37 °C. Prior to the addition of the preformed nanocomplexes, prepared at sub-optimum, optimum and supra-optimum ratios, the medium was replaced with fresh medium (0.3 mL). Cells were then incubated for 48 hours at 37 °C. Thereafter, the medium was removed and fresh medium (0.2 mL) and MTT reagent (0.2 mL, 5 mg/mL in sterile PBS) was added, followed by incubation for 4 hours at 37 °C. The EMEM containing MTT was then removed, cells washed with twice with PBS (0.3 mL), and the resulting purple formazan salt solubilised with 0.3 mL DMSO. The absorbance values of the samples were then recorded at 570 nm in a Mindray MR-96A microplate reader. Percentage cell viability was correlated to the untreated cells (control =100%).

5.2.2.9.2 Transfection and Competition Assay

HeLa-Tat-*Luc* cells were trypsinised and seeded into 48-well plates at a density of 2.1 x 10^4 cells/well, and incubated in 0.3 mL complete medium for 24 hours at 37 °C. Thereafter, the prepared nanocomplexes were added as previously described, and the cells incubated for an additional 48 hours at 37 °C. The old medium was then discarded, cells washed with PBS (2 x 0.5 mL) and lysed with 80 μL/well cell lysis buffer for 15 min on a Scientific STR 6 platform rocker at 30 rpm. Cell lysates were obtained by centrifugation at 12,000×g for 1 min. To 20 μL of each cell-free extract (supernatant), 100 μL luciferase assay reagent (Promega) was added, mixed and the luminescence measured in relative light units (RLU) on a Glomax®-Multi+Detection System (Promega Biosystem, Sunnyvale, USA). Protein concentrations of cell-free extracts were determined using the BCA assay as previously described (Smith *et al.*, 1985), and the luciferase activity was expressed as RLU/mg protein.

For the competition studies, 50 mM of folic acid solution was added to the cells in each well, and incubated for 20 min at 37 °C, prior to addition of the nanocomplexes. Thereafter, the luciferase activity was determined and protein concentration determined as above.

5.2.2.10 Statistical Analysis

Cell viability and transfection studies were performed in triplicate and results expressed as means ± standard deviation (S.D). The experimental data was analyzed by two-way ANOVA and *t* test, using GraphPad Prism 6.0 and statistical significant values are indicated by $*p < 0.05$, $\#p > 0.05$, $**p < 0.01$, and $***p < 0.001$.

5.3 Results and Discussion

5.3.1 Synthesis and Characterisation

The functionalisation of AuNPs with dendrimers has shown to be a promising advancement in the design of highly efficient non-viral delivery vectors (Xiao *et al.*, 2013). NPs and their nanocomplexes were successfully prepared and investigated. The conjugation of G5D onto AuNPs, as well as the attachment of FA moieties onto the G5D was verified using UV (Figure A2-A3, Appendix A) and ^{1}H NMR spectroscopy (Figure A4-A5, Appendix A). The surface plasmon resonance (SPR) peak at 536 nm indicated the formation of AuNPs. The shift in absorption to a longer wavelength of 566 nm, suggested a possible modification of the AuNP surface due to the attachment of G5D. The absorption peak at 287 nm seen in the spectrum of Au:G5D:FA, correlates with that of FA, hence suggesting the successful attachment of the FA moieties (Pan *et al.*, 2003, Mansoori *et al.*, 2010). In the ^{1}H NMR spectroscopy, the chemical shift between 2.25-3.34 ppm, represented the amino (NH_2) and methylene (CH_2) proton peaks of G5D. The characteristic proton peaks between 6.50-8.63 ppm indicated the conjugation of the FA moiety (Chang *et al.*, 2012).

TEM (Figure 5.3 and Figure 5.4) and NTA (Table 5.1), revealed that the NPs were spherical with diameters ranging from 65-128 nm, while their nanocomplexes imaged at their optimum binding weight ratios appeared as globular clusters with diameters ranging from 124.9-162.9 nm. There were no significant differences ($p < 0.05$) in the mean sizes observed in all prepared NPs. Furthermore, both the NPs and their nanocomplexes displayed positive *zeta* (ζ) potentials ranging between +29 mV to +87 mV and 25.2 mV to +40.7 mV, respectively. These *zeta* potential measurements are greater than +25 mV and are hence associated with relatively high colloidal stability (Honary and Zahir, 2013). Au:G5D and Au:G5D:FA nanocomplexes exhibited greater stability than the G5D and G5D:FA nanocomplexes as noted by their significantly higher ζ potentials. The positive *zeta* potentials also indicates that there was little shielding of the positive charges of the dendrimers by the folate moieties and the siRNA.

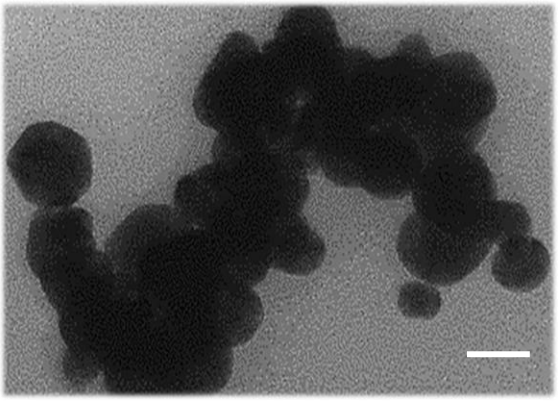

Figure 5.3: TEM micrograph of AuNPs. Scale bar= 100.

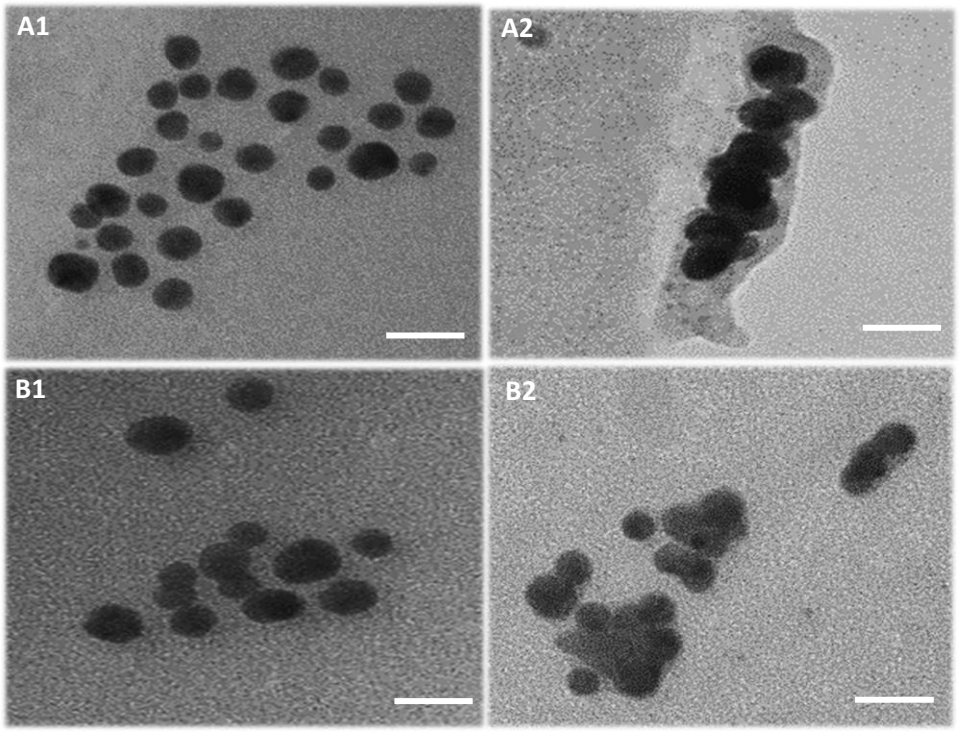

Figure 5.4: TEM micrographs of (A1) Au:G5D NPs, (A2) Au:G5D-siRNA, (B1) Au:G5D:FA, (B2) Au:G5D:FA-siRNA. Nanocomplexes prepared at optimum weight ratio of 5.0:1 and 8.0:1 $^{w}/_{w}$ respectively. Scale bar = 100 nm.

Table 5.1: Mean size and ζ potential measurements of nano-scaffolds and their nanocomplexes. Data presented as mean diameter or ζ potential ± SD.

Nanoparticles and Nanocomplexes	NP:siRNA ($^{w}/_{w}$) Ratio	Mean Diameter (nm) ± SD	ζ Potential (mV) ± SD
Au	-	65.90 ± 9.80	-7.3 ± 1.6
G5D	-	161.3 ± 11.9	+ 87.2 ± 2.4
Au:G5D	-	100.5 ± 44.1	+20.9 ± 2.2
G5D:FA	-	128.0 ± 1.20	+71.2 ± 3.4
Au:G5D:FA	-	77.70 ± 12.5	+29.0 ± 0.5
Au:G5D-siRNA	5.0:1	124.9 ± 19.9 #	+38.5 ± 2.7 *
Au:G5D:FA-siRNA	8.0:1	162.9 ± 51.9 #	+40.7 ± 1.3 #
G5D-siRNA	5.0:1	154.9 ± 9.50 #	+25.8 ± 0.8 *
G5D:FA-siRNA	6.0:1	149.7 ± 5.70 #	+37.2 ± 1.3 #

*$p < 0.05$, #$p > 0.05$ when test nanocomplexes are compared with control nanocomplexes. NTA size and *zeta* potential distribution is reflected in the Appendix.

5.3.2 Binding Studies

Gel Retardation Assay

This assay demonstrated the ability of the prepared NPs to bind and complex the siRNA. It is based on a principle that was initially reported by Hellman and Fried (Hellman and Fried, 2007), that during electrophoresis, nucleic acids migrate freely across the agarose gel, but when they are complexed with carriers such as NPs their mobility is retarded. Figure 5.5, confirms that all prepared NPs were capable of binding and complexing siRNA. The untargeted G5D and Au:G5D NPs both completely retarded at a $^{w}/_{w}$ ratio of 5:1. While the targeted G5D:FA and Au:G5D:FA NPs completely retarded at $^{w}/_{w}$ ratios of 6:1 and 8:1 respectively. The high binding efficiency demonstrated by targeted nano-scaffolds may be attributed to a slight shielding effect subjected by the folic acid on the cationic charges on the G5D, however, no drop in positive charge was not evident in the *zeta* potential measurements, where FA containing nanocomplexes had higher positive *zeta* potentials.

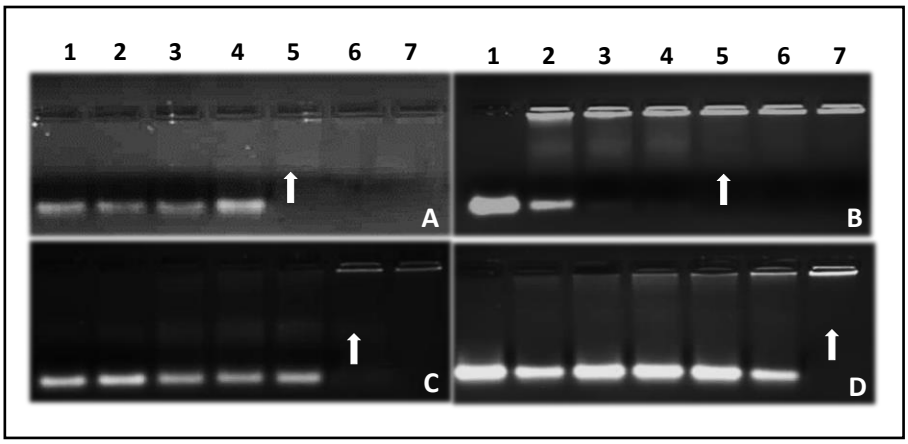

Figure 5.5: Gel retardation assay showing the binding of (A) G5D, (B) Au:G5D, (C) G5D:FA, (D) Au:G5D:FA and siRNA. Incubation mixtures (32 µL) in HBS contained varying amounts of nanoparticle preparation and 0.5 µg siCONTROL Tox siRNA corresponding to weight ratios of 2:1, 3:1, 4:1, 5:1, 6:1, and 7:1 in lanes 2-7 respectively (A-C); and 3:1, 4:1, 5:1, 6:1, 7:1, and 8:1 in lanes 2-7 respectively (D). Lane 1: naked siRNA. Arrows indicate endpoint ratios.

Ethidium Bromide Dye Displacement Assay

The degree of siRNA compaction was explored by measuring the decrease in the ETB fluorescence, upon its displacement from siRNA by NP induced condensation. From figure 5.6, a steady decrease in fluorescence was noted, upon a stepwise addition of the NPs until a plateau was reached where no further condensation occurred. G5D and Au:G5D nanocomplexes attained this endpoint at 55% and 62% respectively, while the G5D:FA and Au:G5D:FA nanocomplexes reached the endpoint at 70% and 78%, respectively. A higher degree of compaction is indicative of weaker binding, and suggests the possibility of easier dissociation of siRNA during transfection (Chuang and Chang, 2015).

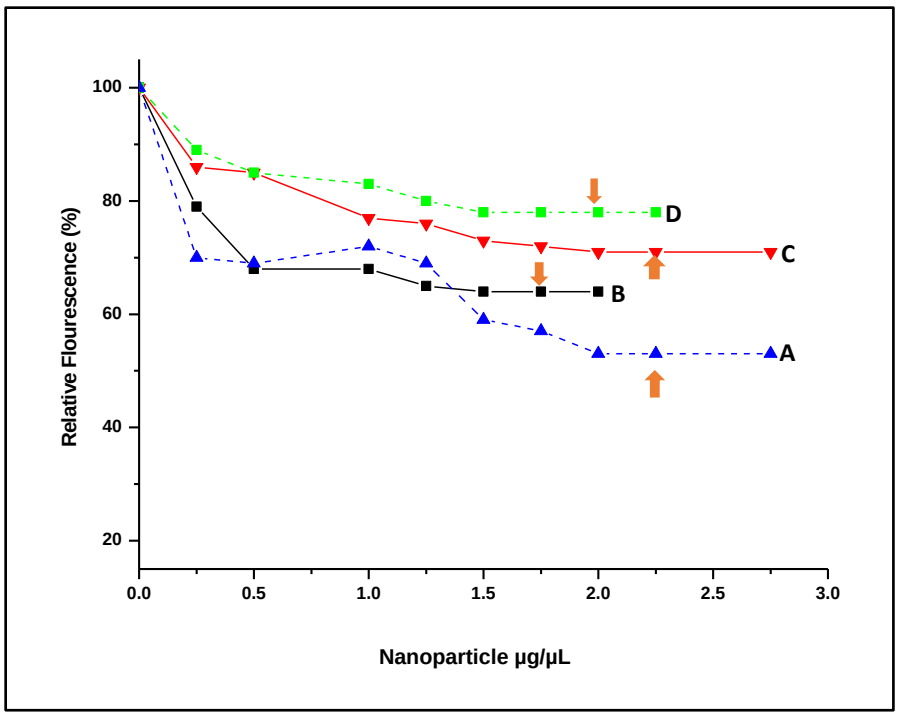

Figure 5.6: Ethidium bromide displacement assay of (A) G5D, (B) Au:G5D, (C) G5D:FA, and (D) Au:G5D:FA nanoparticles. Arrows indicate point of complexation.

5.3.3 Ribonuclease A Digestion Assay

Naked siRNA delivery to a target site may be compromised by degrading serum nucleases. Hence, delivery vectors that will not only bind but also protect the siRNA against such enzymes are vital. Following exposure to 10% RNase A, all NPs showed the ability to protect the siRNA across a range of tested ratios (Figure 5.7). This was not the case for the uncomplexed/naked siRNA as indicated by the absence of a band due to total degradation by the RNase.

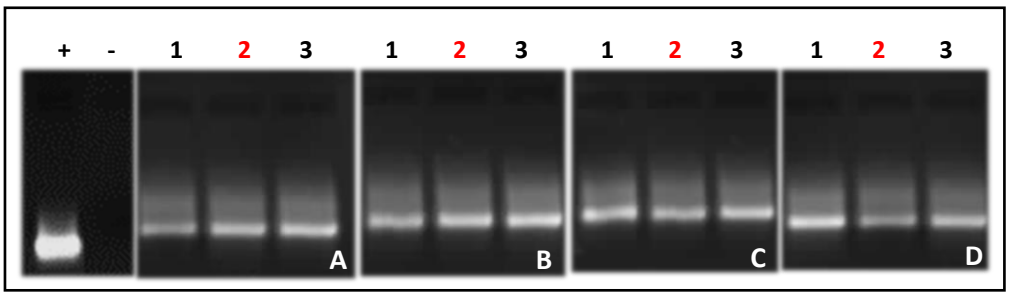

Figure 5.7: Nuclease digestion assay of nanocomplexes. (A) G5D, (B) Au:G5D, (C) G5D:FA, (D) Au:G5D:FA. Control: naked siCONTROL Tox siRNA (0.5 µg) in the absence (+ = positive control) or presence (- = negative control) of RNase A. Lanes 1-3 contains nanocomplexes at sub-optimum, optimum and supra-optimum nanoparticle: siRNA ratios. (A) 4:1, 5:1, 6:1; (B) 4:1, 5:1, 6:1; (C) 5:1, 6:1, 7:1; (D) 7:1, 8:1, 9:1 ($^{w}/_{w}$). Red colored numbers indicate optimum ratios.

5.3.4 MTT Assay

Biomedical applications of nano-scaffolds as gene delivery agents often involve deliberate, direct injection or ingestion into the body. These nano-scaffolds are often coated with bio-conjugates such as nucleic acids, polymers, antibodies and proteins for specific cell targeting. Hence, it is crucial to ensure that such enhancements are not detrimental to the cells (Lewinski *et al.*, 2008). Therefore *in vitro* cytotoxicity evaluation of the nanocomplexes is an important aspect to consider before assessing their *in vivo* potential.

The results presented in Figure 5.8, show some cell specific cytotoxicity as indicated by the differences in % cell viability in the various cell lines. There was no observable pattern/relation between the increasing N/P ratios of the nano-scaffolds and the level of cytotoxicity. There was no significant difference ($p > 0.05$) in cell viability between the tested cell lines, however when the nanocomplexes were compared to the control (cells only), a significant difference ($p < 0.0001$) in % cell viability is seen.

The higher cell viabilities observed with the Au:G5D and Au:G5D:FA nanocomplexes ranging from 70%-90%, suggest that they were less toxic than the G5D and G5D:FA nanocomplexes (50%-70%). This could be due to the presence of the biocompatible, non-immunogenic and non-cytotoxic AuNPs, which reduces some of the amines of G5D (Shukla *et al.*, 2005, Shan *et al.*, 2012, Lee *et al.*, 2008), thereby reducing the cytotoxicity. Hence, the lower cell viability for the G5D and G5D:FA nanocomplexes might be due to the increased cationic charges on the G5D even after the inclusion of a targeting moiety, folic acid. These findings strongly suggest that the inclusion of the non-toxic, inert AuNPs in the formulation of these NP based gene delivery vectors, had a positive and favourable influence on cellular toxicity.

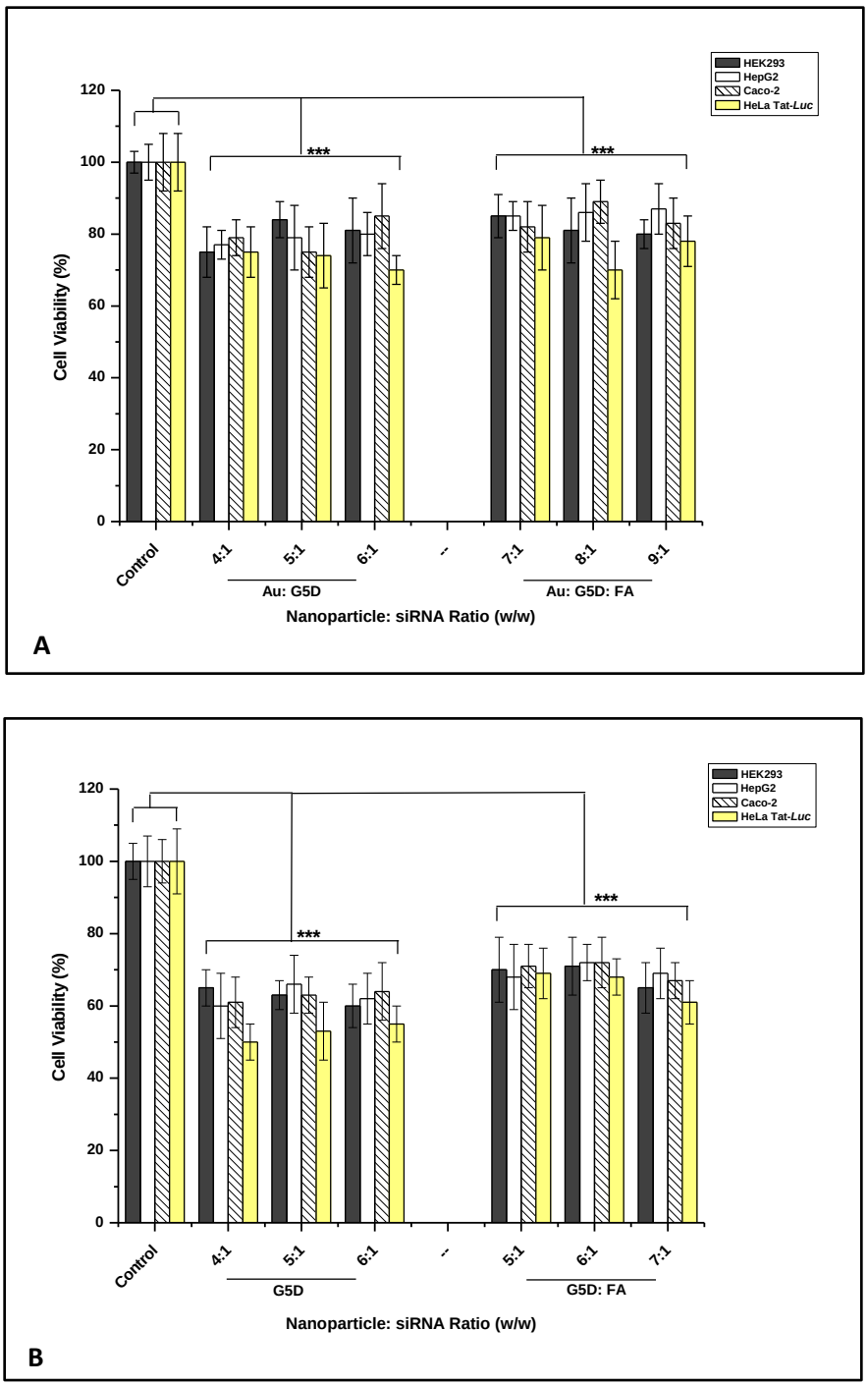

Figure 5.8 (A-B): Cell viability assay of the NP: siRNA nanocomplexes in HEK293, HepG2, Caco-2, and HeLa-Tat-*Luc*. Cells were incubated with nanocomplexes containing 0.67 μg siGENOME non-targeting control siRNA at indicated ratios ($^{w}/_{w}$). Nanocomplexes were prepared at sub-optimum, optimum and supra-optimum ratios. Data are presented as means ± S.D. (n = 3). Control = untreated cells. ***$p < 0.0001$ when compared with the control.

5.3.5 Transfection and Competition Assay

This study evaluated the ability of the nanocomplexes to efficiently deliver siRNA into the folic acid receptor positive HeLa-Tat-*Luc* cells. The HeLa-Tat-*Luc* cell line is a human cervical cell line which stably expresses the firefly luciferase gene (Daniels *et al.*, 2013). The anti-*Luc* siRNA which targets the firefly luciferase mRNA was used to determine the level transfection activity of nanocomplexes indirectly, by measurement of gene knockdown. Results are expressed as RLU/mg protein and as a percentage of luciferase activity, relative to that of untreated control cells (Figure 5.9 A-B).

The experimental data revealed that all nanocomplexes successfully bound and compacted the siRNA into nanometer-sized globular particles small enough to be internalized by the selected cells, either by adsorptive non-specific or specific endocytotic pathways, depending on their formulation. Lower gene silencing efficiency (34%) was seen with the unprotected/naked siRNA. This was expected since, upon delivery into the cell, naked nucleic acid such as siRNA is subjected to enzymatic degradation (Elsabahy *et al.*, 2011). The gene silencing elicited by all prepared nanocomplexes ranged from 42%-70%, with that of the Au:G5D:siRNA and Au:G5D:FA:siRNA nanocomplexes ranging between 50%-70%, while that for the G5D and G5D:FA nanocomplexes ranged between 42%-51% (Figure 5.9B). These significant differences ($p < 0.0001$) in gene silencing efficiency could be due to many reasons. The weaker gene silencing efficiency observed for the G5D and G5D:FA nanocomplexes, could be due to the loss of the structural integrity of the dendrimer due to interaction with interfaces or solid surfaces (Xiao *et al.*, 2013). Another reason could be due to poor dissociation between the siRNA and the cationic G5D due to their strong binding affinity. Earlier studies have demonstrated a direct correlation between the binding affinity of nucleic acids to cationic polymers and the transgene expression (Bettinger *et al.*, 2001). These findings corroborate with studies conducted by Kang and co-workers, who associated unmodified and conjugated G5D with weak gene silencing efficiency (Kang *et al.*, 2005).

Moreover, the high significant gene silencing efficiency elicited by the test nano-scaffolds can be accredited to the presence of AuNPs entrapped in the 1^{o} amines which have been reported to help preserve the morphological aesthetics of dendrimers, permitting efficient interaction with the siRNA (Shan *et al.*, 2012).

These findings are in agreement with reports by Kolhatkar and coworkers on surface tailored PAMAM showing good cell membrane permeability and good delivery of siRNA into the targeted site (Kolhatkar *et al.*, 2007). Recent studies by Shan *et al*. and Waite *et al*. have also demonstrated the effectiveness of internally modified and surface tailored G5D in gene silencing (Shan *et al.*, 2012, Waite *et al.*, 2009). The highest gene silencing was observed at optimum ratios for all nanocomplexes. These findings correlate with previous reports suggesting a possible dependency of the siRNA-dendrimer complex's gene silencing ability on the dendrimer generation, the siRNA concentration and $^{w}/_{w}$ ratio (Patil *et al.*, 2008).

Additionally, to confirm that the uptake of the folate-targeted nanocomplexes was receptor-mediated, a competition study was conducted where the FA-Rs overexpressed on the surface of HeLa-Tat-*Luc* cells were blocked with an excess amount of the free folic acid prior to transfection with the nanocomplexes. A significant ($p < 0.0001$) 30% drop in gene knockdown was seen (Figure 5.10A-B) indicating that much of these nanocomplexes were endocytosed via FA-Rs (Zhang *et al.*, 2015). Overall, these findings suggest that the Au:G5D and Au:G5D:FA NPs appear to be better siRNA delivery vehicles than the G5D and G5D:FA:siRNA NPs, a finding that correlates with the cell viability studies.

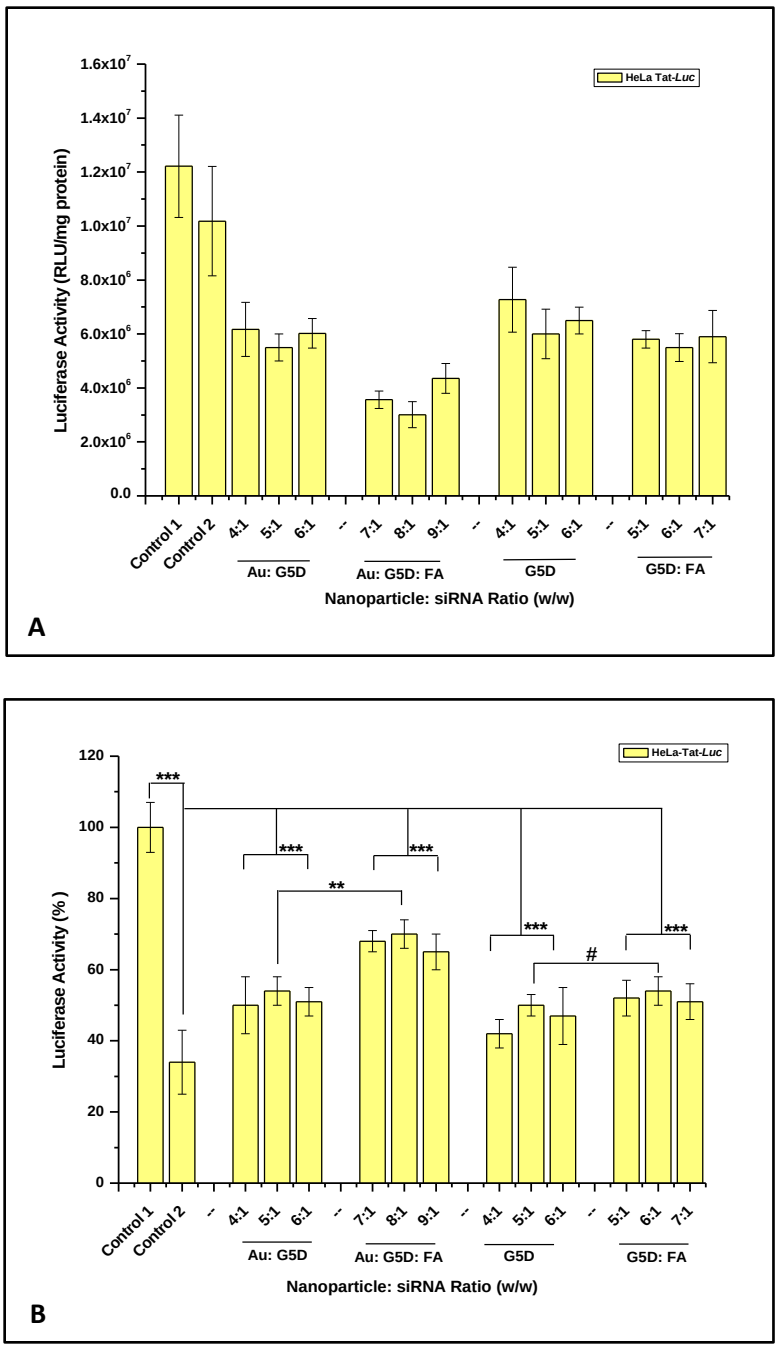

Figure 5.9 (A-B): Luciferase gene silencing using NP:siRNA nanocomplexes. HeLa-Tat-*Luc* cells were exposed to nanocomplexes constituted with 0.27 µg anti-*Luc* siRNA and varying amounts of nanoparticles at sub-optimum, optimum and supra-optimum ratios. Luciferase gene silencing is reported as RLU/mg protein (A), and as a percentage (B). Control 1= untreated cells. Control 2= cells + Anti-*Luc* siRNA. Data are presented as means ± SD (n=3). #$p > 0.05$, **$p < 0.001$ ***$p < 0.0001$.

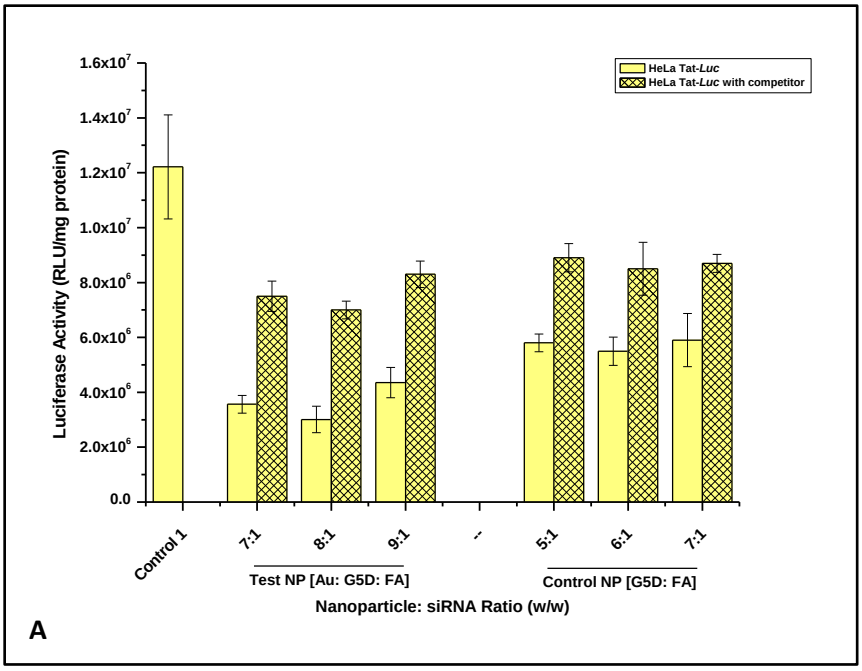

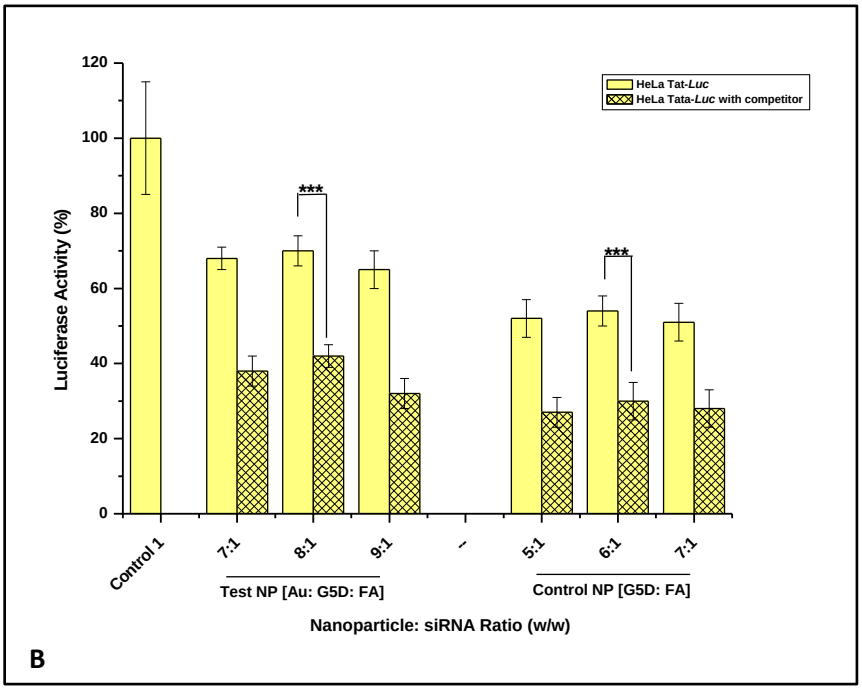

Figure 5.10 (A-B): Competition studies of targeted NP: anti-*Luc* siRNA nanocomplexes. HeLa-Tat-*Luc* cells were exposed to excess folic acid (250 μg), then treated with nanocomplexes at optimum ratios. Luciferase gene silencing is expressed/reported as RLU/mg protein (A) and as a percentage (B). Data are presented as means ± SD (n=3). *$p < 0.05$, **$p < 0.001$, ***$p < 0.0001$.

5.4 Conclusion

Both Au:G5D and Au:G5D:FA NPs were excellent siRNA delivery vehicles. Gel retardation and ethidium bromide dye displacement assays clearly showed their interaction with siRNA, regardless of internal/surface positive charges. They were able to form stable globular nanocomplexes which afforded excellent protection to the siRNA against RNase A. The modification of the surface amines of the dendrimers with the FA targeting ligand, and the internal modification with AuNPs served to produce a reduction of the cytotoxicity of the nanocomplexes (cell viability of up to 90%) and an increased siRNA induce luciferase gene silencing (up to 70%). In summary, we have demonstrated that Au:G5D and Au:G5D:FA NPs have many of the ideal characteristics required for an efficient siRNA delivery vehicle, and future studies would be needed to evaluate these NPs *in vivo.*

5.5 References

AHAMED, M., ALSALHI, M. S. & SIDDIQUI, M. 2010. Silver nanoparticle applications and human health. *Clinica chimica acta,* 411**,** 1841-1848.

AKBARZADEH, A., ZARE, D., FARHANGI, A., MEHRABI, M. R., NOROUZIAN, D., TANGESTANINEJAD, S., MOGHADAM, M. & BARARPOUR, N. 2009. Synthesis and characterization of gold nanoparticles by tryptophane. *American Journal of Applied Sciences,* 6**,** 691-695.

ALIVISATOS, A. P., JOHNSSON, K. P., PENG, X. & WILSON, T. E. 1996. Organization of'nanocrystal molecules' using DNA. *Nature,* 382**,** 609.

ALMEIDA, J. P. M., FIGUEROA, E. R. & DREZEK, R. A. 2014. Gold nanoparticle mediated cancer immunotherapy. *Nanomedicine: Nanotechnology, Biology and Medicine,* 10**,** 503-514.

ANDERSSON, H. A., KIM, Y.-S., O'NEILL, B. E., SHI, Z.-Z. & SERDA, R. E. 2014. HSP70 promoter-driven activation of gene expression for immunotherapy using gold nanorods and near infrared light. *Vaccines,* 2**,** 216-227.

ARIMA, H., YAMASHITA, S., MORI, Y., HAYASHI, Y., MOTOYAMA, K., HATTORI, K., TAKEUCHI, T., JONO, H., ANDO, Y. & HIRAYAMA, F. 2010. In vitro and in vivo gene delivery mediated by lactosylated dendrimer/α-cyclodextrin conjugates (G2) into hepatocytes. *Journal of Controlled Release,* 146**,** 106-117.

ATAR, F. B., BATTAL, E., AYGUN, L. E., DAGLAR, B., BAYINDIR, M. & OKYAY, A. K. 2013. Plasmonically enhanced hot electron based photovoltaic device. *Optics express,* 21**,** 7196-7201.

AYDIN, Z., AKBAS, F., SENEL, M. & KOC, S. N. 2012. Evaluation of Jeffamine®-cored PAMAM dendrimers as an efficient in vitro gene delivery system. *Journal of Biomedical Materials Research Part A,* 100**,** 2623-2628.

BAL, S. M., DING, Z., VAN RIET, E., JISKOOT, W. & BOUWSTRA, J. A. 2010. Advances in transcutaneous vaccine delivery: do all ways lead to Rome? *Journal of controlled release,* 148**,** 266-282.

BALAZS, D. A. & GODBEY, W. 2010. Liposomes for use in gene delivery. *Journal of drug delivery,* 2011.

BANAN, M. & PURI, N. 2004. The ins and outs of RNAi in mammalian cells. *Current pharmaceutical biotechnology,* 5**,** 441-450.

BETTINGER, T., CARLISLE, R. C., READ, M. L., OGRIS, M. & SEYMOUR, L. W. 2001. Peptide-mediated RNA delivery: a novel approach for enhanced transfection of primary and post-mitotic cells. *Nucleic acids research,* 29**,** 3882-3891.

BHAKTA, G., SHRIVASTAVA, A. & MAITRA, A. 2009. Magnesium phosphate nanoparticles can be efficiently used in vitro and in vivo as non-viral vectors for targeted gene delivery. *Journal of biomedical nanotechnology,* 5**,** 106-114.

BHATTACHARYA, R., PATRA, C. R., EARL, A., WANG, S., KATARYA, A., LU, L., KIZHAKKEDATHU, J. N., YASZEMSKI, M. J., GREIPP, P. R. & MUKHOPADHYAY, D. 2007. Attaching folic acid on gold nanoparticles using noncovalent interaction via different polyethylene glycol backbones and targeting of cancer cells. *Nanomedicine: Nanotechnology, Biology and Medicine,* 3**,** 224-238.

BOUSSIF, O., LEZOUALC'H, F., ZANTA, M. A., MERGNY, M. D., SCHERMAN, D., DEMENEIX, B. & BEHR, J.-P. 1995. A versatile vector for gene and oligonucleotide transfer into cells in culture and in vivo: polyethylenimine. *Proceedings of the National Academy of Sciences,* 92**,** 7297-7301.

BOUWMEESTER, H., POORTMAN, J., PETERS, R. J., WIJMA, E., KRAMER, E., MAKAMA, S., PUSPITANINGANINDITA, K., MARVIN, H. J., PEIJNENBURG, A. A. & HENDRIKSEN, P. J. 2011. Characterization of translocation of silver nanoparticles and effects on whole-genome gene expression using an in vitro intestinal epithelium coculture model. *ACS nano,* 5**,** 4091-4103.

BRADLEY, J. S. 1994. The chemistry of transition metal colloids. *Clusters and colloids: from theory to applications***,** 459-544.

BRAUN, G. B., PALLAORO, A., WU, G., MISSIRLIS, D., ZASADZINSKI, J. A., TIRRELL, M. & REICH, N. O. 2009. Laser-activated gene silencing via gold nanoshell− siRNA conjugates. *Acs Nano,* 3**,** 2007-2015.

BRAVO-OSUNA, I., VICARIO-DE-LA-TORRE, M., ANDRÉS-GUERRERO, V., SÁNCHEZ-NIEVES, J., GUZMÁN-NAVARRO, M., DE LA MATA, F., GÓMEZ, R., DE LAS HERAS, B., ARGUESO, P. & PONCHEL, G. 2016. Novel water-soluble mucoadhesive carbosilane dendrimers for ocular administration. *Molecular pharmaceutics,* 13**,** 2966-2976.

BRUST, M., WALKER, M., BETHELL, D., SCHIFFRIN, D. J. & WHYMAN, R. 1994. Synthesis of thiol-derivatised gold nanoparticles in a two-phase liquid–liquid system. *Journal of the Chemical Society, Chemical Communications***,** 801-802.

CHANG, Y., LIU, N., CHEN, L., MENG, X., LIU, Y., LI, Y. & WANG, J. 2012. Synthesis and characterization of DOX-conjugated dendrimer-modified magnetic iron oxide conjugates for magnetic resonance imaging, targeting, and drug delivery. *Journal of Materials Chemistry,* 22**,** 9594-9601.

CHAPLOT, S. P. & RUPENTHAL, I. D. 2014. Dendrimers for gene delivery–a potential approach for ocular therapy? *Journal of Pharmacy and Pharmacology,* 66**,** 542-556.

CHEN, A. A., DERFUS, A. M., KHETANI, S. R. & BHATIA, S. N. 2005. Quantum dots to monitor RNAi delivery and improve gene silencing. *Nucleic acids research,* 33**,** e190-e190.

CHEN, Q., LI, K., WEN, S., LIU, H., PENG, C., CAI, H., SHEN, M., ZHANG, G. & SHI, X. 2013. Targeted CT/MR dual mode imaging of tumors using multifunctional dendrimer-entrapped gold nanoparticles. *Biomaterials,* 34**,** 5200-5209.

CHO-CHUNG, Y. 2005. DNA drug design for cancer therapy. *Current pharmaceutical design,* 11**,** 2811-2823.

CHOI, C. H. J., ALABI, C. A., WEBSTER, P. & DAVIS, M. E. 2010. Mechanism of active targeting in solid tumors with transferrin-containing gold nanoparticles. *Proceedings of the National Academy of Sciences,* 107**,** 1235-1240.

CHUANG, C.-C. & CHANG, C.-W. 2015. Complexation of bioreducible cationic polymers with gold nanoparticles for improving stability in serum and application on nonviral gene delivery. *ACS applied materials & interfaces,* 7**,** 7724-7731.

CONDE, J., DORIA, G. & BAPTISTA, P. 2011. Noble metal nanoparticles applications in cancer. *Journal of drug delivery,* 2012.

CONNOR, E. E., MWAMUKA, J., GOLE, A., MURPHY, C. J. & WYATT, M. D. 2005. Gold nanoparticles are taken up by human cells but do not cause acute cytotoxicity. *Small,* 1**,** 325-327.

COULIE, P. G., VAN DEN EYNDE, B. J., VAN DER BRUGGEN, P. & BOON, T. 2014. Tumour antigens recognized by T lymphocytes: at the core of cancer immunotherapy. *Nature reviews. Cancer,* 14**,** 135.

CROOKS, R. M., ZHAO, M., SUN, L., CHECHIK, V. & YEUNG, L. K. 2001. Dendrimer-encapsulated metal nanoparticles: synthesis, characterization, and applications to catalysis. *Accounts of Chemical Research,* 34**,** 181-190.

CRUZ, L. J., TACKEN, P. J., RUEDA, F., CARLES DOMINGO, J., ALBERICIO, F. & FIGDOR, C. G. 2012. 8 Targeting Nanoparticles to Dendritic Cells for Immunotherapy. *Methods in enzymology,* 509**,** 143.

DANIEL, M.-C. & ASTRUC, D. 2004. Gold nanoparticles: assembly, supramolecular chemistry, quantum-size-related properties, and applications toward biology, catalysis, and nanotechnology. *Chemical reviews,* 104**,** 293-346.

DANIELS, A., SINGH, M. & ARIATTI, M. 2013. PEGYLATED AND NON-PEGYLATED siRNA LIPOPLEXES. *J. Control. Release,* 94**,** 1-14.

DAVIES, J. C., GEDDES, D. M. & ALTON, E. W. 2001. Gene therapy for cystic fibrosis. *The journal of gene medicine,* 3**,** 409-417.

DE OLIVEIRA, R., ZHAO, P., LI, N., DE SANTA MARIA, L. C., VERGNAUD, J., RUIZ, J., ASTRUC, D. & BARRATT, G. 2013. Synthesis and in vitro studies of gold nanoparticles loaded with docetaxel. *International journal of pharmaceutics,* 454**,** 703-711.

DING, Y., ZHOU, Y.-Y., CHEN, H., GENG, D.-D., WU, D.-Y., HONG, J., SHEN, W.-B., HANG, T.-J. & ZHANG, C. 2013. The performance of thiol-terminated PEG-paclitaxel-conjugated gold nanoparticles. *Biomaterials,* 34**,** 10217-10227.

DORASAMY, S., NARAINPERSAD, N., SINGH, M. & ARIATTI, M. 2012. Novel targeted liposomes deliver sirna to hepatocellular carcinoma cells in vitro. *Chemical biology & drug design,* 80**,** 647-656.

DREADEN, E. C., ALKILANY, A. M., HUANG, X., MURPHY, C. J. & EL-SAYED, M. A. 2012. The golden age: gold nanoparticles for biomedicine. *Chemical Society Reviews,* 41**,** 2740-2779.

DUNCAN, B., KIM, C. & ROTELLO, V. M. 2010. Gold nanoparticle platforms as drug and biomacromolecule delivery systems. *Journal of Controlled Release,* 148**,** 122-127.

EDELSTEIN, M. L., ABEDI, M. R. & WIXON, J. 2007. Gene therapy clinical trials worldwide to 2007—an update. *The journal of gene medicine,* 9**,** 833-842.

EDINGER, D. & WAGNER, E. 2011. Bioresponsive polymers for the delivery of therapeutic nucleic acids. *Wiley interdisciplinary reviews: nanomedicine and nanobiotechnology,* 3**,** 33-46.

EL-SAYED, I. H., HUANG, X. & EL-SAYED, M. A. 2005. Surface plasmon resonance scattering and absorption of anti-EGFR antibody conjugated gold nanoparticles in cancer diagnostics: applications in oral cancer. *Nano letters,* 5**,** 829-834.

ELSABAHY, M., NAZARALI, A. & FOLDVARI, M. 2011. Non-viral nucleic acid delivery: key challenges and future directions. *Current drug delivery,* 8**,** 235-244.

FERLAY, J., SOERJOMATARAM, I., ERVIK, M., DIKSHIT, R., ESER, S., MATHERS, C., REBELO, M., PARKIN, D., FORMAN, D. & BRAY, F. 2013. Cancer Incidence and Mortality Worldwide: IARC CancerBase No. 11. Lyon, France: International Agency for Research on Cancer. GLOBOCAN 2012 v1. 0, 2013.

FIGUEROA, E. R., LIN, A. Y., YAN, J., LUO, L., FOSTER, A. E. & DREZEK, R. A. 2014. Optimization of PAMAM-gold nanoparticle conjugation for gene therapy. *Biomaterials,* 35**,** 1725-1734.

FORTUNE, J. A., NOVOBRANTSEVA, T. I. & KLIBANOV, A. M. 2011. Highly effective gene transfection in vivo by alkylated polyethylenimine. *Journal of drug delivery,* 2011.

FRATILA, R. M., MITCHELL, S. G., DEL PINO, P., GRAZU, V. & DE LA FUENTE, J. S. M. 2014. Strategies for the biofunctionalization of gold and iron oxide nanoparticles. *Langmuir,* 30**,** 15057-15071.

FRATODDI, I., VENDITTI, I., CAMETTI, C. & RUSSO, M. 2014. Gold nanoparticles and gold nanoparticle-conjugates for delivery of therapeutic molecules. Progress and challenges. *Journal of Materials Chemistry B,* 2**,** 4204-4220.

GARY, D. J., PURI, N. & WON, Y.-Y. 2007. Polymer-based siRNA delivery: perspectives on the fundamental and phenomenological distinctions from polymer-based DNA delivery. *Journal of Controlled Release,* 121**,** 64-73.

GHOSH, D. & CHATTOPADHYAY, N. 2013. Gold nanoparticles: acceptors for efficient energy transfer from the photoexcited fluorophores. *Optics and Photonics Journal,* 3**,** 18.

GHOSH, P., HAN, G., DE, M., KIM, C. K. & ROTELLO, V. M. 2008a. Gold nanoparticles in delivery applications. *Advanced drug delivery reviews,* 60**,** 1307-1315.

GHOSH, P. S., KIM, C.-K., HAN, G., FORBES, N. S. & ROTELLO, V. M. 2008b. Efficient gene delivery vectors by tuning the surface charge density of amino acid-functionalized gold nanoparticles. *ACS nano,* 2**,** 2213.

GIL, P. R. & PARAK, W. J. 2008. Composite nanoparticles take aim at cancer. *ACS nano,* 2**,** 2200-2205.

GILJOHANN, D. A., SEFEROS, D. S., DANIEL, W. L., MASSICH, M. D., PATEL, P. C. & MIRKIN, C. A. 2010. Gold nanoparticles for biology and medicine. *Angewandte Chemie International Edition,* 49**,** 3280-3294.

GILJOHANN, D. A., SEFEROS, D. S., PRIGODICH, A. E., PATEL, P. C. & MIRKIN, C. A. 2009. Gene regulation with polyvalent siRNA− nanoparticle conjugates. *Journal of the American Chemical Society,* 131**,** 2072-2073.

GUO, S. & HUANG, L. 2014. Nanoparticles containing insoluble drug for cancer therapy. *Biotechnology advances,* 32**,** 778-788.

GUO, S., HUANG, Y., JIANG, Q., SUN, Y., DENG, L., LIANG, Z., DU, Q., XING, J., ZHAO, Y. & WANG, P. C. 2010. Enhanced gene delivery and siRNA silencing by gold nanoparticles coated with charge-reversal polyelectrolyte. *ACS nano,* 4**,** 5505-5511.

GUO, W. & LEE, R. J. 1999. Receptor-targeted gene delivery viafolate-conjugated polyethylenimine. *The AAPS Journal,* 1**,** 20-26.

GUO, X. & HUANG, L. 2012. Recent advances in non-viral vectors for gene delivery. *Accounts of chemical research,* 45**,** 971.

HAENSLER, J. & SZOKA JR, F. C. 1993. Polyamidoamine cascade polymers mediate efficient transfection of cells in culture. *Bioconjugate chemistry,* 4**,** 372-379.

HELLMAN, L. M. & FRIED, M. G. 2007. Electrophoretic mobility shift assay (EMSA) for detecting protein–nucleic acid interactions. *Nature protocols,* 2**,** 1849-1861.

HERZOG, R. W., CAO, O. & SRIVASTAVA, A. 2010. Two decades of clinical gene therapy–success is finally mounting. *Discovery medicine,* 9**,** 105.

HONARY, S. & ZAHIR, F. 2013. Effect of zeta potential on the properties of nano-drug delivery systems-a review (Part 2). *Tropical Journal of Pharmaceutical Research,* 12**,** 265-273.

HONDA, M., ASAI, T., OKU, N., ARAKI, Y., TANAKA, M. & EBIHARA, N. 2013. Liposomes and nanotechnology in drug development: focus on ocular targets. *International journal of nanomedicine,* 8**,** 495.

HU, M., QIAN, L., BRIÑAS, R. P., LYMAR, E. S., KUZNETSOVA, L. & HAINFELD, J. F. 2008. Gold nanoparticle–protein arrays improve resolution for cryo-electron microscopy. *Journal of structural biology,* 161**,** 83-91.

HUANG, Y., YU, F., PARK, Y.-S., WANG, J., SHIN, M.-C., CHUNG, H. S. & YANG, V. C. 2010. Co-administration of protein drugs with gold nanoparticles to enable percutaneous delivery. *Biomaterials,* 31**,** 9086-9091.

IBRAHEEM, D., ELAISSARI, A. & FESSI, H. 2014. Gene therapy and DNA delivery systems. *International journal of pharmaceutics,* 459**,** 70-83.

INDIRA, T. & LAKSHMI, P. 2010. Magnetic nanoparticles–a review. *Int. J. Pharm. Sci. Nanotechnol,* 3**,** 1035-1042.

JANG, H., RYOO, S.-R., KOSTARELOS, K., HAN, S. W. & MIN, D.-H. 2013. The effective nuclear delivery of doxorubicin from dextran-coated gold nanoparticles larger than nuclear pores. *Biomaterials,* 34**,** 3503-3510.

JIANG, W., KIM, B. Y., RUTKA, J. T. & CHAN, W. C. 2008. Nanoparticle-mediated cellular response is size-dependent. *Nature nanotechnology,* 3**,** 145-150.

JIN, L., ZENG, X., LIU, M., DENG, Y. & HE, N. 2014b. Current progress in gene delivery technology based on chemical methods and nano-carriers. *Theranostics,* 4**,** 240.

JUNQUERA, E. & AICART, E. 2014. Cationic lipids as transfecting agents of DNA in gene therapy. *Current topics in medicinal chemistry,* 14**,** 649-663.

KAMBHAMPATI, S. P., CLUNIES-ROSS, A. J., BHUTTO, I., MISHRA, M. K., EDWARDS, M., MCLEOD, D. S., KANNAN, R. M. & LUTTY, G. 2015. Systemic and Intravitreal Delivery of Dendrimers to Activated Microglia/Macrophage in Ischemia/Reperfusion Mouse RetinaRetinal Microglia Uptake of Dendrimers. *Investigative ophthalmology & visual science,* 56**,** 4413-4424.

KANG, H., DELONG, R., FISHER, M. H. & JULIANO, R. L. 2005. Tat-conjugated PAMAM dendrimers as delivery agents for antisense and siRNA oligonucleotides. *Pharmaceutical research,* 22**,** 2099-2106.

KANNAN, R., NANCE, E., KANNAN, S. & TOMALIA, D. 2014. Emerging concepts in dendrimer-based nanomedicine: from design principles to clinical applications. *Journal of internal medicine,* 276**,** 579-617.

KATRAGADDA, C. S., CHOUDHURY, P. K. & MURTHY, P. 2010. Nanoparticles as non-viral gene delivery vectors. *Indian J Pharm Educ Res,* 44**,** 109-111.

KAY, M. A., GLORIOSO, J. C. & NALDINI, L. 2001. Viral vectors for gene therapy: the art of turning infectious agents into vehicles of therapeutics. *Nature medicine,* 7**,** 33-40.

KENDIRCI, M., TELOKEN, P. E., CHAMPION, H. C., HELLSTROM, W. J. & BIVALACQUA, T. J. 2006. Gene therapy for erectile dysfunction: fact or fiction? *european urology,* 50**,** 1208-1222.

KESHARWANI, P., BANERJEE, S., GUPTA, U., AMIN, M. C. I. M., PADHYE, S., SARKAR, F. H. & IYER, A. K. 2015. PAMAM dendrimers as promising nanocarriers for RNAi therapeutics. *Materials Today,* 18**,** 565-572.

KICHEV, A., ROUSSET, C. I., BABURAMANI, A. A., LEVISON, S. W., WOOD, T. L., GRESSENS, P., THORNTON, C. & HAGBERG, H. 2014. Tumor necrosis factor-related apoptosis-inducing ligand (TRAIL) signaling and cell death in the immature central nervous system after hypoxia-ischemia and inflammation. *Journal of Biological Chemistry,* 289**,** 9430-9439.

KILLOPS, K. L., CAMPOS, L. M. & HAWKER, C. J. 2008. Robust, efficient, and orthogonal synthesis of dendrimers via thiol-ene "click" chemistry. *Journal of the American Chemical Society,* 130**,** 5062-5064.

KIM, A., LEE, E. H., CHOI, S.-H. & KIM, C.-K. 2004. In vitro and in vivo transfection efficiency of a novel ultradeformable cationic liposome. *Biomaterials,* 25**,** 305-313.

KIM, C. S., DUNCAN, B., CRERAN, B. & ROTELLO, V. M. 2013. Triggered nanoparticles as therapeutics. *Nano today,* 8**,** 439-447.

KIM, D.-W., KIM, J.-H., PARK, M., YEOM, J.-H., GO, H., KIM, S., HAN, M. S., LEE, K. & BAE, J. 2011. Modulation of biological processes in the nucleus by delivery of DNA oligonucleotides conjugated with gold nanoparticles. *Biomaterials,* 32**,** 2593-2604.

KIM, D. & JON, S. 2012. Gold nanoparticles in image-guided cancer therapy. *Inorganica Chimica Acta,* 393**,** 154-164.

KIM, J.-B., CHOI, J. S., NAM, K., LEE, M., PARK, J.-S. & LEE, J.-K. 2006. Enhanced transfection of primary cortical cultures using arginine-grafted PAMAM dendrimer, PAMAM-Arg. *Journal of controlled release,* 114**,** 110-117.

KLEIN, S., ZOLK, O., FROMM, M., SCHRÖDL, F., NEUHUBER, W. & KRYSCHI, C. 2009. Functionalized silicon quantum dots tailored for targeted siRNA delivery. *Biochemical and biophysical research communications,* 387**,** 164-168.

KNIPE, J. M., PETERS, J. T. & PEPPAS, N. A. 2013. Theranostic agents for intracellular gene delivery with spatiotemporal imaging. *Nano today,* 8**,** 21-38.

KOLHATKAR, R. B., KITCHENS, K. M., SWAAN, P. W. & GHANDEHARI, H. 2007. Surface acetylation of polyamidoamine (PAMAM) dendrimers decreases cytotoxicity while maintaining membrane permeability. *Bioconjugate chemistry,* 18**,** 2054-2060.

KOMPELLA, U. B., AMRITE, A. C., RAVI, R. P. & DURAZO, S. A. 2013. Nanomedicines for back of the eye drug delivery, gene delivery, and imaging. *Progress in retinal and eye research,* 36**,** 172-198.

KRIEG, A. M., YI, A.-K., MATSON, S., WALDSCHMIDT, T. J., BISHOP, G. A., TEASDALE, R., KORETZKY, G. A. & KLINMAN, D. M. 1995. CpG motifs in bacterial DNA trigger direct B-cell activation. *Nature,* 374**,** 546-549.

KUMAR, S. S. D., SURIANARAYANAN, M., VIJAYARAGHAVAN, R., MANDAL, A. B. & MACFARLANE, D. 2014. Curcumin loaded poly (2-hydroxyethyl methacrylate) nanoparticles from gelled ionic liquid–In vitro cytotoxicity and anti-cancer activity in SKOV-3 cells. *European Journal of Pharmaceutical Sciences,* 51**,** 34-44.

LAZARUS, G. G. & SINGH, M. 2016. Cationic modified gold nanoparticles show enhanced gene delivery in vitro. *Nanotechnology Reviews,* 5**,** 425-434.

LEE, I. H., KWON, H. K., AN, S., KIM, D., KIM, S., YU, M. K., LEE, J. H., LEE, T. S., IM, S. H. & JON, S. 2012. Imageable Antigen-Presenting Gold Nanoparticle Vaccines for Effective Cancer Immunotherapy In Vivo. *Angewandte Chemie,* 124**,** 8930-8935.

LEE, J.-S., GREEN, J. J., LOVE, K. T., SUNSHINE, J., LANGER, R. & ANDERSON, D. G. 2009. Gold, poly (β-amino ester) nanoparticles for small interfering RNA delivery. *Nano letters,* 9**,** 2402-2406.

LEE, J. H., LIM, Y.-B., CHOI, J. S., LEE, Y., KIM, T.-I., KIM, H. J., YOON, J. K., KIM, K. & PARK, J.-S. 2003. Polyplexes assembled with internally quaternized PAMAM-OH dendrimer and plasmid DNA have a neutral surface and gene delivery potency. *Bioconjugate chemistry,* 14**,** 1214-1221.

LEE, S. H., BAE, K. H., KIM, S. H., LEE, K. R. & PARK, T. G. 2008. Amine-functionalized gold nanoparticles as non-cytotoxic and efficient intracellular siRNA delivery carriers. *International journal of pharmaceutics,* 364**,** 94-101.

LEWINSKI, N., COLVIN, V. & DREZEK, R. 2008. Cytotoxicity of nanoparticles. *small,* 4**,** 26-49.

LI, J.-M., ZHAO, M.-X., SU, H., WANG, Y.-Y., TAN, C.-P., JI, L.-N. & MAO, Z.-W. 2011. Multifunctional quantum-dot-based siRNA delivery for HPV18 E6 gene silence and intracellular imaging. *Biomaterials,* 32**,** 7978-7987.

LIN, A. Y., ALMEIDA, J. P. M., BEAR, A., LIU, N., LUO, L., FOSTER, A. E. & DREZEK, R. A. 2013. Gold nanoparticle delivery of modified CpG stimulates macrophages and inhibits tumor growth for enhanced immunotherapy. *PLoS One,* 8**,** e63550.

LIU, B., YANG, M., LI, R., DING, Y., QIAN, X., YU, L. & JIANG, X. 2008. The antitumor effect of novel docetaxel-loaded thermosensitive micelles. *European Journal of Pharmaceutics and Biopharmaceutics,* 69**,** 527-534.

LIU, G., LI, D., PASUMARTHY, M. K., KOWALCZYK, T. H., GEDEON, C. R., HYATT, S. L., PAYNE, J. M., MILLER, T. J., BRUNOVSKIS, P. & FINK, T. L. 2003. Nanoparticles of compacted DNA transfect postmitotic cells. *Journal of Biological Chemistry,* 278**,** 32578-32586.

LIU, H., WANG, H., YANG, W. & CHENG, Y. 2012. Disulfide cross-linked low generation dendrimers with high gene transfection efficacy, low cytotoxicity, and low cost. *Journal of the American Chemical Society,* 134**,** 17680-17687.

LIU, Z., ZHAO, F., GAO, S., SHAO, J. & CHANG, H. 2016. The Applications of Gold Nanoparticle-Initialed Chemiluminescence in Biomedical Detection. *Nanoscale research letters,* 11**,** 460.

LLEVOT, A. & ASTRUC, D. 2012. Applications of vectorized gold nanoparticles to the diagnosis and therapy of cancer. *Chemical Society Reviews,* 41**,** 242-257.

LU, S., NEOH, K. G., HUANG, C., SHI, Z. & KANG, E.-T. 2013. Polyacrylamide hybrid nanogels for targeted cancer chemotherapy via co-delivery of gold nanoparticles and MTX. *Journal of colloid and interface science,* 412**,** 46-55.

LUNGWITZ, U., BREUNIG, M., BLUNK, T. & GÖPFERICH, A. 2005. Polyethylenimine-based non-viral gene delivery systems. *European Journal of Pharmaceutics and Biopharmaceutics,* 60**,** 247-266.

LUO, D., HAVERSTICK, K., BELCHEVA, N., HAN, E. & SALTZMAN, W. M. 2002. Poly (ethylene glycol)-conjugated PAMAM dendrimer for biocompatible, high-efficiency DNA delivery. *Macromolecules,* 35**,** 3456-3462.

LUTEN, J., VAN NOSTRUM, C. F., DE SMEDT, S. C. & HENNINK, W. E. 2008. Biodegradable polymers as non-viral carriers for plasmid DNA delivery. *Journal of Controlled Release,* 126**,** 97-110.

LV, H., ZHANG, S., WANG, B., CUI, S. & YAN, J. 2006. Toxicity of cationic lipids and cationic polymers in gene delivery. *Journal of Controlled Release,* 114**,** 100-109.

MANJU, S. & SREENIVASAN, K. 2012. Gold nanoparticles generated and stabilized by water soluble curcumin–polymer conjugate: Blood compatibility evaluation and targeted drug delivery onto cancer cells. *Journal of colloid and interface science,* 368**,** 144-151.

MANSOORI, G. A., BRANDENBURG, K. S. & SHAKERI-ZADEH, A. 2010. A comparative study of two folate-conjugated gold nanoparticles for cancer nanotechnology applications. *Cancers,* 2**,** 1911-1928.

MANSOURI, S., CUIE, Y., WINNIK, F., SHI, Q., LAVIGNE, P., BENDERDOUR, M., BEAUMONT, E. & FERNANDES, J. C. 2006. Characterization of folate-chitosan-DNA nanoparticles for gene therapy. *Biomaterials,* 27**,** 2060-2065.

MARTIN, T. A., YE, L., SANDERS, A. J., LANE, J. & JIANG, W. G. 2013. Cancer invasion and metastasis: molecular and cellular perspective.

MCINTOSH, C. M., ESPOSITO, E. A., BOAL, A. K., SIMARD, J. M., MARTIN, C. T. & ROTELLO, V. M. 2001. Inhibition of DNA transcription using cationic mixed monolayer protected gold clusters. *Journal of the American Chemical Society,* 123**,** 7626-7629.

MENG LIN, M., KIM, H.-H., KIM, H., MUHAMMED, M. & KYUNG KIM, D. 2010. Iron oxide-based nanomagnets in nanomedicine: fabrication and applications. *Nano reviews,* 1**,** 4883.

MERTEN, O.-W. & GAILLET, B. 2016. Viral vectors for gene therapy and gene modification approaches. *Biochemical Engineering Journal,* 108**,** 98-115.

MINTZER, M. A. & SIMANEK, E. E. 2008. Nonviral vectors for gene delivery. *Chemical reviews,* 109**,** 259-302.

MIRKIN, C. A., LETSINGER, R. L., MUCIC, R. C. & STORHOFF, J. J. 1996. A DNA-based method for rationally assembling nanoparticles into macroscopic materials. *Nature,* 382**,** 607-609.

MORILLE, M., PASSIRANI, C., VONARBOURG, A., CLAVREUL, A. & BENOIT, J.-P. 2008. Progress in developing cationic vectors for non-viral systemic gene therapy against cancer. *Biomaterials,* 29**,** 3477-3496.

MOUT, R., MOYANO, D. F., RANA, S. & ROTELLO, V. M. 2012. Surface functionalization of nanoparticles for nanomedicine. *Chemical Society Reviews,* 41**,** 2539-2544.

MÜLLER-REIBLE, C. 1993. Principles, possibilities and limits of gene therapy. *Zeitschrift fur Kardiologie,* 83**,** 5-8.

NAKHLBAND, A., BARAR, J., BIDMESHKIPOUR, A., HEIDARI, H. R. & OMIDI, Y. 2010. Bioimpacts of anti epidermal growth receptor antisense complexed with polyamidoamine dendrimers in human lung epithelial adenocarcinoma cells. *Journal of biomedical nanotechnology,* 6**,** 360-369.

NAM, H. Y., HAHN, H. J., NAM, K., CHOI, W.-H., JEONG, Y., KIM, D.-E. & PARK, J.-S. 2008. Evaluation of generations 2, 3 and 4 arginine modified PAMAM dendrimers for gene delivery. *International journal of pharmaceutics,* 363**,** 199-205.

NAYEROSSADAT, N., MAEDEH, T. & ALI, P. A. 2012. Viral and nonviral delivery systems for gene delivery. *Advanced biomedical research,* 1.

NEU, M., FISCHER, D. & KISSEL, T. 2005. Recent advances in rational gene transfer vector design based on poly (ethylene imine) and its derivatives. *The journal of gene medicine,* 7**,** 992-1009.

NICHOLS, J. W. & BAE, Y. H. 2014. EPR: evidence and fallacy. *Journal of Controlled Release,* 190**,** 451-464.

NIIDOME, T., NAKASHIMA, K., TAKAHASHI, H. & NIIDOME, Y. 2004. Preparation of primary amine-modified gold nanoparticles and their transfection ability into cultivated cells. *Chemical Communications***,** 1978-1979.

NIIDOME, Y., NIIDOME, T., YAMADA, S., HORIGUCHI, Y., TAKAHASHI, H. & NAKASHIMA, K. 2006. Pulsed-laser induced fragmentation and dissociation of DNA immobilized on gold nanoparticles. *Molecular Crystals and Liquid Crystals,* 445**,** 201/[491]-206/[496].

OISHI, M., NAKAOGAMI, J., ISHII, T. & NAGASAKI, Y. 2006. Smart PEGylated gold nanoparticles for the cytoplasmic delivery of siRNA to induce enhanced gene silencing. *Chemistry Letters,* 35**,** 1046-1047.

PAN, D., TURNER, J. L. & WOOLEY, K. L. 2003. Folic acid-conjugated nanostructured materials designed for cancer cell targeting. *Chemical Communications***,** 2400-2401.

PAN, S., CAO, D., HUANG, H., YI, W., QIN, L. & FENG, M. 2013. A Serum-Resistant Low-Generation Polyamidoamine with PEI 423 Outer Layer for Gene Delivery Vector. *Macromolecular bioscience,* 13**,** 422-436.

PAN, Y., NEUSS, S., LEIFERT, A., FISCHLER, M., WEN, F., SIMON, U., SCHMID, G., BRANDAU, W. & JAHNEN-DECHENT, W. 2007. Size-dependent cytotoxicity of gold nanoparticles. *Small,* 3**,** 1941-1949.

PARKER, A. L., NEWMAN, C., BRIGGS, S., SEYMOUR, L. & SHERIDAN, P. J. 2003. Lipoplex-mediated transfection and endocytosis. *Expert Reviews in Molecular Medicine,* 5.

PATIL, M. L., ZHANG, M., BETIGERI, S., TARATULA, O., HE, H. & MINKO, T. 2008. Surface-modified and internally cationic polyamidoamine dendrimers for efficient siRNA delivery. *Bioconjugate chemistry,* 19**,** 1396-1403.

PATIL, M. L., ZHANG, M. & MINKO, T. 2011. Multifunctional triblock nanocarrier (PAMAM-PEG-PLL) for the efficient intracellular siRNA delivery and gene silencing. *ACS nano,* 5**,** 1877-1887.

PERRAULT, S. D. & CHAN, W. C. 2009. Synthesis and surface modification of highly monodispersed, spherical gold nanoparticles of 50− 200 nm. *Journal of the American Chemical Society,* 131**,** 17042-17043.

PETERSEN, H., FECHNER, P. M., MARTIN, A. L., KUNATH, K., STOLNIK, S., ROBERTS, C. J., FISCHER, D., DAVIES, M. C. & KISSEL, T. 2002. Polyethylenimine-graft-poly (ethylene glycol) copolymers: influence of copolymer block structure on DNA complexation and biological activities as gene delivery system. *Bioconjugate chemistry,* 13**,** 845-854.

PISSUWAN, D., NIIDOME, T. & CORTIE, M. B. 2011. The forthcoming applications of gold nanoparticles in drug and gene delivery systems. *Journal of controlled release,* 149**,** 65-71.

QIU, Y., LIU, Y., WANG, L., XU, L., BAI, R., JI, Y., WU, X., ZHAO, Y., LI, Y. & CHEN, C. 2010. Surface chemistry and aspect ratio mediated cellular uptake of Au nanorods. *Biomaterials,* 31**,** 7606-7619.

RAMEZANI, N., EHSANFAR, Z., SHAMSA, F., AMIN, G., SHAHVERDI, H. R., ESFAHANI, H. R. M., SHAMSAIE, A., BAZAZ, R. D. & SHAHVERDI, A. R. 2008. Screening of medicinal plant methanol extracts for the synthesis of gold nanoparticles by their reducing potential. *Zeitschrift für Naturforschung B,* 63**,** 903-908.

RANA, S., BAJAJ, A., MOUT, R. & ROTELLO, V. M. 2012. Monolayer coated gold nanoparticles for delivery applications. *Advanced drug delivery reviews,* 64**,** 200-216.

RAVINDRA, P. 2009. Protein-mediated synthesis of gold nanoparticles. *Materials Science and Engineering: B,* 163**,** 93-98.

ROPERT, C. 1999. Liposomes as a gene delivery system. *Brazilian journal of medical and biological research,* 32.

ROSENBERG, S. A., AEBERSOLD, P., CORNETTA, K., KASID, A., MORGAN, R. A., MOEN, R., KARSON, E. M., LOTZE, M. T., YANG, J. C. & TOPALIAN, S. L. 1990. Gene transfer into humans—immunotherapy of patients with advanced melanoma, using tumor-infiltrating lymphocytes modified by retroviral gene transduction. *New England Journal of Medicine,* 323**,** 570-578.

ROSI, N. L., GILJOHANN, D. A., THAXTON, C. S., LYTTON-JEAN, A. K., HAN, M. S. & MIRKIN, C. A. 2006. Oligonucleotide-modified gold nanoparticles for intracellular gene regulation. *Science,* 312**,** 1027-1030.

ROTH, C. M. & SUNDARAM, S. 2004. Engineering synthetic vectors for improved DNA delivery: insights from intracellular pathways. *Annu. Rev. Biomed. Eng.,* 6**,** 397-426.

SARDAR, R., FUNSTON, A. M., MULVANEY, P. & MURRAY, R. W. 2009. Gold nanoparticles: past, present, and future. *Langmuir,* 25**,** 13840-13851.

SCHOLZ, C. & WAGNER, E. 2012. Therapeutic plasmid DNA versus siRNA delivery: Common and different tasks for synthetic carriers. *Journal of Controlled Release,* 161**,** 554-565.

SEFEROS, D. S., GILJOHANN, D. A., HILL, H. D., PRIGODICH, A. E. & MIRKIN, C. A. 2007. Nano-flares: probes for transfection and mRNA detection in living cells. *Journal of the American Chemical Society,* 129**,** 15477-15479.

SENDROIU, I. E., WARNER, M. E. & CORN, R. M. 2009. Fabrication of silica-coated gold nanorods functionalized with DNA for enhanced surface plasmon resonance imaging biosensing applications. *Langmuir,* 25**,** 11282-11284.

SHAH, N., STEPTOE, R. J. & PAREKH, H. S. 2011. Low-generation asymmetric dendrimers exhibit minimal toxicity and effectively complex DNA. *Journal of Peptide Science,* 17**,** 470-478.

SHAN, Y., LUO, T., PENG, C., SHENG, R., CAO, A., CAO, X., SHEN, M., GUO, R., TOMÁS, H. & SHI, X. 2012. Gene delivery using dendrimer-entrapped gold nanoparticles as nonviral vectors. *Biomaterials,* 33**,** 3025-3035.

SHUKLA, R., BANSAL, V., CHAUDHARY, M., BASU, A., BHONDE, R. R. & SASTRY, M. 2005. Biocompatibility of gold nanoparticles and their endocytotic fate inside the cellular compartment: a microscopic overview. *Langmuir,* 21**,** 10644-10654.

SINGH, M., ROGERS, C. B. & ARIATTI, M. 2007. Targeting of glycosylated lipoplexes in HepG2 cells: Anomeric and C-4 epimeric preference of the asialoglycoprotein receptor. *South African Journal of Science,* 103**,** 204-210.

SINGH, M., SINGH, S., PRASAD, S. & GAMBHIR, I. 2008. Nanotechnology in medicine and antibacterial effect of silver nanoparticles. *Digest Journal of Nanomaterials and Biostructures,* 3**,** 115-122.

SIOUD, M. 2010. Development of TLR7/8 small RNA antagonists. *RNA Therapeutics: Function, Design, and Delivery***,** 385-392.

SMITH, D. K. 2008. Dendrimers and the double helix-From DNA binding towards gene therapy. *Current topics in medicinal chemistry,* 8**,** 1187-1203.

SMITH, P. K., KROHN, R. I., HERMANSON, G., MALLIA, A., GARTNER, F., PROVENZANO, M., FUJIMOTO, E., GOEKE, N., OLSON, B. & KLENK, D. 1985. Measurement of protein using bicinchoninic acid. *Analytical biochemistry,* 150**,** 76-85.

SOMIA, N. & VERMA, I. M. 2000. Gene therapy: trials and tribulations. *Nature Reviews Genetics,* 1**,** 91-99.

STRONG, L. E. & WEST, J. L. 2011. Thermally responsive polymer–nanoparticle composites for biomedical applications. *Wiley Interdisciplinary Reviews: Nanomedicine and Nanobiotechnology,* 3**,** 307-317.

SUN, L., CHEN, P. & LIN, L. 2016. Enhanced Molecular Spectroscopy via Localized Surface Plasmon Resonance. *Applications of Molecular Spectroscopy to Current Research in the Chemical and Biological Sciences.* InTech.

SUN, X., ZHANG, G., KEYNTON, R. S., O'TOOLE, M. G., PATEL, D. & GOBIN, A. M. 2013. Enhanced drug delivery via hyperthermal membrane disruption using targeted gold nanoparticles with PEGylated Protein-G as a cofactor. *Nanomedicine: Nanotechnology, Biology and Medicine,* 9**,** 1214-1222.

SUN, Y.-N., WANG, C.-D., ZHANG, X.-M., REN, L. & TIAN, X.-H. 2011. Shape dependence of gold nanoparticles on in vivo acute toxicological effects and biodistribution. *Journal of nanoscience and nanotechnology,* 11**,** 1210-1216.

TAN, W. B., JIANG, S. & ZHANG, Y. 2007. Quantum-dot based nanoparticles for targeted silencing of HER2/neu gene via RNA interference. *Biomaterials,* 28**,** 1565-1571.

TAVERNIER, G., ANDRIES, O., DEMEESTER, J., SANDERS, N. N., DE SMEDT, S. C. & REJMAN, J. 2011. mRNA as gene therapeutic: how to control protein expression. *Journal of controlled release,* 150**,** 238-247.

THOMAS, C. E., EHRHARDT, A. & KAY, M. A. 2003. Progress and problems with the use of viral vectors for gene therapy. *Nature Reviews Genetics,* 4**,** 346-358.

THOMAS, M. & KLIBANOV, A. M. 2002. Enhancing polyethylenimine's delivery of plasmid DNA into mammalian cells. *Proceedings of the National Academy of Sciences,* 99**,** 14640-14645.

TIWARI, P. M., VIG, K., DENNIS, V. A. & SINGH, S. R. 2011. Functionalized gold nanoparticles and their biomedical applications. *Nanomaterials,* 1**,** 31-63.

TSENG, Y.-C., MOZUMDAR, S. & HUANG, L. 2009. Lipid-based systemic delivery of siRNA. *Advanced drug delivery reviews,* 61**,** 721-731.

UNSOY, G., YALCIN, S., KHODADUST, R., GUNDUZ, G. & GUNDUZ, U. 2012. Synthesis optimization and characterization of chitosan-coated iron oxide nanoparticles produced for biomedical applications. *Journal of Nanoparticle Research,* 14**,** 964.

VILLANUEVA, J. R., NAVARRO, M. G. & VILLANUEVA, L. R. 2016. Dendrimers as a promising tool in ocular therapeutics: Latest advances and perspectives. *International journal of pharmaceutics,* 511**,** 359-366.

WADA, K., ARIMA, H., TSUTSUMI, T., HIRAYAMA, F. & UEKAMA, K. 2005. Enhancing effects of galactosylated dendrimer/α-cyclodextrin conjugates on gene transfer efficiency. *Biological and Pharmaceutical Bulletin,* 28**,** 500-505.

WADHWANI, A., KLEIN, W. & LACOR, P. 2010. Efficient gene silencing in neural cells by functionalized gold nanoparticles. *Nanoscape,* 7**,** 6-10.

WAITE, C. L., SPARKS, S. M., UHRICH, K. E. & ROTH, C. M. 2009. Acetylation of PAMAM dendrimers for cellular delivery of siRNA. *Bmc Biotechnology,* 9**,** 38.

WEBSTER, D. M., SUNDARAM, P. & BYRNE, M. E. 2013. Injectable nanomaterials for drug delivery: carriers, targeting moieties, and therapeutics. *European Journal of Pharmaceutics and Biopharmaceutics,* 84**,** 1-20.

XIA, T., KOVOCHICH, M., BRANT, J., HOTZE, M., SEMPF, J., OBERLEY, T., SIOUTAS, C., YEH, J. I., WIESNER, M. R. & NEL, A. E. 2006. Comparison of the abilities of ambient and manufactured nanoparticles to induce cellular toxicity according to an oxidative stress paradigm. *Nano letters,* 6**,** 1794-1807.

XIAO, T., CAO, X. & SHI, X. 2013. Dendrimer-entrapped gold nanoparticles modified with folic acid for targeted gene delivery applications. *Journal of Controlled Release,* 172**,** e114-e115.

XU, P., VAN KIRK, E. A., ZHAN, Y., MURDOCH, W. J., RADOSZ, M. & SHEN, Y. 2007. Targeted Charge-Reversal Nanoparticles for Nuclear Drug Delivery. *Angewandte Chemie International Edition,* 46**,** 4999-5002.

XU, Q., KAMBHAMPATI, S. P. & KANNAN, R. M. 2013. Nanotechnology approaches for ocular drug delivery. *Middle East African journal of ophthalmology,* 20**,** 26.

XUN, M.-M., LIU, Y.-H., GUO, Q., ZHANG, J., ZHANG, Q.-F., WU, W.-X. & YU, X.-Q. 2014. Low molecular weight PEI-appended polyesters as non-viral gene delivery vectors. *European journal of medicinal chemistry,* 78**,** 118-125.

YAMAMOTO, A., KORMANN, M., ROSENECKER, J. & RUDOLPH, C. 2009. Current prospects for mRNA gene delivery. *European Journal of Pharmaceutics and Biopharmaceutics,* 71**,** 484-489.

YAMANO, S., DAI, J. & MOURSI, A. M. 2010. Comparison of transfection efficiency of nonviral gene transfer reagents. *Molecular biotechnology,* 46**,** 287-300.

YEN, H. J., HSU, S. H. & TSAI, C. L. 2009. Cytotoxicity and immunological response of gold and silver nanoparticles of different sizes. *Small,* 5**,** 1553-1561.

YIN, H., KANASTY, R. L., ELTOUKHY, A. A., VEGAS, A. J., DORKIN, J. R. & ANDERSON, D. G. 2014. Non-viral vectors for gene-based therapy. *Nature reviews. Genetics,* 15**,** 541.

YIN, W., XIANG, P. & LI, Q. 2005. Investigations of the effect of DNA size in transient transfection assay using dual luciferase system. *Analytical biochemistry,* 346**,** 289-294.

YOSHIDA, H., NISHIKAWA, M., YASUDA, S., MIZUNO, Y., TOYOTA, H., KIYOTA, T., TAKAHASHI, R. & TAKAKURA, Y. 2009. TLR9-dependent systemic interferon-β production by intravenous injection of plasmid DNA/cationic liposome complex in mice. *The journal of gene medicine,* 11**,** 708-717.

YUAN, X., WEN, S., SHEN, M. & SHI, X. 2013. Dendrimer-stabilized silver nanoparticles enable efficient colorimetric sensing of mercury ions in aqueous solution. *Analytical Methods,* 5**,** 5486-5492.

ZHANG, J., DU, J., HAN, B., LIU, Z., JIANG, T. & ZHANG, Z. 2006. Sonochemical formation of single-crystalline gold nanobelts. *Angewandte Chemie,* 118**,** 1134-1137.

ZHANG, S., GAO, H. & BAO, G. 2015. Physical principles of nanoparticle cellular endocytosis. *ACS nano,* 9**,** 8655-8671.

ZHENG, D., SEFEROS, D. S., GILJOHANN, D. A., PATEL, P. C. & MIRKIN, C. A. 2009. Aptamer nano-flares for molecular detection in living cells. *Nano letters,* 9**,** 3258-3261.

ZHOU, J., RALSTON, J., SEDEV, R. & BEATTIE, D. A. 2009. Functionalized gold nanoparticles: synthesis, structure and colloid stability. *Journal of Colloid and Interface Science,* 331**,** 251-262.

ZHOU, M., ZHANG, X., YANG, Y., LIU, Z., TIAN, B., JIE, J. & ZHANG, X. 2013a. Carrier-free functionalized multidrug nanorods for synergistic cancer therapy. *Biomaterials,* 34**,** 8960-8967.

ZHOU, Z., MA, X., JIN, E., TANG, J., SUI, M., SHEN, Y., VAN KIRK, E. A., MURDOCH, W. J. & RADOSZ, M. 2013b. Linear-dendritic drug conjugates forming long-circulating nanorods for cancer-drug delivery. *Biomaterials,* 34**,** 5722-5735.

ZHU, H., JIANG, R., XIAO, L. & ZENG, G. 2010. Preparation, characterization, adsorption kinetics and thermodynamics of novel magnetic chitosan enwrapping nanosized γ-Fe 2 O 3 and multi-walled carbon nanotubes with enhanced adsorption properties for methyl orange. *Bioresource technology,* 101**,** 5063-5069.

ZIRAKSAZ, Z., NOMANI, A., SOLEIMANI, M., BAKHSHANDEH, B., AREFIAN, E., HARIRIAN, I. & TABBAKHIAN, M. 2013. Evaluation of cationic dendrimer and lipid as transfection reagents of short RNAs for stem cell modification. *International journal of pharmaceutics,* 448**,** 231-238.

CHAPTER 6

6 CONCLUSIONS AND RECOMMENDATIONS FOR FURTHER RESEARCH

6.1 Introduction and Aim

Gene therapy promises to treat cancer by delivering therapeutic genes, drugs, and adjuvants into the tumours. Throughout the years, a variety of gene delivery treatment modalities (viral and non-viral) have been advanced; however, their clinical application has been limited by high toxicity and low transfection efficiency. Although, non-viral vectors are low in toxicity, their transfection efficiency is questionable, prompting basic research in this area. Dendrimer stabilized metal nanoparticles have shown potential as efficient non-viral modalities. Metal gold nanoparticles (AuNPs) are the most promising non-viral delivery scaffolds, owing to their attractive properties, that presents a platform for the creation of vectors that could bind, condense, protect and deliver therapeutic drugs or genes to target sites with minimal toxicity. This study aimed at evaluating and optimizing the delivery efficiencies of functionalized AuNPs for three nucleic acids e.g. plasmid DNA (pDNA), messenger RNA (mRNA) and small interference RNA (siRNA) *in vitro,* to effect the required gene expression or silencing. The research undertaken involved the synthesis and functionalisation of AuNPs with a dendrimer (G5D) and targeting ligand (folic acid, FA); characterisation; nucleic acid binding assessment; enzyme protection studies; cytotoxicity evaluation; and gene expression and silencing efficiency.

6.2 Overall Findings and Conclusion

All nanoparticles were successfully formulated and confirmed by TEM, NTA, UV spectroscopy and NMR. NPs appeared spherical, well dispersed with mean diameter sizes ranging from 65-128 nm, while their nanocomplexes displayed as clusters with sizes ranging from 100-200 nm. Gel retardation and dye displacement studies showed that both Au:G5D and Au:G5D:FA NPs were highly efficient in pCMV-*Luc* DNA, F*luc*-mRNA, siRNA binding. They also formed stable nanocomplexes affording good protection to pDNA, mRNA and siRNA against nucleases, with high cell viability (>80%) and gene expression activity (up to 6 x 10^8 RLU/mg protein) especially for the mRNA nanocomplexes. Overall, the gene expression and silencing efficiency of Au:G5D and Au:G5D:FA NPs was greater than that of G5D and G5D:FA NPs, indicating the important

and central roles played by both the dendrimer and the AuNPs in their design and formulation. Receptor-mediated delivery was confirmed by the competition assay, where transfection levels in the FA-receptor negative cell lines, were significantly lower ($p < 0.001$) than that in FA-receptor positive cell lines. Overall, we have successfully synthesized and demonstrated efficient gene delivery using dendrimer grafted gold nanoparticles and FA modified dendrimer grafted gold nanoparticles *in vitro*.

6.3 Future Recommendations

Studies to date have demonstrated the potential of gold nanoparticles *in vitro*, with issues that still need to be resolved before clinical applications. Proper investigation of AuNPs' cytotoxicity in a wider panel of cell lines may be necessary, including other detailed toxicological assessments, viz. oxidative stress, cell membrane damage, and genotoxicity evaluations. Furthermore, the cell specific targeting of AuNPs to minimize side effects, is important, necessitating the selection of suitable stabilizing and targeting moieties. Finally, issues of possible immune response will need to be extensively evaluated before these NPs can be tested *in vivo*. Nonetheless, AuNPs present a platform for the advancement of drug and gene delivery vectors that could be used for the treatment of cancer and other inherited disorders.

APPENDIX

Appendix A

Synthesis and Functionalisation

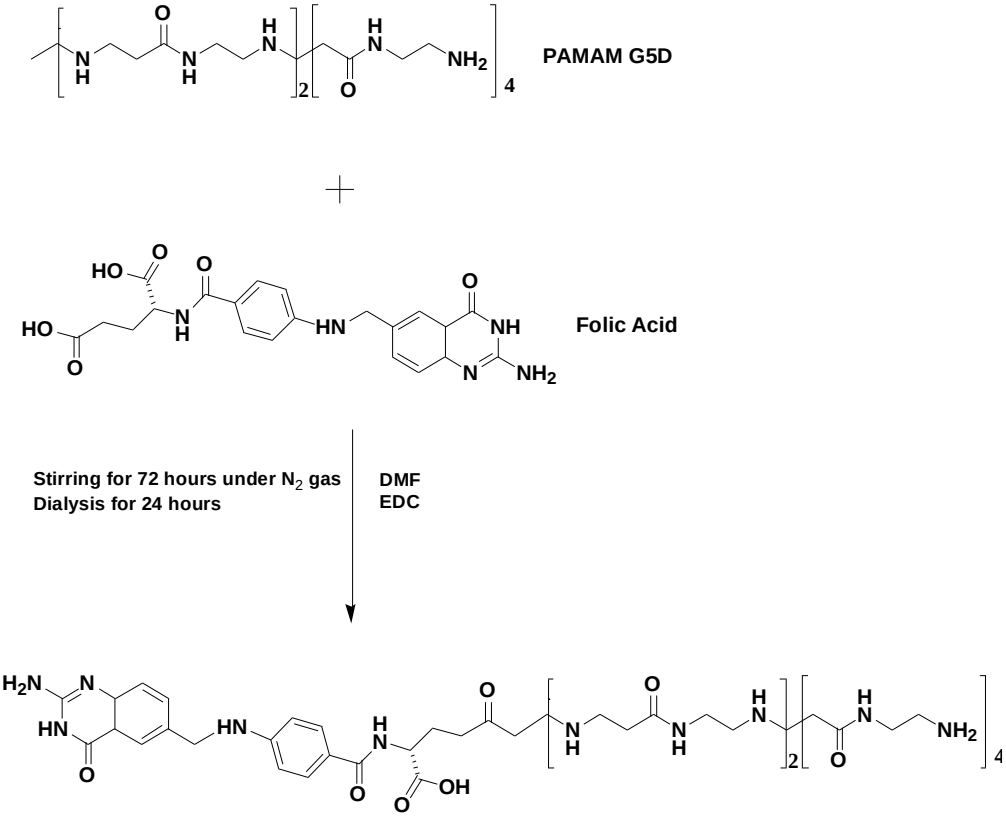

Figure A1: Schematic representation of the synthesis of folic acid conjugated PAMAM G5D.

UV-Spectroscopy

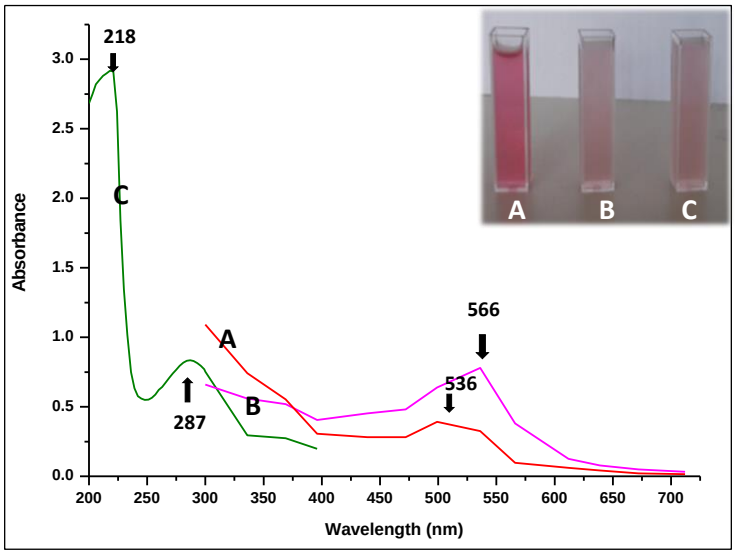

Figure A2: UV- Spectra of (A) AuNPs, (B) Au:G5D NPs and (C) Au:G5D:FA NPs.

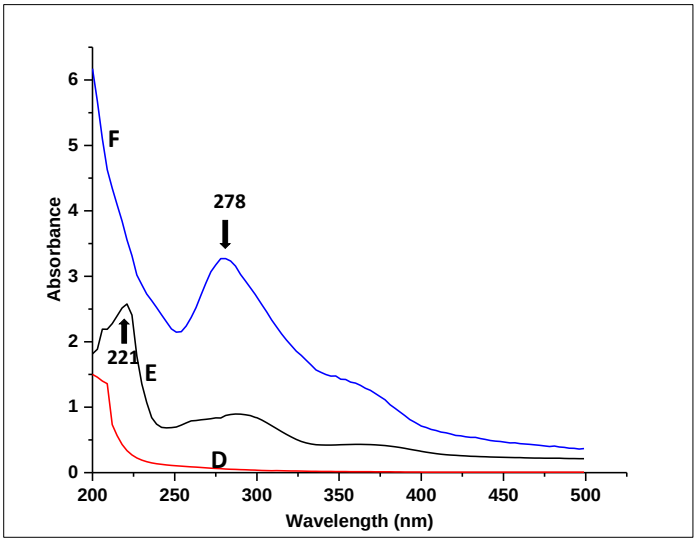

Figure A3: UV- Spectra of (D) G5D, (E) G5D:FA NPs and (F) FA.

^{1}H NMR Spectroscopy

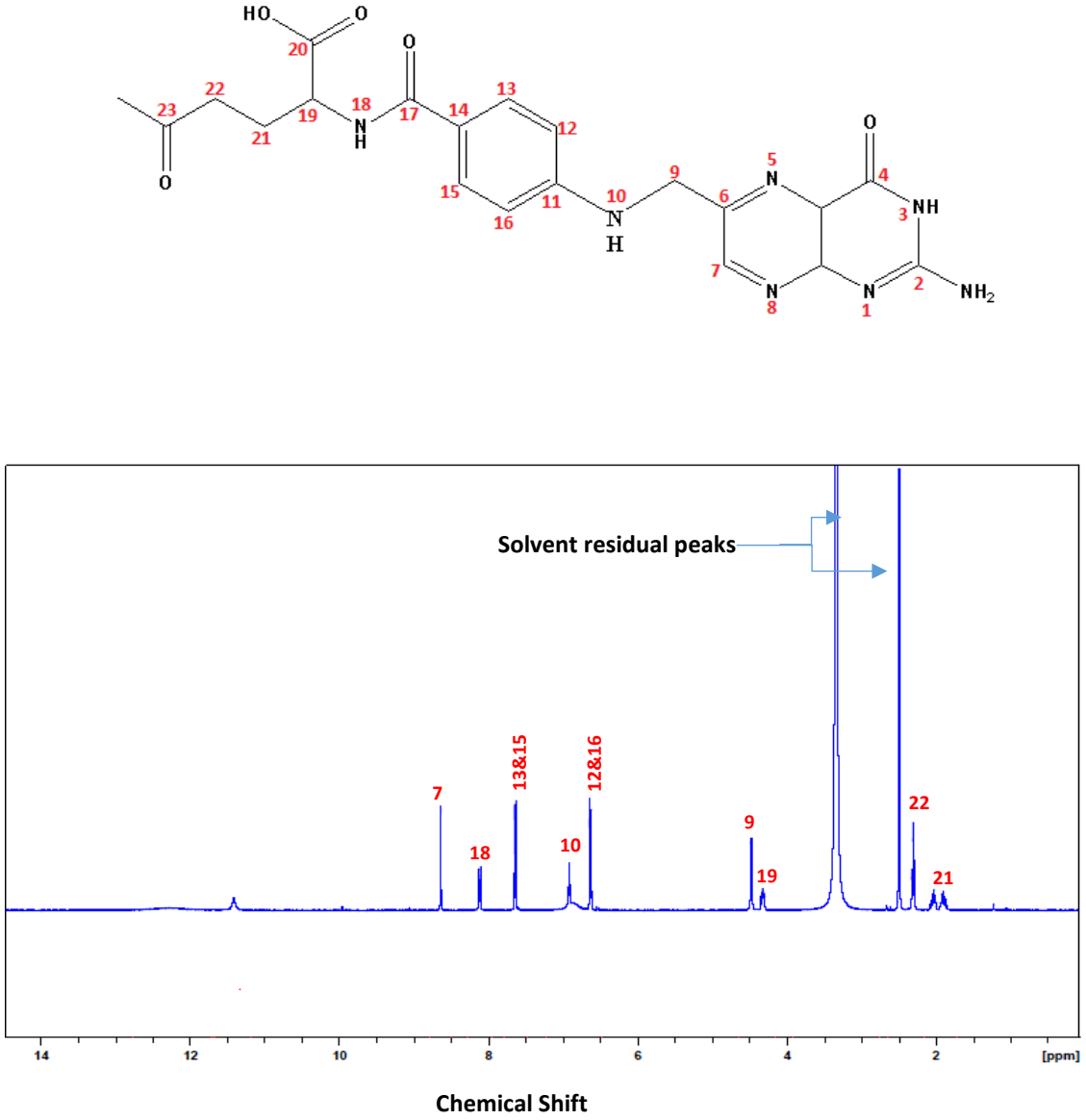

Figure A4: The structure of folic acid and ^{1}H NMR spectrum.

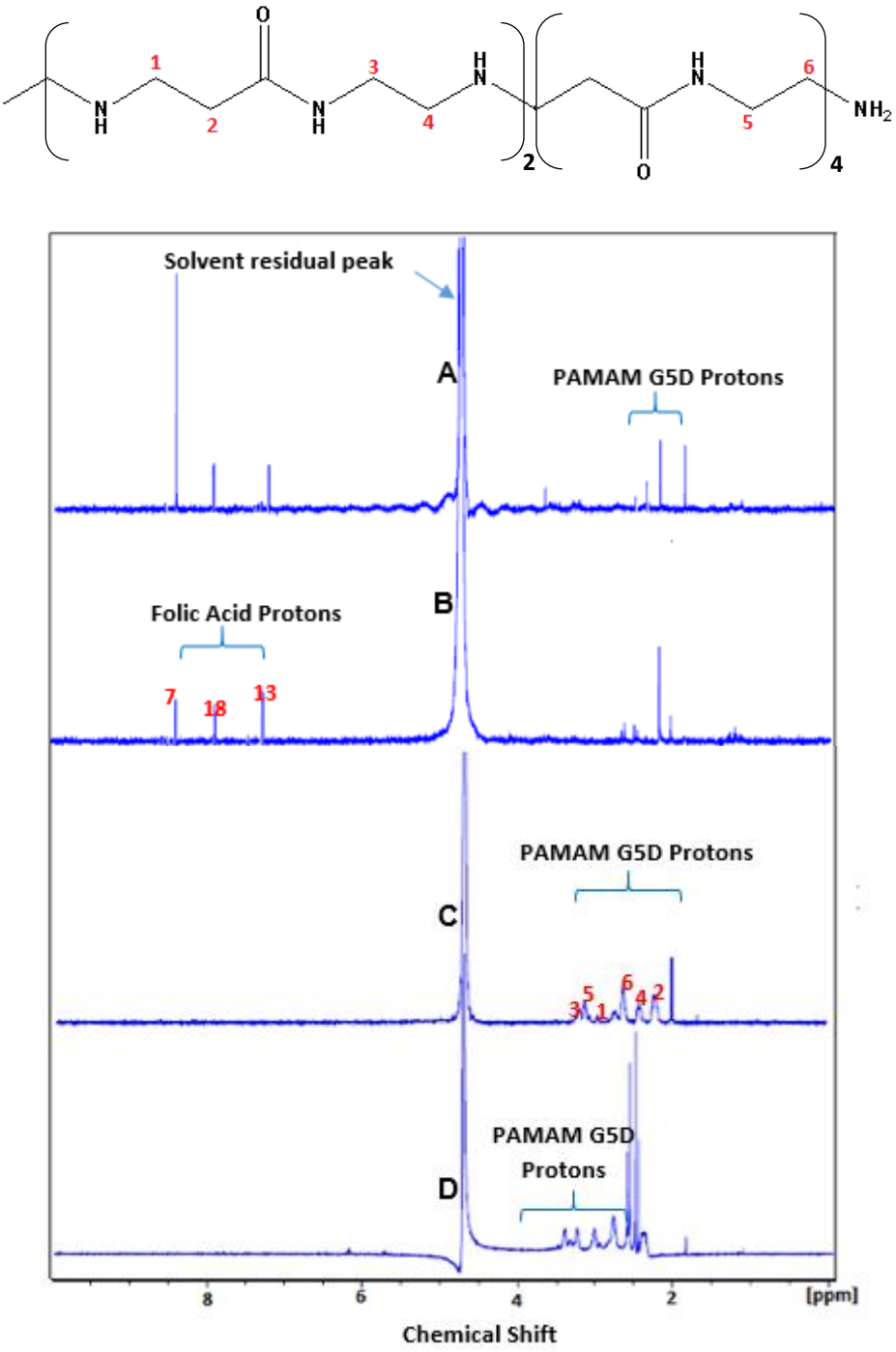

Figure A5: The structure of PAMAM G5 dendrimer and ^{1}H NMR spectra of PAMAM (G5) dendrimer and folic acid functionalised gold nanoparticles in D_2O. (A) G5D:FA, (B) Au:G5D:FA, (C) G5D, (D) Au:G5D.

Nanoparticle Tracking Analysis-Nanoparticles (NPs)

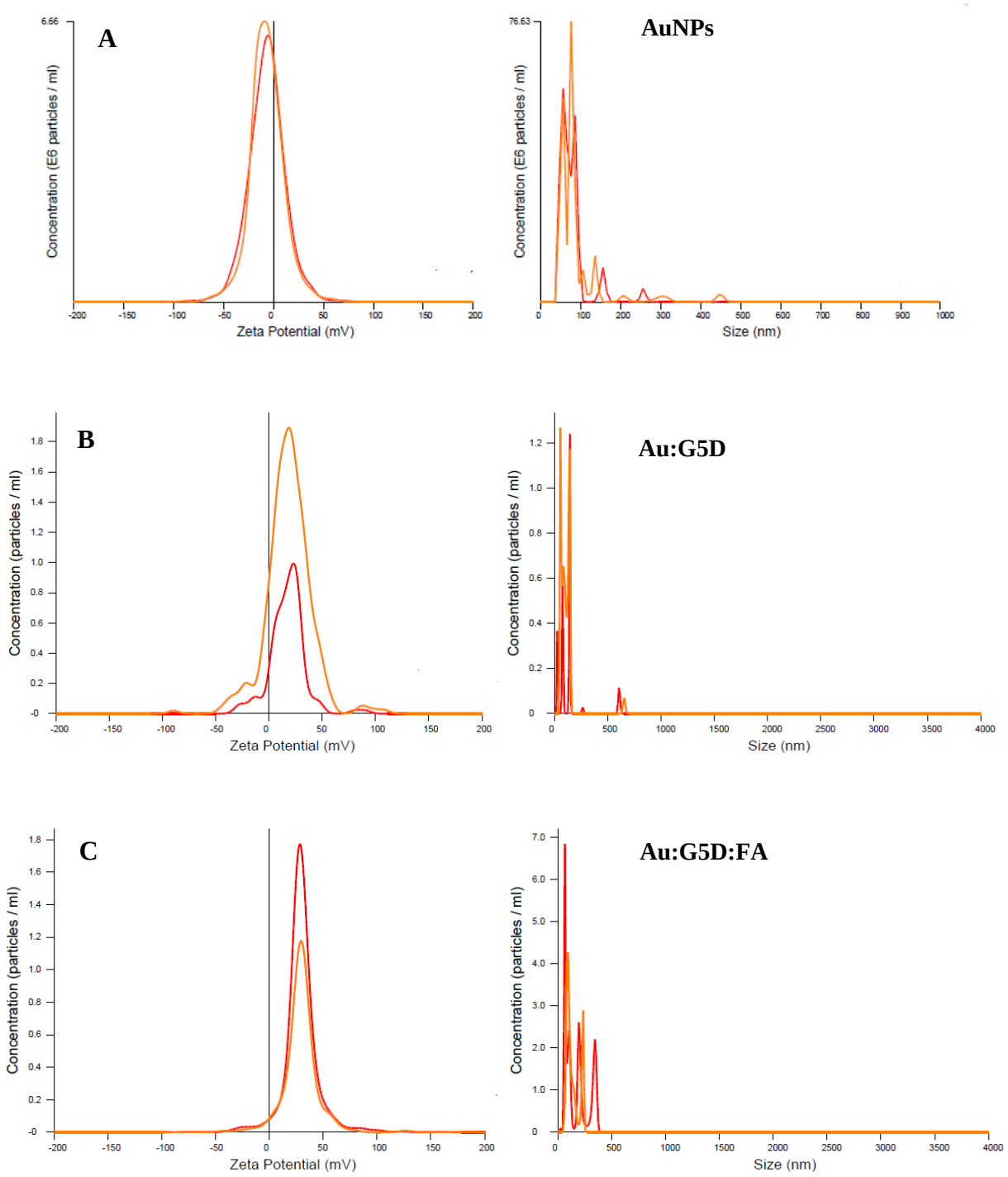

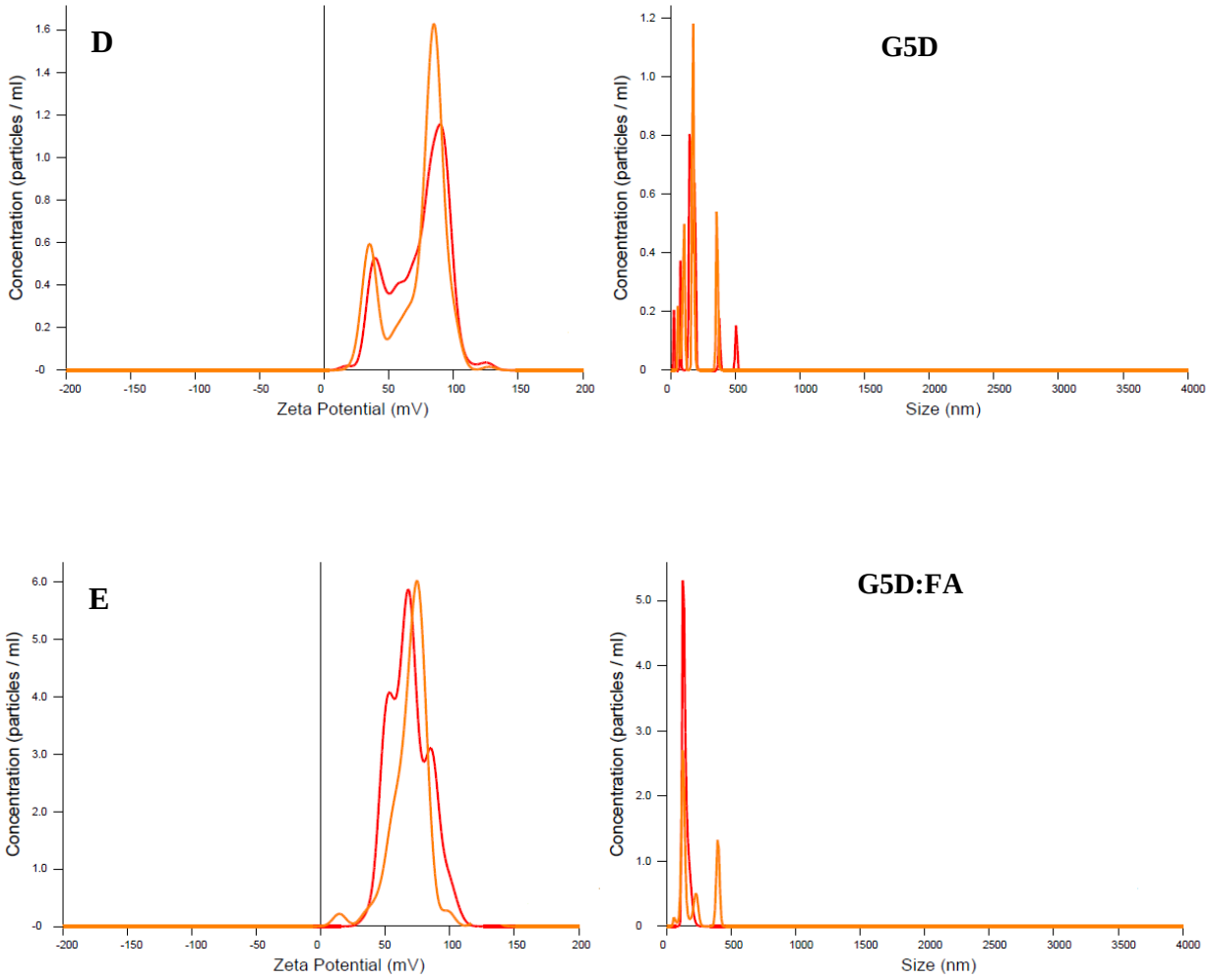

Figure A6: ζ potential (mV) and mean size (nm) images of NPs (A) AuNPs, (B) Au:G5D, (C) Au:G5D:FA, (D) G5D, and (E) G5D:FA.

Nanoparticle Tracking Analysis of pDNA Nanocomplexes

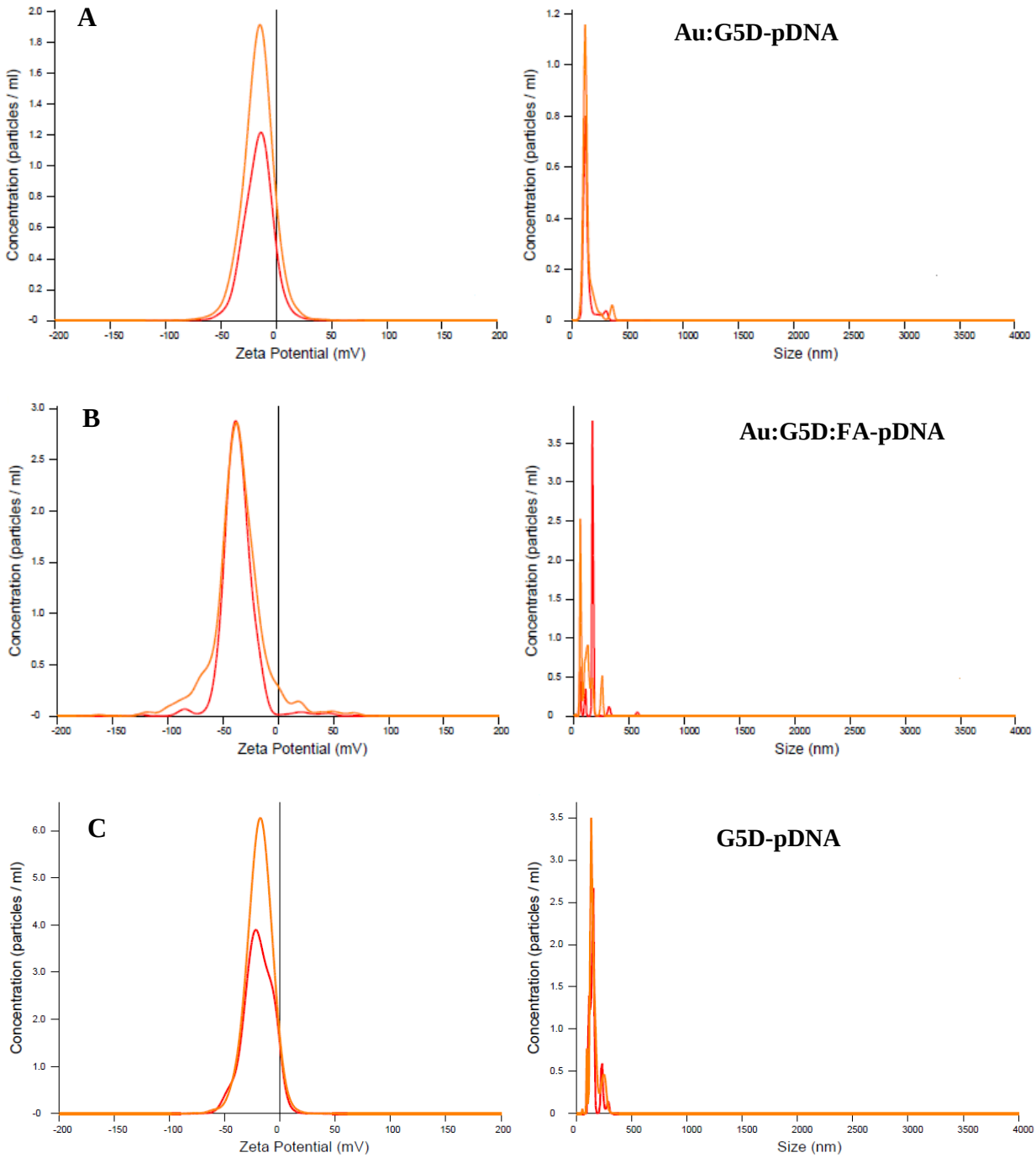

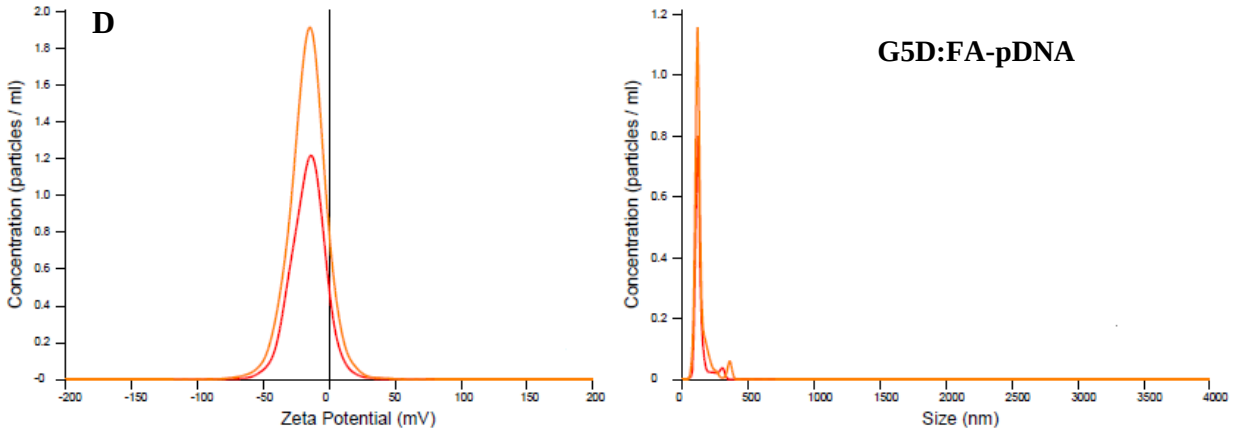

Figure A7: ζ potential and mean size images of nanocomplexes (A) Au:G5D, (B) Au:G5D:FA, (C) G5D, and (D) G5D:FA prepared at optimum ratios ($^{w}/_{w}$).

Nanoparticle Tracking Analysis of mRNA Nanocomplexes

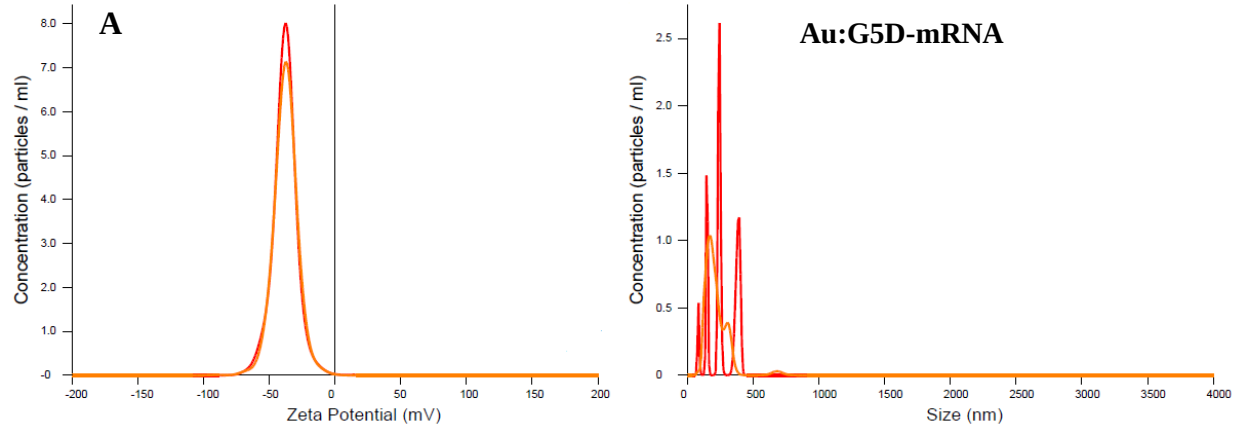

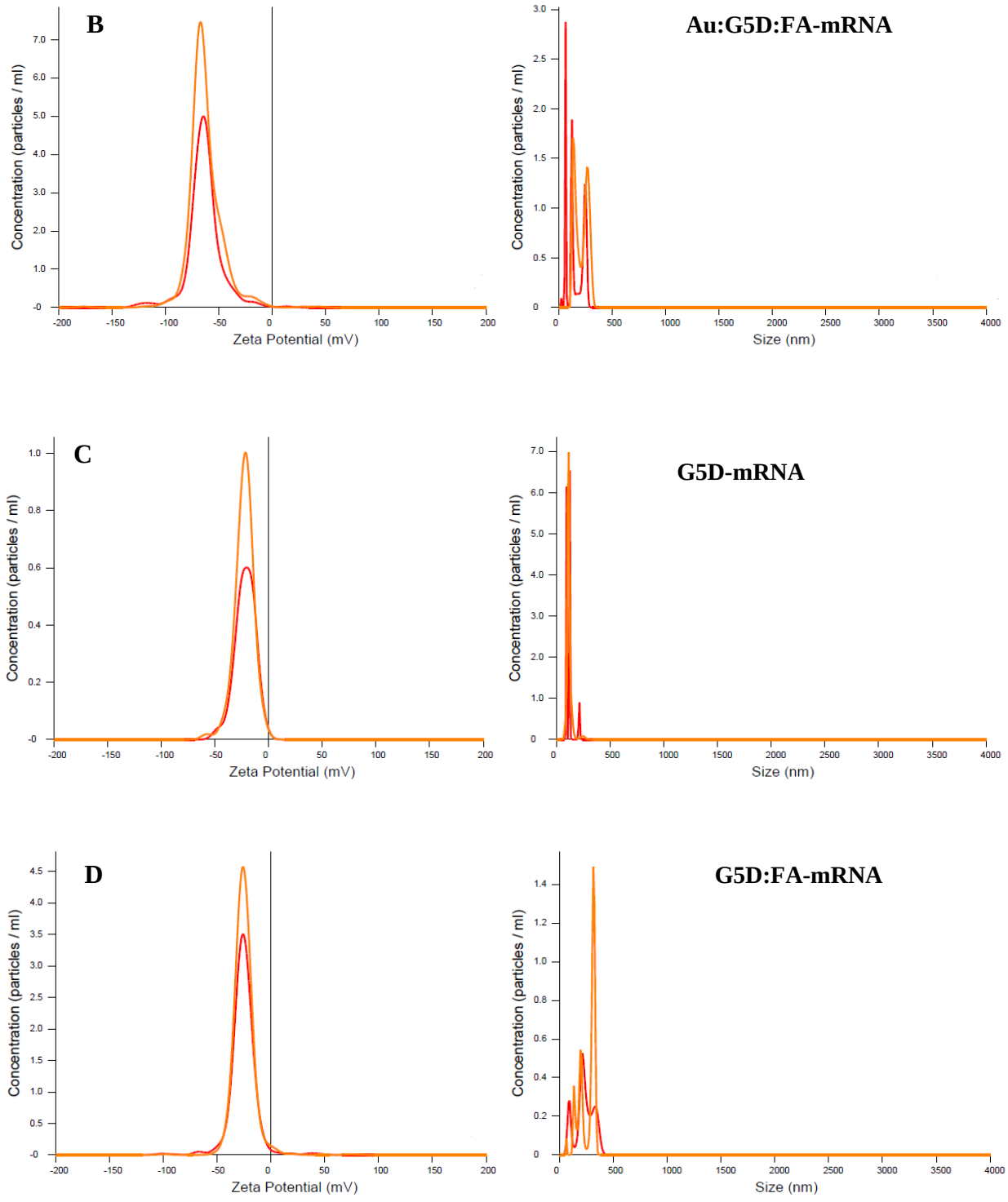

Figure A8: ζ potential and mean size images of nanocomplexes (A) Au:G5D, (B) Au:G5D:FA, (C) G5D, and (D) G5D:FA prepared at optimum ratios ($^{w}/_{w}$).

Nanoparticle Tracking Analysis of siRNA Nanocomplexes

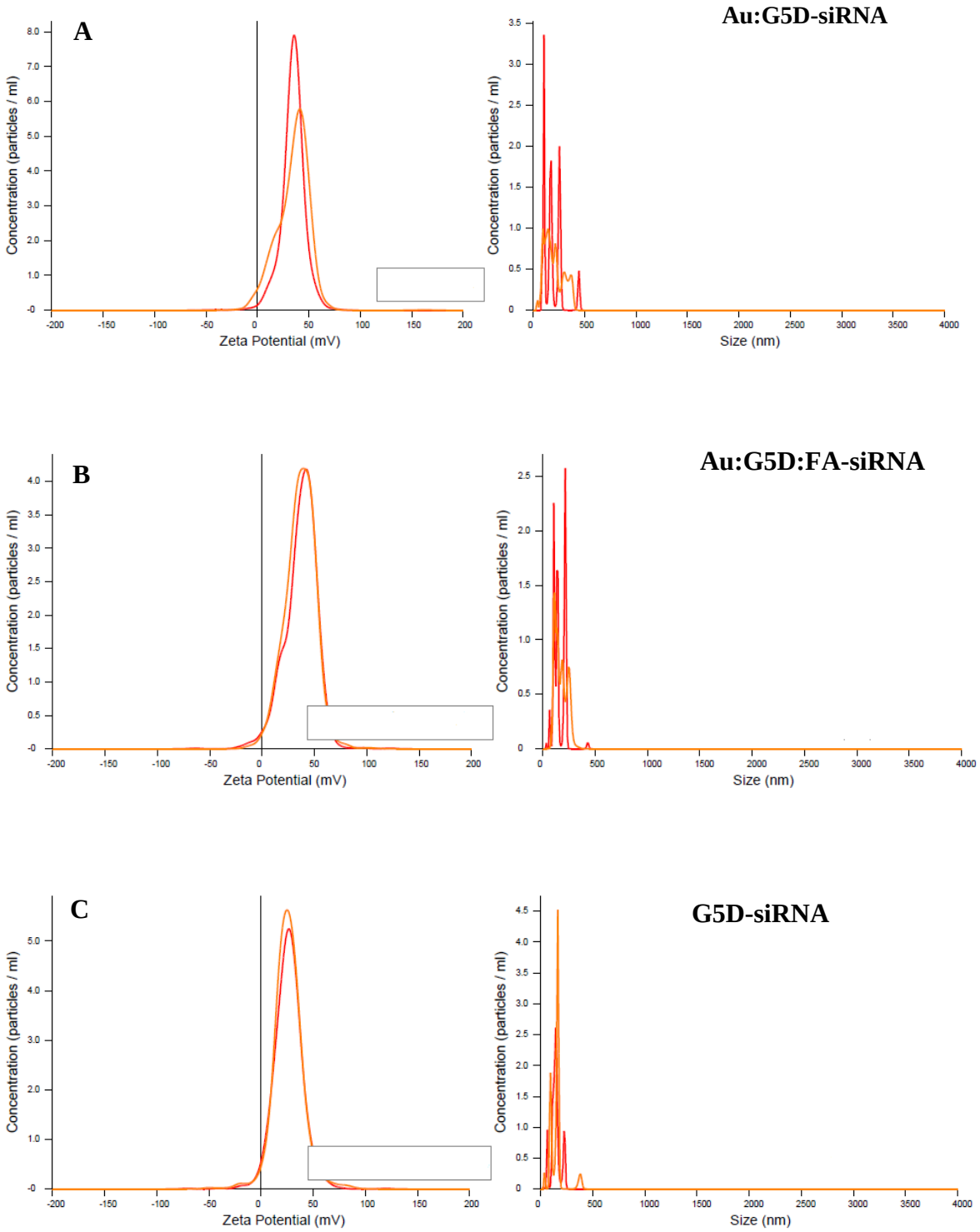

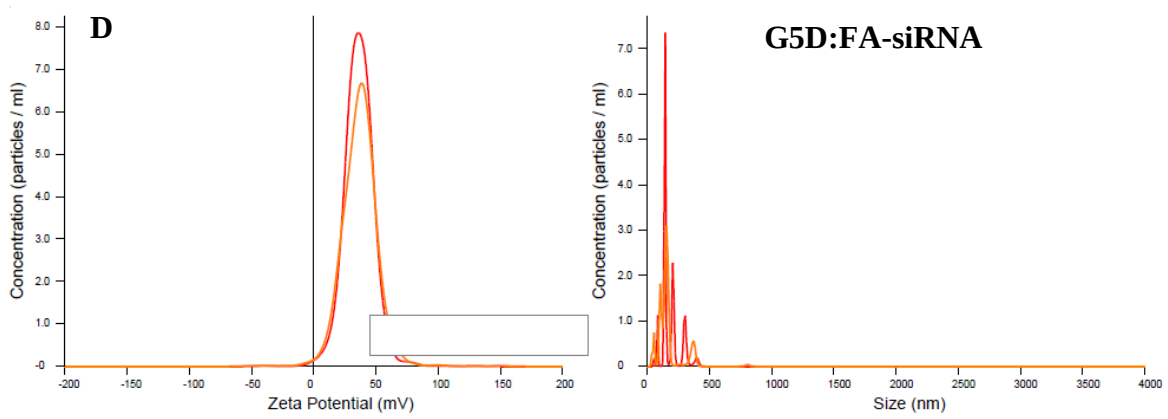

Figure A9: ζ potential and mean size images of nanocomplexes (A) Au:G5D, (B) Au:G5D:FA, (C) G5D, and (D) G5D:FA.

Turnitin Report

Final Thesis PhD 2017

ORIGINALITY REPORT

15%	9%	11%	6%
SIMILARITY INDEX	INTERNET SOURCES	PUBLICATIONS	STUDENT PAPERS

PRIMARY SOURCES

1	Submitted to University of KwaZulu-Natal Student Paper	2%
2	Londiwe Mbatha, Santanu Chakravorty, Charles B. de Koning, Willem A.L. van Otterlo, Patrick Arbuthnot, Mario Ariatti, Moganavelli Singh. "Spacer Length: A Determining Factor in	2%